Investigation of the Functional Significance of MMP-8 in Breast Myoepithelial Cells

Thesis submitted for the degree of Doctor of Philosophy at the University of London

by

Müge SARPER

Centre for Tumour Biology
Barts Cancer Institute
Bart's and the London Queen Mary's
School of Medicine and Dentistry
John Vane Science Centre
Charterhouse Square
London EC1M 6BQ

London, 2013

Abstract

The Matrix Metalloproteinase (MMP) family are conventionally considered as key enzymes contributing to cancer-cell invasion through remodelling of the extracellular matrix (ECM). In contrast, MMP-8 has been shown to exert an anti-cancer role. In normal breast, MMP-8 expression is restricted to tumour suppressor myoepithelial cells (MECs), which form the interface between glandular epithelium and the ECM. In ductal carcinoma *in situ* (DCIS), MECs are altered; a consistent change is up-regulation of αvβ6-integrin, which is associated with loss of suppressor activity. Preliminary observations indicated that there is also loss of MMP-8 expression in DCIS-MEC. The aim of this study is to investigate the impact of loss of MEC derived MMP-8 on MEC function and how this might modulate tumour progression.

To generate a model of DCIS MEC, an αvβ6 over-expressing cell line (Myo-β6) was generated from normal MECs (Myo-Puro). These cells were found to lose MMP-8 expression. To dissect gain-of-function effect, MMP-8 was re-introduced into Myo-β6 (MMP-8 WT). A proteolytic inactive form of MMP-8 was used to dissect the dependence of function on proteolysis.

In-vitro analysis demonstrated that MMP-8 WT but not inactive MMP-8 significantly up-regulates MEC adhesion ($p=0.0001$) and spread ($p=0.0003$) on ECM, but reduces migration towards ECM proteins including Collagen-I ($p=0.006$) and fibronectin ($p=0.01$). Furthermore MMP-8 WT results in reduced numbers of filopodia/retraction fibres ($p=0.01$) and reduced protrusion length ($p=0.0001$) on MEC cell surface. MMP-8 promotes the localisation of α6β4-integrin to hemidesmosomal adhesive structures ($p=0.003$), and inhibits MEC gelatinase ($p=0.002$) and TGF-β activity. Conversely, knock-down of endogenous MMP-8 in Myo-Puro MECs promotes migration and filopodia/retraction fibre formation ($p=0.05$), increases gelatinase activity ($p=0.007$) and TGF-β signalling.

To analyse the paracrine effect of MEC-derived MMP-8 on breast cancer cell invasion, MDA MB 231 or SUM159 cells were co-cultured with modified Myo-β6 cells in Boyden chamber invasion assays. A significant reduction in breast cancer cell invasion was observed only in the presence of MMP-8 WT ($p=0.004$) but not with inactive MMP-8. In contrast, MMP-8 knock-down in Myo-Puro MECs significantly enhanced breast cancer cell invasion ($p=0.001$). In order to recapitulate the DCIS stromal micro-ecology, 3D-organotypic cultures were constructed. In these systems there was a significant reduction in invasion only in the presence of MMP-8 WT MECs ($p<0.001$). Conversely, in the absence of Myo-Puro-derived MMP-8 breast cancer cell invasion was significantly up-regulated ($p=0.007$).

These results suggest that MMP-8 does contribute to MEC tumour suppressor function via mechanisms dependent upon its proteolytic activity. These data support the hypothesis that loss of MMP-8 may contribute to the progression of DCIS to invasive disease.

Declaration

I confirm that the work presented in this thesis is my own, except stated below:

- Tissue sections and organotypic sections were cut by G. Elia, Barts Cancer Institute, London.
- Immunohistochemical analysis of MMP-8 was done by G. Elia and Dr L. Haywood, Barts Cancer Institute, London.
- Primary myoepithelial cells, luminal epithelial cells and fibroblasts were isolated by Dr J. Gomm, Barts Cancer Institute, London.
- Myoepithelial cell lines Myo-β6 and Myo-Puro were generated by Dr M. Allen, Barts Cancer Institute, London. The parental myoepithelial cell line (MEC 1089) was a kind gift from Prof M. O' Hare, and Prof P. Jat, Institute of Neurology, University College London, London.
- MMP-8 wild type and MMP-8 mutant (EA) coding plasmids were kind gifts from Prof D. Edwards, Dr J. Decock and S. Thirkettle, University of East Anglia, Norwich.
- TGF-β responsive MDA MB 231 cell line was a kind gift from Dr C. Hill, London Research Institute, London.
- Neso antibody was a kind gift from Prof M Djamgoz and Dr S. Fraser, Imperial College London.
- MMP-8 *in situ* hybridisation probe was designed by Prof R. Poulsom, Blizzard Institute Queen Mary University of London, London

Contents

Table of Figures

Table of Tables

Abbreviations

16qNL	16q no loss
16qPL	16q partial loss
16qWL	16q whole lost
2D	2 dimensional
3D	3 dimensional
4NQO	4-Nitroquinoline 1-oxide
A	
ABC	Avidin-biotin complex
aCGH	Array comparative genomic hybridisation
ADAM	A disintegrin and metalloproteinases'
ADAMTS	A disintegrin and metalloproteinase with thrombospondin motifs'
ADH	Atypical ductal hyperplasia
Ala	Alanine
ALH	Atypical lobular hyperplasia
APS	Ammonium persulfate
Arg	Arginine
ATCC	American Type Culture Collection
AU	Arbitrary unit
B	
Bcl	B-cell lymphoma
BM	Basement membrane
Bp	Base pair
BP	Bullous pemphigoid
BPAG	Bullous pemphigoid antigen
BRCA-1	Breast cancer gene
BSA	Bovine serum albumin
C	
C/EBP	CCAAT/enhancer-binding protein-β site
Ca	Calcium
CAF	Cancer associated fibroblast
CALLA	Common Acute Lymphoblastic Leukemia Antigen
CD	Cluster of designation
CGH	Comparative genomic hybridisation
CK	Cytokeratin
CM	Conditioned media
COX	Cyclo-oxygenase
CXCL	C-X-C ligand
CXCR4	C-X-C receptor
Cy3	Cyanine
D	
DAB	Diaminobenzidine
DAPI	4',6-diamidino-2-phenylindole
DCIS	Ductal carcinoma *in situ*
Dcs	Desmocollin

DMBA	7,12-dimethylbenz[a]anthracene
DMEM	Dulbecco's modified Eagle's medium
DMSO	Dimethyl sulfoxide
DPX	Distyrene tricresyl phosphate xylene
Dsg	Desmoglein
E	
ECL	Enhanced chemiluminescence
ECM	Extracellular matrix
EDTA	Ethylenediaminetetraacetic acid
EGF	Epidermal growth factor
EGFR	Epidermal growth factor receptor
EHS	Englebreth-Holm Swarm
ELISA	Enzyme-linked immunosorbent assay
EMT	Epithelial mesenchymal transition
EpCam	Epithelial cell adhesion molecule
ER	Oestrogen receptor
ERK	Extracellular signal-regulated protein kinase
F	
FAK	Focal adhesion kinase
FB	Fibroblast
FBS	Foetal bovine serum
FEA	Flat epithelial atypia
FFPE	Formalin fixed paraffin embedded
FITC	Fluorescein isothiocyanate
FN-EDA	Oncofetal form of fibronectin
G	
GP	Glycosylphosphatidylinositol
GRB	Growth factor receptor-bound protein
H	
H&E	Hematoxylin and eosin
HaCat	Cultured human keratinocyte
HD	Hemidesmosome
HER	Human epidermal growth factor receptor
HGF	Hepatocyte growth factor
HPV	Human papilloma virus
HRP	Horseradish peroxidise
HSC70	Heat shock cognate 70
h-TERT	Human telomerase reverse transcriptase
HUVEC	Human unbilical vein endothelial cell
I	
IDC	Invasive ductal carcinoma
IF	Immunofluorescence
IGF	Insulin like growth factors
IHC	Immunohistochemistry
IL	Interleukin
ISH	*In situ* hybridization
K	
kDA	Kilodalton

KGF	Keratinocyte growth factor
L	
LAP	Latency associated peptide
LCIS	Lobular carcinoma *in situ*
LEC	Luminal epithelial cell
Leu	Leucine
LIF	Leukemia inhibitory factor
LIX	Lipopolysaccharide induced CXC chemokine
LLC	Lung Lewis carcinoma
LOH	Loss of heterozygosity
LOX	Lysyl oxidase
LTBP	Latent TGF-β binding protein
Lys	Lysine
M	
MAPK	Mitogen-activated protein kinase
MCA	Methylcholanthrene
MEC	Myoepithelial cell
MFI	Mean fluorescent intensity
Mg	Magnesium
MIP-1α	Macrophage inflammatory protein-1α
MMP	Matrix metalloproteinase
MMPI	Matrix metalloproteinase inhibitor
MMTV	Mouse mammary tumour virus
Mn	Manganese
MSI	Microsatellite instability
MT-MMPs	Membrane Type MMPs
mTOR	Mammalian target of rapamycin
MTS	3-(4,5-dimethylthiazol-2-yl)-5-(3-Carboxymethoxyphenyl)-2-(4-sulfophenyl)-2H-tetrazolium
MW	Molecular weight
MWCO	Molecular weight cut off
N	
NaOH	Sodium hydroxide
NCBI	National Center for Biotechnology Information
Neso	Neonatal splice variant of Nav1.5
NF-κβ	Nuclear Factor-κβ
NHSBSP	National Health Service Breast Screening Programme
Ni-NTA	Nickel-nitrilotriacetic acid
NMU	N-nitrosomethylurea
NOD/SCID	Nonobese diabetic/severe combined immunodeficiency
NS	Not significant
O	
OD	Optical density
P	
PAI	Plasminogen activator inhibitor
PBS	Phosphate buffered saline

PCR	Polymerase chain reaction
PDGF	Platelet derived growth factor
PFA	Paraformaldehyde
PI3K	Phosphoinositide 3-kinase
PMN	Polymorphonuclear cells
PR	Progesterone receptor
PTEN	Phosphatase and tensin homolog
Q	
QRT-PCR	Quantitative reverse transcription polymerase chain reaction
R	
RGD	Arginyl-glycyl-aspartic acid
rhMMP-8	Recombinant human matrix metalloproteinase -8
RIPA	Radio immunoprecipitation assay
ROS	Reactive oxygen species
RPMI	Roswell Park Memorial Institute
RT	Room temperature
RTK	Receptor tyrosine kinases
RT-PCR	Reverse transcription polymerase chain reaction
S	
SAGE	Serial analysis of gene expression
SCC	Squamous cell carcinoma
SDS	Sodium dodecyl sulphate
SEM	Standard errors of mean
Ser	Serine
SFM	Serum free media
siRNA	Small interfering RNA
SMA	Smooth muscle actin
SMAD	Small mothers against decapentaplegic
SMMHC	Smooth muscle myosin heavy chain
SNP	Single nucleotide polymorphism
SRKs	Src family kinases
STS	Steroid sulphatase
T	
TDLU	Terminal duct lobular units
TAE	Tris acetate-EDTA
TEMED	Tetramethylethylenediamine
TGF-β	Transforming growth factor-β
TGF-βR	Transforming growth factor-β receptor
Thr	Threonine
TIMP	Tissue inhibitor of metalloproteinase
TNF	Tumour necrosis factor
TP53	Tumor protein 53
TPA	12-O-tetradecanoyl-phorbol-13-acetate
U	
UB	Unbound
uPAR	Urokinase-type plasminogen activator receptor
UV	Ultraviolet

V	
Val	Valine
VEGF	Vascular endothelial growth factor
VEGFR	Vascular endothelial growth factor receptor
Wnt	Wingless-int
W	
WT	Wild type
WT-1	Wilms' tumor suppressor
Z	
Zn	Zinc

Chapter 1: Introduction

1 Introduction

1.1 Breast Cancer Incidence

1.1.1 Incidence of Ductal Carcinoma *in situ*

The frequency of detection of *in situ* breast cancer has increased dramatically in the last two decades (Figure 1-1) (CRUK Statistics 2010). This increase is concomitant with the advent of the National Health Service Breast Screening Programme (NHSBSP) which was introduced in 1988. According to NHSBSP, women aged between 50 and 70 are invited for mammographic screening every three years. A recent trial is ongoing to extend breast screening to 47-73 age limits (CRUK Statistics 2010).

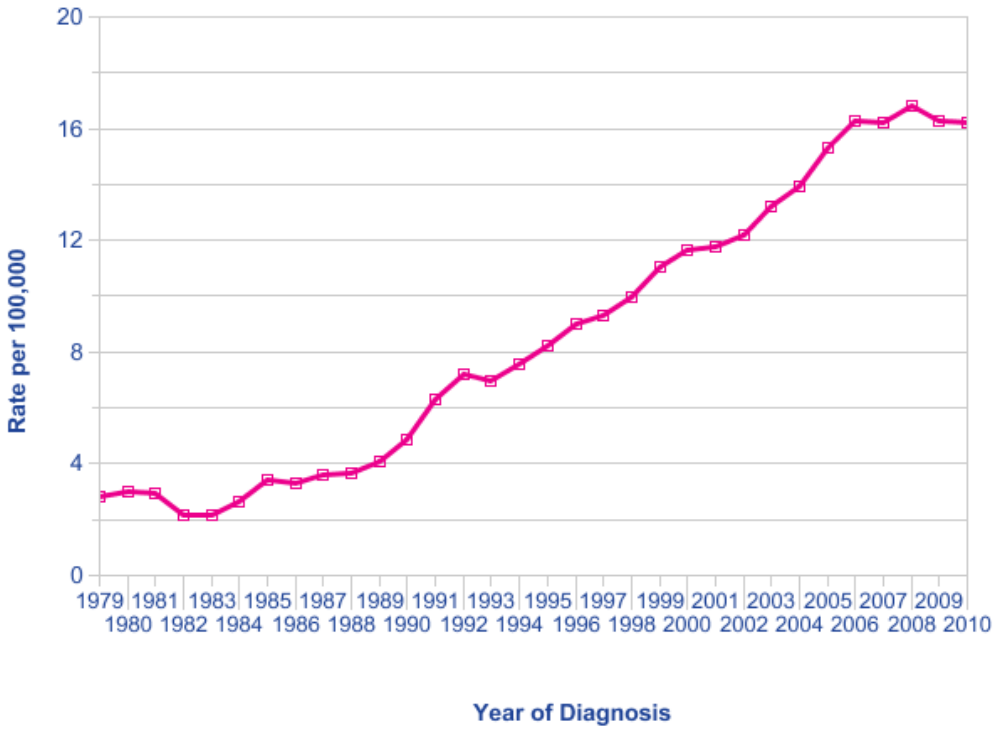

Figure 1-1: *In situ* breast carcinoma age-standardised incidence rates between 1979 and 2010. The rates were substantially increased after NHSBSP introduced in 1988-1989 financial year (Figure extracted from www.cancerresearchuk.org).

Ductal carcinoma *in situ* (DCIS) forms the majority of *in situ* breast carcinoma cases with 90% of detected *in situ* breast carcinomas diagnosed as DCIS and 10% as lobular carcinoma *in situ* (LCIS). The incidence of DCIS is higher in women aged 50-69 which also corresponds to the screening strategy (Figure 1-2) (CRUK Statistics 2010).

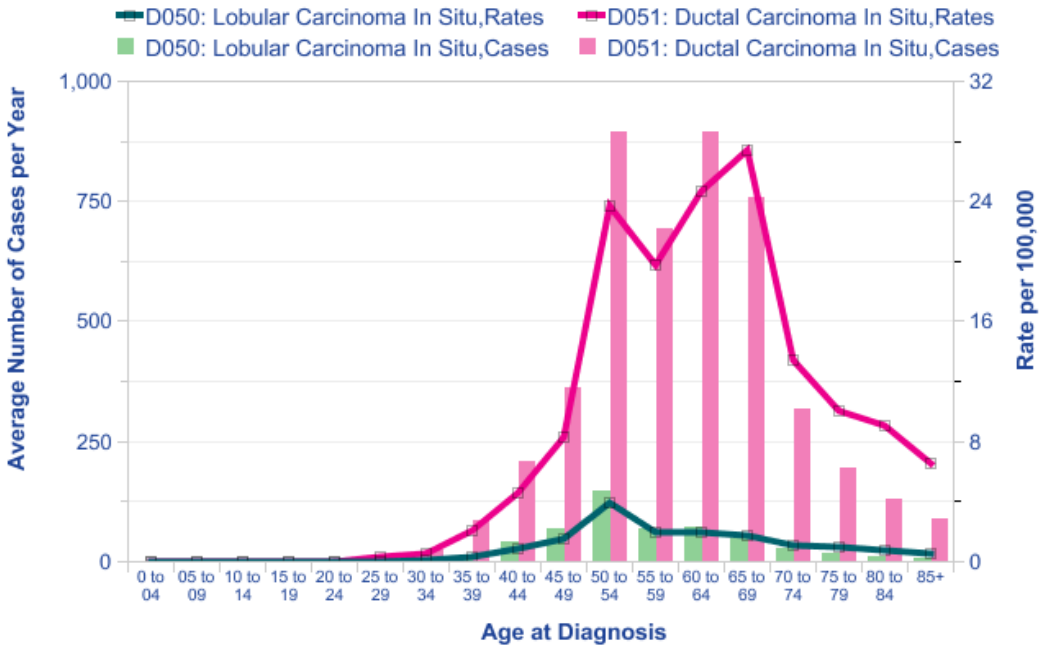

Figure 1-2: Distribution of average number of new cases per year and incidence of *in situ* breast cancer according to age group and histological type (2008-2010). The highest incidence rate of *in situ* breast carcinoma is in women in 50s and 60s. DCIS has an approximately 9 times higher incidence rate than that of LCIS (Figure extracted from www.cancerresearchuk.org).

Women diagnosed with *in situ* breast cancer have twice the risk of developing invasive breast cancer when compared to women with no *in situ* breast cancer history [1]. In 2010 83% of total diagnosed *in situ* breast cancer cases and 20% (3100 cases) of total breast cancer cases in women were DCIS (CRUK Statistics 2010).

1.1.2 Invasive Breast Carcinoma Incidence

Breast cancer is the most common cancer in females in the UK, with 31% of newly diagnosed cancer cases in women being breast cancer (CRUK Statistics 2010). The lifetime risk for a woman to develop breast cancer in the UK is 1 in 8 (CRUK Statistics 2010). It is the third most common cause of cancer related deaths in UK and second most common cause of death from cancer in women, responsible for 15% of cancer related deaths for females in UK (CRUK Statistics 2010).

The incidence rate of invasive breast cancer, similar to *in situ* disease, was substantially affected by the introduction of the NHSBSP and due to the pool of undetected breast cancer cases, increased more rapidly until 1992 then showed a slight increase until 2010 (Figure 1-3) (CRUK Statistics 2010).

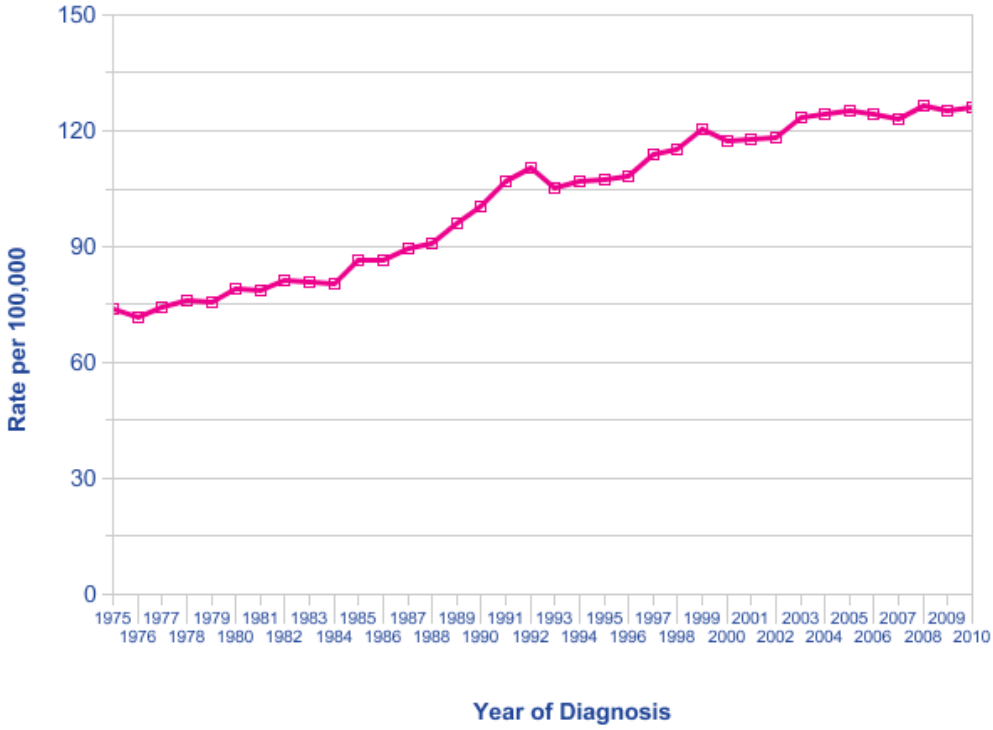

Figure 1-3: Invasive breast carcinoma age-standardized incidence rates between 1975 and 2010. The rates increased between 1975 and 1992 then slightly dropped and remained relatively stable until 2010 when compared to the increase between 1980 and 1992 (Figure extracted from www.cancerresearchuk.org).

Nearly half (48%) of diagnosed breast cancer cases occur in women aged 50-70 years. Despite the fact that breast cancer is rare in women under or in their early 20s, it is the most common cancer in females under the age of 39 accounting for 1,350 new cases per year (CRUK Statistics 2010).

Interestingly, breast cancer incidence is higher in economically developed countries [2, 3] such as Western Europe. Risk factors for development of breast cancer include late first pregnancy, late menopause, high breast density, alcohol consumption and taking hormone replacement therapy (CRUK Statistics 2010).

There is an overall decrease in breast cancer mortality rates when compared to the early 1970s. This has been attributed to facts such as improvements in screening, surgical techniques, radiotherapy and adjuvant therapies including tamoxifen [4, 5].

1.2 Ductal Carcinoma *in situ*

1.2.1 Structure of Breast

Breast tissue is composed of a branching ductal network which terminates in functional acini called terminal duct lobular units (TDLU) [6]. These structures are made up of an epithelial-bilayer: an inner columnar luminal epithelial cell (LEC) compartment and outer myoepithelial cell (MEC) compartment (Figure 1-4) [6]. Physiologically these cell groups are responsible for milk production and ejection, respectively [7-9]. During lactation, LECs synthesise milk components, which are collected in the duct lumen as a result of MEC contraction, and transported to the nipple [7-9]. In resting breast these compartments are represented in approximately the same cell number, however the proliferation of the luminal group is dependent on hormonal activity, and fluctuates with menstrual cycle and expands with pregnancy [10, 11]. This functional bilayer epithelium is embedded in stroma which consists of adipose and fibrous tissue in varying proportions [8, 12-14]. The MEC organisation differs between ducts and lobules; in excretory ducts, MEC are arranged in an almost continuous layer around LECs but form more of a basket like structure in lobules [8]. MECs are separated from the connective tissue by the underlying basement membrane (BM) [15]. BM is produced

mainly by MECs and consists of Collagen-IV, fibronectin, laminin, Nidogen, glycosaminoglycans and proteoglycans. Receptors of BM components, especially cell adhesion molecules such as integrins, present in MECs, are responsible for interaction with the BM and neighbouring cells [8, 16].

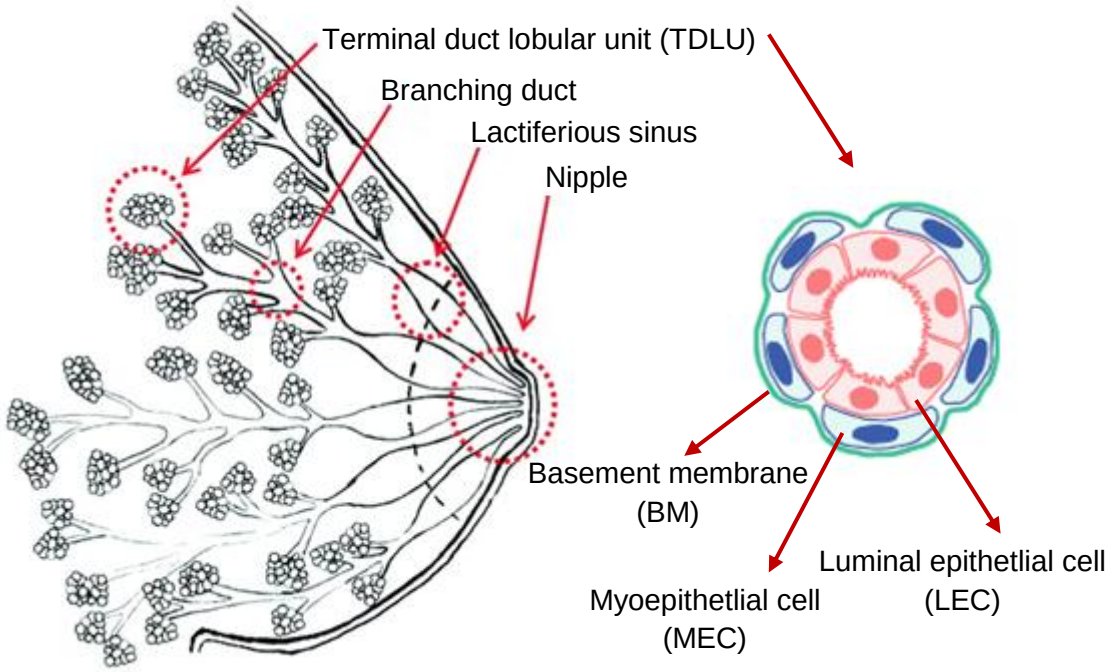

Figure 1-4: Schematic of the structure of normal breast. Human breast comprises a branching ductal network terminating in TDLU. These functional units are lined with a dual epithelial layer consisting of LECs and MECs. Once milk is produced by LECs it is transferred by the contractile action of MEC into interconnecting ducts, lactiferous sinuses and ultimately to the nipple. Figure taken and adapted from Allred et al 2010 and Cichon et al 2010 [7, 17].

DCIS is the proliferation of malignant cells enclosed by the surrounding MEC layer and BM without stromal invasion (Figure 1-5) [18, 19]. It represents the earliest definable stage of breast cancer and is the non-obligate precursor to invasive disease. Therefore, DCIS is regarded as the ideal target for breast

cancer treatment [18, 19]. Although DCIS was diagnosed very rarely until 1980, as a result of widespread mammographic screening, 20% of breast cancer cases detected today are classified as DCIS (CRUK Statistics 2010) [20]. It is difficult to study the natural history of DCIS, however, it is reported that 50% of untreated cases may progress to invasive disease and that the time to progression is variable up to 4 decades [19, 21, 22]. There is no single molecular marker identified hitherto that predicts *in situ* to invasive disease progression [23, 24]. To evaluate whether the tumour is likely to progress into invasive cancer is the main challenge in DCIS treatment [23, 24].

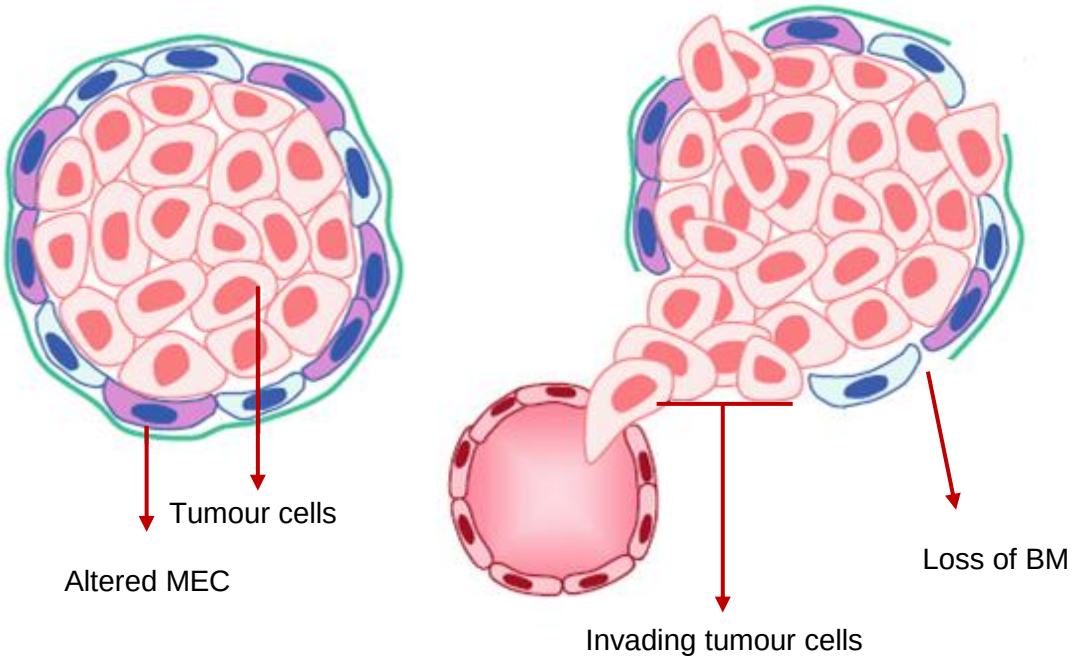

Figure 1-5: Schematic of DCIS versus invasive ductal carcinoma. In DCIS the proliferative tumour cells fill the duct lumen, retained by the BM and MEC layer. During invasion MEC-BM integrity is lost and tumour cells invade through disrupted foci. Figure taken and adapted from Cichon et al 2010 [17].

1.2.2 DCIS Classification

DCIS shows heterogeneity in both morphology and cell biology as evidenced by proliferation index, signalling pathway activation and cellular composition, and reflected in clinical behaviour [19]. Traditionally DCIS classification is based on nuclear morphology, growth rate, cytonuclear differentiation and the presence or absence of necrosis [19]. The Van Nuys classification system uses nuclear grade and necrosis. This approach classifies DCIS into three subgroups: non-high-grade without necrosis, non-high-grade with necrosis and high-grade with or without necrosis [19]. Another system is recommended by National Coordinating Group for Breast Screening Pathology in the UK. This system is based on cytological and architectural features and divides DCIS into low, intermediate or high grade DCIS [19]. The first group contains small regular cells and shows cribriform or micropapillary patterns. High grade DCIS is often called comedo DCIS and in contrast to low grade disease the malignant cells show marked pleomorphism with mitotic figures and is frequently characterised by a central mass of necrotic tumour cells. Intermediate DCIS exhibits nuclear characteristics between these groups [19, 25]

With regard to the heterogeneous biology of DCIS, histological classifications present an over simplified approach and provide limited information about the complex structure and outcome of the disease. The classification based on nuclear morphology divides DCIS into three groups which are low-, intermediate-, and high grade DCIS. This system provides a degree of

predictive value, in that high-grade DCIS has higher risk of recurrence but the system has limited reproducibility due to subjective interpretation [19, 26].

Additional classification methods may assist better treatment choice. Gene expression profiling can also categorize *in situ* disease as well, intermediate and poorly differentiated DCIS [19].

Differences observed between well and poorly differentiated DCIS includes genes associated to metabolism and cell communication [21]. The cases which carry high diversity also show high levels of p53 mutation [27, 28]. High expression of anti-apoptotic protein B-cell lymphoma (Bcl) -2 and oestrogen receptor (ER) positivity characterise low-grade (well differentiated) DCIS [28].

Over recent years there have been considerable advances in the classification of invasive breast cancer and this is partly reflected in DCIS. In invasive ductal carcinoma (IDC) the classification, based on parameters such as morphology, histologic grade, expression of steroid and growth factor receptors, oestrogen inducible genes and mutation in the p53 gene, remains over simplified with respect to the repeatedly observed great variability in behaviour between cases [29-31]. Gene expression arrays have identified gene signatures that classify breast cancer into 5 main groups: Luminal A, Luminal B, HER-2 amplified, Basal-like and normal-like [29]. Whilst identified through microarray analysis, considerable progress has been made in generating surrogate immunohistochemical signatures [29].

Luminal tumours express luminal cytokeratins (CK) -8 and CK-18 and are characterised by ER expression. This group can be further divided into at least two subtypes according to ER and progesterone receptor (PR) expression levels with Luminal A group (ER^+/PR^+/ Human epithelial growth factor receptor- $HER\text{-}2^-$) having higher ER and PR levels than Luminal B group (ER^+/PR^+or-/$HER\text{-}2^-$). In comparison to the other groups Luminal tumours show better prognosis and response to therapies, particularly Luminal A [29-31].

HER-2 amplified, Basal-like and normal-like groups are characterised by down regulation of ER and most of the ER related genes. $HER\text{-}2^+$ tumours are characterised by amplification of HER-2 and several genes related to HER-2 on chromosome 17 such as Growth factor receptor-bound protein (GRB) -7. This group also frequently shows p53 mutation and are identified on immunohistochemistry (IHC) as ER^-, PR^-, $HER\text{-}2^+$ [29-31]. The normal-like breast cancers show high expression of genes related to MEC and adipose cells and low expression of the genes related to LECs. However, they have been more difficult to identify as a distinct entity in further studies and it is unclear if this is a true subgroup [29-31].

Basal-like tumours express CK-5, 14, 17 and laminin, which are characteristics of MECs. They generally lack ER, PR and HER-2 expression and so frequently are referred as Triple Negative tumours. Whilst there is considerable overlap between Basal-like and Triple Negative tumours, they

are not in fact identical [29-31]. It has been suggested that Basal-like tumours are best characterised on 5 markers consisting of ER, PR, HER-2, epidermal growth factor receptor (EGFR) and CK5/6. Basal-like tumours are negative for ER, PR, HER-2 and positive for EGFR and CK5/6, whilst 'triple negative' may be classified according to negativity for all 5 markers [32] . The Basal-like group is also associated with breast cancer gene (BRCA)-1 mutation. This mutation is linked with high proliferation, p53 mutation and often lack of HER-2 expression. Basal like tumours have the highest frequency of distant metastasis and shortest survival and relapse free survival time [29-31]. This classification based on molecular signatures indicates that the transcriptional programme and genetic alterations have significant impact on disease prognosis [29-31].

Further comparative use of histological markers and gene expression analysis between DCIS and IDC demonstrate that DCIS also can be categorised as Basal-like, HER-2+ and luminal type tumours in a similar fashion to invasive disease [21, 28, 33, 34]. Hannemann and colleagues employed microarray analysis to compare gene expression profile of 40 *in situ* and 40 invasive breast cancers. By performing two-dimensional hierarchical clustering they showed that the basal-like, HER-2 type and luminal type can also be observed in DCIS [21].

Cheang and colleagues used a panel of 5 markers similarly classified DCIS [35]. However, differences in clinical behaviour observed within the same groups based on these markers suggest that this panel is too limited. Clark

and co-workers evaluated a greater number of biomarkers, including ER, PR, HER-2, CK5/6, CK14, topoisomerase IIα, β4 integrin, β6 integrin, Bcl-2, maspin and p53, in a large cohort of 188 DCIS cases [26]. The most significant variability in gene expression was seen in maspin, p53, EGFR and topoisomerase IIα. A strong correlation was observed between ER and PR whereas there was an inverse correlation with HER-2. The basal markers CK5/6 and CK14 were positive in approximately 10% of the cohort, indicating the rare existence of the basal type in DCIS. Bcl-2 expression is also associated with well differentiated DCIS and good prognosis. It is noteworthy that Bcl-2 is also identified as an independent predictive tool for good prognosis in IDC [26, 33, 36]. A cluster analysis developed based on these markers identified 4 subtypes of DCIS (Figure 1-6).

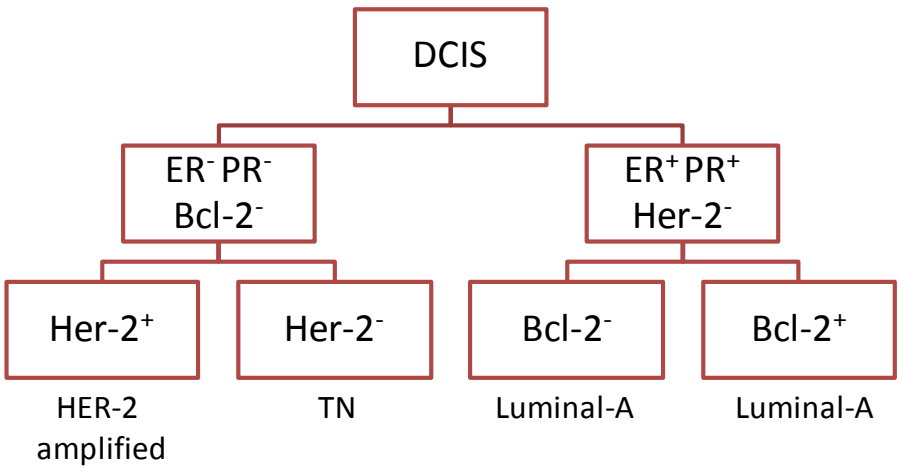

Figure 1-6: The classification of DCIS according to molecular markers. This classification is indicating that the subgroups identified for IDC already exist in DCIS. TN subtype contains tumours with basal-like features. Figure adapted from Clark et al 2010 [26].

Although the molecular subgroups identified for IDC can be detected at the DCIS stage, the relative frequency of each subtype is different; for example in DCIS, the basal subtype is rarely found (10% of the cohort accounts for approximately 18% of invasive carcinoma) [26]. Importantly, HER-2 positivity shows a higher frequency in DCIS than in IDC [37, 38]. HER-2 amplification and over-expression was reported for 50% of DCIS cases and is considered as a particular characteristic of DCIS [38, 39]. In fact HER-2 over-expression in MCF10A cells results in the generation of DCIS-like structures, which are composed of proliferating cells filling the lumen encapsulated by an intact Collagen-IV layer with no invasion into BM, in 3D culture systems [40], and based on these findings the authors suggest that HER-2 amplification is considered an early event in breast cancer development [21]. However only ~20% of invasive breast cancers show HER-2 amplification, so this cannot be essential for breast cancer development.

The different frequencies of HER-2 positivity in DCIS and IDC lead to two hypotheses; HER-2 amplification might be lost during the DCIS-IDC switch, or HER-2 positive DCIS cases may not develop into invasive disease. To investigate these possibilities Park and colleagues compared HER-2 levels between pure DCIS cases and DCIS associated with IDC, furthermore they compared the intraductal and invasive components of the same IDC case. They showed that HER-2 amplification is significantly more frequently detected in DCIS and, interestingly the intraductal and invasive component of the same case is similar in terms of HER-2 amplification which shows that progression to invasive disease is not a function of a change (loss) of HER-2

amplification. Taking this result into consideration it can be concluded that a clonal expansion model which supports the differential progression of DCIS and IDC in early stages of breast cancer would be a better explanation of the discrepancy observed in HER-2 status [37].

1.2.3 Pathways of Progression of DCIS

The first progression model of breast cancer suggested that breast tumours would originate either from ducts or lobules and therefore were named after the location from which they arose; ductal carcinoma or lobular carcinoma, respectively. However Wellings and colleagues showed that breast cancer is mostly generated from the TDLU [41]. The demonstration of a single anatomical site of origin for breast carcinoma was followed by the proposition of a linear evolutionary pathway for breast cancer progression through which TDLUs transform into flat epithelial atypia (FEA) that give rise to atypical ductal hyperplasia (ADH) that develop into low grade DCIS (Figure 1-7). It was suggested that low grade DCIS can progress into high grade DCIS by accumulation of genetic and epigenetic alterations and therefore gain the ability to invade [41].

Lobular breast neoplasia differs from ductal types based on cell morphology. Lobular cancer consists of small, non-polarised, discohesive low-cuboidal luminal cells whereas the ductal type is composed of larger mostly polarised cells showing characteristics of low columnar cells of the duct [41, 42]. Atypical lobular hyperplasia (ALH) and lobular carcinoma *in situ* (LCIS) are

non-obligate (risk indicators) of ILC, the equivalent ductal lesions FEA, ADH and DCIS being non-obligate precursors for IDC [41].

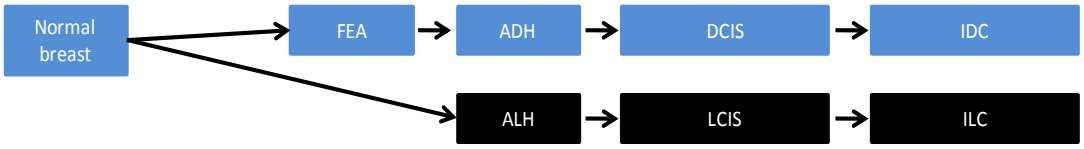

Figure 1-7: The linear model proposed for breast cancer evolution based on histomorphological characteristic. This model is now regarded as an oversimplified approach. Figure adapted from Simpson, 2005 and Sgroi, 2010 [41, 43]

It is now recognised that the linear model of breast cancer progression oversimplifies the extensive genotypic and phenotypic differences in breast cancer. An accumulating body of evidence shows that ER+ and ER- breast cancers are distinct diseases which follow two genetically distinct molecular routes; those leading to the development of low grade (well differentiated) and high grade (poorly differentiated) group of carcinomas, respectively [29, 30]. This underlines the critical role of expression of ER and activation of the ER pathway [29, 30]. In the ER^+ group the variety and number of genetic abnormalities in cancer cells are associated with the histological grade (the degree of differentiation). The ER^- group is a much more heterogenous group of lesions including the Basal and HER-2 amplified tumours.

One of the main findings supporting this proposal of two distinct disease pathways is the demonstration of the recurrent (> 80% of cases) loss of long arm of chromosome 16 (16q) in low grade DCIS and low grade invasive cancers whereas in high grade cancers, despite having a more complex genome, 16q loss is infrequent (<30%). Therefore, it was hypothesised that

the vast majority of high grade disease does not originate from low grade lesions since the regaining of a lost region of genomic material is an unlikely event. In fact, Balleine and colleagues [44] employed microarray based gene expression profiling and array based genomic hybridization techniques to establish the gene expression profile of DCIS associated with low grade and high grade invasive breast carcinoma and the DCIS classification generated relates to the coexisting invasive cancer grade. This classification clusters DCIS into low molecular grade and high molecular grade (rather than stage), again suggesting these are distinct molecular entities [45, 46].

Buerger and colleagues took a comparative genomic hybridization (CGH) approach in order to investigate specific genomic alterations in DCIS (pure or associated with invasion). 38 cases were classified morphologically as well, intermediate or poorly differentiated then microdissected and CGH was performed. A number of aberrations were observed in almost all chromosomes. They found that 16q loss is seen commonly in well and intermediate grade DCIS. Intermediate grade DCIS frequently displayed 1q gain and 11q loss. The average number of genetic imbalances (overall gains and losses) increased from well to poorly differentiated DCIS. The poorly differentiated DCIS showed frequent 1q gain and amplification of 11q, and 17q where BRCA1 gene is located. Although it has greater number of genetic imbalances when compared to well differentiated DCIS; 16q loss was very rarely detected. Interestingly, 11q amplification was restricted to DCIS associated with invasion when compared to pure DCIS. Furthermore, DCIS and the invasive compartment adjacent to DCIS are almost identical in terms

of genetic pattern. The multitude of aberrations observed in all cases identifies DCIS as a genetically advanced stage of breast cancer progression and a direct precursor of IDC [46-48].

Although ADH and low grade DCIS are immunophenotypically and genomically similar diseases, the risk of low grade DCIS to progress into invasive cancer is greater than the risk of ADH [41, 43].

Since the molecular subtypes determined for invasive breast cancer are shown to be already definable at the DCIS stage; the existence of distinct evolutionary paths for each subtype from early stages of breast cancer development can be argued. The potential ability to invade is determined already at the DCIS stage mostly through specific genetic alterations, and is preserved through breast cancer evolution [28, 49-51]

In contrast, Allred and co-workers reported that different DCIS subtypes can coexist in the same case and that the degree of diversity within cases is correlated with p53 mutation which leads to genetic instability [28]. They speculate that this implies that high grade DCIS can develop from low grade DCIS.

Taking into consideration that low grade breast cancers are strongly associated with ER positivity and ER expression is one of the features that is demonstrated to be highly preserved through breast cancer progression [52]; Natrajan et al hypothesised that if low grade tumours can develop into

higher grade than this progression should result in ER+ high grade tumours encompassing 16q loss [53]. Therefore they compared changes in 16q by microarray based CGH (aCGH) in fresh-frozen high versus low grade tumours and grouped cases according to degree of 16 q loss: 16q whole lost (16qWL), 16q partial loss (16qPL) and no loss in 16q (16qNL). Interestingly, this revealed a pattern associated with molecular breast cancer subgroups. Tumours harbouring 16qWL strongly associated with ER+ luminal phenotype, tumours with16qPL associated with Basal-like phenotype and 16qNL associated with HER-2 amplified phenotype. They found that nearly 30% of ER+ high grade tumours have 16qWL, which indicates that upgrading from low to high grade occurs uncommonly and that it occurs preferentially in tumours with the luminal phenotype. Furthermore overall genetic instability was higher in ER+ high grade tumours with 16qWL, when compared to low grade tumours with 16qWL. The authors suggested that tolerance to genetic instability, such as displaying homologous recombination DNA replication defects, which is rarely reported in low grade tumours, can drive progression from low to high grade [53]. The finding of relatively more common 16q loss in high grade luminal type tumours in comparison to low grade tumours may indicate that low grade precursors can develop into high grade luminal subtype cancer [53].

To conclude pre-invasive stages of breast cancer are non-obligate precursors of invasive breast carcinoma and they progress into grade matched invasive disease. The latter observation is translated into an alternative progression model for breast cancer in which low and high grade

cancers follow two distinct evolutionary routes, though there is some evidence to indicate that in some circumstances low grade may progress to high grade (Figure 1-8).

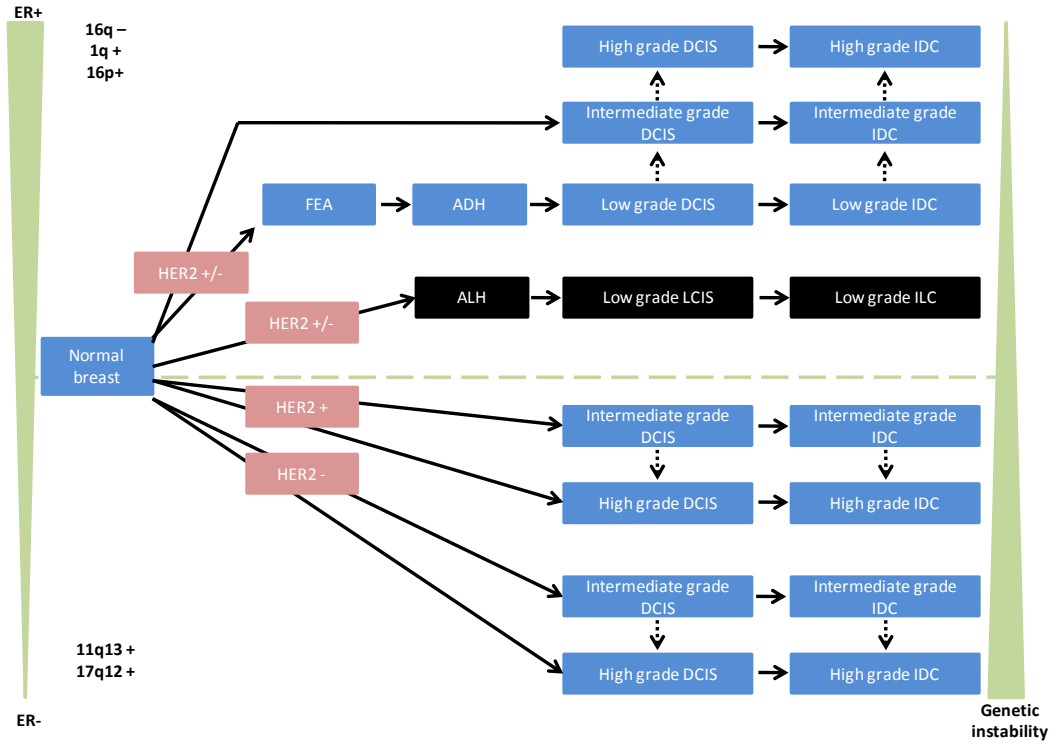

Figure 1-8: Postulated lines of progression of breast cancer. ER+ low grade breast neoplasia family: ER+ PR+ HER-2-, lack basal markers, carry diploid or near diploid karyotypes, and show 16q deletion and 1q and 16p gains. High grade breast neoplasia family: ER+/- PR+/-, HER-2 amplification, expression of basal markers and carry a complex karyotype, 11q and 17q gain. Figure adapted from Simpson, 2005 and Sgroi, 2010 [41, 43]

1.2.4 Molecular Factors Determining The Transition of DCIS to Invasive Disease

Phenotypic, gene expression and genomic studies have shown that; when matched by histological grade and ER expression, high grade DCIS and high grade invasive breast cancer show similar profiles [49, 54, 55]. Interestingly,

when focused on breast tumour cells, stage specific signatures that could be used as a marker for invasive disease progression could not be identified [49, 54, 55]. Ma and colleagues integrated laser capture micro dissection with genome wide DNA microarray analysis to identify genes differentially expressed at different stages of breast cancer progression [49]. They revealed that the pre-invasive and invasive breast cancer cells are almost identical at transcriptome level. Moreover the gene expression signatures from different stages in the same sample are more similar than the matched stage from other samples. When gene expression was examined by a function of tumour stage (ADH, DCIS or IDC) and cluster analysis was done, intriguingly, a cluster pattern corresponding to tumour grade rather than stage was revealed; low grade and high grade tumours show reciprocal gene expression signatures and intermediate grade tumours exhibit hybrid patterns of high and low grade clusters. This overlap of gene expression patterns in intermediate grade might again indicate a link of progression from low to high grade. To analyse whether there is a difference in gene expression that contributes to the transition of DCIS to IDC; expression levels of a test gene set was analysed in DCIS versus IDC. They identified a set of consistently up-regulated genes in a set of high grade IDC compared to its DCIS conponent. These were genes involved in cell cycle, centrosomal function and DNA repair, and implicate these as playing a role in the progression of high grade disease [49].

Similarly Schuetz and colleagues [56] investigated the gene expression profile of case matched DCIS and IDC samples using laser capture

microdissection and affymetrix oligonucleotide microarray analysis. In keeping with previous studies they found that matched DCIS and IDC from the same patient cluster more closely than grade matched lesions from different patients. They also revealed a group of differently expressed genes between consecutive stages. The majority of these genes are involved in cell-cell and cell-microenvironment interaction, for example matrix metalloproteinase (MMP) -11 was found to be up-regulated and BP180 (Bullous pemphigoid antigen -BPAG -1), a component of hemidesmosomes, was shown to be down-regulated in IDC.

Recently it was shown that $p16^{+}$, cyclo-oxygenase (COX) -2^{+} and $Ki67^{+}$ (triple positive) DCIS cases have a higher risk of development of subsequent invasive cancer than $p16^{-}$, COX-2^{-} and $Ki67^{-}$ cases [57].

To conclude, whilst in a subset of high grade disease, there appears to be changes in cell cycle related genes, in the majority of cases, most of the genetic aberrations of invasive breast cancer are already present in DCIS [41, 45].

1.2.5 Role of Microenvironment

The great similarity shared between DCIS and invasive tumour cells, and the association of cancer invasion with loss of an intact MEC layer and BM, prompted the hypothesis that the stromal environment could be a major component that triggers invasion, perhaps in combination with a gain of

function in malignant cells [56, 58-60]. In fact the heterogeneous nature of malignant cells is accompanied by dramatic changes in stroma such as activation and proliferation of fibroblasts, infiltration of immune cells, and angiogenesis [12, 17, 61, 62]. The accumulation of these changes leads to a tumour-favourable microenvironment termed the tumour associated stroma. In breast cancer there is a growing body of evidence that this stroma co-evolves with the tumour epithelium, even before tumour invasion occurs [17, 18, 51] and cell-cell and cell-matrix interactions between epithelia and stroma via paracrine mechanisms play a significant role in progression [51, 63]. This cross-talk includes exchange of soluble factors such as chemokines, growth factors, and MMPs between tumour and stromal cells at the host tumour interface as well as direct cell-matrix interactions [64, 65].

Normal adult tissue stroma compromises both an extracellular matrix (ECM) -structural compartment and a cellular compartment, and provides regulatory information to maintain normal tissue architecture and homeostasis. In contrast, with malignant transformation of epithelial cells this regulatory interaction is disturbed [62]. Fibroblasts are a major component of the stroma, therefore much of the evidence for tumour related changes in stroma is based on work on cancer associated fibroblasts (CAFs) [62].

A major insight into the role of CAFs came from the classic tissue recombination studies described by Olumi et al [66]. They isolated normal fibroblasts from prostate and CAFs from prostate tissue containing carcinoma. They combined either CAFs or normal fibroblasts with

immortalised prostate epithelial cells in Collagen-I and implanted these co-cultures in male mice. Those recombinants containing CAFs showed greater epithelial cell proliferation than those with normal fibroblasts and histological analysis revealed features of a poorly differentiated adenocarcinoma, with 80% epithelium and 20% stroma, in contrast to those recombinants containing normal fibroblasts which showed no evidence of tumour formation.

This indicates that CAFs significantly differ from their normal counterparts in terms of contributing towards cancer progression. Aberrant signalling derived from CAFs can interfere with the normal physiological epithelial cell-microenvironment communication [66].

Another study used a model of chemical carcinogenesis to address whether the target of the carcinogen was the epithelial or stromal compartment. Mammary epithelium was isolated from rat, cultured *in vitro* for several passages to reduce the risk of fibroblast contamination and exposed to N-nitrosomethylurea (NMU) (a model carcinogen with a short half life) or vehicle control and transplanted into the cleared fat pad of rats (hosts) which were treated with NMU or vehicle control. Tumour formation was observed only in NMU treated animals regardless of whether the injected epithelial cells were treated with NMU or control. Immunohistochemical analysis showed that all the neoplastic cells were CK positive and vimentin negative which demonstrated that tumours were of epithelial origin. This suggests that the host must be exposed to the carcinogen, with exposure of epithelial cells

alone being insufficient to generate transformation. A number of studies have started to define the characteristics of CAFs that contribute to their tumour promoting function. They show altered expression of several growth factors such as platelet derived growth factor (PDGF), insulin like growth factors (IGF) -I and II, transforming growth factor (TGF-β) -I, hepatocyte growth factor (HGF), EGF and keratinocyte growth factor (KGF) compared to normal counterparts [67].

One established paracrine interaction between CAFs and tumour cells is via secretion of CXC ligand (CXCL) -12 chemokine. This chemokine is expressed in CAFs and acts through binding to its receptor CXC receptor (CXCR) -4 which is on tumour cells and induces tumour cell proliferation [68]. It is also shown that this chemokine can promote angiogenesis by acting on endothelial cells and enhance endothelial precursor cell infiltration to tumour side. In addition CXCR4 expression is shown to be a predictor for poorer overall and disease free survival [69].

Another similar interaction is the activation of COX-2 in MCFDCIS cells in the presence of CAFs which leads to promotion from *in situ* to invasive cancer in mice (Miller et al., 2000). When CAFs and MCFDCIS cells are co-injected with a COX inhibitor, transition to invasive stage disease is completely ablated [70, 71].

One striking change in CAFs is the up-regulation of alternative spliced variants of ECM proteins such as tenascin and fibronectin [72, 73]. The

oncofetal form of fibronectin (FN-EDA) is up-regulated in the breast cancer microenvironment [72, 73] and is involved in activation of the pro-form of TGF-β which is regarded as a major pathway leading to generation of myofibroblasts from normal fibroblasts [74].

There are different explanations about the origin of CAFs [61, 64, 75]. The source of CAFs can be sustained paracrine interactions such as chronic inflammation which may lead residual fibroblasts to develop into myofibroblasts [67, 76]. Alternatively CAFs can be generated from bone marrow derived cells that differentiate into CAFs in tumour related stroma [77]. Indeed it was shown in prostate cancer that bone marrow derived progenitor cells can differentiate into stromal cells that have altered epigenetic mechanisms [78].

Microenvironment related gene expression alterations have been repeatedly reported in breast cancer [12, 51, 79, 80]. Several proteins are up-regulated in DCIS associated stroma; most notably ECM components, MMPs and cell cycle related genes. Another interesting observation is the down-regulation of cytoplasmic ribosomal proteins whereas mitochondrial ribosomal proteins are up-regulated. This decrease in cytoplasmic ribosomal proteins may cause a subtle alteration in ribosomal structure that ultimately allows the translation of proteins involved in tumour growth [51].

In keeping with gene expression changes, there are controversial data on genetic abnormalities in tumour associated stroma. Allinen and colleagues

reported that genetic changes are exclusive to tumour cells using aCGH and single nucleotide polymorphism (SNP) array approaches on isolated cell populations [8, 12-14]. Conversely; a body of evidence reports loss of heterozygosity (LOH), microsatellite instability (MSI) and point mutations related to tumour suppressor genes such as tumour protein 53 (TP53) and phosphatase and tensin homolog (PTEN) and oncogenes in tumour associated stroma. It is of note that these studies were performed on formalin fixed paraffin embedded (FFPE) tissue [81]. The techniques used in these studies, such as mutlisatellite PCR, are prone to produce artefactual results with poor quality DNA input from a limiting number of cells (or template) is employed [27, 82-84]. The reports showing somatic TP53 mutation in stroma propose that the existence or absence of this mutation in stromal cells could be used as a prognostic marker to predict nodal metastasis [85]. Despite the evidence from several other reports for TP53 mutations in CAFs [27, 85-88] no mutations have been detected in fresh frozen samples [89] and immunohistochemical analysis and SNP array showed that p53 mutation was found in only 4% of isolated primary breast cancer CAF samples [90]. In keeping with this there are also conceptual problems in understanding somatic mutation occurrence in the microenvironment. From an evolutionary point of view the function of a somatic mutation is the establishment of a selective advantage against environmental pressure, however the alterations seen in the microenvironment is for the benefit of cancer cells. In other words, if the somatic mutation model is correct therefore these changes should result in a sarcoma [75]. However CAFs do not exert *in vivo* tumourigenicity and

undergo senescence after several passages [91] but, intriguingly, senescent CAFs were shown to still be able to contribute to tumourigenesis of ovarian surface epithelial cells [92].

Stable phenotypical abnormalities in cancer related stroma may, in part, be explained by epigenetic regulation mechanisms [61, 75]. Several studies have identified distinct patterns of methylation in the stromal compartment, MEC population and epithelial cell populations, suggesting this may contribute to the generation of an altered microenvironment, though the functional significance of these changes has not been established [79, 93, 94]**.**

All cell types and ECM components of a tissue contribute distinct mechanical properties such as elasticity and stiffness. Altogether these characteristics determine the tissue response to forces. Intracellular or extracellular forces, mechanoresponsive elements and interactions with intracellular signalling pathways ultimately modulate cellular response to ECM such as adhesion and spread [95].

Microenvironment dependent physical forces in breast cancer, (ECM strength and stiffness) strongly affect the topography and hence the presentation of ligands to their cell-ECM receptors (integrins) [96-98]. This disruption of normal cell-ECM interaction can result in induction of cell proliferation and gaining of cancer related properties such as proliferation and a migratory phenotype [97, 98].

Particularly in DCIS the continuous growth of tumour cells in a confined volume (the duct) could increase cell and tissue tension [95, 99, 100]. In addition compression of an expanding tumour mass by the surrounding tissue interferes with the normal tissue architecture and may ultimately affect cell-cell junctions and hence, cellular polarisation [95]. In high grade DCIS the intratumour pressure could be further increased due to hypoxia and a central necrotic mass [101]. This increase is associated with the release and activation of several growth factors including angiogenic factors anchored in the ECM [95]. In addition the shrinkage of interstitial volume results in enhanced concentration of the growth factors [102]. In a model system it has been shown that neovascularisation enhances the interstitial flow within tumour associated stroma, which can trigger transformation of tumour stroma residential fibroblasts into myofibroblasts via TGF-β signalling [103]. Thus, the mechanical changes in the environment can contribute directly to altered function of stromal cells [102, 103]. Myofibroblasts can establish stronger adhesions and show enhanced cellular contractility which, through a positive feedback mechanism, further increases ECM tension and TGF-β activation [103]. Enhanced Collagen cross linking is one of the major factors contributing to ECM stiffness [95]. Lysyl oxidase (LOX) which has the ability to crosslink Collagen-I and ultimately stiffens the breast tissue, has been implicated in progression of breast cancer [104, 105]. Collagen crosslinking was shown to induce integrin clustering, focal adhesion maturation and consequently upregulate migration-related signalling pathways (mechanosignalling) such as phosphoinositide 3-kinase (PI3K), which results in acquisition of an invasive phenotype in breast cancer cells [105, 106]. The

mechanical properties of a tumour evolve according to the disease stage; DCIS and invasive breast cancer could differ significantly in terms of mechanical characteristics but this remains to be further studied [95, 107].

1.3 Myoepithelial Cells

1.3.1 Myoepithelial Cells in Normal Breast

A unique component of the microenvironment of DCIS is the MEC population. MECs are regarded as a hybrid cell type which exhibit both smooth muscle cell and epithelial cell characteristics. They express smooth muscle actin (SMA), smooth muscle myosin heavy chain (SMMHC) and calponin [108-110]. They also express desmosomal proteins which compose adhesive intercellular structures and attach MECs to each other and to LECs. The desmosomes that exist between a MEC and a LEC are composed of desmoglein-2 (Dsg-2) and desmocollin-2 (Dcs-2) whereas the desmosomes exist between two MECs are composed of Dsg-3 and Dcs-3. These structures have a central role in correct LEC-MEC positioning [108-110]. MEC of the normal breast are responsible for the maintenance of apico-basal polarity and hence the integrity and assembly of the LEC layer. In normal breast they are the major source of laminin-I-I-I ,which is a component of ECM, and its robust effect on correct polarisation of LECs has been demonstrated [13, 111, 112]. Moreover MECs show expression of basal cytokeratins CK5, CK14 and CK17 [113].

MECs are natural tumour suppressor cells, which are directly involved in the interaction between LECs and ECM [114, 115]. They surround LECs, produce BM [79] and secrete several tumour suppressor proteins which underline the importance of paracrine regulations in tumour suppressor function [114, 115]. They show high expression of ECM proteins, proteinase inhibitors and anti-angiogenic factors [114, 115]. Therefore not only do MECs form a physical barrier but also they are ideally positioned to direct the communication between BM and LECs; to act as a checkpoint for factors such as nutrients or growth factors secreted from or targeted to LECs and to supply signals for maintenance of normal breast tissue polarization [8, 13, 116].

MEC form the interface with the BM and in keeping with this they express high levels of BM receptors, most importantly integrins [16, 117]. MECs form unique hemidesmosomal structures in which α6β4 integrin is involved. This complex acts as a laminin-3-3-2 receptor, and therefore has a key role in attachment of MECs to BM [8, 13, 14]. The loss of HD complexes in tumourigenesis underscores the mechanism involved in the detachment of MECs from their micro-ecology.

The origin of MECs is still unclear since the phylogeny in human breast tissue is not fully understood [8, 14, 116, 118]. A stem cell which gives rise to a common progenitor of LECs and MECs was identified to exhibit cluster of designation (CD) $49f^{hi}$ (integrin α6 subunit), Epithelial cell adhesion molecule (EpCAM) $^{-}$/low, $CD24^{-}$, $CD133^{-}$, ER^{-}, PR^{-}, $HER\text{-}2^{-}$ phenotype (Figure 1-9). A

luminal progenitor can develop into a LEC or during pregnancy into an alveolar cell. There may be a distinct myoepithelial progenitor differentiated from a common progenitor or they may arise from luminal or alveolar ancestors which result in differences in cell morphology (mirroring the amount of myofilaments that exist in the cell) [13]. MECs have been shown to exhibit a CD49f^{hi}, EpCAM$^{-/low}$ basal phenotype, which shares several cell markers with mammary stem cells [14].

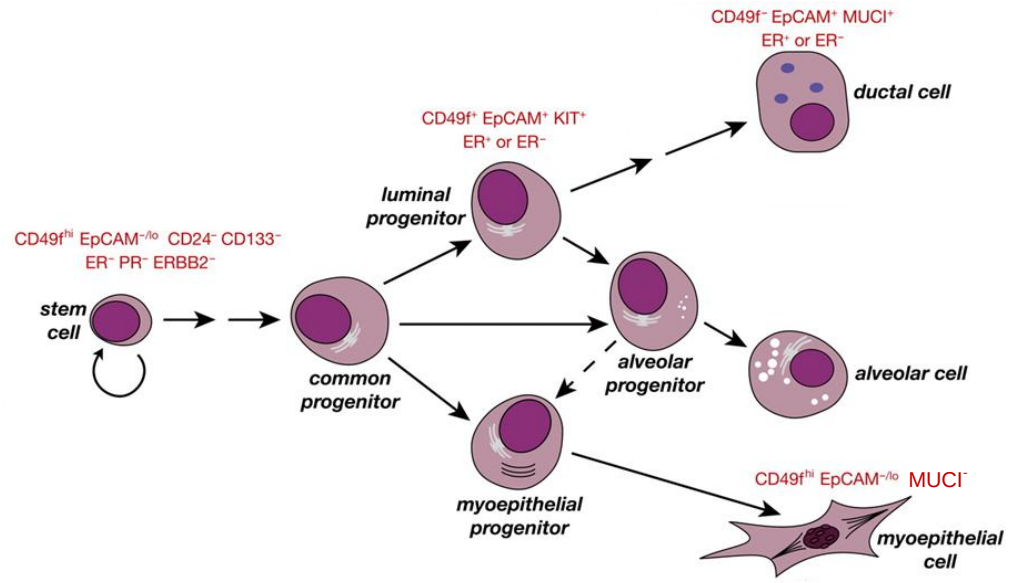

Figure 1-9: Model of phylogeny proposed within mammary epithelium. MEC layer may arise from a myoepithelial progenitor, or a luminal progenitor might develop into alveolar progenitor which can give rise to MEC [14].

In vitro and *in vivo* studies show that MECs have a central role during mammary gland morphogenesis during embryological development [13, 119]. Proteases and growth factors produced mainly by MECs are involved in ECM remodelling and can affect LEC proliferation and branching morphogenesis [120-125].

MEC rarely form tumours and those that do develop are usually benign neoplasms which show no degradation of BM [125, 126]. Sternlicht and co-workers [125] have developed MEC lines and xenografts that are derived from benign breast (and salivary gland) myoepitheliomas. MEC lines were characterized by immunoreactivity for maspin and other protease inhibitors such as plasminogen activator inhibitor (PAI) -1, similar to normal breast tissue MECs. In transwell invasion assays these cell lines inhibited melanoma and breast cancer cell invasion, partly by a maspin dependent mechanism. Furthermore, the matrix generated from the xenografts (Humatrix), composed of both BM and non-BM components, down-regulated cancer cell invasion compared to Matrigel. Similarly, conditioned media from MEC lines was sufficient to show an invasion suppressor effect in transwell assay. Moreover Humatrix abolished (melanoma) tumour invasion and metastasis *in vivo* [125].

Jones and colleagues [117] investigate the interaction of MECs with breast cancer cells and fibroblasts in transwell invasion assays. Normal MECs and fibroblasts were isolated from reduction mammoplasty tissue. MECs were characterised by expression of myoepithelial markers such as β4 integrin, CK-14, Common acute lymphoblastic leukemia antigen (CALLA) and Dsg-3, and lack of expression for luminal associated proteins such as CK-18 or EMA, whereas fibroblast populations were negative for these markers by IHC or at mRNA level. When MECs were co-cultured with a panel of ER positive or ER negative breast cancer cells in transwell invasion assays the breast cancer cell invasion was negatively regulated compared to baseline levels, in

contrast when fibroblasts were co-cultured with breast cancer cells the invasion was increased. Interestingly when three cell populations were cultured the invasion was down-regulated indicating a dominant suppressor role for MECs. In addition when conditioned media collected from MECs were substituted for the MEC population it was sufficient to reproduce similar results. This supports the importance of secreted factors in the tumour suppressor role of MEC. Moreover when fibroblasts or breast cancer cells were co-cultured with MECs; this resulted in a consistent decrease of MMP expression and activity. This might in part explain the invasion suppressor role of MECs to modulate fibroblast or cancer cell function [117].

Another tumour suppressor protein expressed by MECs is maspin which is a serine protease shown to inhibit tumour growth, invasion and metastasis [8, 127, 128]. MECs also express p63 and p73 which play central roles in the control of cell growth and survival [113]. Other examples of suppressor proteins include tissue inhibitor of metalloproteinase-1 (TIMP-1) which decreases invasion and CD44 which blocks adhesion and migration of human malignant cells *in vitro* [114, 115]. MECs can control steroid hormone metabolism within breast tissue by their ability to express steroid sulphatase (STS) and process inactive precursors which are therefore available for LECs as active steroid hormones [8, 129].

MECs can also modulate cell proliferation. Their ability to induce growth arrest (G_2/M status) in breast cancer cells has been demonstrated [128]. In addition, Hu and co-workers used MCF10ADCIS.com cells to resemble

human breast cancer to investigate the importance of MECs in disease progression. *In vivo* these cells give rise to comedo DCIS-like structures; surrounded by a cell layer which shows positivity for MEC markers (such as CALLA and p63) and BM rich in laminin-3-3-2, which can spontaneously develop into invasive tumours. When MCF10ADCIS.com cells are co-injected into mice with normal primary MECs or MECs isolated from a normal cell line, they develop smaller tumours (compared to MCF10ADCIS.com cells alone) than when injected together with fibroblasts derived from invasive breast carcinoma or rheumatoid arthritis. When all three cell groups were injected together smaller tumours developed, once again showing the dominant suppressor effect of MECs over both tumour cells and fibroblasts. Histology of the tumours also differed between different co-injection groups; MCF10ADCIS.com alone or together with normal MECs formed DCIS-like lesions while all the fibroblast co-injections (including fibroblast derived from normal breast tissue) resulted in invasive tumours. Intriguingly the differences observed in tumour growth or histology were not a result of permanent genetical alterations in the tumour cells since when MCF10ADCIS.com cells of invasive tumours were isolated and injected alone in mice again they generated DCIS structures [130].

1.3.2 Myoepithelial Cells in DCIS

During the development and progression of DCIS, MECs undergo several dramatic alterations which potentially could result in compromised suppressor function [79]. Gene expression and epigenetic profiles demonstrate that DCIS associated MECs exhibit a phenotype distinct from normal MECs [79]. In DCIS, MECs appear to show reduced differentiation [12, 79, 93, 131]. In addition epigenetic analysis has revealed distinct methylation profile alterations [93].

DCIS associated MECs up-regulate genes involved in promoting proliferation, migration, invasion and angiogenesis, whereas they show reduced expression of genes coding for certain tumour suppressor proteins also genes involved in the normal function of the cell such as thrombospondin and oxytocin receptor [79].

One of the most notably over-expressed proteins in DCIS associated MECs is the chemokine CXCL14 which can bind to leukocytes as well as LECs, and has previously been shown to influence cell proliferation, differentiation, migration and invasion [12]. Furthermore MECs in DCIS have been shown to increase MMP expression especially MMP-14, and cathepsin secretion which may aid ECM degradation [79].

Consistent with the gene profiling studies, DCIS associated MECs exhibit alteration in many markers; reduced immunohistochemical staining has been

shown for SMA, Calponin, CALLA, CK 5/6, p63 and a dramatic loss in SMMHC in DCIS associated MECs in comparison with the normal MECs of the same breast [131]. These differences again indicate that MECs are losing normal cell function.

One consistent change in DCIS-associated MECs noted in our lab is the up-regulation of αvβ6. This has been shown to activate TFG-β and leads to up-regulation of MMP-9 in MECs, which promotes tumour cell invasion [132, 133].

In DCIS, focal disruption of the intact MEC layer leads to rearrangement of normal tissue boundaries and is accompanied by BM breakdown [59, 60]. The focal loss of the intact MEC layer and consequent aberrant exposure of DCIS tumour cells to ECM was extensively studied by Man et al. They showed that the cancer cells in juxtaposition to the MEC layer disruption become invasive and show dramatic reduction in ER expression and LOH at different chromosomal loci including the Wilm's tumour suppressor (WT) -1 gene [59, 60]. They also up-regulate invasion and metastasis related gene expression. In addition an increased level of leukocyte infiltration was observed around disrupted MECs [59, 134]. The implication is that the loss of the MEC results in acquisition of the tumourigenic phenotype in adjacent cells.

1.4 Matrix Metalloproteinases

1.4.1 Classification and Roles in Cancer

The protease clan compromises 5 classes: Metalloproteinases, serine, cysteine, threonine and aspartic proteases [135]. MMPs are a large family of endopeptidases which have the ability to remodel ECM and are up-regulated in many cancers, such that the MMP family is conventionally regarded a key factor contributing to the process of cancer cell invasion and metastasis [22, 136-141]. In addition to remodelling ECM they can process many non-structural substrates such as cytokines and growth factors and influence cell proliferation, differentiation, angiogenesis and apoptosis [142-144], thus they impact on a diverse range of biological processes [22, 139, 145].

MMPs belong to the metzincins super-family which also includes 'a disintegrin and metalloproteinases' (ADAMs) and 'a disintegrin and metalloproteinase with thrombospondin motifs' (ADAMTSs) members. In humans there are 24 MMP genes, including duplicated MMP-23 genes. The total set of proteases expressed in human tissues and cells is called the human degradome and contains 569 enzymes. This information comprises 1.7% of the human genome [146, 147].

MMPs share common structural features [140]. From the N to C terminus (Figure 1-10 A); MMPs have a signal peptide involved in secretion, a prodomain which contains a cysteine residue, a catalytic domain which

contains a zinc (Zn) ion, a linker hinge region and a haemopexin domain that confers substrate specificity [140, 145, 148, 149]. MMPs become activated in a process called the cysteine switch. The interaction between the cysteine residue and the zinc ion allows the enzyme to stay in the latent phase by stopping a water molecule necessary for catalysis from binding to the zinc atom. This link needs to be interrupted for activation either by complete removal of the prodomain or chemical alteration of the cysteine residue to release active enzyme [13, 139, 140, 150, 151]. MMPs can be activated extracellularly by other MMPs, serine proteases such as plasmin or reactive oxygen species (ROS). An alternative intracellular activation can also occur by furin, but the intracellular roles of MMPs remain elusive [145].

MMPs are traditionally classified according to their substrate specificity and structure into 5 main categories (Figure 1-10 B) [140, 145]:

1. Collagenases: This family contains MMP-1, MMP-8 and MMP-13. They can process interstitial fibrillar collagens; Collagen-I, II and III into ¾ N terminus and ¼ C terminus fragments which denaturate to gelatine spontaneously, and also can cleave other ECM proteins (such as gelatine) and non structural substrates such as interleukin (IL) -10 [145, 152, 153]. The haemopexin domain has been shown to facilitate collagen cleavage by controlling binding and mediating the unwinding of the triple helix structure [154, 155]. Collagenases are involved in embryonic development, tissue regeneration and wound repair. There are many links between collagenases and cancer. MMP-1 is the first identified MMP

[156] and its over-expression has been shown to be related to increased metastasis to bone in breast cancer and poor prognosis in breast cancer as well as colorectal cancer and malignant melanoma [157, 158]. MMP-13 expression is restricted to a few physiological conditions involving extensive collagenous ECM remodelling such as fetal bone development [159]. Over-expression of MMP-13 is seen mainly in squamous cell carcinoma of head and neck and correlates with invasion and metastasis [152].

2. Gelatinases: This family contains MMP-2 and MMP-9. They carry three fibronectin type II repeats which mediate binding to their substrate gelatin [160]. They can also process Collagen-IV and to a lesser Collagen V and XI, laminin and aggrecan. MMP-9 can convert cryptic vascular endothelial growth factor (VEGF) into its bioavailable form for its receptor (VEGFR) [140, 145]. The gelatinases have frequently been implicated in cancer [161-169]

3. Stromelysins: The members of this family are MMP-3, MMP-10 and MMP-11. They are structurally similar to collagenases but they do not have the ability to cleave interstitial collagens. MMP-3 and MMP-10 are involved in proMMP activation (including MMP-8), and MMP-11 cleaves serpins, and also can be activated intracellularly via a furin recognition sequence, but the intracellular function of this enzyme is unknown [140, 152].

4. Matrilysins (Minimal domain arrangement): This family consists of MMP-7 and MMP-26. MMP-7 is involved in apoptosis by processing Fas ligand and pro tumour necrosis factor (TNF) -α, and interacts with E-cadherin [139]. Unlike most of the members of the MMP family MMP-26 can be stored mainly intracellularly and secreted upon exposure to appropriate stimuli [140, 152].

5. Membrane Type MMPs (MT-MMPs): This family contains four transmembrane enzymes MT1-MMP, MT2-MMP, MT3-MMP, MT5-MMP (MMP-14, 15, 16 and 24) and two glycosylphosphatidylinositol (GP)-anchored enzymes MT4-MMP MT6-MMP (MMP-17 and 25). They all have a furin recognition motif therefore can be activated intracellularly. Their main function is to activate other MMPs, localising proteolytic activity to the cell membrane [140, 152]. MT-MMPs can also regulate cytokine function [140, 152].

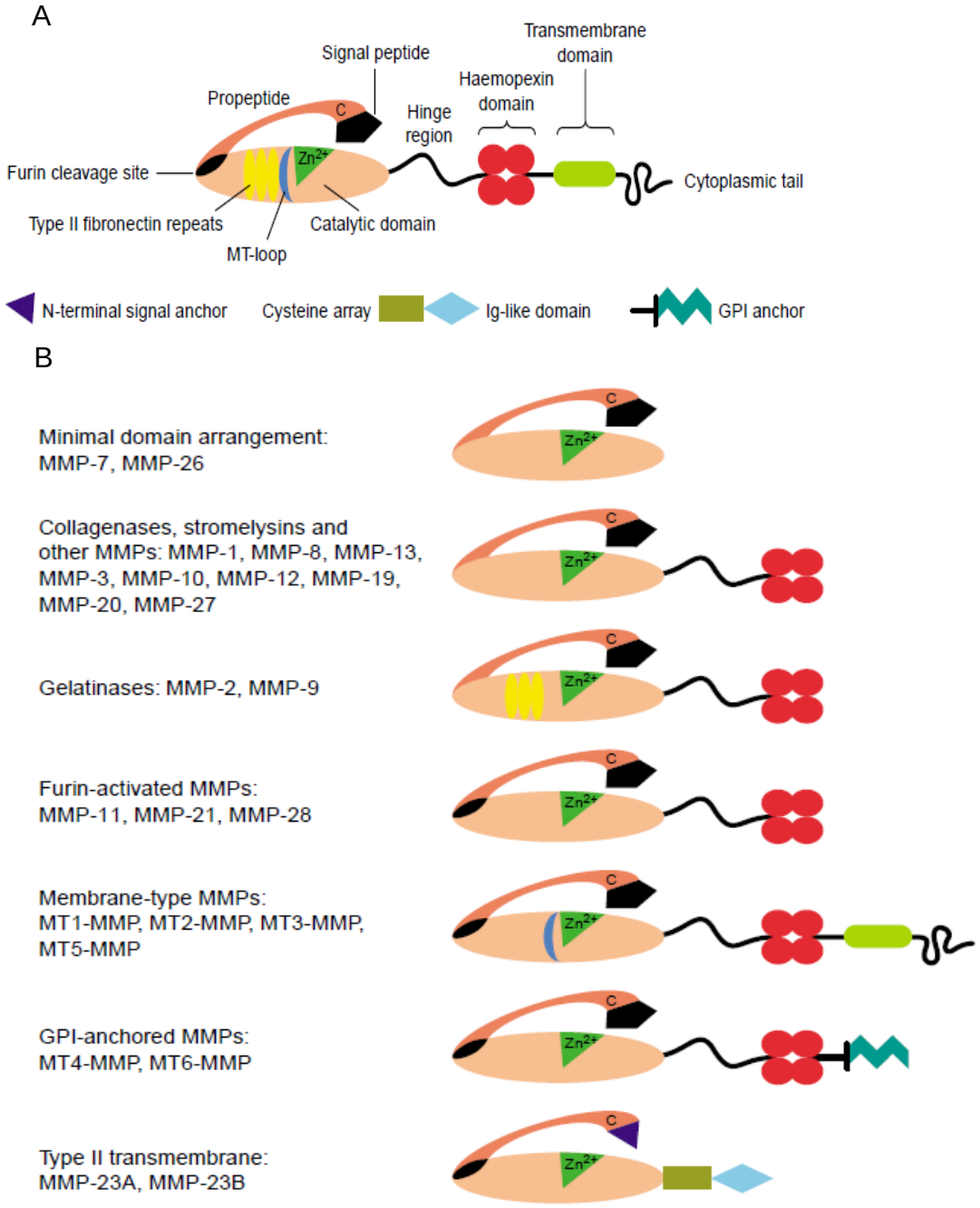

Figure 1-10: Structural characteristics and classification of MMPs. A Structural features of MMPs. All MMPs have a signal peptide, a propeptide and a catalytic domain. All regions that vary between different subgroups are shown. B The classification of MMPs, which is based on structure. Other than MMP-7,MMP26 and MMP-23A/B all MMPs have a haemopexin region, MT-MMPs contain a transmembrane domain and a cytoplasmic tail or a GP anchor. Gelatinases have fibronectin type II repeats and MMP-23 possess an Ig-like domain. Figure extracted from Lafleur et al., 2003 [140].

MMP function can be regulated in four main ways: transcriptional and translational regulation [170], compartmentalisation, proenzyme activation and through endogenous inhibitors –TIMPs [139]. Transcriptional control is the major physiological mechanism since most of the MMP family share common cis-acting elements which in part explain their co-activation and co-repression upon various signals [149, 171].

In humans there are 4 TIMPs [172]. TIMP-1, TIMP-2, and TIMP-4 are soluble proteins whereas TIMP-3 is anchored to ECM [140, 145]. They contain 184-194 amino acids and have a rather simple structure with an N-terminus domain which is responsible for inhibitory function and a highly variable C-terminus domain [140, 145]. TIMPs have a “wedge like” shape and form a non covalent complex with their binding partners in a 1:1 stoichiometry via the N terminus [145]. This contact interferes with the catalytic site of MMP and inhibits its function. The roles of TIMPs are more complicated than a simple inhibitory function, also their interaction with substrates other than proteases is not precisely known [140, 145]. TIMPs are also shown to be up-regulated in many cancer conditions. This apparent contradiction reflects the limitations in knowledge of TIMP function and raises the question whether increased activity of MMPs is due to up-regulation of MMP or deregulation of inhibitors [22].

Given the central roles of MMPs in BM penetration, this family is a promising target for anti-cancer therapy. The main support for the association of MMPs with cancer progression comes from *in vivo* studies [165]. As an example

MMP-1 has been shown to control the metastatic activity of breast cancer cells. When MMP-1 expression is knocked down in MDA MB 231 cells and then implanted in mice by tail vein injection, this results in reduced lung metastatic capacity [173]. Tester and co-workers generated proMMP-2 over-expression in MDA MB 231 cells which endogenously express the proMMP-2 activator MT1-MMP. When these cells were injected into the mammary fat pad of nude mice, orthotopic tumour growth was enhanced compared to vector control. Also metastasis to brain, liver, bone and kidney was enhanced after intracardiac inoculation [161].

It has recently been recognised that MMPs can exert tumour suppressor functions [135, 147, 174-176]. Broad range MMP inhibitors (MMPIs) can counterbalance the host protective effects of MMPs. Therefore anti-target MMPs should be identified and trials need to be tailored carefully to avoid targeting these MMPs. Furthermore the same MMP can act both as a target and an anti-target at different stages of a disease as shown by *in vivo* studies [135, 147, 174-176].

There is a growing body of evidence to show that MMPs can be involved in early stages of breast cancer progression [177]. For example; in the mouse mammary tumour virus (MMTV) driven breast carcinoma model, MMP-11 knockout mice generated fewer spontaneous tumours compared to wild type (WT) counterparts [178]. Similarly MMP-7 over-expression in the MMTV system leads to development of mammary hyperplasias, and increased the rate of tumour formation [179].

MMP expression has also been associated with the progression of breast cancer. Gene expression levels of MMP-1 and MMP-9 make up part of the 70 gene signature that predicts distant metastasis in lymph node negative breast cancer [162]. High levels of MMP-1 in fibroblasts detected by IHC staining correlates with a high rate of distant metastases [180]. Interestingly MMP-1 expression in patients with ADH can be used as a predictive marker for developing breast cancer [181]. High MMP-9 expression in the stromal compartment and in mammary tumour cells also is associated with poor prognosis [163]. Similarly a general increased expression of MMPs in stroma (fibroblasts and macrophages) including MMP-1,7,9,13 and MT1-MMP correlates with higher risk of distant metastasis [180]. An enhanced ratio of MMP-2/TIMP-2 or MMP-9/TIMP-1 also has been associated with lymph node metastasis and poor prognosis [164].

Other evidence suggests a more complex role for MMPs in tumour progression. MMP-9 plays a dual role in angiogenesis. MMP-9 is a key element in the angiogenic switch in pancreatic carcinoma [167]. MMP-9 null mice show reduced tumour growth and neovasculature [167]. Conversely plasminogen degradation by MMP-3, 7, 9 and 12 can produce angiostatin which is an anti-angiogenic factor [168]. In addition MMP-7 and MMP-9 over-expression, in an integrin α1 knock out system, can reduce angiogenesis and tumour growth *in vivo* [169].

Furthermore, depending on tumour stage, MMP-9 can exhibit both anti and pro-tumourigenic function [165]. In a human papilloma virus (HPV) -16 multistage skin carcinogenesis model, mice lacking MMP-9 (HPV16/MMP-9$^{-/-}$) generated fewer tumours and exhibited an extended latency period when compared to HPV16/MMP-9 proficient mice. However when these tumours were assessed for differentiation, using CK as a phenotypic marker, it was revealed that in MMP-9 null tumours keratinocytes were less differentiated, which is an indication of more aggressive behaviour. Interestingly in MMP-9 proficient tumours, MMP-9 expression is restricted to infiltrating immune cells such as neutrophils, macrophages, and mast cells whereas the tumour cells were negative [166].

MMP-12 plays an anti-angiogenic role via cleavage of plasminogen generating angiostatin [182]. In fact MMP-12 over expression in melanoma cells reduced tumour growth and vascularisation [182] and in colorectal carcinomas is correlated with increased survival [183]. However, there is evidence of tissue specificity since in other carcinomas such as non small cell lung cancer it associates with worse prognosis [184]. It is of note that the source of MMP-12 is also important; when it is expressed by stromal cells it is favourable but when tumour cell derived MMP-12 appears to confer a poor prognosis [185, 186]. Further, MMP-12 was also shown to be involved in urokinase-type plasminogen activator receptor (uPAR) processing [187].

TIMP-1 levels can be a marker of good or poor prognosis and better understanding of its dual role is needed [188]. Plasma levels TIMP-1 in

patients with metastatic breast cancer were evaluated by ELISA and higher levels of TIMP-1 correlated to reduced survival [189]. Interestingly high TIMP-3 mRNA levels in breast tumours indicate good prognosis and longer disease free survival [188]. Conversely TIMP-3 levels have been shown to be elevated in dense breast tissue which carries higher risk for breast cancer development compared to non-dense breast [190]. It is also of note that TIMP-3 expression is absent in the normal breast epithelial compartment and tumour cells of DCIS but highly up-regulated in myofibroblasts and MECs surrounding the DCIS [12].

Several MMP inhibitors have reached phase III clinical trials, but nevertheless have failed to show any significant effect on patient survival [147]. The failure of broad spectrum MMP inhibitors (MMPI) in anticancer trials suggests an incomplete understanding of the complex function of this family; of precisely when and how they act in cancer [22, 138-140]. This may also be affected by the tumour suppressor function of some MMPs [146]. The majority of MMPI act via chelating the Zn ion which is a consensus structure for proteases [147]. Therefore these inhibitors can target ADAMTSs as well, which considering their anti-cancer function, should be avoided [191-197]. Moreover, targeting one MMP can influence other MMPs being activated or inhibited by the target, or a feedback loop to compensate the target MMP can be triggered [146, 147]. In addition the administration of MMPIs to patients with advanced cancer might not have a significant effect on prognosis considering the role of MMPs in early cancer stages [174, 177].

Taken together it is clear that MMPs can have stage- and source-specific functions. This spatiotemporal change in MMP activity may be in part explained by the availability of specific substrates at a particular site of MMP expression [175]. Therefore identification of the substrate repertoire for each MMP will contribute to a better understanding of the protease web, and potentially lead to more informed development of MMPI [175].

1.4.2 Matrix Metalloproteinase-8

MMP-8 (also known as neutrophil collagenase or collagenase-2) is the second member of the collagenase family of MMPs. Although MMP-8 was originally reported to be expressed exclusively by neutrophils, where it locates to specific granules and is secreted upon neutrophil activation [198, 199], it has become evident that it can be produced by many other cell types including endothelial cells, odontoblasts, and benign and malignant keratinocytes [175, 200, 201]. The gene is located to the telomeric site of chromosome 11 with the other members of the collagenase family [152].

MMP-8 preferentially targets Collagen-I; to a lesser extent it can cleave Collagen-III and Collagen-II [202]. Collagens are the main component of the ECM with Collagen-I being the major collagen. These molecules have three α-chains and form a triple helix. Collagen-I is cleaved at Gly^{775}- Ile^{776} residues of the α1 chain and Gly^{775}- Leu^{776} residues of α2 chain. This cleavage yields to ¾ N-terminal and ¼ C-terminal fragments [202]. These

fragments spontaneously denature to gelatine at body temperature as previously described [152].

MMP-8 shows an archetypal structure, like other collagenases it consists of a signal peptide, a propeptide, a catalytic domain, a hinge region and a haemopexin like domain [140]. It is secreted as an 85kDA inactive form [152] and can be activated extracellularly by other MMPs such as MMP-3 and MMP-10 [203, 204]. The activated MMP-8 form varies in molecular weight depending on its cellular source [205, 206] which may reflect the degree of glycosylation levels [201]. MMP-8 has 6 different glycosylation sites and enhanced glycosylation may block its secretion and be associated with its storage in the intracellular granules [201]. In addition, an alternative 870bp splice variant of MMP-8 has been identified which has an extra exon of 91bp between residues 174 and 175 and lacks the signal peptide. The function of this form is not known [207].

There is accumulating evidence that MMP-8 acts as a tumour suppressor since the demonstration that MMP-$8^{-/-}$ male mice exhibit increased incidence of skin tumours in a chemically induced carcinogenesis model system [208]. The progression rate of these benign lesions to malignancy did not differ between MMP-8 null or WT mice, which implies that MMP-8 is particularly involved in suppression of early stages of tumourigenesis [208]. Similarly in MMP-$8^{-/-}$ mice subjected to Methylcholanthrene (MCA), as a different model of chemically induced carcinogenesis, the rate of development and the number of fibrosarcomas were significantly enhanced compared to WT

littermates [208]. Since there was no difference in MMP-8$^{-/-}$ female mice and WT mice; in order to understand the action of sex hormones the ovaries of female mice were removed, or alternatively, the mice were treated with tamoxifen. In these cases MMP-8$^{-/-}$ female mice showed significantly higher susceptibility to develop skin tumours when exposed to 7,12-dimethylbenz[a]anthracene (DMBA) and 12-O-tetradecanoyl-phorbol-13-acetate (TPA). Thus ovarian-derived oestrogen might have a protective role on tumour development in this system [208]. Moreover bone marrow transplantation from WTmice to MMP-8$^{-/-}$ mice was sufficient to rescue the expression of MMP-8 in (bone marrow derived) neutrophils and the susceptibility of MMP-8$^{-/-}$ mice to tumourigenesis after exposure to MCA [208].

Histopathological analysis of skin tumours or wounds in MMP-8 null mice revealed that the lack of MMP-8 down regulates early neutrophil infiltration to the wounded skin site (determined by Ly-6G neutrophil marker immunostaining) and delayed wound closure, but once the immune response is established it is abnormally sustained in wounds and skin tumours [208, 209]. The delay in early response may in part be due to the reduced ability of leukocytes to migrate towards the tumour or inflammatory site without MMP-8 dependent activity against Collagen-I [208-210].

Importantly, a non-matrix substrate of MMP-8 has been identified [208]. A chemoattractant - lipopolysaccharide induced CXC chemokine (LIX) (IL-8 and CXCL5 murine homolog), which is involved in the chemotaxis of

polymorphonuclear cells (PMNs), was shown to be cleaved at Ser^{4}-Val^{5} and Lys^{79}-Arg^{80}, and subsequently activated by MMP-8 [208, 211, 212]. The resultant processed form exerts enhanced chemotactic activity on neutrophils. Therefore the absence of MMP-8 dependent activation of LIX, may result in reduced PMN cell influx. The sustainment of the late immune response was, however, explained by a defective apoptosis mechanism in neutrophils [213]. It was hypothesised by the authors (Balbin et al., 2003) that the persistent accumulation of infiltrating leukocytes may result in chronic inflammation through generation of ROS, which in turn may interact with DNA in proliferating epithelium resulting in permanent genomic alteration and instability which predisposes to tumour development. This hypothesis might in part explain the link between MMP-8 loss and cancer development via chronic inflammation [139, 214].

Furthermore, evidence for a tumour suppressor role for MMP-8 was provided by Gutierrez-Fernandez and co-workers who over-expressed MMP-8 in B16F10 melanoma cells and inoculated these cells in MMP-$8^{-/-}$ back crossed C57BL/6 mice (with an intact immune system) via the lateral tail vein to study metastasis formation [215]. MMP-8 over-expression significantly down-regulated lung metastasis formation (size and number) compared to Empty vector transfected B16F10 cells. Interestingly, over-expression of an inactive form of MMP-8 in B16F10 cells was unable to suppress metastasis, indicating the involvement of enzymatic activity in the metastasis protective function of MMP-8 [215]. Furthermore, MMP-8 expression did not alter B16F10 cell proliferation *in vitro*, or tumour weight *in vivo* when B16F10 cells

were injected sub-cutaneously. In addition MMP-8 over-expressing B16F10 melanoma cells showed reduced invasion *in vitro* in Matrigel-coated Boyden chamber assays, and decreased transmigration through human unbilical vein endothelial cell (HUVEC) monolayers compared to the control tranfection group. In addition when neutrophils from MMP-$8^{-/-}$ mice were isolated and a transwell invasion assay was set up, these neutrophils showed reduced invasion when compared to the invasion of neutrophils isolated from WT mice. Interestingly MMP-8 transfected B16F10 cells adhered more strongly to Collagen-I and spread more on laminin-I-I-I than Empty vector transfected cells, suggesting that MMP-8 modulates adhesion and spreading on ECM [215].

In order to explore the role of host derived MMP-8 rather than tumour derived MMP-8; B16F10 (parental) cells were injected tail veins of MMP-$8^{-/-}$ or WT mice to investigate experimental metastasis. There was a significant increase in the number of lung metastasis in MMP-$8^{-/-}$ mice when compared to WT mice. In order to assess spontaneous metastasis formation, Lewis lung carcinoma (LLC) cells were injected sub-cutaneously to MMP-$8^{-/-}$ or WT mice. There was no difference on primary tumour growth but MMP-8 deficient mice developed significantly increased number of lung metastasis which shows that host derived MMP-8 can also contribute to metastasis protective function [215].

MMP-8 expression has also been shown to correlate with improved survival in patients with squamous cell carcinoma (SCC) of the tongue [198, 216,

217]. To evaluate the suppressor role of MMP-8 Korpi and colleagues used a chemical induced model of tongue SCC by exposing MMP-$8^{-/-}$ or WT mice to 4-Nitroquinoline 1-oxide (4NQO). Female MMP-8 null mice were significantly more susceptible to SCC than WT mice [216]. This is in contrast with the hypothesis of Balbin and colleagues that ER might play a protective role in tumour formation in MMP-8 deficient system [175] but may indicate site-specific differences. Korpi et al also showed that MMP-8 can cleave ER-α in a dose dependent manner [216]. The MMP-8 promoter does not contain an ER response element, however it includes CCAAT/enhancer-binding protein-β site (C/EBP) element which has been shown to associate with ER-α. This complex can act as a transcription factor [152, 216, 218]. Therefore, in the future detailed studies scoping the interaction of MMP-8 with the ER pathway would be warranted.

In contrast to tumour suppressor function; in head and neck squamous cell carcinoma and ovarian carcinoma, MMP-8 expression was associated with the presence of metastasis [200, 219]. Polymorphism in the MMP-8 gene (MMP-8 78K/E) is associated with increased bladder cancer risk [220], and in pancreatic cancer MMP-8 has been shown to be up-regulated [221] and demonstrated to cleave the C terminus of Eph receptor ligand, Ephrin B1, which makes pancreatic cancer cells more invasive [222, 223]. Thus MMP-8 appears to have different functions in different settings.

Macrophage inflammatory protein-1α (MIP-1α) has also been identified as a non-matrix substrate of MMP-8 [209, 224], and MMP-8$^{-/-}$ mice also showed down regulation of active TGF-βI and reduced activation of IL-10 [153].

Mutational analysis in malignant melanoma identified a number of frequent mutations in MMP-8 which were accompanied with LOH and reduced Collagenolytic activity [217]. Based on the nonsynonymous to synonymous mutation ratio, these mutations are identified as driver mutations. The mutated forms or WT MMP-8 was stably over-expressed in Mel-STR human melanocytes. The WT but not the mutated forms significantly blocked anchorage independent colony growth in soft agar colony formation assays *in vitro*. *In vivo*, Mel-STR cells over-expressing WT MMP-8 when injected subcutaneously into Non obese diabetic/severe combined immunodeficiency (NOD/SCID) mice did not form ulceration (an indicator of aggressiveness of melanoma) or lung metastasis whereas cells expressing mutated MMP-8 developed numerous lung metastases though no difference in primary tumour growth rate, once again demonstrating the suppressor role of MMP-8 on metastatic potential [217]. In keeping with the reduced enzymatic activity in the mutated forms this study once again implicates the role of enzymatic action in its biological role. According to recent findings whether the loss of tumour suppression depends on the absence of WT MMP-8 or presence of mutant MMP-8 is not clear [225]. To date, no such mutations have been reported in breast cancer or its microenvironment.

Gutierrez-Fernandez and colleagues demonstrated the formation of specific MMP-8/MMP-9 complexes in isolated bone marrow cells of WT mice (this complex did no longer exist in bone marrow cells of MMP-8 knockout or MMP-9 knockout mice). The biological significance of these complexes is under investigation but binding of MMP-8 might change activity of MMP-9 and vice versa [209].

Recently it was reported that over-expression of catalytically active MMP-8 enhanced expression of IL-6 and IL-8 in a number of breast cancer cell lines including MDA MB 231 and MCF-7 but not in the non-cancerous mammary epithelial cell line HMT-3522 S1 [212]. This effect may involve nuclear factor-κβ (NF-κβ) signalling since a pharmacological inhibitor of NF-κβ significantly down-regulated the IL-6 and IL-8 secretion. In contrast, MMP-8 WT over-expressing MDA MB 231 cells reduced colony formation *in vitro* compared to Empty vector or inactive MMP-8 over-expressing cells. Furthermore treatment of parental MDA MB 231 cells with recombinant IL-6 significantly induced MMP-8 expression, which indicates an immunomodulatory circuit generated in this system [212].

Previous work from our own lab has shown that the expression of MMP-8 in normal breast is almost exclusively restricted to the MECs (Figure 1-11) [215]. The expression of MMP-8 by MECs shows a gradual loss through cancer progression which correlates with their loss of suppressive activity [215]. When total mRNA was isolated from invasive breast cancers and an RT-PCR approach was taken, invasive breast cancers showing expression

of MMP-8 were associated with lower lymph node metastasis and good prognosis [215]. In addition four SNPs have been identified for MMP-8 in breast cancer patients and the T allele (minor allele) is once again associated with reduced risk of lymph node metastasis [226].

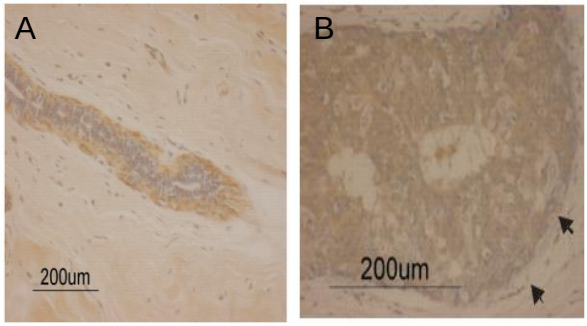

Figure 1-11: MMP-8 localisation in normal breast versus DCIS. A: Localisation of MMP-8 staining to MEC-BM interface in normal breast, B: Diffuse cytoplasmic staining of neoplastic cells and loss of MEC-BM staining in DCIS (arrow heads) [215].

To conclude, the mechanism by which MMP-8 acts as a tumour suppressor in normal breast is not fully understood, and the biologic significance of its loss in MECs during DCIS progression remains to be elusive.

This project is focused on the interaction of the microenvironment with the cancer cell, particularly on the paracrine interaction between MECs, LECs and stroma via MMP-8 and loss of this mechanism in DCIS.

1.5 Integrins

1.5.1 Classification

Integrins are a superfamily of transmembrane cell adhesion molecules which can directly bind components of ECM and act as a transmitter between the external environment and cytoskeleton to supply traction for cell migration and invasion [227]. Integrins consist of heterodimers of distinct α and β subunits in various combinations. In humans, at least 18α and 8β subunits form 24 heterodimers which have distinct but partially overlapping ligand repertoire (Figure 1-12) [227, 228]. The extracellular part of each subunit generates a specific surface for ligand binding. Most integrins have a short cytoplasmic domain comprising less than 75 amino acids; the β4 integrin subunit is unique in having a cytoplasmic domain of 1000 amino acids. The β integrin cytoplasmic tail has a tyrosine residue, the phosphorylation of this residue can result in various responses in integrin function (Figure 1-13) [227, 228]. Upon ligation to ligand, integrins cluster in the cell membrane, α and β units show conformational change and recruit adaptor molecules such as talin which binds and therefore provides connection to the actin cytoskeleton, and signalling molecules such as focal adhesion kinase (FAK) which acts as a phosphorylation-regulated bridge for Src family kinases (SRKs) and facilitates assembly of focal adhesion structures. Recruitment of FAK activates signalling through several pathways such as PI3K, Rac, NFκβ and ERK/MAPK [229]. Focal adhesions are dynamic structures that transduce the outside information such as differences in extracellular forces

or ligands into the cell in a mechanism known as outside-in signalling. Divalent cations exist in the matrix microenvironment and are involved in initial cell-ECM engagement. Both extracellular integrin subunits have cation binding sites; cations such as calcium (Ca^{++}), magnesium (Mg^{++}), and manganese (Mg^{++}) are required for formation of the tertiary structure of integrin-ligand complexes, and an abundance of divalent cations can influence integrin binding affinity [227, 230].

Integrin affinity can be also regulated by inside-out signaling that controls integrin activity. The binding of talin to β integrin cytoplasmic tail triggers the disassociation of α and β cytoplasmic units and straightens the folded extracellular integrin structure. These conformational changes in extracellular regions result in increased ligand affinity [227, 230].

The repertoire of integrins on the cell surface dictates ECM sensing and response, as well as modulating signalling pathways involved in cell behaviour such as proliferation, survival, adhesion, and motility on different substratum [227, 230].

Some integrins, such as β1, are ubiquitously expressed whilst others are restricted to defined cell types, for example, α6β4 is expressed in basal cells at the cell-BM interface, including keratinocytes and MECs.

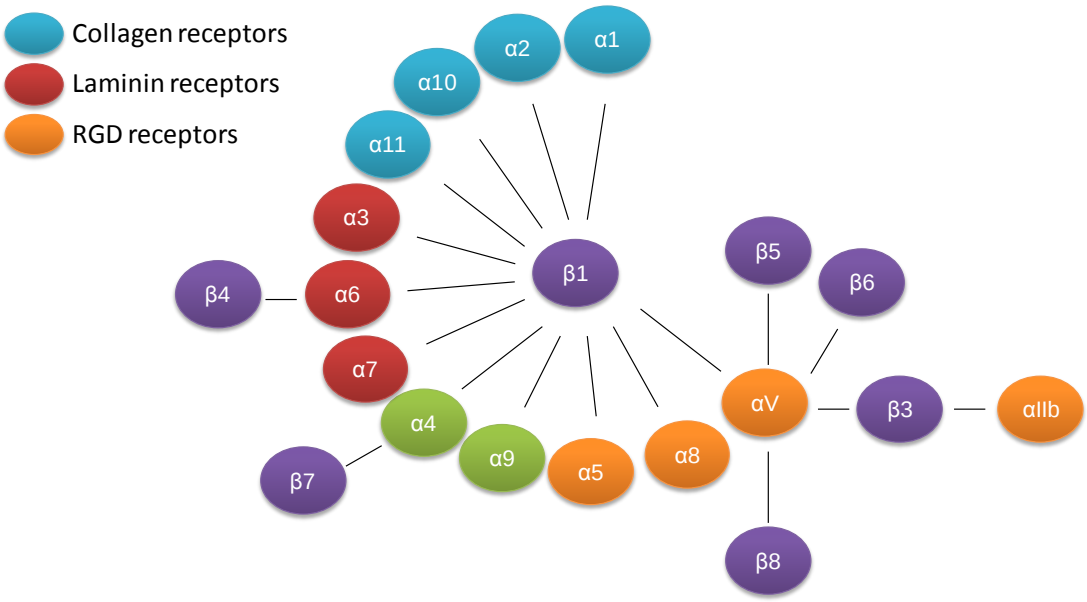

Figure 1-12: The classification of integrins according to ligand. The black lines indicate heterodimer formation. Figure adapted from Hynes., 2002, Takada et al., 2007 and Thomas, Nystorm, Marshall, 2006 [227, 231, 232]

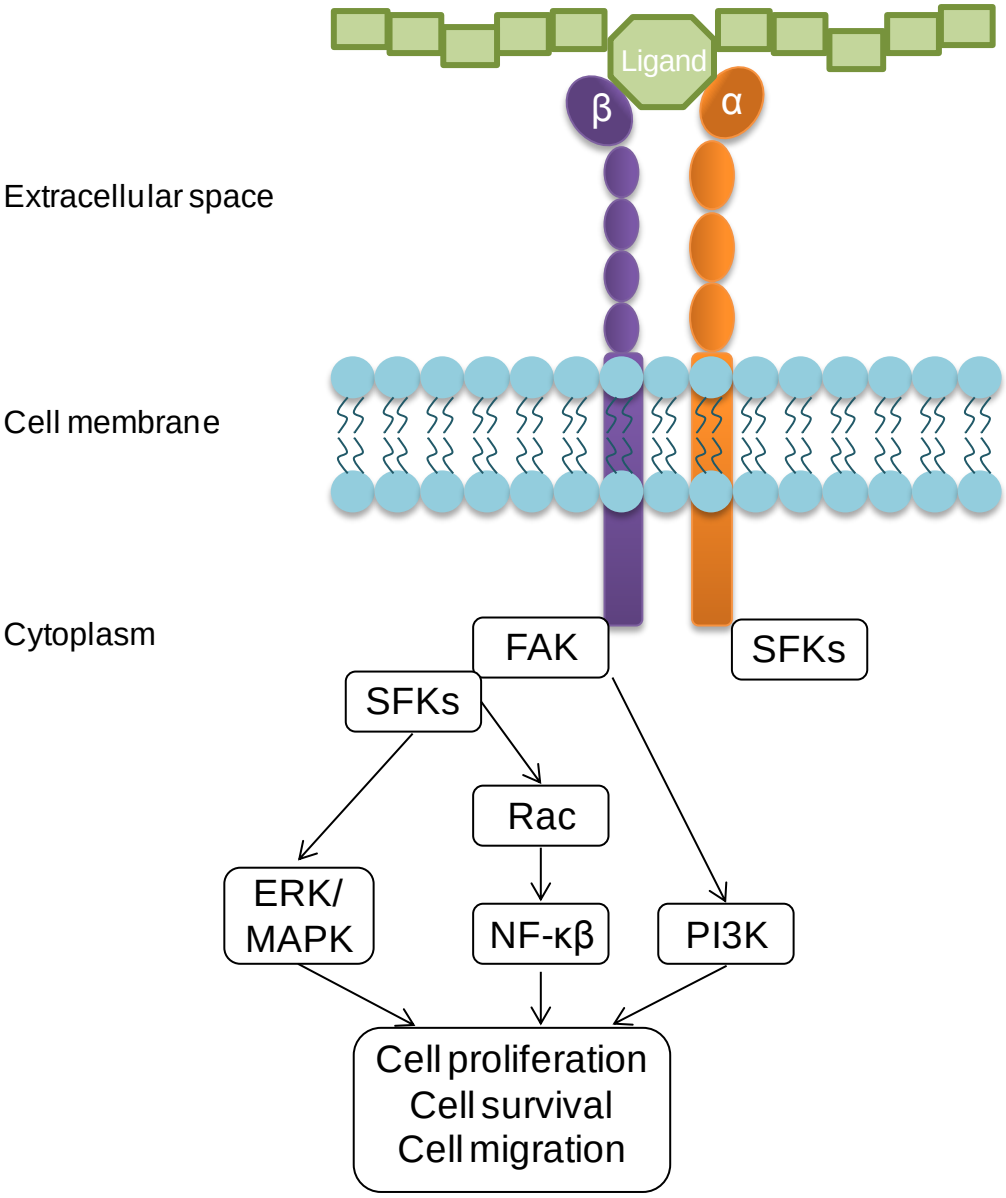

Figure 1-13: Integrin structure (α and β subunits) and signalling pathways downstream of integrin activation. Phosphorylation of the β subunit activates various pathways including ERK/MAPK, Rac and PI3K which modulate cell proliferation, cell survival and migration. Figure adapted from Guo et al., 2004 [229].

1.5.2 Integrins in Cancer

Altered integrin expression profiles in cancer cells compared to normal tissue have been repeatedly reported [227-229]. Given the central functions of integrins in ECM sensing and regulation of cell behaviour; cancer cells may be expected to down-regulate integrins that mediate stable adhesion to ECM and maintain cell quiescence (resting state) and differentiation, and up-regulate integrins that provide growth advantage and motility [233]. The context of aberrant integrin expression in cancer is complex and varies according to cell type [227-229]. The impact of a particular integrin therefore will depend on the overall integrin repertoire of the cell and the environment to which it is exposed [233]. It is also well established that integrins are associated with receptor tyrosine kinases (RTKs) and growth factor receptors [227-229].

Immunohistochemical profiling of integrins in normal, DCIS and invasive breast cancer tissue reveals that in normal breast MECs are the dominant source of α1, α2, α3, α6, αv, α9, and β1 and β4 subunits, with β4 being almost exclusive to MECs (Table 1-1) [234-237]. These subunits are polarised at MEC-BM interface. In DCIS this phenotype is largely maintained (Table 1-1) but in invasive breast cancer an overall decrease in integrin expression is reported [234-237]. However, expression of certain integrins are correlated with clinical outcome. Expression of the β4 subunit is strongly correlated with increased tumour size and higher nuclear grade [238]. Similarly expression of the α6 subunit is correlated with metastasis formation and reduced survival [239]. More recently, it also has been demonstrated

that α6 and β4 sub units are over-expressed in aggressive Basal-type breast tumours [240].

Integrin	Normal Breast		DCIS	
	MEC	LEC	MEC	Cancer
α1	++	+/-	+++	-
α2	++	+	++	-
α3	+++	+	+++	+
α6	+++	+/-	++	+/-
αv	+	+/-	+/-	+
β1	++	+/-	++	+
β4	++	+/-	++	-

Table 1-1: Comparison of the integrin repertoire of normal LEC and MEC and the same cell components in DCIS.– not expressed, +/- unclear expression, + low expression, ++ intermediate expression, +++ high expression. Table adapted from Koukoulis et al., 1991, Shaw, 1999 and Lambert et al., 2012 [235-237]

1.5.3 α6β4 Integrin and Hemidesmosomes

Stable attachment of basal cells to BM is achieved by anchor like structures called hemidesmosomes (HDs) which link the keratin cytoskeleton to the BM [109, 241-243]. These structures (Type I HD) are composed of α6β4 integrin, CD151 tetraspanin protein, Bullous pemphigoid (BP) 180 transmembrane protein, BP240 and plectin (HD-1) [244, 245]. The β subunit of α6β4 contains two pairs of fibronectin type III repeats and a connecting domain. α6β4 can attach to plectin at two regions; one spans the second fibronectin repeat and connecting segment, and the other spans the third fibronectin repeat carboxyl terminal [246, 247]. The extracellular domain of α6β4 acts as a receptor for laminin 3-3-2. [248]. CD151 interacts with α6β4 and mediates outside-in signalling [249, 250].

The basal layer of the skin is made up of basal keratinocytes. MECs and keratinocytes share a number of characteristics including integrin repertoire [251]. The function of α6β4 has been extensively studied in keratinocytes. An α6β4 knock out system revealed the role of α6β4 in skin integrity, since α6β4 null mice show severe skin blistering [252]. The epidermis of $\alpha6\beta4^{-/-}$ mice detached immediately after birth and the offspring die shortly after. Further investigation of the skin in $\alpha6\beta4^{-/-}$ mice by immunostaining for HD molecules and electron microscopy showed that neither integrin α6 subunit nor plectin was nucleated at the basal surface of basal keratinocytes indicating lack of HD formation. Furthermore, it was shown that keratin filaments of keratinocytes were unable to anchor to basal plasma membrane [252]. Residual keratinocyte attachment may be due to the activity of α3β1 [252].

The HD structure is dynamic and can disassociate upon a migratory signal (Figure 1-14), mainly from growth factors such as EGF [244, 248, 253, 254] which mediates α6β4 tyrosine or serine phosphorylation [255, 256]. α6β4 can be phosphorylated at specific serine residues by PKC-α which also has been shown to have play a role in HD dynamics [247, 248, 257]. This post transcriptional alteration disrupts α6β4-HD linkage, and α6β4 dislocates from HD and shuttles to actin rich filopodia where it promotes cell migration (Figure 1-14). α6β4 lacks an actin binding site therefore a linker protein is employed to achieve α6β4-actin association. Plectin contains an actin binding site (as well as a keratin binding site), and this site can also bind to α6β4 [258]. Therefore actin and α6β4 compete for plectin binding; in other words if plectin is bound to α6β4 its binding to actin is inhibited. In keeping

with this BP230 is proposed to be the actin-α6β4 linker in filopodia [244, 248, 253, 254]. This might explain the contradictory effects of α6β4; that it can be both involved in stationary cell adhesion and migration dependant on its localisation in the cells [245]. Therefore, inhibition of kinase activity is a key process to maintain intact hemidesmosomal structures. This is in contrast with the formation of focal contacts where phosphorylation of integrin β subunit is needed [233].

Phosphorylation of the intracellular β4 subunit can also amplify several signal transduction pathways (Figure 1-15). There is some dispute about the interaction between α6β4 and FAK. The early reports showed that α6β4 does not bind FAK mainly due to absence of intracellular FAK binding domain in both α and β intracellular subunits [259]. Nevertheless recent articles reported co-immunoprecipitation of α6β4, FAK and adaptor molecule Src in endothelial cells [260, 261]. It is also shown that α6β4 intracellular domains lack binding a sequence for PI3K [259]. However α6β4 can still activate PI3K-Akt and affect downstream of Rac which mediates invasion of MDA MB 435 in transwell invasion assays [262]. Mammalian target of rapamycin (mTOR) which is a downstream element of Akt was shown to be activated by α6β4 and signal via eIF-4E and induce expression of VEGF [263] in MDA MB 231 breast carcinoma cells. As well as enhancing tumour angiogenesis; VEGF expression by this α6β4 dependent mechanism triggers PI3K signalling which creates an autocrine circuit and contributes to breast cancer cell survival [263]. This shows that α6β4 can regulate growth factor expression.

Laminin-3-3-2 ligation by α6β4 can also be involved in anchorage independent cell survival via a mechanism dependent on Rac, involving NF-κβ activation and shuttling to the nucleus where it can induce transcription of anti-apoptotic factors [264, 265]. This mechanism is independent of PI3K. Weaver and colleagues generated a 3D reconstituted BM (Matrigel) system in which they grow the normal mammary LECs model (isolated from reduction mammoplasty) and by sustained passaging and growth factor withdrawal they have generated cells that spontaneously acquired tumourigenic properties. They showed that normal but not their tumourigenic counterparts polarised correctly in the 3D system, judged by α6β4 and laminin-3-3-2 staining on the cell-BM interface, and generate acini which are resistant to apoptosis in part due to the activation of endogenous NF-κβ. Moreover they showed that HD assembly is important in maintaining correct polarity, active NF-κβ and resistance to apoptosis [265]. It should be noted that in this study the glandular structures are composed only of LEC, whereas in human breast tissue LECs are surrounded with MECs which are the predominant source of α6β4.

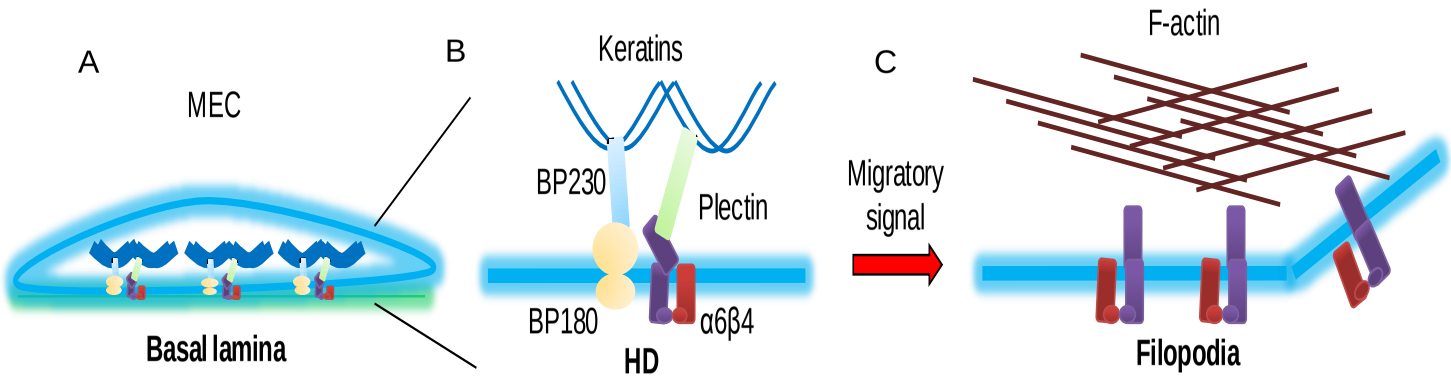

Figure 1-14: Shuttling of α6β4 after migratory signal. A; The localisation of HDs to the basal surface and the association with keratin skeleton. B; the detailed structure of HDs composed of α6β4, plectin, BP230 and BP180. C; Localisation of α6β4 in actin rich filopodia upon migratory signal. Figure adapted from Tsuruta et al., 2011

HD disassembly is a well established mechanism of keratinocyte migration in wound healing and re-epithelisation [245, 266]. Ozawa and colleagues compared the dynamics of focal adhesion and HD like structure formation in HaCat keratinocyte cells. Although cultured cells maintain the expression of HD proteins they failed to construct bona fide HD assembly whereas the cells form HD rich protein clusters [245, 266]. In contrast, keratinocytes form focal adhesions under tissue culture conditions while the importance of these adhesions *in vivo* intact skin is debatable [245, 266]. Ozawa and co-workers employed scratch wound assay and showed that focal adhesions assemble where filopodial structures are formed and HD structures are located immediately behind focal adhesions. α6β4 was needed to establish directed migration since treatment with an α6 integrin function blocking antibody (repeated with β4 antibody) disrupted HD structures. Cell movement was random, not directed [267, 268]. Moreover under this condition in which α6β4 activity is blocked, cell polarity was lost and HaCat cells showed rounded morphology implying a role for α6β4 in cellular spread. In contrast when α3 integrin-function blocking antibody was used to interrupt focal adhesions the cell migration was inhibited and HD structures were stabilised in the plane of the cell membrane. When plectin was knocked down keratinocyte migration was induced. Therefore assembly and disassembly of focal adhesions and HD structure are intricately linked in order to regulate cell migration (during wound closure).

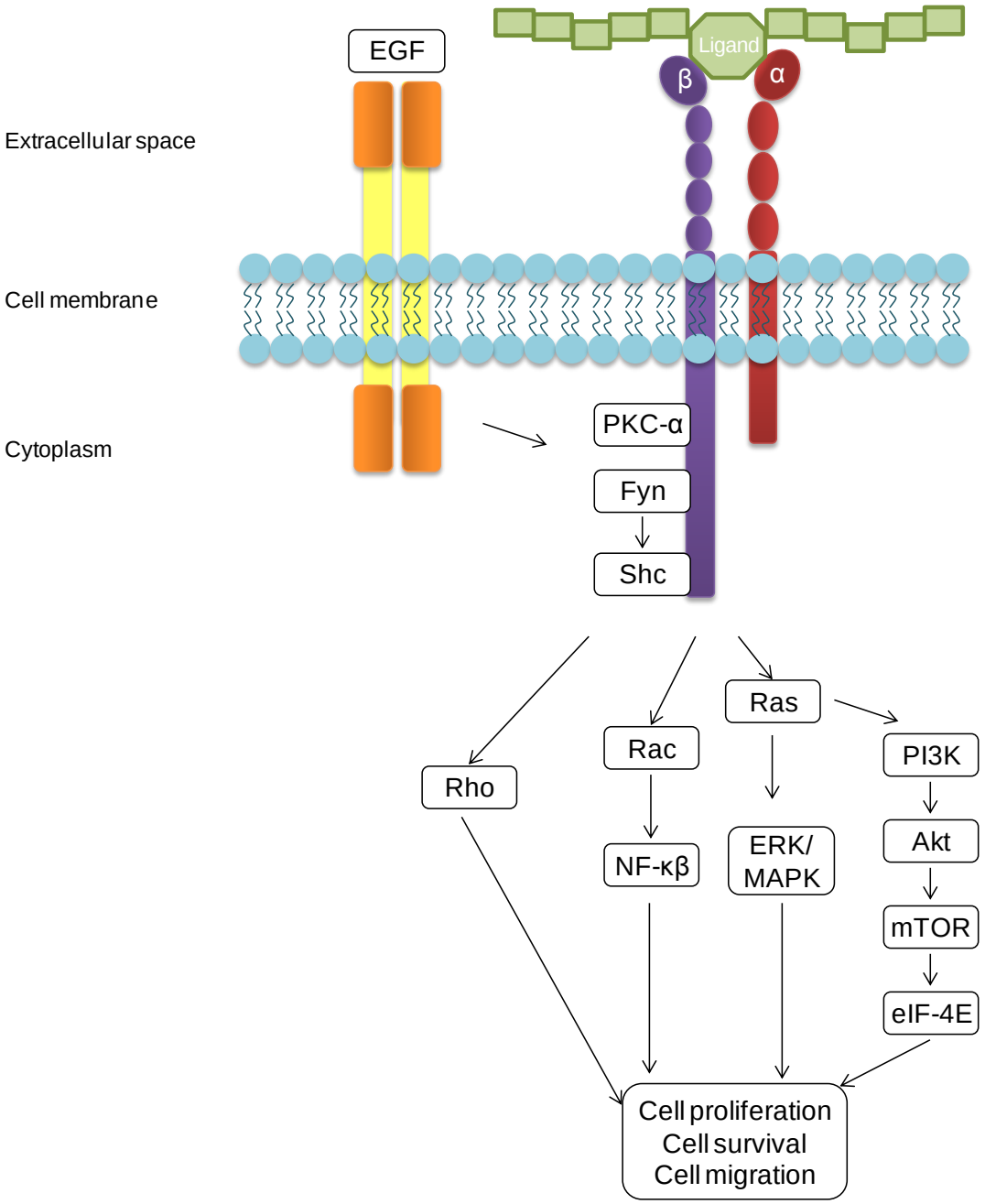

Figure 1-15: Summary of the signalling pathways associated with α6β4. α6β4 can be phosphorylated either with PKC-α or Fyn under the control of binding EGF to its receptor and activates several downstream pathways including Rho, Rac, Ras, PI3K which result into cell proliferation, survival and migration. Figure adapted Mariotti et al., 2001, Dans et al 2001., Mainiero et al., 1996, Santoro et al., 2003, Cantley et al., 1994, Shaw et al 1997, Chung et al., 2002, Zahir et al., 2003, Weaver et al., 2002 [253, 255-257, 259, 262-265].

Epithelial cell migration on laminin-3-3-2 can be modulated by the cleavage of γ2 chain by MMPs and concomitant revealing of specific binding sites

involved in signalling in cell migration [269-271]. MMP-2, 3, 12, 13, 20 and MT1-MMP can process laminin γ2 chain at an identical N terminus sequence (Ala^{586}-Leu^{587}), whereas α3 and β3 chains remain intact, which triggers mammary epithelial cell migration over laminin-3-3-2 in transwell migration assays, in which MCF-7 or MCF10A cells were plated on laminin-3-3-2 coated transwells and incubated in presence of the various MMPs listed [269-271]. Moreover MCF10A cells seeded on processed laminin-3-3-2 showed microscopic features of a migratory phenotype filopodial and lamellipodial structures [269]. It is further shown that processed laminin γ2 chain is found in tissue extracts from mouse skin carcinoma or breast of pregnant rat but not in quiescent rat breast [269]. Interestingly MMP-8 was also shown to cleave laminin γ2 chain at a distinct sequence (Leu^{587}-Thr^{588}) from other MMPs, but this does not result in significant induction of cell migration [270]. Intriguingly, in contrast with the γ2 chain cleavage, laminin-3-3-2 can be also proteolysed at α3 chain by plasmin which promotes HD assembly formation and hampers cell motility [272].

MMP-2 is expressed by stromal cells around the tumour and laminin-3-3-2 is expressed by and nucleated at the invasive front of colon and breast cancer cells [269]. Therefore cancer cell-microenvironment crosstalk can be fundamental for cancer cell invasion.

MMP-2 activation occurs via a unique mechanism in which the MT1-MMP and TIMP-2 are involved [273]. Further detailed information by Koshikawa and colleagues revealed the dependence of MT1-MMP activity in MMP-2

derived the γ2 chain processing [271]. Dual-immunofluorescent staining of human breast tissue for either laminin-3-3-2 and MT1-MMP or laminin-3-3-2 and MMP-2 showed that laminin-3-3-2 is predominantly expressed at the outer (invasive) edge and it is well co-localised with MT1-MMP or MMP-2 [271]. MT1-MMP is anchored to the cell membrane; therefore it can spatially cluster MMP-2 activation and laminin-3-3-2 cleavage to invasive interior and forms migration promoter cues along BM. This is of importance especially in early stages of invasion such as during the *in situ* stage where the local invasion depends on the context of external factors (BM).

1.5.4 Integrin αvβ6

αvβ6 integrin is an epithelial cell specific integrin that is largely undetectable in normal tissue but is up-regulated in many cancers and in wound healing [227, 231, 232, 274]. Over-expression of αvβ6 has been described in several cancer types including breast cancer [275], oral cancer [227, 231, 232, 276], colon cancer [277-280], basal cell carcinoma [281] and squamous cell carcinoma [282]. αvβ6 is a receptor for the RGD motif (arginyl-glycyl-aspartic acid), therefore it binds to fibronectin, vitronectin and tenascin as well as the latency associated peptide (LAP) of TGF-β [227, 231, 232, 283]. Binding of αvβ6 to LAP activates TGF-β [227, 231, 232]. There is accumulating evidence showing that αvβ6 is involved in cancer progression by promoting tumour cell invasion, blocking apoptosis, up-regulating MMP expression, and activating TGF-β and therefore modulating TGF-β signalling [227, 231, 232, 275, 278]. The role of αvβ6 integrin in inducing normal oral keratinocyte

migration was shown to be dependent on up-regulation of MMP-9 [274]. Moreover, a switch from αvβ5 to αvβ6 occurs in keratinocytes during transformation to malignancy and this contributes to anchorage independent growth of malignant keratinocytes [282].

1.6 Transforming Growth Factor-β

TGF-β is a growth factor widely implicated in cancer metastasis [284-286]. There are three TGF-β isoforms and receptors. TGF-βI preferentially signals through TGF-β receptor (TGF-βR) II. TGF-βRII and ligand complex has high affinity for TGF-βRI. Therefore TGF-βRII and TGF-βRI form a heteromeric signalling complex. This complex triggers phosphorylation of downstream elements SMAD-2 and SMAD-3 which than form a complex with mediator SMAD-4 [285]. These complexes then shuttle to the nucleus where they regulate transcription of various TGF-β responsive genes [285]. In addition TGF-β can act in a SMAD-independent manner [285, 286].

The genes under control of TGF-β induced transcription include integrins, integrin ligands and integrin-related proteins such as adaptor proteins [286]. TGF-β is secreted as a latent form non-covalently conjugated with LAP and latent TGF-β binding protein (LTBP). During the activation of TGF-β it is disassociated from the inactive complex. TGF-βI and TGF-β3 contain RGD motifs in LAP-1 and LAP-3 respectively which is a recognition sequence for integrins particularly αv integrins [286]. Binding of αvβ6 to the LAP N terminus results in a conformational change and therefore activates TGF-β

[283, 286]. The activation of TGF-β by integrins is found to be physiologically relevant since mice devoid of αvβ6 and αvβ8 show similar defects to those seen in TGF-βI and TGF-β3 knockout mice, such as severe autoimmunity syndrome, cleft palate and lack of Langerhans cells [287]. Interestingly active TGF-β has been reported to be restricted to the epithelial cell surface in the normal mammary gland suggesting that activation of latent TGF-β takes place locally on a cell by cell basis [288].

TGF-β plays a dual role during cancer progression; in early stages it acts as a tumour suppressor for epithelial cells, mainly by inhibiting cell proliferation, but in later stage disease, TGF-β is associated with tumour progression, via mechanisms including cancer cell and host-tumour interactions [284-286]. This dual role is mainly due to the involvement of TGF-β in complex mechanisms influencing cell survival, proliferation and differentiation. In keeping with this the over-expression of TGF-β is correlated with many cancer types including breast, prostate and colorectal cancer [284-286, 289]. The serum level of TGF-β was found to be elevated in breast cancer patients [290], and Yang et al hypothesised that there may be a critical level of TGF-β in tissues and when this is exceeded the undesirable effects of TGF-β might be triggered [291]. Yang and colleagues generated a transgenic mouse model expressing soluble TGF-βRII antagonist under the regulation of MMTV. When isogenic melanoma cells were injected via the tail vein, these mice were resistant to development of liver metastases, moreover when crossed with MMTV-neu to generate a metastatic breast cancer model, interestingly primary tumourigenesis was not accelerated, but there was a

significant reduction in formation of lung metastasis. This mouse model did not show other pathological features of lack of TGF-$\beta^{-/-}$ mice, such as immune system dysfunction and it was hypothesised by the authors that the soluble antagonist might only block the metastasis-associated action of TGF-β whereas the regulatory action of TGF-β in normal tissue remains functional [291].

In human breast cancer secreted TGF-βI was shown by immunohistochemistry to be localised at the invading front of the primary tumours following collagen tracks and metastases of lymph nodes [289].

Yin and colleagues used MDA MB 231 cells to over-express a dominant negative mutant of TGF-βRII lacking most of the cytoplasmic domain, in order to block TGF-β responsiveness [292]. When treated with TGF-β *in vitro*, proliferation of mutant TGF-βRII transfected cells was not altered but that of control MDA MB 231 cells was down-regulated [292]. Conversely, in an experimental *in vivo* bone metastasis model when injected in the left cardiac ventricle of female nude mice, mutant TGF-βRII transfected MDA MB 231 cells reduced bone metastasis formation when compared to non-transfected MDA MB 231 counterparts while there was no difference between mutant TGF-βRII bearing or control cells in terms of primary tumour formation after cells were administered intramuscularly into the right thigh of female nude mice [292]. This study again underscores the role of TGF-β to act as metastasis promoter rather than influencing primary tumour growth.

In this study, Transwell invasion assays and 3D organotypic assays were used. In the first assay, cancer cells were plated onto a cell permeable membrane coated with Matrigel, which represents BM, and MECs were seeded in the outer chamber as described in 2.8. During the assay cancer cells cross the Matrigel barrier, this requires degradation of Matrigel and migration. The assembly of this assay allows study of the paracrine interactions between two cell types. The advantages of the Transwell invasion assay incudes short incubation period (24 or 48 hours according to cancer cell type) and requirement for low cell numbers [320]. However this set up lacks the fibroblast compartment of the microenvironment and the 3D assembly of breast tissue, therefore 3D invasion assays which recapitulate the breast tissue architecture is needed for a better understanding of breast cancer cell invasion [309, 319, 320]. As a 3D model, organotypic gels were prepared using a Matrigel-Collagen mixture. Fibroblasts were embedded in the organotypic gels to create physiological-like microenvironmental effects. MECs and breast cancer cells were seeded onto gels to mimic the double layered breast duct. In comparison to Transwell invasion assays, organotypic cultures require longer incubation time (10 days) and greater cell numbers. In the current study, normal breast fibroblasts were used, since they are available in our laboratory. Although normal fibroblasts have been shown to be sufficient to induce formation of invasive breast tumours, probably via tumour cells inducing a myofibroblast phenotype [74, 117, 130], recently it was shown that CAFs behave significantly different to normal fibroblasts in organotypic assays [330]. When fibroblasts were collected from different stages (pre-invasive and invasive) of the MMTV-PyMT mouse model and

embedded in organotypic gels, CAFs promoted significantly more cancer cell invasion and contracted the gel significantly more than normal fibroblasts, indicating a greater ability of CAFs to remodel the ECM [330]. Thus, to understand the effect of cancer related stroma, there is an argument that CAFs should be used in organotypic cultures in place of normal fibroblast populations.

Chapter 2: Materials and Methods

2 Materials and Methods

2.1 Cell Lines and Cell Culture

All breast cancer cell lines were obtained from American Type Culture Collection (ATCC) and verified with STR profiling (LGC Standards, Teddington, UK, tracking number 710081047). MDA MB 231 and MCF-7 cells were cultured in Dulbecco's modified Eagle's medium (DMEM, PAA, E15-843) containing 10% (volume/volume, v/v) Fetal Bovine Serum (FBS, PAA, A15-14), hereafter termed complete medium. SUM159 cells were grown in complete HAM F12 (PAA, E15-817) with hydrocortisone (Sigma, HO 888, 1µg/ml) and insulin (Sigma, I9278, 1µg/ml).

Cell line	Media	Supplement	Concentration
MDA MB 231	DMEM	Fetal Bovine Serum	10%
MFC-7	DMEM	FBS	10%
SUM159	HAM F12	FBS	10%
		Hydrocortisone (Sigma, HO 888)	1µg/ml
		Insulin (Sigma, I9278)	1µg/ml

Table 2-1: List of breast cancer cell lines used and the details of media and supplement.

2.2 Generation of MEC Lines

The human telomerase reverse transcriptase (h-TERT) immortalised MEC 1089 cell line was a kind gift from Prof M. O' Hare, and Prof P. Jat, Institute of Neurology, UCL, London. These cells were isolated from reduction mammoplasty tissue as described by Gomm et al., 1995 [293], immortalised

as described by O'Hare et al., 2001 [294] and termed as Myo 1089 cell line. This cell line originally was a mixed population composed of MECs express differing levels of α6β4. These cells were sorted by their α6β4 expression using β4 antibody (Millipore, MAB 1964) coated magnetic beads (Dynal Invitrogen, 110.31). The cell line generated by this selection was called β4-1089 and fully characterised to demonstrate MEC features including expression of vimentin, SMA, p63 (Dr. M.D. Allen personal communication). In order to generate an αvβ6 integrin over-expressing cell line, AM12 packaging cell line was transfected with either empty pBABE-puro vector, or vector containing β6 integrin insert (Addgene plasmid:1734). β4-1089 cells were cultured with the media collected from control or β6 carrying AM12 cells and selected for puromycin (Sigma, P8833, 1μg/ml) resistance. Control and αvβ6 over-expressing cell lines were called 1089-N (Myo-puro) and 1089-β6 (Myo-β6) respectively. These cell lines were shown to switch their phenotype over time in culture; most notably they show gradual α6β4 integrin down regulation. In order to maintain α6β4 expression, cells are enriched by positive selection on β4 antibody-coated anti-mouse magnetic beads every 10-13 weeks. Along with this enrichment 1089-β6 cells are re-sorted by positive selection on αvβ6 coated beads, whereas 1089-N cells are negatively selected.

These cells were cultured in the presence of hydrocortisone (1μg/ml), Epidermal Growth Factor (EGF, Sigma, 9644, 10ng/ml), insulin (1μg/ml) and puromycin.

2.3 Isolation of Primary LEC and MEC Populations from Normal Breast and DCIS

The cell isolation protocol was adapted from Gomm et al 1995 [293]. Reduction mammoplasty tissue was collected and used to prepare breast organoids. The tissue was chopped and digested overnight at 37˚C with collagenase (1 mg/ml, Sigma, C2674) and hyaluronidase (Sigma, H3506) on a roller-mixer. The following day the fat layer was separated by decanting and organoids and single cells were washed three times with RPMI (PAA, E15-840) and followed by 3 sedimentation steps at room temperature (RT) to isolate the fibroblast-containing stromal compartment. After each 30 minutes sedimentation step the supernatant was removed and kept. In order to get a single cell suspension, the sedimented organoids were digested with 1X trypsin/EDTA (PAA, L11-004) –Dnase (Roche Diagnostics, 10104159001) for 30 minutes after washing with phosphate buffered saline (PBS). The digest was stopped with RPMI containing 10% FBS and the cell suspension was filtered through gauze (pore size: 56µm^2, Henry Simon, Stockport). Cells were counted and incubated in a 1:1 ratio sequentially with magnetic beads coated with CALLA antibody (AbD serotech, MCA1556) to isolate MECs, followed by magnetic beads coated with EpCAM (Ber-EP4) antibody (Invitrogen, 161.02) to isolate LECs, at 4˚C for 15 minutes on a roller-mixer. This bead/antibody complex-cell suspension was diluted with RPMI and bound cells were isolated using a magnet (Dynal, MPC-1, 120-01). Further incubations with magnetic beads were employed until depletion of each cell type was achieved. The bead/cell pellet was washed and grown in tissue

culture according to conditions described in Gomm et al 1995 [293]. For DCIS associated MEC and LECs, cells were isolated from DCIS tissue; organoid digests were incubated with β4-integrin antibody coated magnetic beads as explained above to select MECs and followed by an incubation step with anti-EpCam beads for LECs.

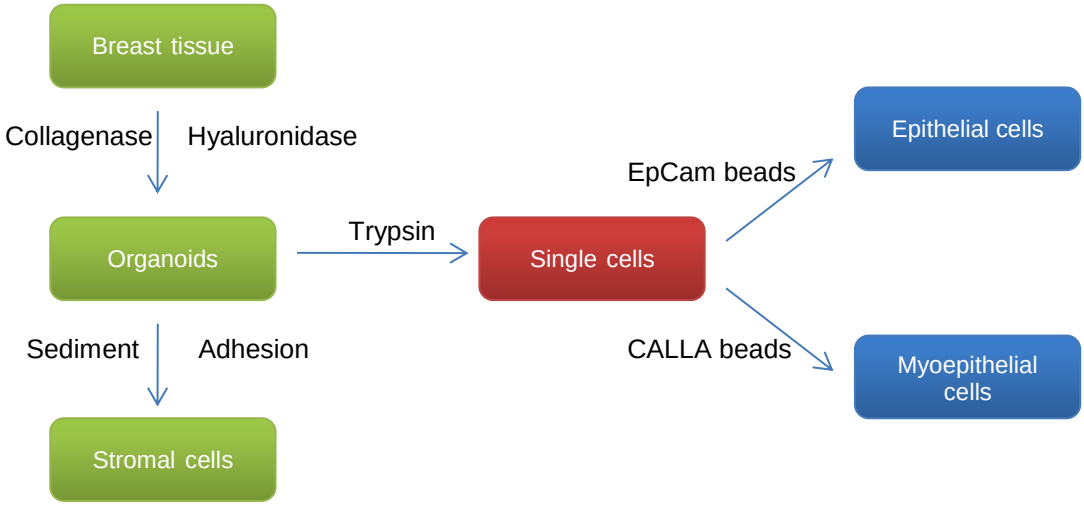

Figure 2-1: Diagram showing isolation of normal primary cells from reduction mammoplasty tissue. For DCIS associated cells, DCIS tissue was used and anti-β4 antibody was used to isolate MECs. Adapted from Gomm et al., 1995 [293].

2.4 MMP-8 Gene Over-expression

The MMP-8 WT and inactive MMP-8 EA (E198A) plasmids were kind gifts from Dr Dylan Edwards, Dr Julie Decock and Sally Thirkettle, University of East Anglia, Norwich [212]. Empty pcDNA4/TO (Invitrogen, K103002) was used for generation of control group.

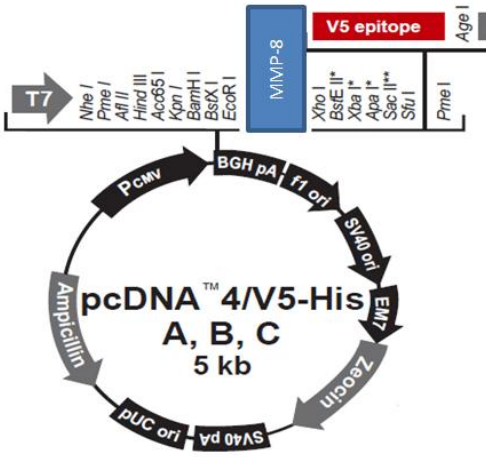

CMV promoter: bases 209-863
T7 promoter/priming site: bases 863-882
Multiple cloning site: bases 895-1008
V5 epitope: bases 1009-1050
Polyhistidine tag: bases 1060-1077
BGH reverse priming site: bases 1100-1117
BGH polyadenylation signal: bases 1009-1313
f1 origin: bases 1366-1789
SV40 promoter and origin: bases 1854-2178
EM7 promoter: bases 2186-2241
Zeocin™ resistance gene: bases 2261-2635
SV40 polyadenylation signal: bases 2764-2894
pUC origin: bases 3278-3951
Ampicillin resistance gene: bases 4095-4956 (complementary)

Figure 2-2: Map of pcDNA.4/V5-His A vector contains MMP-8 insert. Adapted from pcDNA.4/V5-His A, B, and C User manual, Version D 11/09/11, Invitrogen.

500ng of plasmid was digested with a digest mixture (Table 2-2) for 2 hours at 37˚C. The digest products were ran in 1% (weight/volume, w/v) agarose (Invitrogen,16500-500) in Tris acetate-EDTA (TAE), for 45 min at 100v.

Component	Amount (µl)
EcoR1 (NEB, RO1O1T)	1
Xho1 (NEB, R0146S)	1
Bovine serum albumin (BSA) (NEB, B9001S)	0.25
EcoR1 buffer (NEB, B0101)	2.5

Table 2-2: Mixture prepared for plasmid digest. Total volume was adjusted to 25µl with nuclease free water.

The sequence was confirmed with sequencing using T7 primers. For detailed information see appendix.

Myo-β6 cells were plated 24 hours prior to transfection at a density $7x10^4$ cells per well onto a 6-well plate in complete HAM F12. On the day of

transfection, media was replaced with 2ml of fresh complete media. For one well of a 6 well plate 6µl Gene juice reagent (Novagen, 70967) was added to 100µl Opti-MEM (Gibco, 51985, 026). This transfection cocktail was mixed quickly by vortex and incubated for 5 minutes at RT. 1µg of DNA (plasmid contains MMP-8 WT or MMP-8 EA insert, Empty vector) was added to media/gene juice complex and mixed gently by pipetting, then incubated at RT for 20 minutes. After incubation DNA/gene juice complex was added to cultured cells (100µl per well) drop wise and the flask was swirled to ensure equal transfection coverage, then incubated for 5 hours at 37˚C. After that the media containing transfection complexes was changed to 2ml complete media and incubated for 24 hours. All functional assays were done 24 hours after transfection. For conditioned media (CM) generation, complete media was changed to 2ml serum free media (SFM) after two washes with 1ml SFM per well and harvested after 24 hours incubation. CM were collected, spun at 1200 rpm for 3 minutes to remove dead cells and kept at -80˚C. Cells were harvested for RNA or protein extraction.

2.5 MMP-8 Gene Knock-down

Myo-Puro cells were seeded onto 6-well plates at a density $7x10^4$ cells per well and incubated for 24 hours at 37˚C in 2ml complete HAM F12. After 24 hours the media was replenished and Myo-Puro cells were transfected with pooled MMP-8 small interfering RNA (siRNA) (Thermo Scientific, MU-005969-00-0020), MMP-9 siRNA (Thermo Scientific) or Luciferase GL3 Duplex control siRNA (Thermo Scientific, D-001400-01-20) [295] by using

Interferin transfection reagent (Polyplus tranfection, Peqlab, 409-01). All siRNAs are kept at 20µM stock and used at 4nM final concentration (For MMP-9 1nM final concentration was used). Therefore 24µl interferin transfection reagent was added to 13.2µl siRNA in 1200 µl SFM and mixed with vortexing for 10 seconds. Then the siRNA mixture was incubated for 10 minutes at RT. After that the mixture was added to the 6 well plate (200µl per well) drop wise and the plate was immediately swirled to give a homogenous distribution of the siRNA mixture. All functional assays were carried out 96 hours after transfection. CM was generated as described in 2.4.

2.6 Reverse Transcription and Real Time Polymerase Chain Reaction

RNA was extracted with QuickRNA miniprep kit (Zymo Research, R1054) and reverse transcribed by Super Script II (Invitrogen, 11064-014) according to manufacturer's instructions. 100ng cDNA were used per reaction. Primer sequences (Invitrogen) and polymerase chain reaction (PCR) cocktail are as shown in Tables 2-3, 2-4, 2-5 and 2-6. All primers were kept at 100mM stock concentration and used at 0.4mM final concentration. 18s was used as housekeeping gene.

MMP-8 Primers	Sequence 5'-3'	Exon
Forward	GGTAGAGTTTGAAGAGAAGATCATGTTC	1
Forward	GCCGAAGAAACATGGACCAAC	4
Forward	ACTCCTCTGACCCTGGTGCC	5
Reverse	TCCATT GGGTCCATCAAATGG	4
Reverse	TGAGGATGCCTTCTCCAGAAG	8
Reverse	GGATACAGCCACATTTGATTTTGC	10

Table 2-3: Primer sequences designed for MMP-8 and used in reverse transcription PCR.

18s Primers	Sequence 5'-3'
Forward	CACGGGAAACCTCACCCGGC
Reverse	AACGGCCATGCACCACCACC

Table 2-4: Primer sequences designed for 18s and used in reverse transcription PCR.

β6 Primers	Sequence 5'-3'
Forward	GAAGGAATGATCACGTACAAG
Reverse	AGCAGGGAGTCTTCACAGGT

Table 2-5: Primer sequences designed for β6 integrin and used in reverse transcription PCR.

Component	Amount (µl)
Immomix Red (Bioline,Bio 25-022)	11
Forward Primer	1
Reverse Primer	1
Nuclease free water	10

Table 2-6: PCR cocktail prepared for reverse transcription PCR.

For nested PCR targeting MMP-8 mRNA; in the first run of PCR the 4F forward and 8R reverse primers were used and run for 35 cycles. 2µl product was used for a second run in which nested 5F forward and 8R reverse primers were used and run for 25 cycles to end the reaction in the linear phase. PCR cycle conditions were as summarised in Table 2-7 and for αvβ6 in Table 2-8). 18s was used as internal standard. The products from first and

second run of PCR were run on a 1% agarose/TAE gel for 45 min at 100v and visualised under ultraviolet (UV) light (AutoChemi System).

Step	Temperature (C)	Duration
Hot Start	95	8 min
Denaturation	94	30 sec
Annealing	56	30 sec
Extension	72	43 sec
Extension	74	10 min
Cooling	16	

Table 2-7: Cycle details for MMP-8 PCR

Step	Temperature (C)	Duration
Initial Denaturation	95	1 min
Denaturation	95	30 sec
Annealing	50	30 sec
Extension	72	1 min
Extension	72	5 min
Cooling	16	

Table 2-8: Cycle details for αvβ6 PCR

Real Time PCR was done by using SYBR green chemistry (Applied Biosystems, 4367659) according to manufacturer's instructions. 100ng cDNA input was used per reaction. Primers were used at 0.3mM final concentration. A PCR mix was prepared for each reaction as shown in Table 2-9 for 10µl total volume. Reactions were run using a step one plus instrument (Applied Biosystems).

Component	Amount (µl)
SYBR Green	5
Forward Primer	1
Reverse Primer	1
Nuclease free water	2

Table 2-9: PCR cocktail prepared for real time PCR.

2.7 Western Blotting

The CM collected from Myo-Puro or Myo-β6 cells was concentrated 20 times with centrifugal units (Millipore, 4FC 800324) with 3K molecular weight cut off (MWCO) at 4000g for 45 minutes at 4˚C. The same volume of sample was prepared from each condition and boiled in reducing (β-Mercaptoethanol containing) or non reducing Laemmli buffer for 5 minutes at 95˚C. The cell lysates were prepared with radio immunoprecipitation assay (RIPA) buffer containing proteinase inhibitors (Calbiochem, 539131). The protein concentration was quantified by Biorad DC protein assay (Biorad, reagent A: 500-0113, reagent B: 500-0114, reagent S: 500-0115) according to manufacturer's instructions.

10% Acrylamide -sodium dodecyl sulphate (SDS) separating gel (Table 2-10) and 5% stacking gel (Table 2-11) were cast. Samples were carefully loaded onto the gel. Recombinant human MMP-8 western blot (WB) standard (R&D Systems, WBC017) was loaded as a positive control and the gels run at 125v for 90 minutes at RT. After protein separation, the gel was removed from the cassette and placed in a transfer assembly where it faces towards a nitrocellulose membrane (Hybond C extra, RPN203E) and was run at 30v for 90 minutes at RT. After transfer the membrane was blocked with 5% (w/v) non-fat milk (Marvel) and 0.1% (v/v) Tween 20 (Applichem A 1389,0500) in phosphate buffered saline (PBS-T) for 1 hour at RT then probed with primary antibody prepared in blocking solution or 5% (w/v) bovine serum albumin (BSA, PAA, K45-001) containing PBS-T according to antibody manufacturer's instructions, and incubated at 4˚C overnight. Primary

antibodies used are listed in Table 2-12. For MMP-8 over-expressing cell samples the membrane was probed with anti V5 antibody (Invitrogen, R960-25) to detect the V5 tag. The membrane was washed with PBS-T 3 times for 5 minutes. Depending on the species in which the primary antibody is raised, horseradish peroxidase (HRP) conjugated mouse secondary (Dako, P0447), rabbit secondary (Dako, P0448) or goat secondary (Dako, P0160) antibody was prepared in 5%milk PBS-T at 1/2000 dilution and added after 3 washing steps for 5 minutes with PBS-T, then incubated for 1 hour at RT. Finally the membrane was washed as described and developed with enhanced chemiluminescence (ECL- GE healthcare, RPN 2106). For antibodies against phosphorylated forms of SMAD-2 and SMAD-3 ECL prime was used (Amersham, RPN2135).

Component	Amount	Company	Cat no
Sterile distilled water	4.6ml	N/A	N/A
30% Acrylamide	2.7ml	National Diagnostics	EC-890
1.5M Tris (pH 8.8)	2.5ml	Sigma	T1503
10% (w/v) SDS	100µl	National Diagnostics	EC-874
Tetramethylethylenediamine (TEMED)	6µl	Flowgen Bioscience	H17459
10% Ammonium persulfate (APS)	100µl	AGTC Bioproducts	EC-504

Table 2-10: Recipe of the separating gel prepared for WB. This recipe is for 1 gel.

Component	Amount
Sterile distilled water	3.4ml
30% Acrylamide	830µl
1M Tris (pH 6.8)	630µl
10% (w/v) SDS	50µl
TEMED	5µl
10%APS	50µl

Table 2-11: Recipe of the stacking gel prepared for WB. This recipe is for 1 gel.

Antibody name	Host	Dilution	Company	Cat no
MMP-8	Mouse	1/500	R&D Systems	mAb 908
MMP-8	Rabbit	1/1000	Millipore	81016
SMAD-2	Rabbit	1/1000	Cell signalling	3122
pSMAD-2	Rabbit	1/1000	Cell signalling	3101
SMAD-3	Rabbit	1/1000	Cell signalling	9523
pSMAD-3	Rabbit	1/1000	Cell signalling	9520
HSC70	Mouse	1/10000	Santa Cruz	sc-7298
Actin	Goat	1/1000	Santa Cruz	sc-1615
αvβ6	Goat	1/500	Santa Cruz	sc-6632
V5	Mouse	1/5000	Invitrogen	R960-25

Table 2-12: Primary antibody list used for WB.

2.8 Invasion Assay

$2x10^4$ modified Myo-β6 or Myo-Puro cells were seeded into one well of a 24 well plate in 500µl complete HAM F12 and incubated for 24 hours. After incubation 500µl complete media was replaced with 500µl SFM after 2 washes with SFM to remove residual serum.

One volume of Matrigel (9mg/ml, BD Biosciences, 354234) was mixed with 2 volumes of ice-cold SFM according to the breast cancer cell line used, to give 3mg/ml concentration; for MCF-7, MDA MB 231 DMEM was used and

for SUM159 HAM F12 was used. Boyden chamber transwells (pore size: 8µm[2], Corning, 3422) were coated with 70µl diluted Matrigel and allowed to set for 1 hour at 37˚C. After 1 hour transwells were placed in wells of a 24 well plate containing the appropriate transfected cell type. Then, 3x10[4] MDA MB 231, SUM159 or MCF-7 cells were seeded onto Matrigel and incubated for 24 hours for MDA MB 231 or SUM159 cells and for 48 hours for MCF-7 cells at 37˚C. Following this, the cells that had invaded through Matrigel and attached to the underside of the transwell were harvested with 10x trpsin/ Ethylenediaminetetraacetic acid (EDTA- PAA, L11-003) for 1 hour at 37˚C. Cells were removed by washing the well and underside of the transwells 3 times with 500µl trypsin then diluted 1/10 in isoton solution (BD, 342003) and counted with a CASY counter (Schärfe System).

For Collagen-I invasion assay; transwells were coated with 50µl 200µg/ml Rat Tail Collagen-I (BD Biosciences, 354236) [296]. Collagen-I was set according to manufacturer's instructions and as shown in Table 2-13.

Component	Calculation (µl)
Total volume	$50 * well\ number$
10x PBS	$Total\ volume/10$
Stock Collagen-I	$\frac{Final\ concentration * Final\ volume}{Stock\ concentration^{1}}$
1M NaOH	$Volume\ of\ stock\ collagen * 0.023$
Distilled water	$total\ volume - 10x\ PBS - stock\ collagen - 1M\ NaOH$

Table 2-13: Calculation of Rat tail Collagen-I preparation for Collagen-I invasion assay (same calculation method was used for Collagen-I zymography).

[1]This concentration is different for every lot.

Collagen-I was mixed with 10x PBS and distilled water then neutralised with 1M NaOH (Sigma, S8045). All reagents were kept on ice until needed. Collagen-I solution was mixed gently by inverting.

50µl diluted and neutralised Collagen solution was aliquoted into each transwell and set at RT overnight [107]. The invasion assay was constructed as described above by co-culturing with modified Myo-β6 or Myo-Puro cells. The number of invaded cells was counted as described previously.

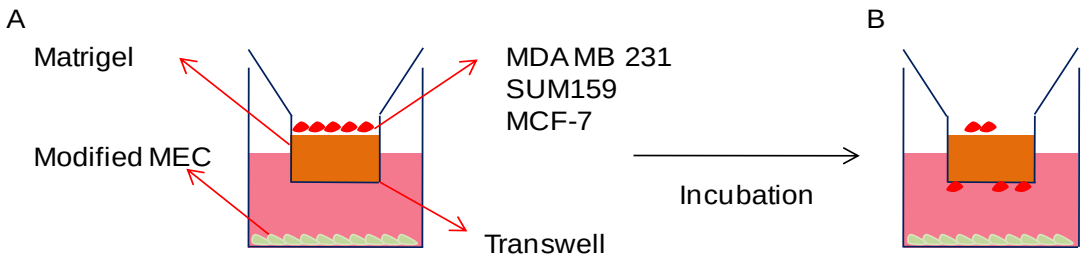

Figure 2-3: Diagram showing the invasion assay set up. A. Breast cancer cells seeded on top of Matrigel. B. Cancer cells invaded through Matrigel after incubation.

2.9 Proliferation Assay

To analyse MEC proliferation; $3x10^4$ Myo-β6 or Myo-Puro cells were seeded per well onto a 24 well plate and incubated for 24 hours at 37˚C. After incubation, the media was replaced with 400µl fresh media, and 80µl 3-(4,5-dimethylthiazol-2-yl)-5-(3-carboxymethoxyphenyl)-2-(4-sulfophenyl)-2H-tetrazolium (MTS) reagent (Promega cell titer 96 Aqueous, G5421) was added (5:1 media:MTS v/v ratio) then incubated for 1 hour at 37˚C. Following this the MTS containing media was mixed by pipetting and transferred to a

96 well plate as 120µl aliquots. The plate was read at A°_{495} (Tecan, infinite F50).

To analyse breast cancer cell proliferation $3x10^4$ MDA MB 231, SUM159 or MCF-7 cells were treated with CM collected from modified Myo-β6 or Myo-Puro cells. Incubation was 24 hours for MDA MB 231 and SUM159 cells and 48 hours for MCF-7 cells, corresponding to the duration of the invasion assay. Proliferation was quantified by using MTS reagent as described above.

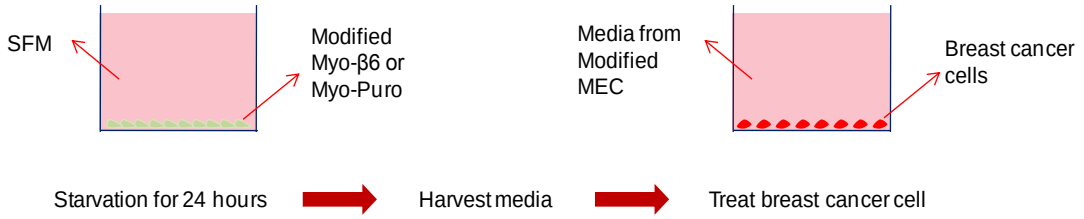

Figure 2-4: Diagram showing MTS assay set up and regimen. This set up is for analysing the paracrine activity of MMP-8.

2.10 Gelatine Zymography

A gelatine solution (porcine skin type A gelatine, Sigma, G2500) of 2.8mg/ml was prepared by dissolving 28mg of stock gelatine in 10ml sterile distilled water in a microwave for 20 seconds (900w) and kept at -20˚C. The resolving gel was prepared with 4.6ml sterile distilled water, 2.7ml 30% acrylamide, 2.5ml 1.5M Tris (pH 8.8), 100µl 10%SDS, 285µl 8% gelatine, 6µl TEMED and 100µl 10%APS to reach 8% acrylamide concentration. Stacking gel was

prepared with 3.4ml sterile distilled water, 830µl 30% acrylamide, 630µl 1M Tris (pH 6.8), 50µl 10%SDS, 50µl 10% APS and 5µl TEMED.

The CM collected from modified MECs and concentrated as described in section 2.4 was added to non-reducing Laemmli buffer. Recombinant human MMP-2 (Calbiochem, PF037) and recombinant human MMP-9 (Calbiochem, PF038) were prepared as stock solutions of 10µg/ml and diluted with sterile water to reach a final concentration of 10ng/ml and 20ng/ml respectively, then added to non-reducing Laemmli buffer.

Samples and standards were loaded onto the gelatine gel and run for 50 minutes at 200V using running buffer as explained in section 2-7. After that separation the gel was carefully removed from the cassette and placed in an air tight container and washed with 2.5% (v/v) Triton X-100, in sterile distilled water 4 times for 15 minutes. The gel was developed with developing buffer (10ml 1M Tris (pH 7.5), 8ml 5M NaCl (Fisher Scientific, BP358), 1ml 1M $CaCl_2$ (Sigma, C7902), 1.6ml 2.5%Triton X-100 and 179.4 ml sterile distilled water). 20ml developing buffer was added and incubated overnight at 37˚C. Coomasie blue staining solution was prepared with 0.5g Coomasie blue R-250 (Thermo Scientific, 20278), 250ml methanol (Fisher Scientific, M/4000, 17), 100ml acetic acid (Sigma, A6283) and 150ml sterile distilled water. After incubation the gel was carefully transferred to a 150mm petri dish and stained with Coomasie blue for 1 hour, following which the staining solution was decanted and the gel was rinsed with destaining solution containing 1.5L methanol, 50ml Formic acid (Sigma, F0507) and 3.5L sterile distilled water.

Destaining solution was replenished and the gel was placed on a shaker until lytic gelatine bands appear.

2.11 Collagen-I Zymography

For Collagen-I zymography 2ml Collagen-I solution per gel was prepared as described in Section 2.8. Separating gel and stacking gel components were mixed in the order listed in the Tables 2-14 and 2-15 and allowed to polymerise.

Component	Amount
1.5M Tris (pH 8.8)	1.3ml
Collagen-I solution	1.9ml
30% Acrylamide	1.7ml
10% (w/v) SDS	50µl
TEMED	2µl
10%APS	0µl

Table 2-14: Recipe for the separating gel prepared for Collagen-I zymography. This recipe is for 1 gel.

Component	Amount
Distilled water	3.05mL
1M Tris (pH 6.8)	1.25mL
30% Acrylamide	650ul
10% SDS	50ul
TEMED	5ul
10% APS	25ul

Table 2-15: Recipe for the stacking gel prepared for Collagen-I zymography. This recipe is for 1 gel.

After the gels set, samples were prepared, run and developed as described for gelatine zymography in Section 2.10.

2.12 Adhesion Assay

Non-tissue culture treated 96 well plates were coated with 100µl of Plasma fibronectin, Rat tail Collagen-I, tenascin-C, laminin-I-I-I, Collagen–IV and LAP in triplicate (at concentrations listed in Table 2-16), 3 wells of each plate were coated with 0.1%BSA in PBS as a control. Coated plates were incubated for 1 hour at 37°C after which the wells were washed 2 times with 100 µl PBS per well.

ECM	Conc. (µg/ml)	Company	Cat no
Laminin-I-I-I	10	Sigma	L2020
Collagen-I	0.5	BD Biosciences	354236
Collagen-IV	10	Sigma	C6745
Fibronectin	1	Sigma	F1141
Tenascin-C	3	Millipore	CC065
LAP	0.5	Sigma	L3408

Table 2-16: List of ECM used in adhesion assay and concentration details. The same ECM are used at the same concentrations in migration the assay.

Modified MECs were serum starved for 24 hours in serum free HAM F12 prior to the experiment. $3x10^3$ cells were seeded in 100 µl of SFM per well and allowed to adhere for 1 hour at 37°C, then 0.25µl of Calcein AM (Invitrogen, C1430) cell tracker was added and incubated for 15 minutes at 37°C. After this the plate was washed twice with 100µl PBS per well and 100µl SFM was added. The plate was read at $A^{\circ}_{490/520}$ on a fluorescent plate reader (BMG Labtech, FL40star Optima) and the adhesion was calculated from the fluorescence of adherent cells.

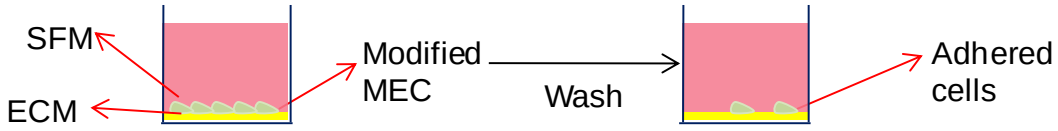

Figure 2-5: Diagram showing adhesion assay set up.

2.13 Immunoprecipitation for Conditioned Media

Protein A sepharose beads (GE Healthcare, CL-4B) were prepared in PBS according to manufacturer's instructions (10% v/v). 200µl bead/PBS solution was spun at 6000 rpm for 2 minutes at 4°C. Supernatant was removed and the remaining 20µl of bead pellet was washed 3 times with 100µl serum free HAM F12 at 6000 rpm for 2 minutes at 4°C. To minimise non-specific binding of the CM to beads 200µl, 20X concentrated CM samples were cleared with 20µl Protein A sepharose beads for 1 h at 4˚C on rotation. After that, samples were spun at 6000 rpm for 2 minutes at 4˚C and the supernatants were collected. Pre-cleared CM were divided into 100µl aliquots and incubated with 5mg MMP-8 antibody (R&D Systems, mAb 908) or mouse IgG (Sigma, I5381) overnight at 4°C on rotation. For MMP-8 antibody at 500 µg/ml stock solution; 10µl antibody was used. For non-immuno mouse IgG at 1 mg/ml stock solution; 5µl antibody was used.

Antibody treated CM were then added to 20µl fresh beads and incubated for 4 hours at 4°C with rotation. Samples were centrifuged as previously described. Supernatant was carefully collected and kept as the unbound fraction. The remaining pellet was washed with SFM as explained. In order to remove the precipitates from the beads; 40µl non-reducing Laemmli buffer

was added to 20µl cleared bead pellet and incubated for 10 minutes at RT then spun once again at 6000 rpm for 1 minute at 4˚C. Supernatant was collected with a fine ended loading tip and kept as the bound fraction. Laemmli buffer was added to unbound fraction and incubated for 10 minutes at RT. 20µl of prepared sample of bound or unbound fractions were loaded and separated on an SDS Acrylamide gel and transferred to nitrocellulose membrane as described in Section 2.7. Membrane was probed with anti MMP-8 or anti V5 antibody as the pcDNA4 vector into which MMP-8 is cloned carries a V5 epitope (Figure 2-2).

2.14 Invadopodia Assay (*In vitro* zymography)

To prepare the gelatine solution; 178.12mg NaCl, 94.57mg $NaBH_4$ (Aldrich, 21,346-2) and 100mg gelatine was dissolved in 50ml PBS for 1hour at 37˚C (pH=9.3). After this 1.8mg rhodamine (Sigma) was added to the solution and mixed for 2 hours in the dark to fluorescently label the gelatine. This gelatine solution was dialysed against PBS for 48 hours in the dark using Slide-A-Lyzer Dialysis Cassettes (MWCO: 10K, Volume: 30ml, Pierce, 66830). PBS was replenished every 24 hours. After dialysis, gelatine was collected and centrifuged at 1200 rpm for 10 minutes to remove un-dissolved particles, and then 1g sucrose (Fisher Scientific, 8060153) was added and dissolved.

Rhodamine-conjugated gelatine was spun at 1200prm for 10 minutes then heated up to 37°C. 40µl drops were aliquoted onto a 10cm tissue culture plate. 13mm coverslips were placed on each drop and incubated for 20

minutes. All incubation steps were done in the dark since rhodamine is sensitive to light. In another dish 1% (v/v) glutaraldehyde solution (Sigma, G5882) in PBS was aliquoted as 40µl drops. After 20 minutes; gelatine covered coverslips were placed on the glutaraldehyde solution to create a dual layer and incubated for 15 minutes. Then the coverslips were placed in a 24 well plate (dual layered side facing up) and washed 3 times with 500µl PBS. After this washing step 500µl 5mg/ml $NaBH_4$ was added and incubated for 20 minutes then washed as previously described. For sterilisation, the coverslips were incubated with 500µl 70% ethanol for 5 minutes, followed by a washing step with PBS then equilibrated with 500µl complete HAM F12 for 20 minutes at 37˚C. Finally $4x10^4$ modified Myo-β6 or Myo-Puro cells were layered onto the coverslips and incubated for 24 hours (Figure 2-6).

After incubation the cells were washed 3 times with 500µl PBS and fixed in 4% paraformaldehyde (PFA, Sigma, P6148) (w/v) in PBS for 15 minutes at RT then washed once again as described. Cells were blocked in 0.1%BSA and 0.1% (w/v) NaN_3 (Fisher Scientific, S227I) in DMEM for 15 minutes in the dark at 4°C. Cells were stained with Fluorescein isothiocyanate (FITC) labelled phalloidin (Invitrogen, A22283) for 20 minutes in the dark at RT then mounted in ProLong Gold Antifade aqueous mounting reagent (Invitrogen, P-36931) with 4',6-diamidino-2-phenylindole (DAPI). Images were taken on a confocal microscope (Section 2.24). Images from ten random fields on each coverslip were taken and the total area degraded was analysed using ImageJ software (National Institute of Health, version: 1.39u) (Figure 2-7). In the case of MMP-9 inhibition, cells were incubated with 25, 50 and 100nM

MMP-9 inhibitor (Calbiochem, 4444278). Control cells were generated by treating with Dimethy Sulphoxide (DMSO) vehicle only.

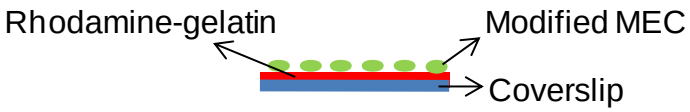

Figure 2-6: Diagram showing invadopodia assay set up.

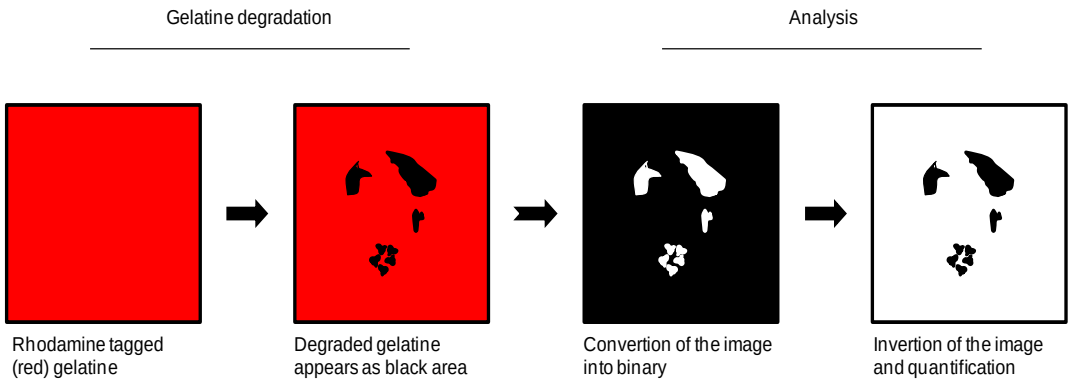

Figure 2-7: Illustration of the steps of image taking and analysis. Degraded gelatine appears as black dots on a red background. Images were taken using confocal microscopy and analysed using ImageJ by converting the image into binary and inverting the image in order to analyse black area on white background.

2.15 Migration Assay

The underside of Boyden chamber transwells were coated with 100µl of ECM or 0.1% BSA in PBS as a control and incubated for 1 hour at RT. ECM components and concentrations were the same as used for the adhesion assay (Section 2.12). After this incubation step, transwells were washed carefully with 100µl PBS avoiding disruption of the transwell membrane with the pipette tip, and placed into 500µl of SFM in the well of a 24 well plate.

$3x10^4$ modified Myo-β6 or Myo-Puro cells were added into the inner chamber in 200µl SFM and incubated for 8 hours at 37˚C. After that the media in the inner and outer chambers were replaced with 200µl and 500µl 10x trpysin/EDTA, respectively and incubated for 1 hour at 37˚C. The trypsin solution with cells was harvested and collected as described for the invasion assay (Section 2.8). The number of migrated cells as well as the number of cells in the inner chamber which have not migrated was counted using a CASY counter. The total cell number was calculated by adding the counts of matching tubes from the inner and the outer chambers. The percentage of migrated cells was calculated by using the counts of the outer chamber versus total cell number.

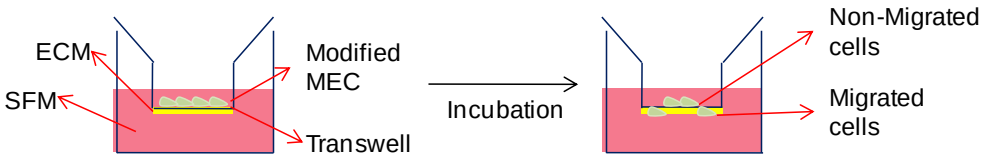

Figure 2-8: Diagram showing the migration assay set up.

2.16 Organotypic Culture

Organotypic gels were constructed using Rat tail Collagen-I and Matrigel. The Collagen telopeptide is intact. For 10 gels; 4.9 ml Rat tail Collagen-I was mixed with 2.1 ml Matrigel (7:3 v/v ratio), 1ml 10x DMEM (Sigma, D2429) and 1 ml FBS on ice. The pH of the solution was neutralised by adding 1M NaOH drop wise until the mixture turn an orange-pink colour. $5x10^6$ MRC5 fibroblasts or primary normal breast fibroblasts were suspended in 1ml complete DMEM and added to the neutralised gel mixture. 1ml gel mixture

was poured into 1 well of a 24 well plate and set for 1 hour at 37˚C. After that complete DMEM was added drop wise on top of the gels and the gels were equilibrated at 37˚C overnight. The following day, media was aspirated from the top of the gels, $2.5x10^5$ (per gel) modified Myo-β6 or Myo-Puro cells were suspended in 500µl complete HAM F12 and added on top of the gels, then incubated for 4 hours at 37˚C. After this $2.5x10^5$ (per gel) MDA MB 231 or SUM159 cells in 500 µl complete DMEM were added and incubated overnight at 37˚C.

In order to provide a stand for the organotypic gels, sterile 1 $inch^2$ nylon membranes (pore size:100µm2, Tetko Inc) were coated with Rat tail Collagen-I as follows; 7 volumes of Rat tail Collagen-I was mixed with 1 volume of 10x DMEM, 1 volume of FBS and 1 volume of complete DMEM. This mixture was adjusted to neutral pH with 1M NaOH as explained. 250µl coating mixture was aliquoted onto each membrane and incubated for 20 minutes at 37˚C. In order to induce crosslinking of Rat tail Collagen-I; the membranes were then covered with 1%glutaraldehyde solution in PBS, and incubated for 1 hour at 4˚C. The glutaraldehyde solution was then removed and membranes were washed 3 times with PBS, followed by 2 more washing steps with complete DMEM. Finally fresh complete DMEM was added and incubated overnight at 4˚C. After that the coated nylon membranes were put on top of steel grids (coated side facing up) in a well of a 6 well plate. Then the gels were carefully removed from the 24 well plate with a sterile spatula and placed on top of the nylon membranes. The well was filled with complete DMEM until the liquid reached the grid-membrane interface level. Media was

replenished every 2 days, and gels were harvested 11 days after rising for the over-expression system and 5 days for the siRNA system. The gels were then fixed in 10% neutral buffered formalin (Cell Path, BAF-0010-037) overnight, then transferred to 70% ethanol for 24 hours. Gels were mounted in paraffin and sectioned (4 mμ thickness) (BCI pathology core facility).

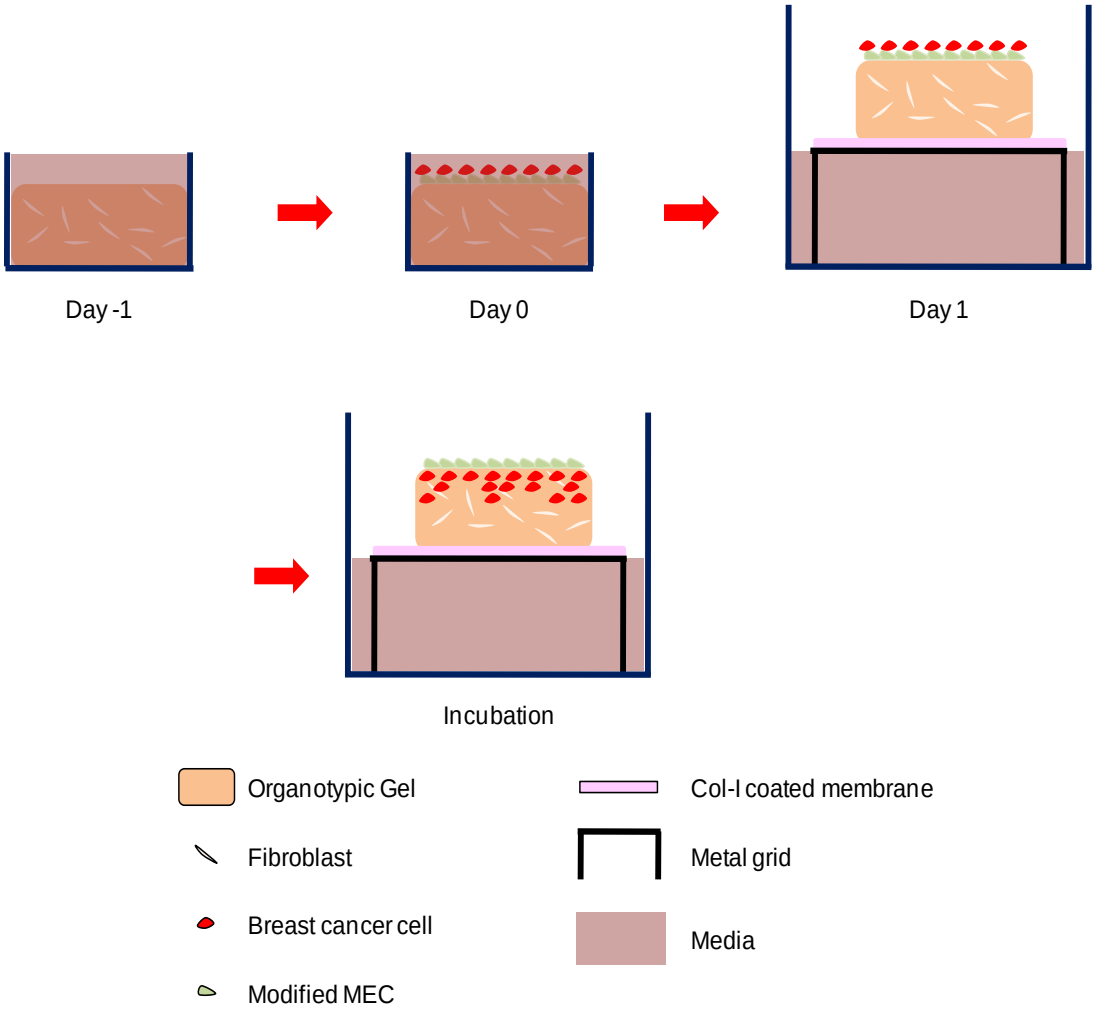

Figure 2-9: Diagram illustrating organotypic culture set up. On Day -1 the gel was cast and covered with complete DMEM, on Day 0 modified MECs and breast cancer cells were added, on Day 1 organotypic cultures were raised to an air liquid interface. Col-I., Collagen-I. Adapted from Froeling et al., 2008, Froeling et al., 2011, Holliday et al., 2009 and Chioni et al., 2012 [297-300].

The organotypic sections were stained with Hematoxylin and Eosin (H&E) (BCI pathology core facility). Bright field images were taken using a 10x objective on a light microscope (Section 2.24) , and processed and analysed with ImageJ [301]. The images were converted into binary and the depth of invaded cells was measured (3 measurements from each photograph). To quantify the area of invaded cells the holes in the binary image were filled. The non-invaded cell layer on the top of the gel was removed and the total number of particles and total area was measured (Figure 2-10).

The invasion index was calculated as the multiplication of the average of the depth of invading cells, the number of invading particles and the total area of invading particles.

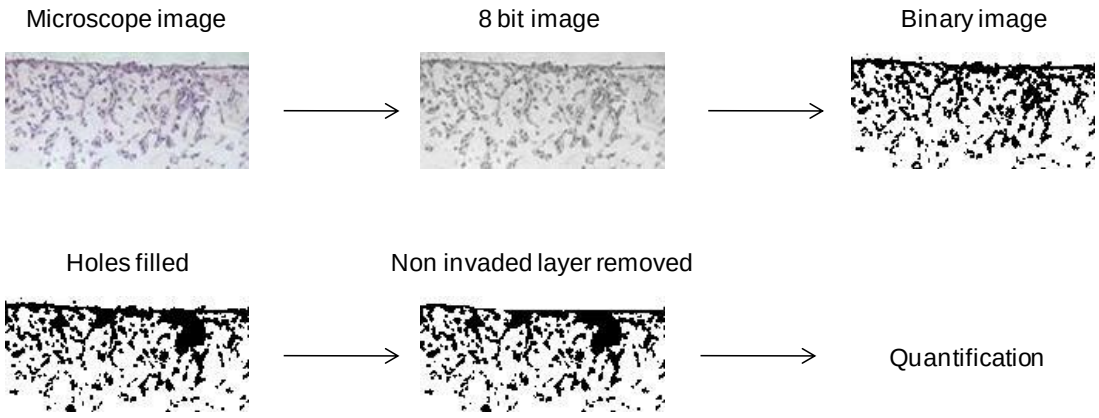

Figure 2-10: Diagram summarising the steps of organotypic gel quantification. The image was converted into 8 bit type, and brightness and contrast were adjusted. Then the processed image was converted into binary. The holes were filled and the top later of the gel was cleared. Then the particle number and area was quantified.

In order to analyse proliferation, gels were stained with Ki67 proliferation marker (Section 2.19). The Ki67 index is calculated as the percentage of

Ki67 positive cells in total cell number (calculate with DAPI staining). This analysis was done for the cells invaded into the gel.

2.17 Immunohistochemistry on Frozen Sections and Paraffin Blocks

FFPE sections were dewaxed at 60˚C for 10 minutes and rehydrated by xylene (Fisher Scientific, X5-1) followed by alcohol dilutions. Several antigen retrieval methods were used: 2.1% (w/v) Citric acid (pH 6) (Fischer Scientific, Cat no: 5949-29-1), 0.1M Tri-sodium Citrate (pH 6), Tris–EDTA (Fischer Scientific, 6381-92-6) (pH 9). Antigen retrieval solution was boiled for 6 minutes in microwave. Then slides were added for another 11 mins. For citric acid, the slides are boiled for 5 minutes twice (antigen retrieval solution level was checked and topped up with distilled water) and incubated on the bench for 20 minutes.

Sections were incubated in horse serum for 20 minutes then MMP-8 antibody diluted in 0.1%BSA/PBS was added and incubated for 1 hour. A number of different MMP-8 antibodies were evaluated, and these are detailed in Table 3-1. After a washing step with PBS the secondary horse anti-mouse antibody (Vector labs, PK 610-2) diluted 1/200 (in PBS) was added and incubated for 40 minutes. The avidin-biotin complex (ABC) layer (Vector labs, PK 610-2) was added after the second washing step and incubated for 30 minutes. Sections were developed in diaminobenzidine (DAB) (Vector lab, SK-4100) following the third washing step. Mayer's

hematoxylin (Sigma, MHS32) was used for counter staining. Sections were then dehydrated through graded alcohol to xylene and mounted in Distyrene-tricresyl phosphate-xylene (DPX) (VWR, BDH Prolabo, 360294H)

A double staining procedure was also carried out. The protocol for double staining was as described above for the first antibody then as follows. A second incubation with horse serum was carried out. Mouse anti- human Calponin antibody (Abcam, ab700-500) diluted 1/100 in 0.1%BSA/PBS, was added and incubated for 1 hour. After a washing step, secondary mouse antibody was added and incubated as described above. Following a further washing step, alkaline phosphatase (Vector labs, SA5100) was then added and incubated for 40 minutes. The sections were then developed with the Vector blue kit (Vecto labs, SK 5300) after the third washing step and counterstained in Mayer's hematoxylin. Glycergel (Dako, C0563) was used to mount the sections since vector blue kit is xylene sensitive.

2.18 Immunofluorescence Staining for Cells

For immunofluorescence staining (IF) 13mm^2 glass coverslips were coated with 200µl of 1µg/ml fibronectin solution and incubated for 1 hour at 37˚C. After that the coating solution was removed and coverslips were washed twice with 500µl PBS. 2x10^4 modified Myo-β6 or Myo-Puro cells were seeded per coverslip in complete HAM F12 and incubated for 24 hours at 37˚C. Following incubation, cells were washed once with 500µl PBS then fixed with 4%PFA in PBS for 10 minutes at RT. PFA was removed and cells were

washed 3 times with 500µl PBS. The cells were then blocked and permeabilised with 2% BSA and 0.1% Triton 100X in PBS for 15 minutes and incubated with primary antibody prepared in blocking solution at 1/100 dilution for 1 hour at RT. Primary antibodies are listed in Table 2-17. Then cells were washed as described above and incubated with secondary antibody conjugated with FITC or cyanine (Cy) -3 diluted in 2% BSA in PBS, for 45 minutes in dark at RT. Details of secondary antibodies used are given in Table 2-18. The cells were washed again, followed by an extra washing step with distilled water and mounted in ProLong Gold Antifade aqueous mounting reagent with DAPI.

Antibody name	Host	Company	Cat no
α6β4	Mouse	Millipore	1964
Plectin	Rabbit	Epitomics	1399

Table 2-17: List of primary antibodies used in IF staining.

Antibody name	Dye	Host	Company	Cat no
Anti Mouse	FITC	Goat	Invitrogen	A11029
Anti Mouse	Cy3	Goat	Invitrogen	A11030
Anti Rabbit	FITC	Goat	Invitrogen	A11008
Anti Rabbit	Cy3	Goat	Invitrogen	A11035

Table 2-18: List of secondary antibodies used in IF staining.

2.19 Immunofluorescence Staining for Organotypic Culture Paraffin Sections

Sections were dewaxed and rehydrated as described in Section 2.17. Antigen retrieval was achieved by boiling the sections in 10mM Tri-sodium Citrate (pH 6) for twice 10 minutes in the microwave (900w) (antigen retrieval solution level was checked and topped up with distilled water), followed by

incubation for 15 minutes at RT. The sections were then washed with PBS for 3 times 1 minute and blocked with 5% BSA/PBS for 1 hour at RT and incubated with primary antibodies diluted in blocking solution for 1 hour at RT. After that the sections were washed with PBS 3 times 5 minutes and incubated with secondary antibodies (diluted in blocking solution) conjugated with FITC or Cy3 dye (Table 2-18) and incubated 45 minutes at RT. The sections were then washed as described followed by an extra washing step with distilled water. Finally the sections were mounted in ProLong Gold Antifade reagent with DAPI and stored at 4°C. Details of primary antibodies used are given in Table 2-19.

Antibody name	Host	Dilution	Company	Cat no
p63	Mouse	50	Dako	M7247
Neso	Rabbit	300	N/A	N/A
Ki67	Mouse	100	Novocastra	NCL-L-Ki67-MM1

Table 2-19: List of primary antibodies used in IF staining of paraffin organotypic culture blocks.

2.20 TGF-β Stimulation Assay

Modified Myo-β6 or Myo-Puro cells were serum starved for 24 hours, following which the cells were stimulated with 5ng/ml recombinant human active TGF-β (R&D Systems, 240-B-002) for 5, 10 and 15 minutes. The TGF-β-containing media was then removed and the cells were washed with PBS and kept on ice to stop stimulation. Cells were scraped in RIPA buffer (containing protease inhibitors) (50µl buffer/well) then lysates were prepared and subjected to WB as described in Section 2.7.

2.21 MMP-8 Stimulation Assay

Parental Myo-β6 cells were seeded on 1µg/ml fibronectin and grown overnight. The following day complete media was removed and Myo-β6 cells were washed twice with SFM. Recombinant human MMP-8 (rhMMP-8, R&D Systems, 908-MP-010) was reconstituted with assay buffer containing 50 mM Tris, 10 mM $CaCl_2$, 150 mM NaCl and 0.05% (w/v) Brij-35 (Sigma, 16005) (pH 7.5) according to the manufacturer's instructions and diluted to 50ng/ml in SFM. Myo-β6 cells were treated with rhMMP-8, and the control group was incubated with assay buffer (vehicle only).

2.22 Luciferase Reporter Assay

MDA MB 231 cells transfected with firefly and renilla luciferase reporter gene fused with the PAI-promoter (MDA MB 231-Luc) were a gift from Dr Caroline Hill, London Research Institute. These were cultured in DMEM in the presence of 50µg/ml blasticidine (Sigma, 15205). MDA MB 231- Luc cells were seeded into a 96-well plate at a density of $4x10^4$ cells per well and incubated overnight at 37˚C then serum starved for 4 hours. After that $5x10^4$ modified Myo-β6 or Myo-Puro cells were seeded on top of MDA MB 231- Luc cells in SFM and co-cultured overnight. The following day media was removed and cells were washed with 100µl PBS. Cell lysis and luciferase activity quantification was done using Dual-Luciferase reporter assay system (Promega, E-1910) according to the manufacturer's instructions.

2.23 MMP-8 Purification

MMP-8 was purified from MMP-8 WT transfected Myo-β6 cells under native conditions using Pro-Bond Purification system (Invitrogen, 45-0055) for polyhistidine-containing recombinant proteins (MMP-8WT is tagged with hexahistidine and V5- section 2.4).

$1x10^6$ cells were seeded in a T175 flask. After 24 hours Myo-β6 cells were transfected with MMP-8 WT construct as described in Section 2.4 and incubated for 24 hours at 37˚C. After that complete media was aspirated and cells were serum starved for 24 hours. The CM was then collected and spun for 3 minutes at 1200 rpm. Supernatant was kept and dead cells were removed as a pellet. Harvested media were kept at - 80˚C until needed.

Media were dialysed against native purification buffer. To prepare 5x purification buffer; 35g NaH_2PO_4 (Sigma, S5011) and 146g NaCl were dissolved in 1L distilled water then adjusted to pH 8 with 10M NaOH. This stock concentration (250mM NaH_2PO_4 and 2.5M NaCl) was diluted 5 times with distilled water before use. 50ml of CM was placed in a dialysis cassette (Slide-A-Lyzer Dialysis Cassettes, MWCO: 10K, Volume: 70ml, Pierce, 87733). Air was removed from the cassette with a 30ml syringe (BD Plastipak, 301229) to maximise the media-membrane interface area. The dialysis cassette was put in a beaker containing 5L 1x native purification buffer and left on slow speed stirring overnight at 4˚C.

The media was removed from the dialysis cassette and put in a 50 ml tube containing Nickel-nitrilotriacetic acid (Ni-NTA) agarose resin (washed and prepared according to manufacturer's instructions). The tube was placed on a roller and incubated overnight at 4˚C to allow binding of MMP-8 WT to the resin. Then media was centrifuged for 1 minute at 800G at 4˚C and the supernatant kept as the unbound fraction. The remaining agarose resin was washed, and MMP-8 was eluted according to manufacturer's instructions.

2.24 Microscopy

Confocal images were taken using a confocal laser scanning microscope LSM510 (Carl Zeiss). FITC dye was excited with the argon laser at 488 nm, Cy3 dye was excited by a HeNe laser at 543 nm. Images were captured at 1084x1084 resolution. Images of the coverslips were acquired using 63x oil immersion objective and images of organotypic sections were taken with 40x objective. Co-localisation analysis was done on at least 4 different fields per experimental condition by Carl Zeiss confocal Meta software. Total field was analysed and co-localisation was displayed as the green (FITC- Plectin) pixels overlapping with red (Cy3- α6β4) pixels.

Bright images of organotypic sections were taken with light microscope (Axiophot, Zeiss) using 10x objective.

2.25 Statistical Analysis

Statistical significance was determined by two tailed Student's *t*-test using Prism (Graphpad Software) or Microsoft Excel. Results were considered as significant with p value less than 0.05.

Chapter 3: Effect of MMP-8 on MEC Functions

3 Effect of MMP-8 on MEC Functions

3.1 Introduction and Aims

MMP-8 has previously been shown to exert a tumour suppressor effect. Balbin et al., demonstrated that MMP-8 knockout male mice show higher susceptibility to skin cancer than WT mice after exposure to chemical carcinogens [208]. Moreover Gutierrez-Fernandez and colleagues showed that MMP-8 over-expression in B16F10 melanoma cells reduces formation of lung metastasis after injected into tail vein of MMP-8 knockout mice (back crossed with C57BL/6 mice) when compared to control vector over-expression [215]. Importantly, they showed that MMP-8 expression in melanoma cells enhances the spread and adhesion to ECM and reduced migratory phenotype *in vitro* [215]. Furthermore Palavalli and co-workers revealed that there frequently is LOH at the MMP-8 locus in melanoma, which is a hallmark of tumour suppressor genes [217]. In fact when mutated forms were over-expressed in Mel-STR melanoma cells and injected subcutaneously in NOD/SCID mice, these cells formed lung metastases whereas the Mel-STR cells over-expressing the WT form did not generate any lung metastases [217].

MECs in normal breast exhibit a tumour suppressor phenotype [117], but there is evidence that function becomes altered in at least some cases of DCIS, and this may contribute to progression of DCIS to invasive disease [275]. Previously in our lab we have shown that a consistent change in DCIS-associated MECs is up-regulation of αvβ6. We have shown that this leads to

a switch in MEC function, and these cells promote tumour cell invasion in a TGF-β dependent and MMP-9 dependent manner [275]. Furthermore, in a series of DCIS cases with long term follow-up, the expression of αvβ6 on DCIS MECs can predict recurrence and progression [275]. We also have shown that in normal breast, MECs are the major source of tumour suppressor MMP-8 but this expression is lost in DCIS associated MECs [215]. The functional significance of this loss in DCIS MECs is not known.

The aims of this chapter are:

- To confirm the localisation of MMP-8 in MECs in normal breast and its loss in DCIS associated MECs
- To evaluate MMP-8 expression in an αvβ6 over-expressing MECs recapitulating DCIS and in a normal MEC model, lacking αvβ6
- To use MEC lines to evaluate the effect of loss or gain of MMP-8 on MEC function.
- Specifically;
    - To over-express MMP-8 in αvβ6 positive DCIS MEC model to study gain-of-function effect, using
        - WT MMP-8
        - Mutant inactive MMP-8 to investigate the dependence of biological function on enzymatic activity
        - An appropriate control DCIS model which carries Empty vector

- To knock-down MMP-8 expression in normal αvβ6 negative MEC model to study loss-of-function effect using
  - MMP-8 siRNA treated normal MEC model
  - Comparable control for normal MEC model treated with control (non-targeting) siRNA

- To dissect whether MMP-8 influences MEC adhesion and migration on different ECM.

3.2 Results

3.2.1 Localisation of MMP-8 in Tissue Sections

In order to analyse the localisation of MMP-8 in breast tissue; IHC was performed on normal breast, DCIS and invasive breast cancer sections as described in Section 2.17. A number of antibodies were tested for IHC staining (Table 3-1). FFPE materials as well as frozen samples were stained. Antigen retrieval was done by pressure cooking or microwaving FFPE sections in antigen retrieval buffer, for frozen samples no antigen retrieval was done. Normal breast tissue was used as a positive control. High level of background staining was present for all the antibodies used and no specific staining was observed (data not shown). Based on the previous findings [215] staining of endothelial cells and of MECs in breast tissue was used as an endogenous positive control but no specific staining in these cell types was detected with any of the antibodies or staining conditions applied

indicating that the MMP-8 antibodies available were not adequate for IHC staining.

Company	Host	Cat no	Outcome
Abcam	Rabbit	11609	High background
Abcam	Rabbit	81286	High background
Millipore	Mouse	3316	High background
Millipore	Rabbit	81016	High background
R&D Systems	Mouse	9081	High background
R&D Systems	Mouse	908	High background
Santa Cruz	Goat	sc-8848	No staining
Sigma	Rabbit	021221	High background

Table 3-1: List of antibodies used in IHC staining for MMP-8 on FFPE and frozen sections.

3.2.2 MMP-8 Expression Levels in Breast Cell Populations

In order to confirm MEC dependent expression of MMP-8 in normal breast and loss of this expression in DCIS, primary normal MECs and LECs (and fibroblasts), and their DCIS-associated counterparts were isolated from normal breast (reduction mammoplasty) and DCIS tissue respectively [293]. Total RNA was isolated and reverse transcribed. A nested PCR targeting MMP-8 mRNA was carried out; eukaryotic ribosomal 18s was amplified as a house keeper control. A poorly metastatic melanoma cell line, G361, was used as a positive control [302, 303]. Figure 3-1 shows that normal breast MECs express MMP-8 whereas no band was observed in DCIS associated MEC. MMP-8 expression was not detected in LEC or fibroblast populations derived from either normal or DCIS tissue.

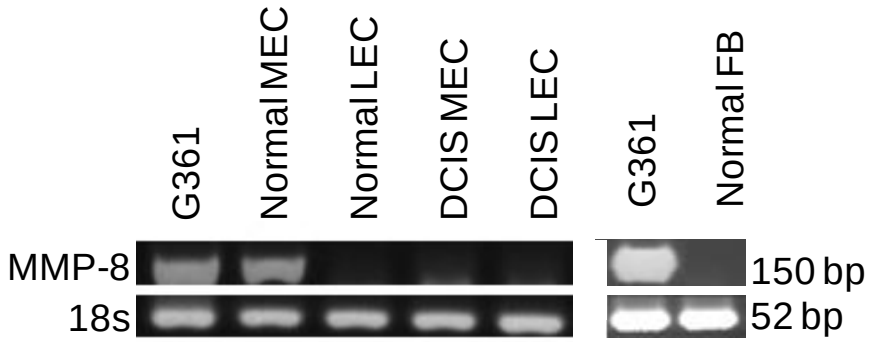

Figure 3-1: Analysis of MMP-8 expression profile in normal versus DCIS tissue. Primary normal MECs LECs and fibroblasts were isolated from normal breast; DCIS associated MECs and LECs were isolated from DCIS tissue as described in Section 2.3. Nested RT-PCR confirmed the expression of MMP-8 in the normal breast MECs and lack of this expression in DCIS MECs, with no expression in normal or DCIS associated LECs, or fibroblasts. FB., Fibroblast, bp., base pair, representative for 2 independent experiments.

3.2.3 Comparison of MMP-8 Expression Levels in Normal Versus DCIS Cell Line Models

To establish a model for DCIS-associated MECs an αvβ6 integrin over-expressing cell line termed Myo-β6 was generated from a normal MEC line, termed Myo-puro as described in Section 2.2. To confirm that the MEC lines recapitulate the *in vivo* phenotype of MEC populations thus showing down-regulation of MMP-8 upon gaining αvβ6 integrin expression, a nested RT-PCR and a quantitative RT-PCR (QRT-PCR) for MMP-8 was undertaken in both Myo-β6 and Myo-Puro cell lines. The G361 metastatic melanoma cell line [302, 303] was used as a positive control. As shown in Figure 3-2 A and B, MMP-8 expression was decreased at mRNA level in Myo-β6 cells compared to Myo-Puro cells. This observation was confirmed at the protein level (Figure 3-2 C); CM was collected from both cell lines, concentrated 20x

and separated by acrylamide gel under reducing conditions as described in Section 2.7. A reduction in MMP-8 expression at protein levels was also observed in CM from Myo-β6 cells reflecting mRNA expression.

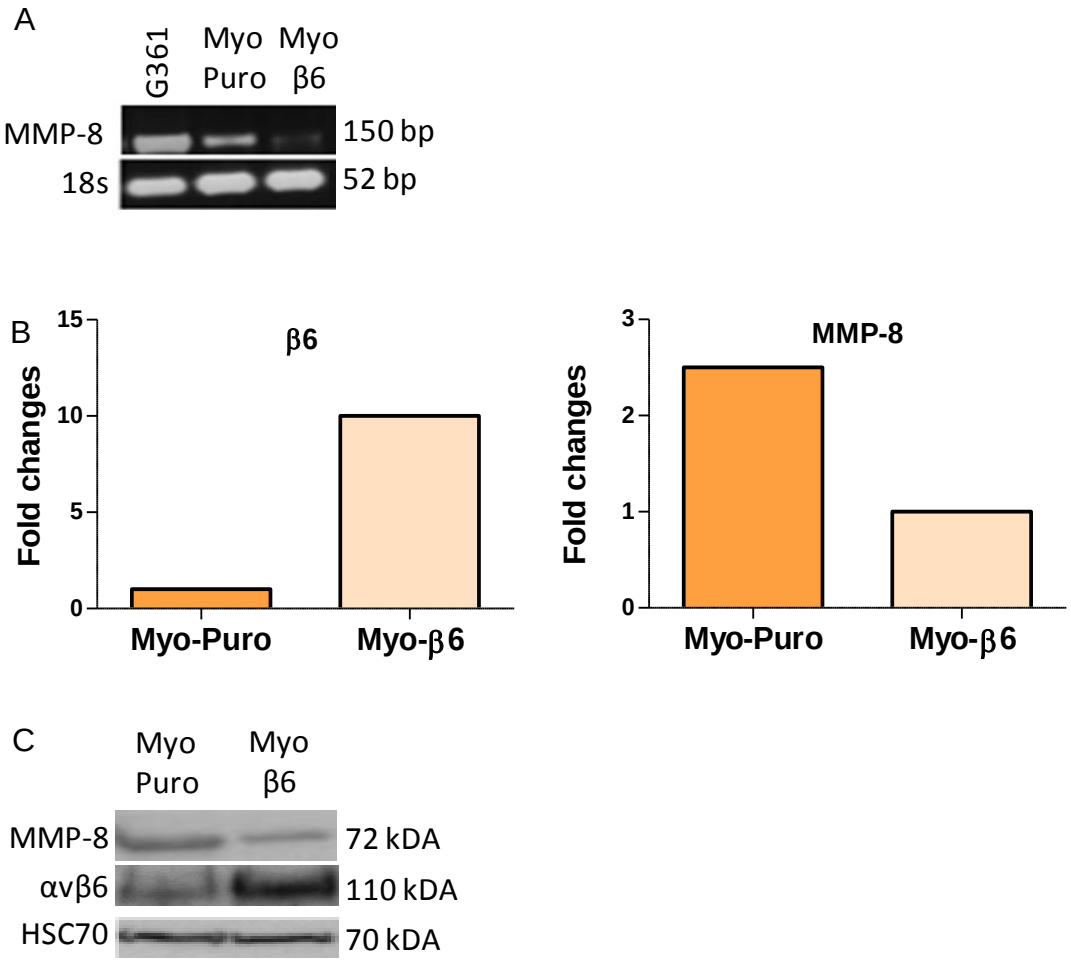

Figure 3-2: MMP-8 expression in Myo puro versus Myo-β6 cell lines. A; Nested RT-PCR and B; QRT-PCR showed that MMP-8 expression was down-regulated upon β6 over-expression at the mRNA level. β6 subunit was analysed. In addition amplification was also detected in the G361 positive control. C; 20x concentrated conditioned media collected from Myo Puro and Myo-β6 cells were separated by WB and probed for MMP-8, for αvβ6; cell lysates were prepared separated by WB and probed for αvβ6. Protein levels of MMP-8 reflected mRNA levels and an inverse correlation was observed between MMP-8 and αvβ6. kDa., kilodalton, Figures are representative of 3 independent experiments.

3.2.4 Over-expression of Wild Type or Inactive MMP-8 in Myo-β6 Cells

To analyse the gain-of-function effect of MMP-8 in the DCIS associated system, MMP-8 was over-expressed in Myo-β6 cells by plasmid transfection (MMP-8 WT) as described in Section 2.4. To further dissect the involvement of proteolytic activity of MMP-8 in its biological role; an enzymatically inactive form of MMP-8 (MMP-8 EA), was also over-expressed in Myo-β6 cells. This form carries a point mutation in the catalytic domain thus retaining the enzyme in the latent form [212]. Figure 3-3 A illustrates the mutation within the catalytic site. To compare MMP-8 expression at mRNA level, RNA was collected 24 hours after transfection and reverse transcribed. PCR targeting MMP-8 mRNA was carried out. Figure 3-3 B shows a similar level of expression of MMP-8 mRNA with WT and EA constructs in Myo-β6 cells. In order to compare protein expression levels; CM were collected from MMP-8 WT and MMP-8 EA or Myo-β6 cells transfected with Empty pcDNA4 after 24 hours serum starvation and concentrated 20x, then immunoprecipitated for MMP-8 using protein A beads coated with MMP-8 antibody (R&D, mab908) as described in Section 2.13. Unbound and immunoprecipitated (bound) fractions were subjected to western blotting under non-reducing conditions. Membrane was probed with V5 antibody. Figure 3-3 C upper panel confirms similar protein expression levels of the two constructs in CM.

To examine the proteinase activity of MMP-8 WT and MMP-8 EA mutant, CM were collected from modified Myo-β6 cells as explained above and were subjected to Collagen-I zymography, since MMP-8 is the major MMP processing Collagen-I [201]. As shown in Figure 3-3 C lower panel

degradation of Collagen-I was solely observed in CM collected from MMP-8 WT whereas MMP-8 EA or Empty vector control failed to show any degradation.

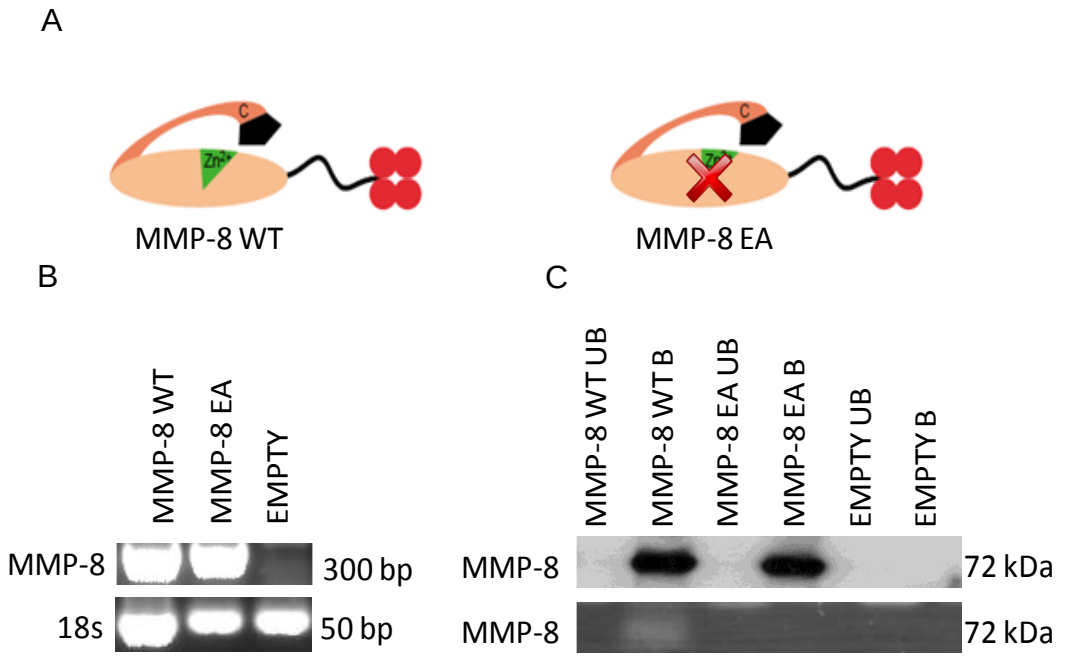

Figure 3-3: Investigation of MMP-8 over-expression in Myo-β6 cells.
A; Schematic illustration of MMP-8 WT and MMP-8 EA indicating the site of mutation.
B; PCR targeting MMP-8 revealed similar expression levels for MMP-8 WT and MMP-8 EA at mRNA level.
C; MMP-8 WT and inactive form (EA) was over-expressed in Myo-β6 cells, CM were collected after 24 hours of starvation and concentrated 20x. MMP-8 was immunoprecipitated with MMP-8 antibody conjugated protein A sepharose beads. Upper panel; WB confirms the presence of MMP-8 protein in MMP-8 WT coding plasmid or MMP-8 EA coding plasmid transfected cells. WB was blotted for V5. Lower panel; Collagen degradative activity of different forms of MMP-8 was analysed with Collagen-I zymography. Substrate degradation was solely observed in MMP-8 WT bound fraction whereas no activity was seen in MMP-8 EA bound or unbound fractions. bp., base pair, kDa., kilodalton, B., bound fraction, UB., unbound fraction, representative for 3 independent experiments.

3.2.5 The Effect of MMP-8 Over-expression on Myo-β6 Proliferation

In order to analyse whether MMP-8 WT or EA over-expression in Myo-β6 cells influence cell proliferation, modified Myo-β6 cells were cultured (on plastic) for 24 hours, and MTS assay was done and normalised to the proliferation of the Myo-β6 cells transfected with Empty vector control as described in Section 2.9. There was no significant difference in proliferation rate between different transfection groups ($p>0.05$, $n=3$) (Figure 3-4).

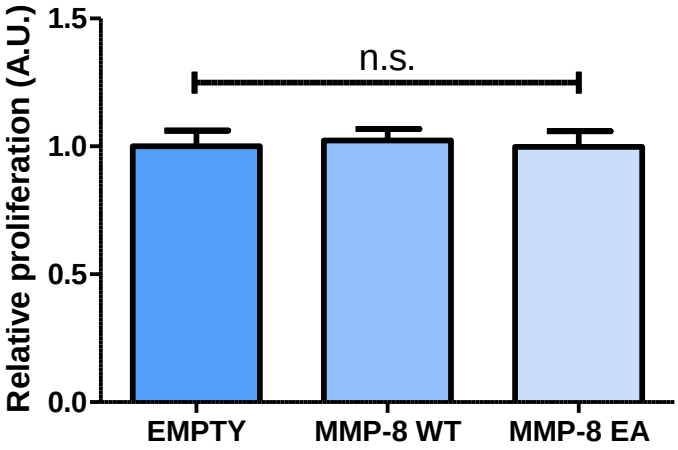

Figure 3-4: Effect of MMP-8 loss on Myo-β6 proliferation. Myo-β6 cells were grown and MTS proliferation assay was done as described in Section 2.9. Proliferation rates showed no significant difference between MMP-8 WT, MMP-8 EA or Empty vector transfected Myo-β6 cells. A.U., arbitrary unit, n.s., not significant, representative for 3 experiments.

3.2.6 Effect of MMP-8 Over-expression on Myoepithelial Phenotype

To evaluate the effect of MMP-8 on myoepithelial phenotype, MMP-8 WT or Empty vector transfected control Myo-β6 cells were seeded onto fibronectin (1µg/ml) coated coverslips in SFM and grown for 24 hours. On this matrix, MMP-8 WT cells showed more spreading with a significant increase in occupied area (in pixels) (Figure 3-5 A and B) compared to Empty vector control ($p=0.02$, $n=1$). In order to eliminate the possibility that increased area occupation was a result of increased proliferation in MMP-8 WT cells, proliferative activity of modified Myo-β6 cells after 24 hours incubation on fibronectin was quantified using the MTS assay as described in materials and methods. In contrast to data related to cell spreading, MTS assay showed that MMP-8 over-expression did not alter the proliferation of Myo-β6 cells throughout the same incubation period (Figure 3-5 C) ($p=0.91$, $n=1$).

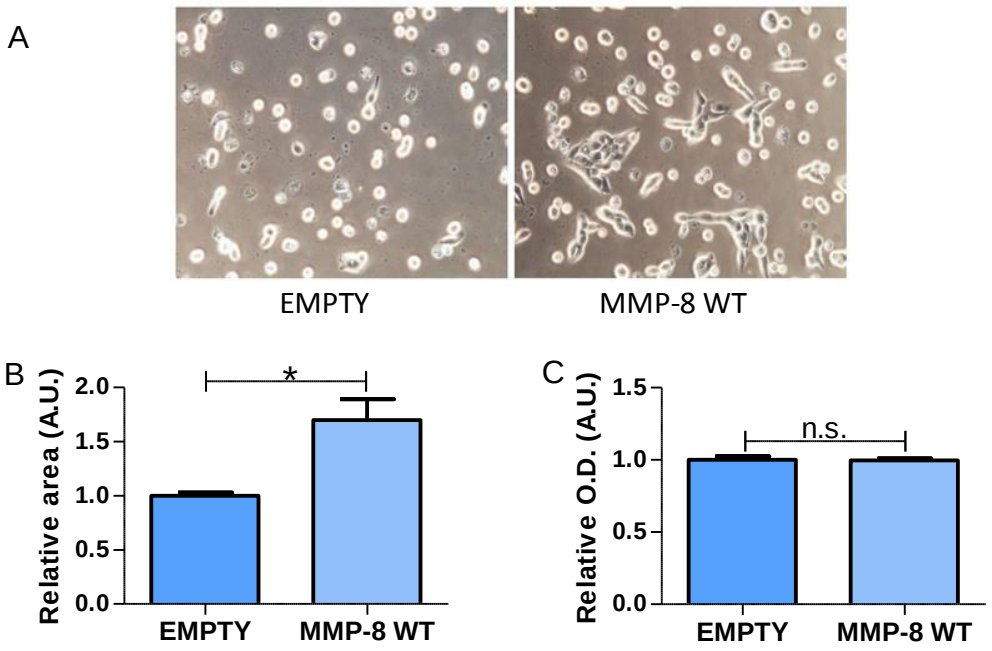

Figure 3-5: Effect of MMP-8 on spreading on ECM. A; MMP-8 WT or Empty vector transfected cells were seeded on fibronectin coated coverslips and pictures were taken after 24 hours. B; Quantification of occupied area by ImageJ, a significant increase in spreading was seen in MMP-8 WT over-expressed cells. C; MTS assay run for 24 hours on fibronectin and showed no significant difference in proliferation rate. *, P ≤ 0.05 (Student's *t* test). Error bars show means +/- SEM. A.U., arbitrary unit, O.D., optical density, n.s., not significant.

3.2.7 Effect of MMP-8 Over-expression on Myoepithelial Adhesion

To dissect the effect of MMP-8 on MEC adhesion to ECM, MMP-8 WT, MMP-8 EA or control cells were seeded onto different ECM coated wells of a 96 well plate, allowed to adhere for 1 hour and tracked fluorescently by Calcein AM cell tracker (Figure 3-5 A). Fluorescence obtained from adherent cells in MMP-8 WT and MMP-8 EA was normalised to Empty vector. All experiments were performed at least 3 times. Figure 3-6 B shows that over-expression of MMP-8 WT significantly enhanced adhesion to fibronectin, Collagen-I, laminin-I-I-I and tenascin-C whereas there was a significant decrease in adhesion to the N terminus latency associated peptide of TGF-β, LAP, when compared to Empty vector (fibronectin p=2.02E-07, Collagen-I p=3.35E-05, laminin-I-I-I p=0.0006 , tenascin-C p=0.01, LAP p=0.03) and EA form transfected Myo-β6 cells (fibronectin p=4.85212E-06, Collagen Type-I p=0.001, laminin-I-I-I p=0.002, tenascin-C p=0.01, LAP p=0.04). MMP-8 WT did not significantly alter the adhesion to Collagen-IV compared to Empty vector (p=0.29) or MMP-8 EA (p=0.63).

MMP-8 EA did not show a significant effect on MEC adhesion in comparison to Empty vector (Fibronectin p=0.12, Collagen-I p=0.44, Collagen-IV p=0.69, laminin-I-I-I p=0.69, tenascin-C p=0.225 LAP p=0.37).

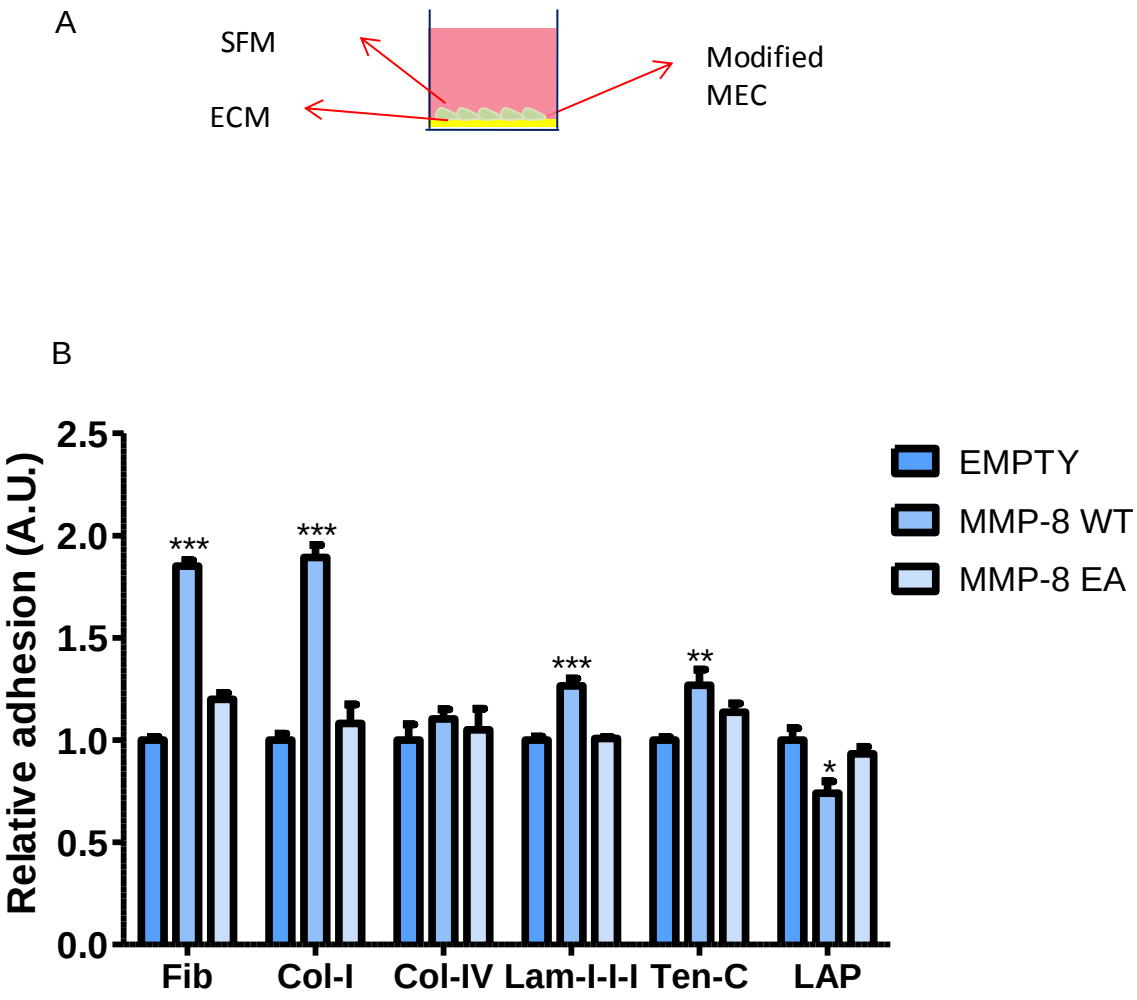

Figure 3-6: Effect of MMP-8 on adhesion to ECM. A;MMP-8 WT, MMP-8 EA or Empty vector transfected Myo-β6 cells were seeded on different ECM molecules in a 96 well plate and stained with Calcein AM cell tracker. B; Adhesion was quantified as the amount of fluorescence measured after washing step to remove non-adherent cells and normalised to the Empty vector. In MMP-8 WT transfected cells a significant increase was observed in adhesion to fibronectin, Collagen-I, laminin-I-I-I and tenascin-C, however adhesive activity to LAP was significantly reduced compared to Empty vector transfected control Myo-β6 cells. In contrast inactive mutant did not show any significant effect. *, P ≤ 0.05; **, P ≤ 0.01; ***, P ≤ 0.001 (Student's *t* test). Error bars show means +/- SEM. A.U., arbitrary unit, Fib., fibronectin, Col-I., Collagen-I, Col-IV., Collagen-IV, Lam-I., laminin-I-I-I, Ten-C., tenascin-C, representative for 3 independent experiments.

3.2.8 Effect of MMP-8 Over-expression on Myoepithelial Migration

In order to explore the effect of MMP-8 over-expression on MEC migration, transwell migration assays were performed by coating the underside of the transwell with different ECM molecules as shown in Figure 3-7 A. In this system Myo-β6 cells were seeded on top of the transwell, and therefore are separated from the ECM by the cell permeable membrane. According to the potential of ECM to establish a gradient to trigger a movement response, cells migrate towards particular ECM and attach to the underside of the transwell. All experiments were performed a minimum of 3 times. Migration towards fibronectin, Collagen-I, laminin-I-I-I, tenascin-C and LAP was significantly abrogated in MMP-8 WT MEC (fibronectin p=0.012003, Collagen-I p=0.006206, laminin-I-I-I p=0.002, tenascin-C p=0.006731, LAP p=0.013) but not in MMP-8 EA MEC (fibronectin p=0.12783, Collagen-I p=0.68, Lam-I-I-I 0.068046, tenascin-C p=0.205279, LAP p=0.734778) compared to Empty vector controls. Migration towards Collagen-IV was not affected by MMP-8 WT or MMP-8 EA over-expression (Figure 3-7 B).

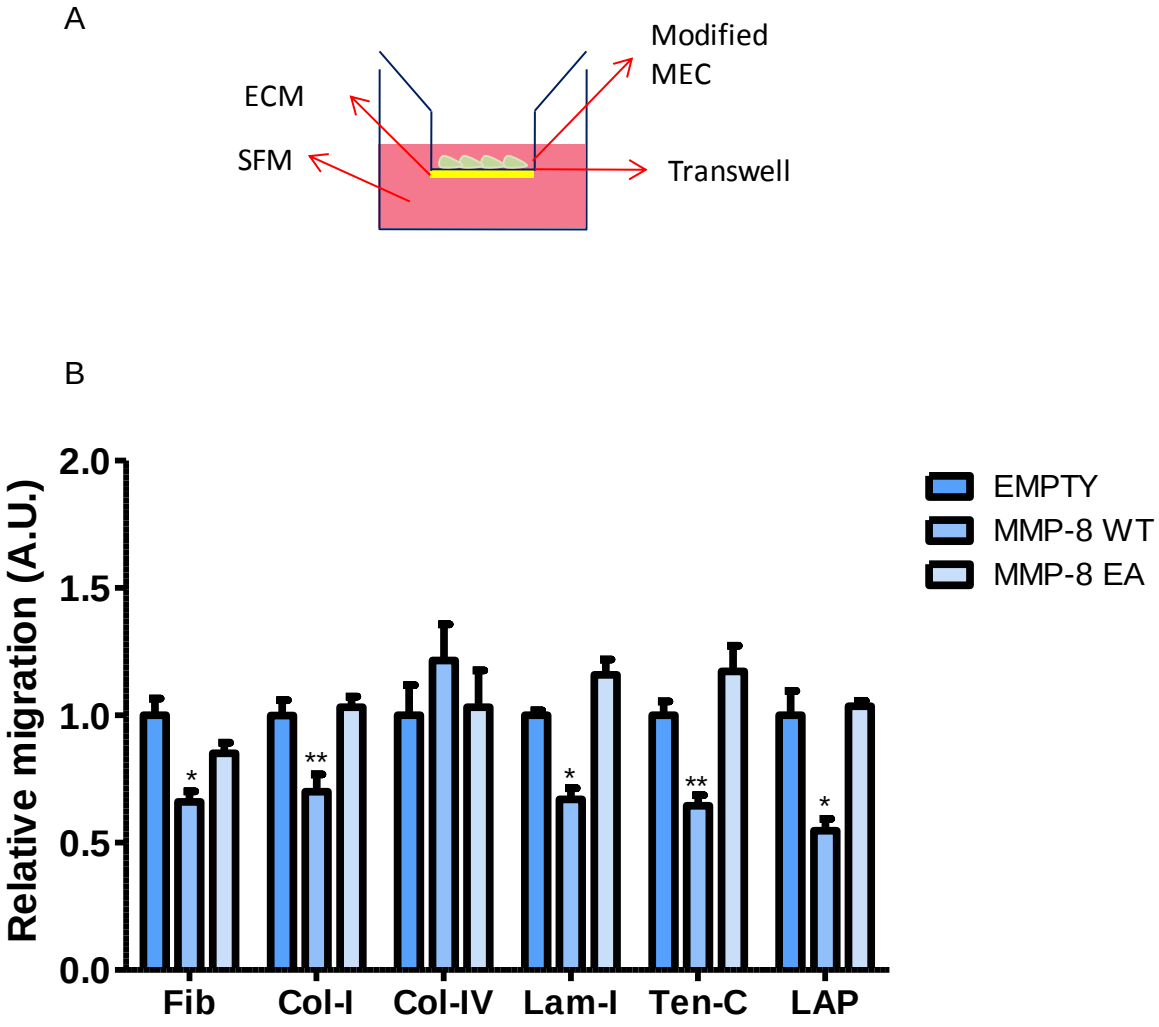

Figure 3-7: Effect of MMP-8 on migration towards ECM. A; Migration of modified Myo-β6 cells was analysed using Boyden chamber migration assays with different ECM molecules. B; After 8 hours incubation the total cell number and migrated cell number were counted and percentage migration was calculated. The graph shows a significant decrease in percentage cell migration towards fibronectin, Collagen type-I, laminin-I-I-I, tenascin-C and LAP in MMP-8 WT with no change in migration for MMP-8 EA transfected MEC. Counts were normalised to migration rate of Empty vector control transfected MEC. *, P ≤ 0.05; **, P ≤ 0.01 (Student's *t* test). Error bars show means +/- SEM. A.U., arbitrary unit, Fib., fibronectin, Col-I., Collagen-I, Col-IV., Collagen-IV, Lam-I., laminin-I-I-I, Ten-C., tenascin-C. Data is mean of 3 independent experiments.

3.2.9 Effect of MMP-8 Over-expression on Myoepithelial Hemidesmosome Formation in Myo-β6 Cells

To further assess the mechanism by which MMP-8 exerts its migration suppressor role on MEC, the distribution of the major myoepithelial integrin, -α6β4- was examined by IF. α6β4 integrin is a major component of hemidesmosome structures which are involved in the attachment of the basal cell surface of normal MECs to the BM.

In order to investigate the localisation of α6β4 integrin to HD, modified Myo-β6 cells were grown for 24 hours on fibronectin, fixed and subjected to dual IF for α6β4 and an established hemidesmosomal marker plectin (HD-1) [254] (Figure 3-8). Co-localisation analysis was carried out and normalised to the co-localisation quantified in control Myo-β6 cells. As shown in Figure 3-8, plectin staining revealed characteristic HD “Swiss cheese” like structures and co-localisation analysis on merge images showed that more α6β4 localised to plectin in MMP-8 WT compared to MMP-8 EA ($p=0.04$, $n=3$) and control cells ($p=0.003$, $n=3$) (Figure 3-9). In addition, α6β4 staining also revealed that this integrin can be found at cell membrane protrusions. In order to identify whether these structures represent filopodial protrusions, modified Myo-β6 cells were dual stained immunofluorescently for α6β4 and phalloidin as shown in Figure 3-10. However without dynamic information it cannot be distinguished whether these structures are filopodias or retraction fibres. Therefore hereafter a hybrid label ‘filopodia/retraction fibres’ will be used for these structures.

The higher magnification shows actin protrusions with co-localised α6β4. The quantification of length (Figure 3-11 A) and number (Figure 3-11 B) of each of these structures based on α6β4 staining in MMP-8 WT, MMP-8 EA or Empty vector transfected control cells on at least 4 different fields per condition containing at least 5 cells, revealed that the filopodia/retraction fibres are significantly shorter and fewer in number in MMP-8 WT compared to either EA (length p=0.0001, number p= 0.05, n=3) or Empty vector transfected MEC (length p=0.0001, number p=0.01, n=3). To investigate the spreading of modified Myo-β6 cells, phalloidin staining was further quantified by ImageJ to analyse the area occupied by the cells on fibronectin matrix (Figure 3-11 C). There was a significant increase in cell size in MMP-8 WT over-expressing cells in comparison to MMP-8 EA over-expressing (p=0.0002, n=3) or control vector transfected Myo-β6 cells (p=0.0003, n=3).

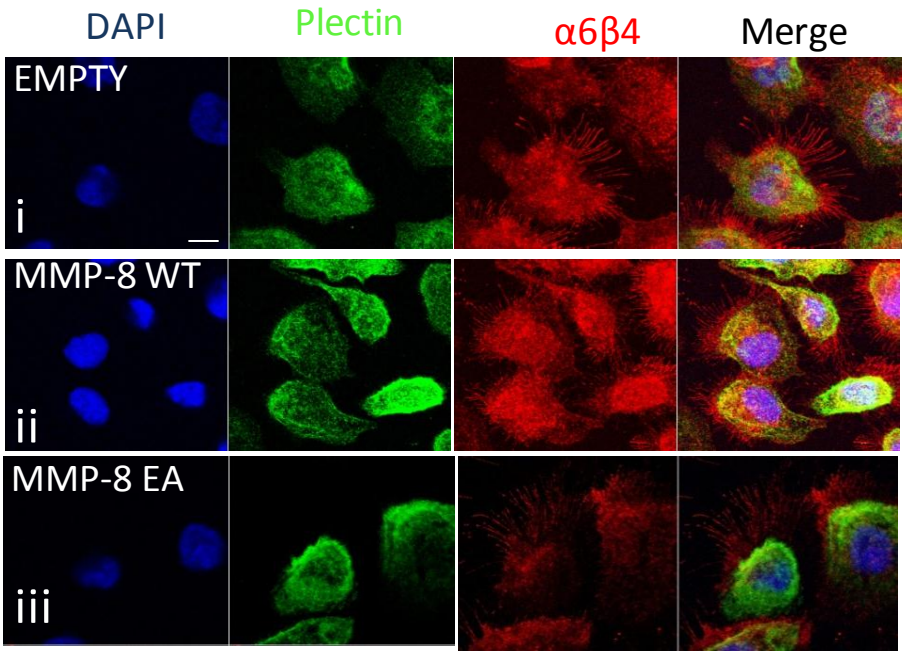

Figure 3-8: Effect of MMP-8 on myoepithelial α6β4 integrin distribution. Confocal sections of modified Myo-β6 cells grown on fibronectin for 24 hours, fixed with 4% PFA and co-stained for plectin (green) and α6β4 (red). Bar, 20μm.

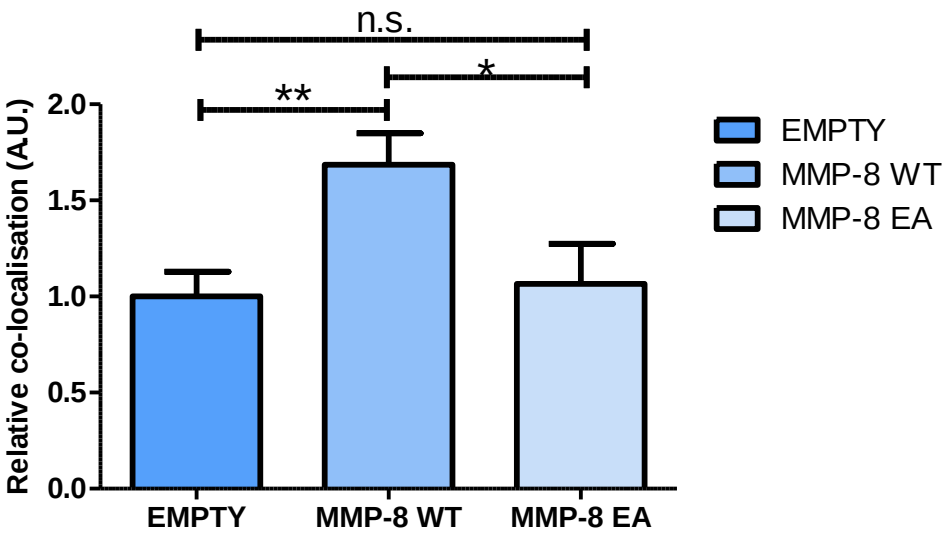

Figure 3-9: Analysis of α6β4 and plectin co-localisation. Co-localisation was analysed. There was a significant increase in α6β4 and plectin co-localisation in MMP-8 WT compared to EA form or Empty vector transfection. Error bars show means +/- SEM. n.s., not significant, A.U., arbitrary unit, data from 3 independent experiments.

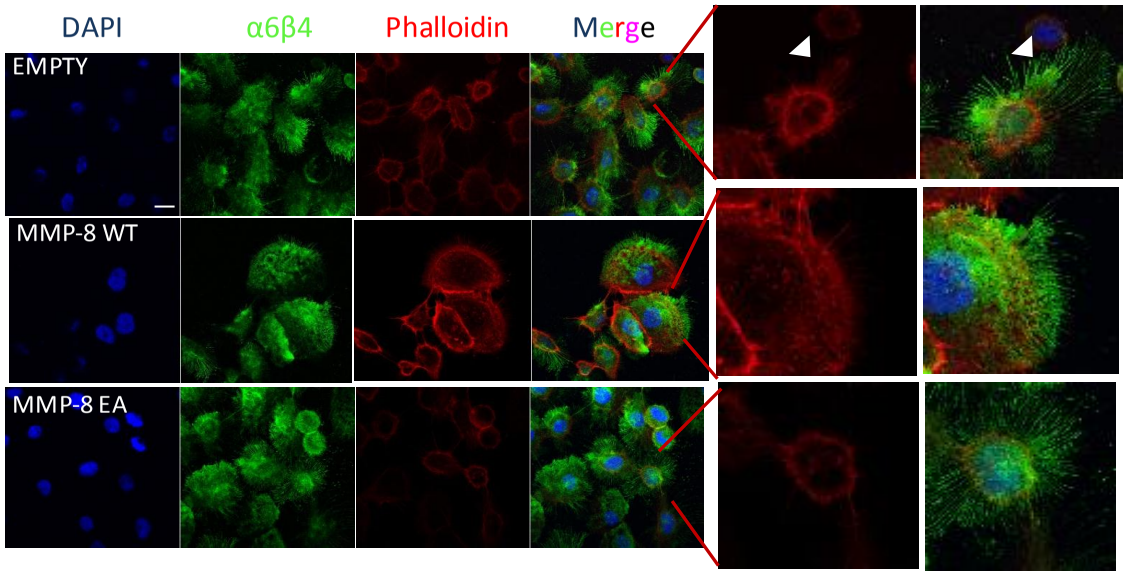

Figure 3-10: Effect of MMP-8 on myoepithelial filopodia/retraction fibre length, number and cell size. A; Modified Myo-β6 cells were grown on fibronectin and co-stained for α6β4 and phalloidin. Staining revealed an altered phenotype in formation of filopodia/retraction fibres in MMP-8 WT transfected Myo-β6 cells. Bar, 50μm. Representative for 3 independent experiments.

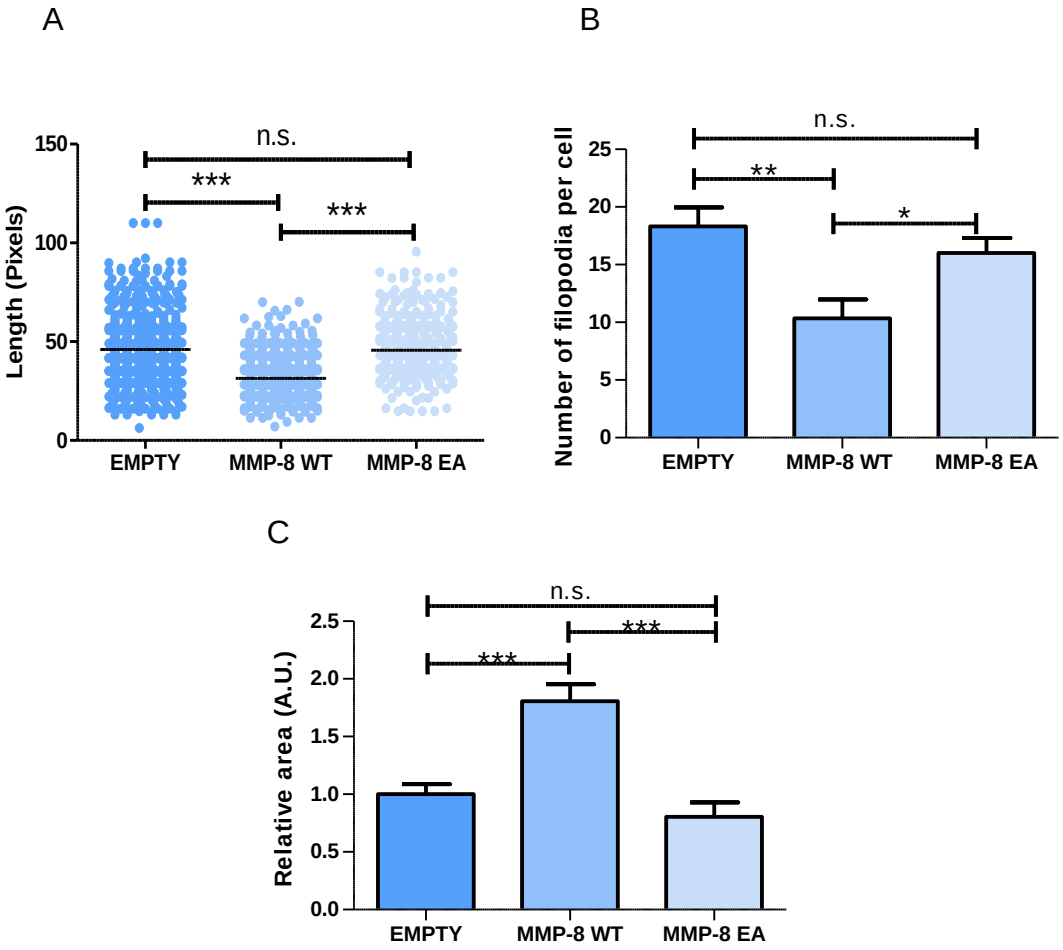

Figure 3-11: Effect of MMP-8 on myoepithelial filopodia/retraction fibre length, number and cell size. A; Length of each filopodia/retraction fibre of at least 5 different cells in a minimum of 4 different fields was measured using ImageJ. A significant decrease in overall filopodia/retraction fibre length was observed in MMP-8 WT compared to EA or Empty vector transfected Myo-β6 cells. B; The number of filopodia/retraction fibre per cell was calculated for each field by dividing the filopodia/retraction fibre number by cell number in each field and showed a significant reduction in MMP-8 WT compared to EA or control vector transfected Myo-β6 cells. C; Cell spreading on fibronectin was quantified by ImageJ as area occupied by cells based on phalloidin staining and normalised to the occupied area of the Empty vector transfected Myo-β6 cells. There was a significant increase in area occupied by MMP-8 WT transfected cells compared to EA or Empty vector transfected cells. *, $P \leq 0.05$, **, $P \leq 0.01$; ***, $P \leq 0.001$ (Student's *t* test). Error bars show means +/- SEM. A.U., arbitrary unit, representative for 3 independent experiments.

3.2.10 Effect of MMP-8 Over-expression on MMP-9 Expression and Function in Myo-β6 Cells

Previous work in our lab has shown that over-expression of αvβ6 – which appears to be associated with down-regulation of MMP-8 – leads to increased MMP-9 expression. Therefore, in order to analyse the alterations in MMP-9 expression in Myo-β6 cells upon MMP-8 WT , EA or Empty vector transfection, total mRNA were harvested from modified Myo-β6 cells 24 hours after transfection and subjected to QRT-PCR. Experiments were performed a minimum of 3 times. There was no significant change in MMP-9 expression at mRNA level in Myo-β6 cells after transfected with MMP-8 WT or MMP-8 EA compared to Empty vector transfection (MMP-8 WT p=0.552, MMP-8 EA p=0.807) (Figure 3-12).

To evaluate the effect of MMP-8 over-expression on proteolytic activity of MMP-9, modified Myo-β6 cells were seeded on rhodamine-conjugated gelatine coated coverslips as described in Section 2.14 and incubated for 24 hours. After incubation the cells were fixed and stained with FITC-conjugated phalloidin (Figure 3-13). The area of degraded gelatine was quantified by ImageJ and demonstrates a significant reduction in gelatine degradation in MMP-8 WT compared to EA form (p=0.03, n=3) or Empty vector (p=0.002, n=3) transfected cells (Figure 3-14 A). There was no difference in cell number per field between different transfection groups (n=3) (Figure 3-14 B).

To confirm the effect of MMP-8 over-expression on MMP-9 function, modified MECs were starved for 24 hours and CM were prepared, and then subjected

to gelatine zymography as described in Section 2.10 (Figure 3-15 A). Densitometric analysis of lytic bands was done using ImageJ and normalised to Empty vector transfection. There was a decrease in the lytic band corresponding to MMP-9 in Myo-β6 cells transfected with MMP-8 WT compared to Empty vector controls ($p=0.057$, $n=4$) and MMP-8 EA carrying Myo-β6 cells ($p=0.067$, $n=4$), but this decrease was not significant (Figure 3-15 B). There was no lytic band detected corresponding to MMP-2 activity (Figure 3-15 B).

Recombinant MMP-9 was used as a control, however, bands generated from this were inconsistent. In the absence of a gelatinolytic band, the MW ladder was used to identify the size of the lytic bands from the samples.

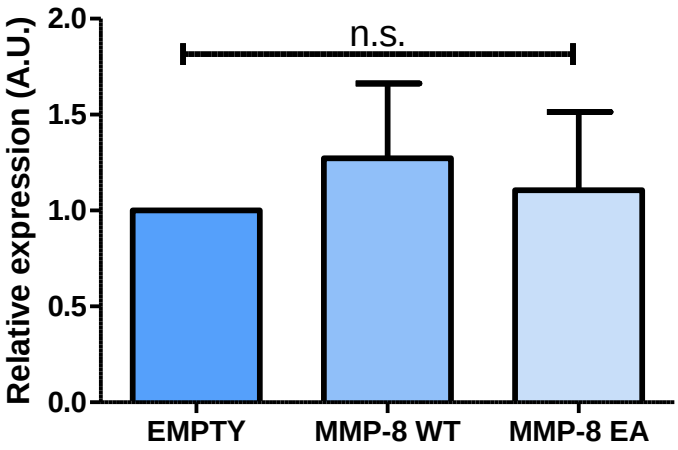

Figure 3-12: Effect of MMP-8 over-expression on MMP-9 expression at mRNA level. QRT-PCR targeting MMP-9 mRNA showed that there was no significant difference in MMP-9 mRNA level in MMP-8 WT or MMP-8 EA transfected Myo-β6 cells compared to Empty vector transfected Myo-β6 cells 24 hours after transfection. Error bars show means +/- SEM. n.s., not significant, A.U., arbitrary unit, representative for 3 independent experiments.

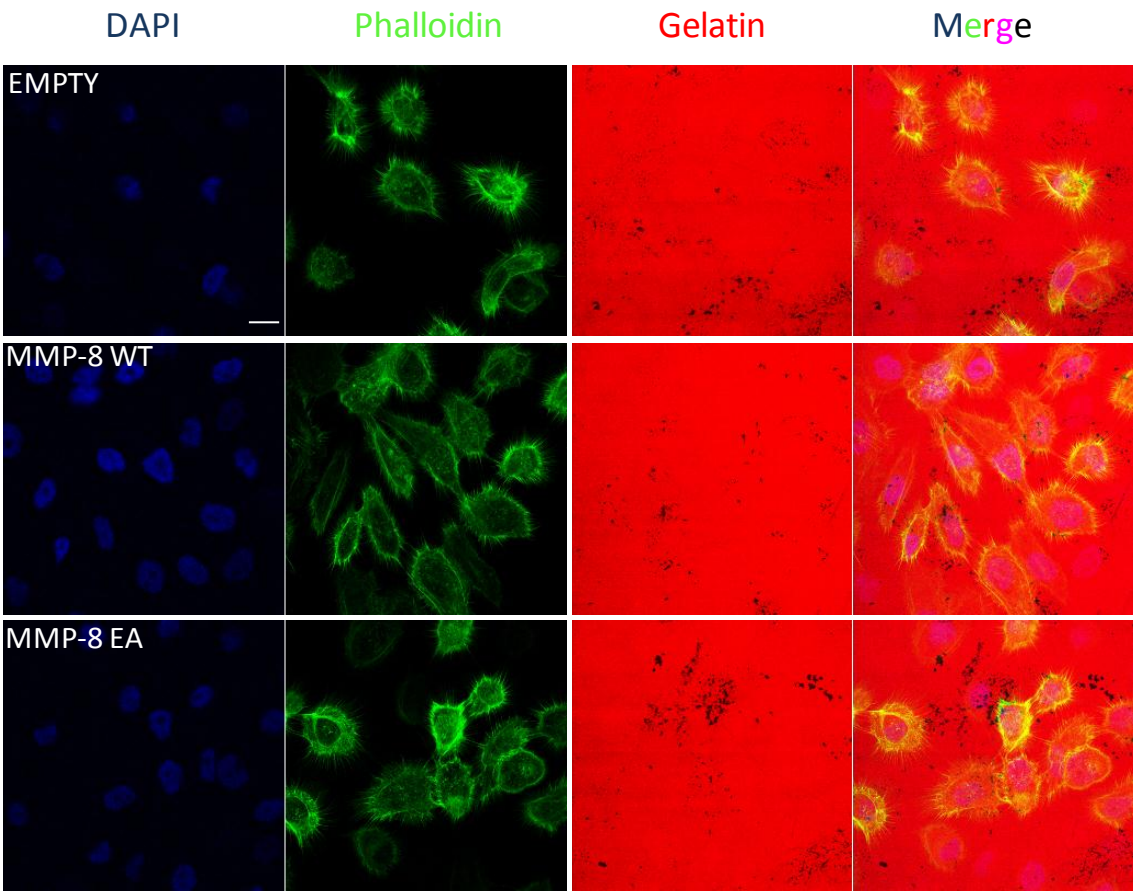

Figure 3-13: Effect of MMP-8 over-expression on gelatine degradation in *in vitro* zymography. MMP-8 WT, MMP-8 EA or EMPTY vector transfected Myo-β6 cells were seeded on rhodamine tagged (fluorescently red) gelatine and incubated for 24 hours, then fixed with 4%PFA and stained for FITC-tagged phalloidin as described in Section 2.14. Degraded gelatine appeared as black dots on red background. Bar, 50μm.

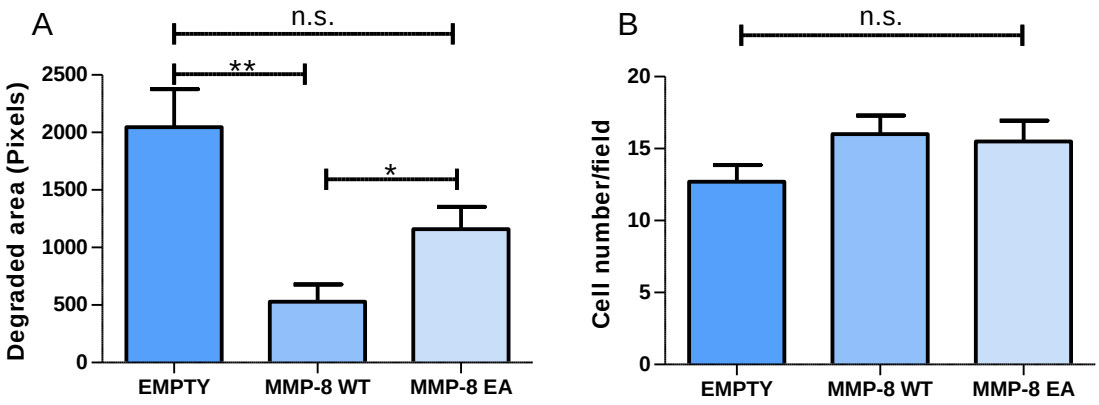

Figure 3-14: Quantification of the effect of MMP-8 over-expression on gelatine degradation in *in vitro* zymography. A; 10 pictures were taken per coverslip and gelatine degradation was quantified as the total area of black dots occupied per field. There was a significant reduction in fluorescent gelatine degradation in MMP-8 WT but not in MMP-8 EA when compared to Empty vector transfected control cells. B; the cell number per field was counted and no significant difference was observed among MMP-8 WT, MMP-8 EA or Empty vector transfected cells. *, P ≤ 0.05, **, P ≤ 0.01; (Student's *t* test). Error bars show means +/- SEM. representative of 3 independent experiments

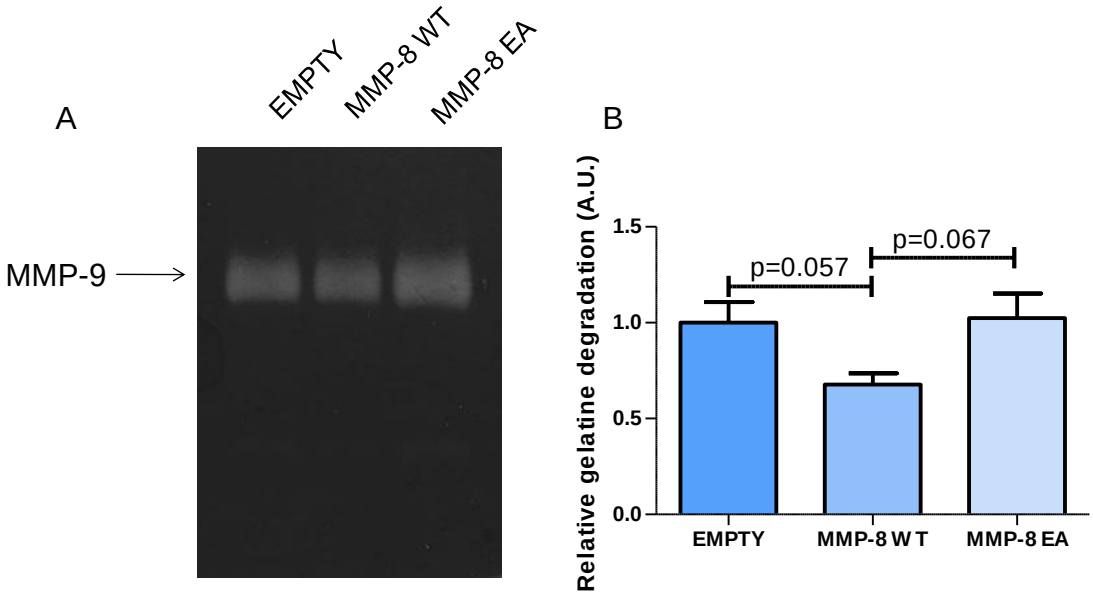

Figure 3-15: Effect of MMP-8 over-expression on gelatine degradation in gel zymography. A; CM were collected from modified and 24 hours serum starved Myo-β6 cells and gelatine zymography was run as described in Section 2.10. Degraded gelatine bands correspond to MMP-9 activity. No bands for MMP-2 were observed. B; Densitometric analysis was done with ImageJ and normalised to the Empty vector transfected control cells. There was a non-significant decrease in MMP-9 activity in MMP-8 WT carrying Myo-β6 cells compared to other transfection groups (p values, student's *t* test). Error bars show means +/- SEM. A.U., arbitrary unit, representative for 4 independent experiments.

3.2.11 MMP-8 Expression Knock-down in Myo-Puro Cells

In order to study the loss-of-function effect of MMP-8 in a normal myoepithelial system, endogenous MMP-8 was knocked down using siRNA targeting MMP-8 mRNA in Myo-Puro cells as explained in Section 2.5, and siRNA targeting luciferase mRNA (siLUC) was used as a control. To evaluate MMP-8 expression after siRNA treatment, total RNA and protein was harvested 96 hours after transfection, then QRT-PCR and WB was run. QRT-PCR results showed a significant loss in MMP-8 expression upon MMP-8 siRNA treatment (p=0.0025, n=3) (Figure 3-17 A) compared to control siRNA transfected Myo-Puro cells. WB results confirmed a loss in MMP-8 expression after MMP-8 siRNA treatment (Figure 3-17 B).

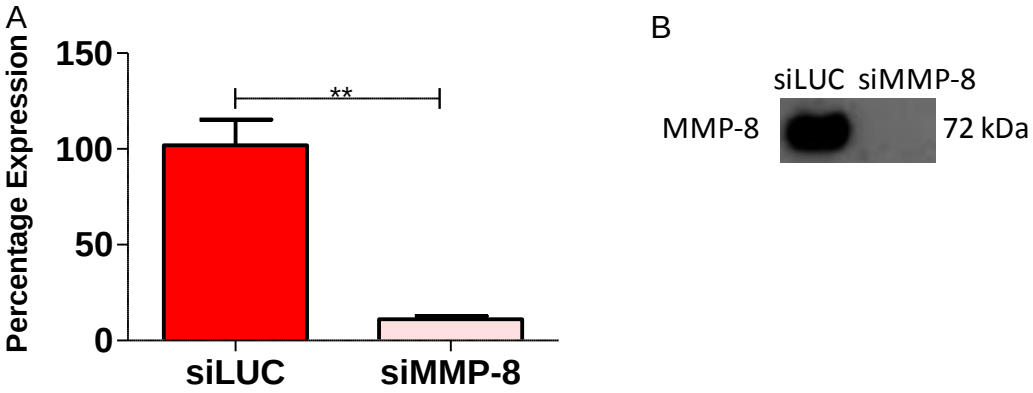

Figure 3-16: Knock-down of MMP-8 expression in Myo-Puro cells using MMP-8 siRNA. A; MMP-8 expression was knocked down by siRNA treatment as described in Section 2.5. MMP-8 expression was checked at RNA level and protein level 96 hours after transfection. QRT-PCR targeting MMP-8 mRNA was run, MMP-8 expression was significantly reduced at RNA level following siRNA transfection. B; Conditioned media was prepared for WB as described in Section 2.4 and subjected to WB. MMP-8 expression was lost at protein level. **, P ≤ 0.01; (Student's *t* test). Error bars show means +/- SEM., representative for 3 independent experiments.

3.2.12 The Effect of MMP-8 Knock-down on Myo-Puro Proliferation

To explore whether MMP-8 loss has an effect on Myo-Puro cell proliferation, proliferation rates were determined in modified Myo-Puro cells as described in Section 2.9. There was no difference in proliferation in siMMP-8 transfected Myo-Puro cells in comparison to siLUC transfection (Figure 3-18) (p=0.4, n=3).

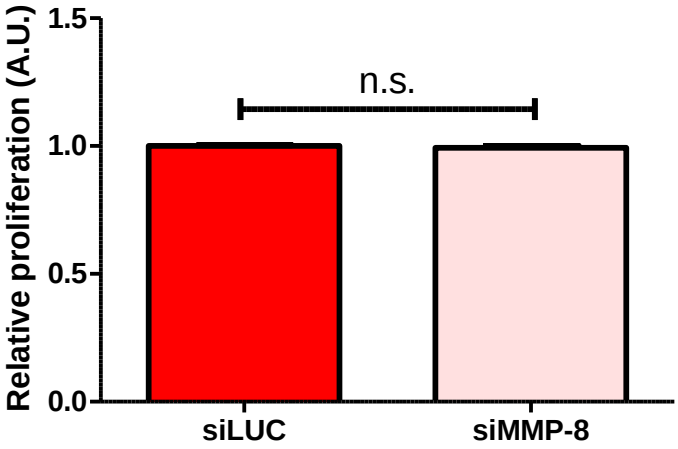

Figure 3-17: Effect of MMP-8 loss on Myo-Puro proliferation. Myo-Puro cells were grown for 24 hours and proliferation was analysed by MTS assay as described in Section 2.9. There was no significant difference in siMMP-8 treated Myo-Puro cells when compared to control group. A.U., arbitrary unit, n.s., not significant, representative for 3 experiments.

3.2.13 Effect of MMP-8 Knock-down on Myo-Puro Adhesion

To explore the impact of MMP-8 loss in the normal MEC system on cell-ECM interactions, myoepithelial adhesion to several ECM molecules was assessed. MMP-8 or control siRNA (siLUC) transfected Myo-Puro cells were seeded on ECM coated wells of a 96 well plate as described in Section 2.12. Experiments were repeated a minimum of 3 times. Myoepithelial adhesion to fibronectin (p=0.01), Collagen-I (p=1.1E-06), Collagen-IV (p=0.0003), laminin I-I-I (p=0.004) and tenascin-C (p=0.003) was significantly reduced in the absence of MMP-8 compared to control siRNA tranfected cells (Figure 3-19). Interestingly there was no significant difference in adhesion to the αvβ6 ligand LAP (p=0.32).

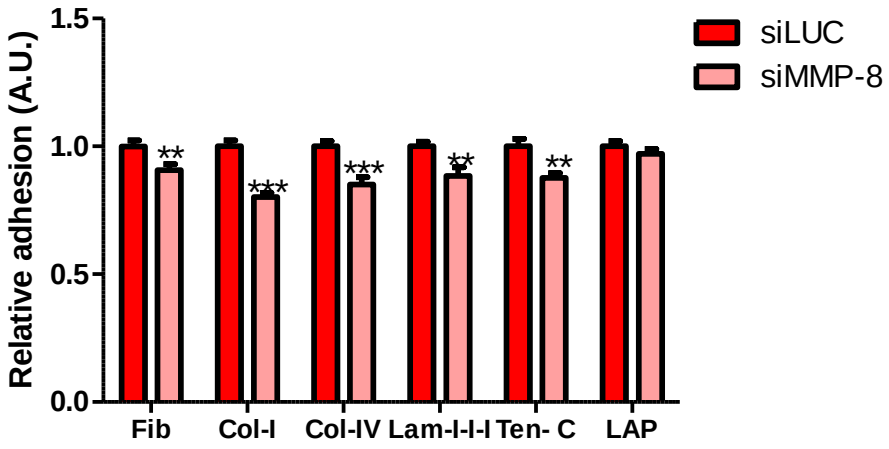

Figure 3-18: Effect of MMP-8 loss in normal Myo-Puro cell line on myoepithelial adhesion to several ECM molecules. Myoepithelial adhesion to ECM was evaluated as described in Section 2.12 and normalised to siLUC transfected control cells. Adhesion to fibronectin, Collagen-I, Collagen-IV, laminin-I-I-I and tenascin-C was significantly reduced in MMP-8 siRNA transfected cells. No significant difference in adhesion to LAP. **, P ≤ 0.01; (Student's *t* test). Error bars show means +/- SEM. A.U., arbitrary unit, Fib., fibronectin, Col-I., Collagen-I, Col-IV., Collagen-IV, Lam-I., laminin-I-I-I, Ten-C., tenascin-C, representative for 3 independent experiments.

3.2.14 Effect of MMP-8 Knock-down on Myo-Puro Migration

MEC migration was studied using Boyden chamber assays in which MMP-8 siRNA or control siRNA transfected Myo-Puro cells were separated from different ECM molecules by a transwell membrane and incubated for 8 hours as described in Section 2.15. All experiments were repeated a minimum of 3 times. MMP-8 loss resulted in a significant increase in the percentage of cells migrating towards Collagen-IV (0.001), laminin-I-I-I (p=8.9E-5), tenascin-C (p=0.002) but not to fibronectin (p=0.64), Collagen-I (p=0.70) and LAP (p=0.81) (Figure 3-20).

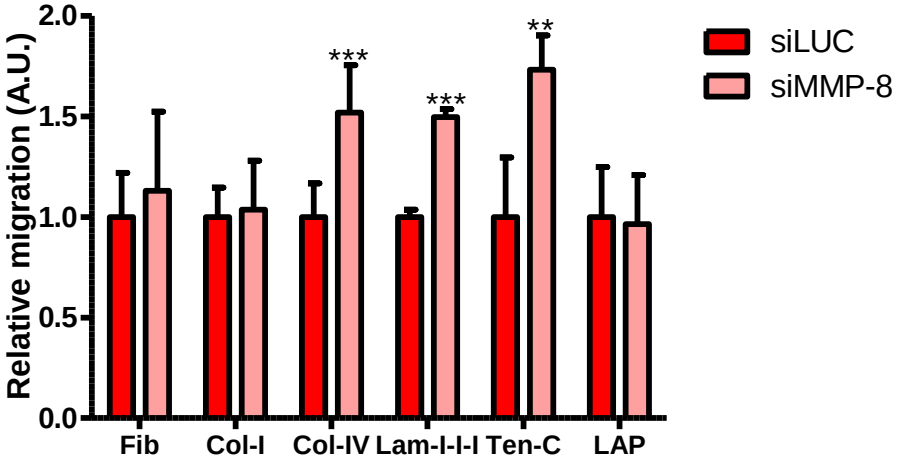

Figure 3-19: Effect of loss of MMP-8 expression in Myo-Puro cells on migratory behaviour. Transwell migration assays were performed and quantified as described in Section 2.15. There was a significant increase in percentage cell migration towards Collagen-IV, laminin-I-I-I, tenascin-C, no significant difference was determined for other ECM molecules. ***, P ≤ 0.001 (Student's *t* test). Error bars show means +/- SEM. n.s. not significant, Fib., fibronectin, Col-I., Collagen-I, Col-IV., Collagen-IV, Lam-I., laminin-I-I-I, Ten-C., tenascin-C, representative for 3 independent experiments.

3.2.15 Effect of MMP-8 Knock-down on Myo-Puro Filopodia/Retraction Fibre Formation

Investigation of filopodia/retraction fibre formation was performed as described in Section 2.18 and 3.3.7 by staining the modified Myo-Puro cells with α6β4 integrin and phalloidin after 24 hour incubation on fibronectin (n=3) (Figure 3-21 A). In each experiment at least 4 different fields containing at least 5 cells were quantified per condition. The quantification of filopodia/retraction fibre length (Figure 3-21 B) and number (Figure 3-21 C) was undertaken on α6β4 staining by ImageJ. There was a significant increase in filopodia/retraction fibre length ($p=0.0009$) and filopodia/retraction fibre number per cell ($p=0.05$) in MMP-8 knock-down Myo-Puro cells when compared to siLUC transfected Myo-Puro cells.

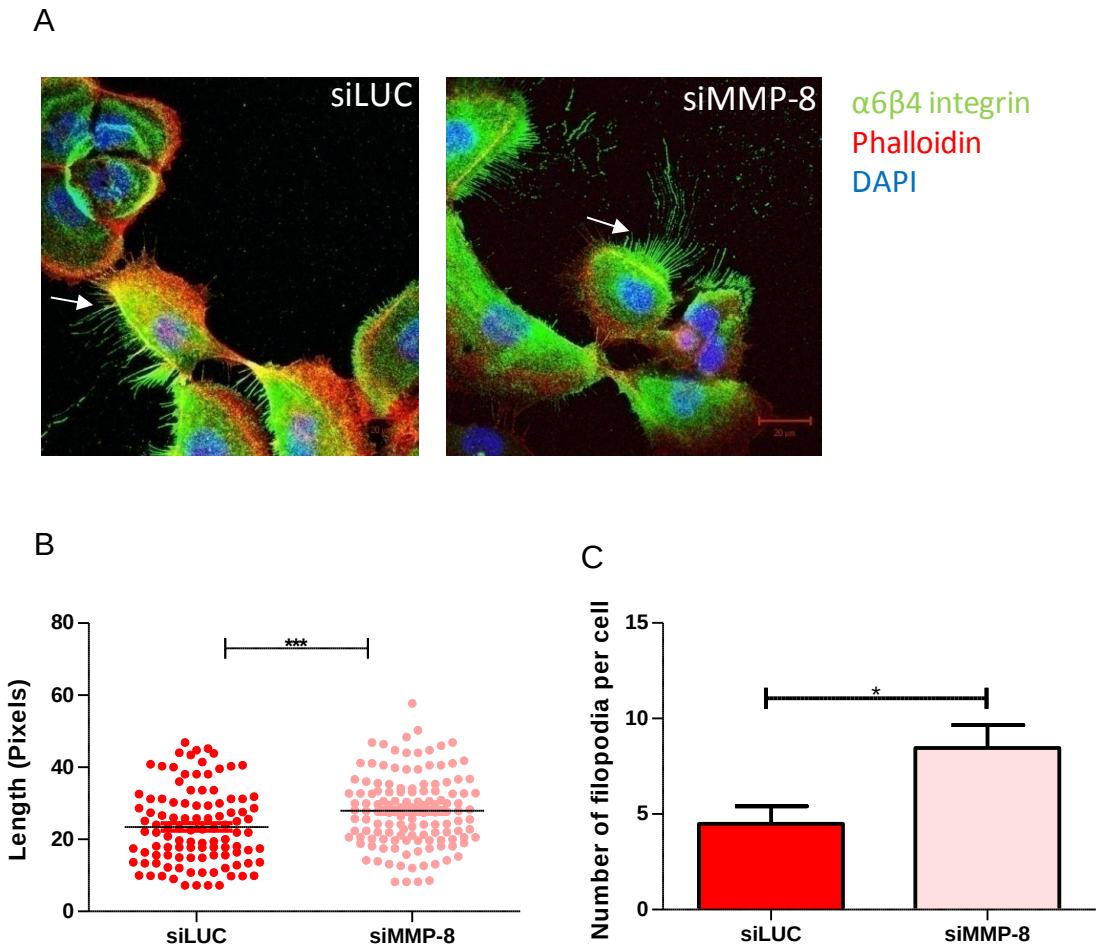

Figure 3-20: Effect of MMP-8 loss in Myo-Puro cells on filopodia/retraction fibre length and number. A; Filopodia/retraction fibre formation (arrows) analysis staining in modified Myo-Puro cells was done as described in 2.18 and 3.3.7. For each condition at least 4 different fields containing at least 5 cells were quantified by ImageJ. Bar 20µm. B; Filopodia/retraction fibre length and C; number was significantly increased in siMMP-8 transfected Myo-Puro cells compared to Myo-Puro cells transfected with siLUC. *, $P \leq 0.05$, ***, $P \leq 0.001$ (Student's *t* test). Error bars show means +/- SEM., representative for 3 independent experiments.

3.2.16 Impact of MMP-8 Loss on MMP-9 Protease Function in Myo-Puro Cells

To evaluate whether MMP-8 loss has an impact on MMP-9 activity; MMP-8 or control siRNA transfected cells were seeded on rhodamine conjugated gelatine (red), incubated for 24 hours and stained for phalloidin (green) and DAPI (blue) (Figure 3-22 A). All experiments were done 3 times. The gelatine degradation was quantified as the total black (degraded) area on red background by ImageJ in at least 10 different fields per condition as described in Section 2.14. Gelatine degradation was significantly greater for MMP-8 knock-down Myo-Puro cells in comparison to the control cell group ($p=0.007$) (Figure 3-22 B). Cell number was counted for every field analysed and revealed no significant difference between MMP-8 knock-down or control siRNA treated groups indicating that enhanced gelatine degradation was not a result of increased cell number ($p=0.65$, $n=3$) (Figure 3-22 C). Furthermore, enhanced gelatinase activity could be inhibited by MMP-9 siRNA or MMP-9 inhibitor (Section 3.2.9).

The level of proteolytic activity was further studied by gel zymography, in which CM samples collected from modified Myo-Puro cell populations were run on a gelatine gel zymography (Figure 3-23 A). Cell counts of modified Myo-Puro cells were counted when CM was collected and showed no significant difference (data not shown), therefore equal volume of CM from each condition was loaded on the gel. Recombinant MMP-2 and recombinant MMP-9 were loaded as positive controls however inconsistent bands were

observed. In order to determine the MW, protein ladder was used (data not shown). Densitometric analysis of the lytic bands was done by ImageJ. MMP-2 levels did not differ ($p=0.986$, $n=3$). There was an increase in MMP-9 activity in siMMP-8 treated Myo-Puro cells when compared to control group, however, this did not reach significance ($p=0.060$, $n=3$) (Figure 3-23 B).

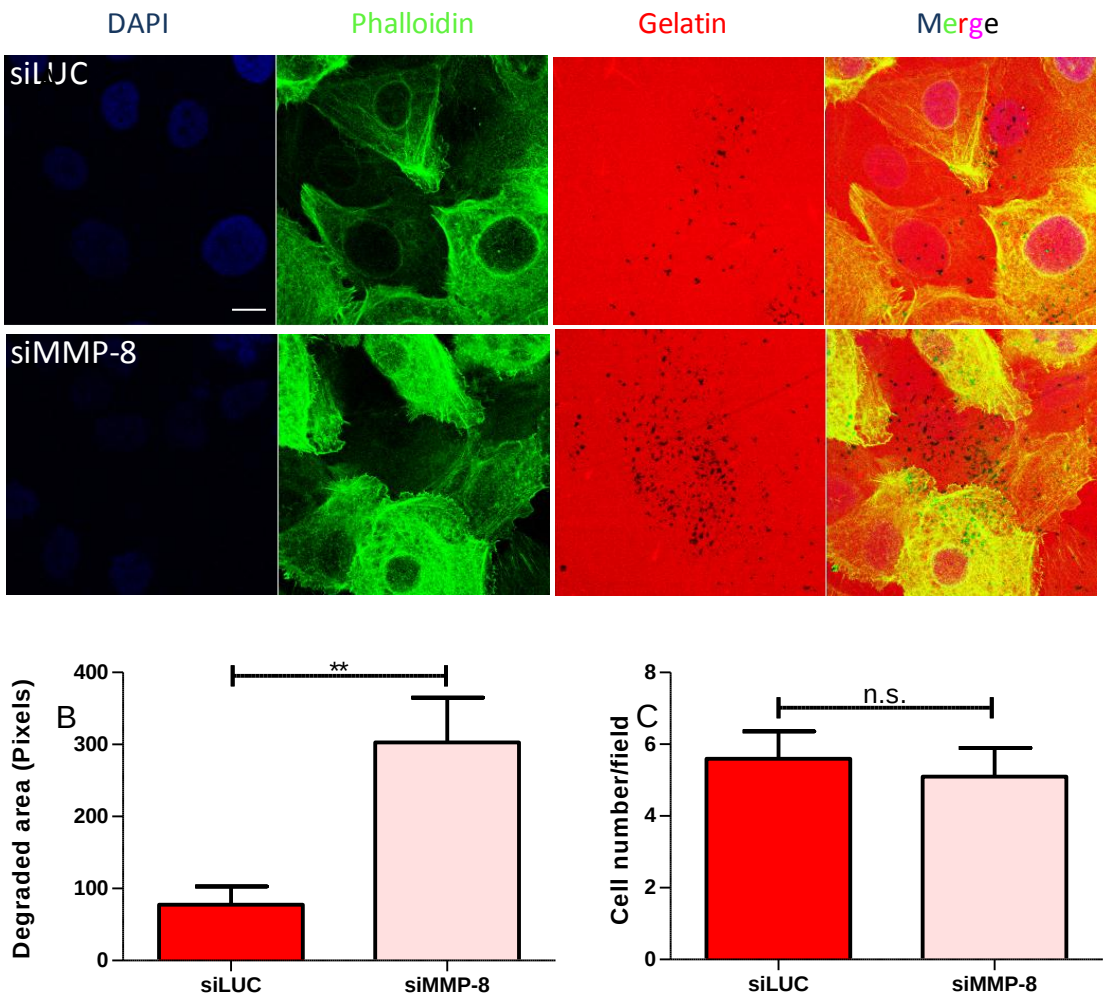

Figure 3-21: Effect of MMP-8 knock-down on gelatine degradative activity of Myo-Puro cells in *in vitro* zymography. A; siLUC or siMMP-8 treated Myo-Puro cells were seeded on rhodamine tagged gelatine and incubated for 24 hours, fixed and stained for FITC-conjugated phalloidin described in Section 2.15. The total area of degraded gelatine (black dots on red gelatine) was analysed on 10 fields by using ImageJ and normalised to the degraded area found in Myo-Puro cells transfected with siLUC. Bar 10µm. B; Degraded area was significantly increased in MMP-8 knocked down cells. C; Cell counts per each field revealed that there was no significant difference between siMMP-8 treated or control groups. **, P ≤ 0.01; (Student's *t* test). Error bars show means +/- SEM, n.s., not significant, representative for 3 independent experiments.

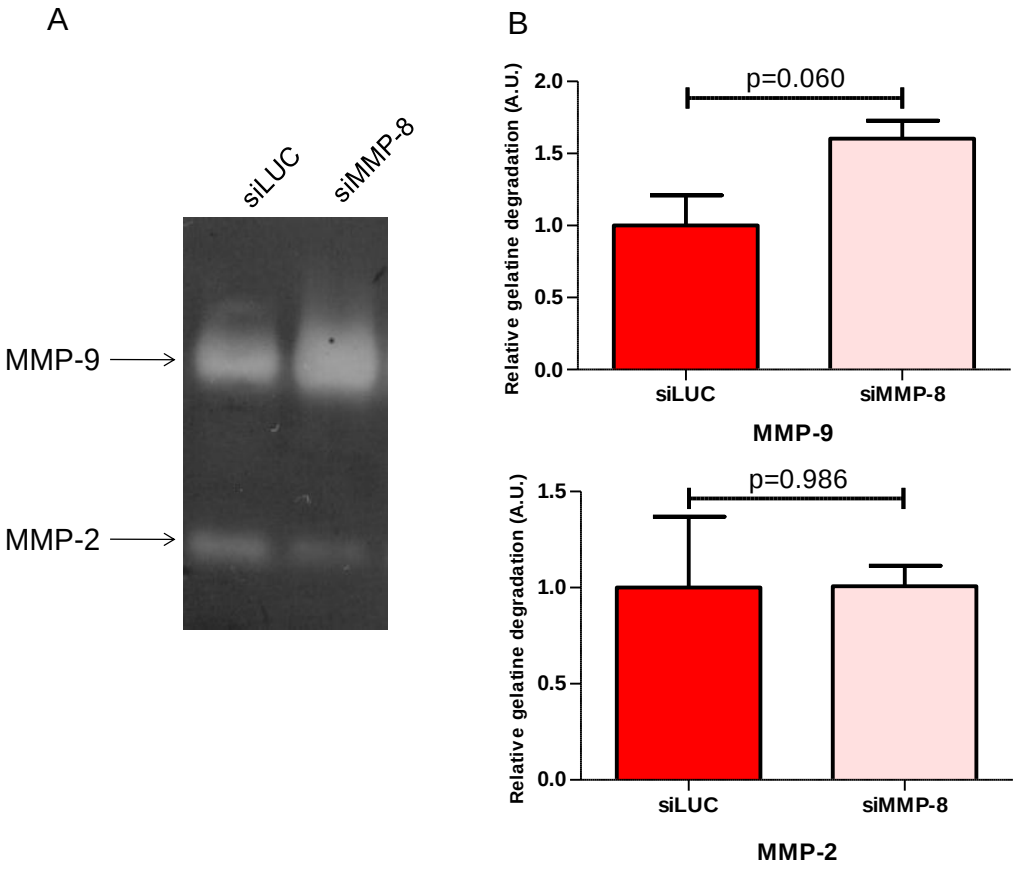

Figure 3-22: Effect of MMP-8 knock-down on MMP-9 and MMP-2 activity in gel zymography. A; CM were collected from modified Myo-Puro cells after 24 hours serum starvation and subjected to gelatine zymography as described in Section 2.10. Bands corresponding to MMP-9 and MMP-2 were observed. B; Quantification was done by the densitometric analysis of the degraded gelatine bands with ImageJ. There was an increase in MMP-9 activity upon MMP-8 knock-down, but this was not significant. There was no significant alteration in MMP-2 levels (p values, student's *t* test). Error bars show means +/- SEM. A.U., arbitrary unit, representative for 3 independent experiments.

3.2.17 The Effect of Inhibition of MMP-9 Activity on Gelatine Degradation of Modified Myo-Puro Cells

In order to analyse whether MMP-9 activity is involved in enhanced gelatine degradation upon MMP-8 loss in Myo-Puro cells (Section 3.2.18), MMP-9 was knocked down by siRNA treatment in the Myo-Puro cells transfected with MMP-8 siRNA (MMP-9 knock-down was verified by RT-PCR -data not shown) or the cells were treated with an MMP-9 inhibitor as described in Section 2.5. Figure 3.25 shows that the gelatine degradation was significantly down-regulated upon MMP-9 knock-down in siMMP-8 treated Myo-Puro cells ($p=0.0003$). In addition, there was a gradual decrease in degraded gelatine area, in relation to increasing concentrations of MMP-9 inhibitor (50nm MMP-9 inhibitor, $p=0.0005$, 100nm inhibitor $p=2.66E-05$). There was no difference in DMSO vehicle only control in gelatine degradation compared to siMMP-8 treatment suggesting that the increased gelatine degradation is derived from increased MMP-9 activity after MMP-8 knock-down. Unfortunately due to time constraints this experiment was performed only once, with analysis of 10 different fields from each condition.

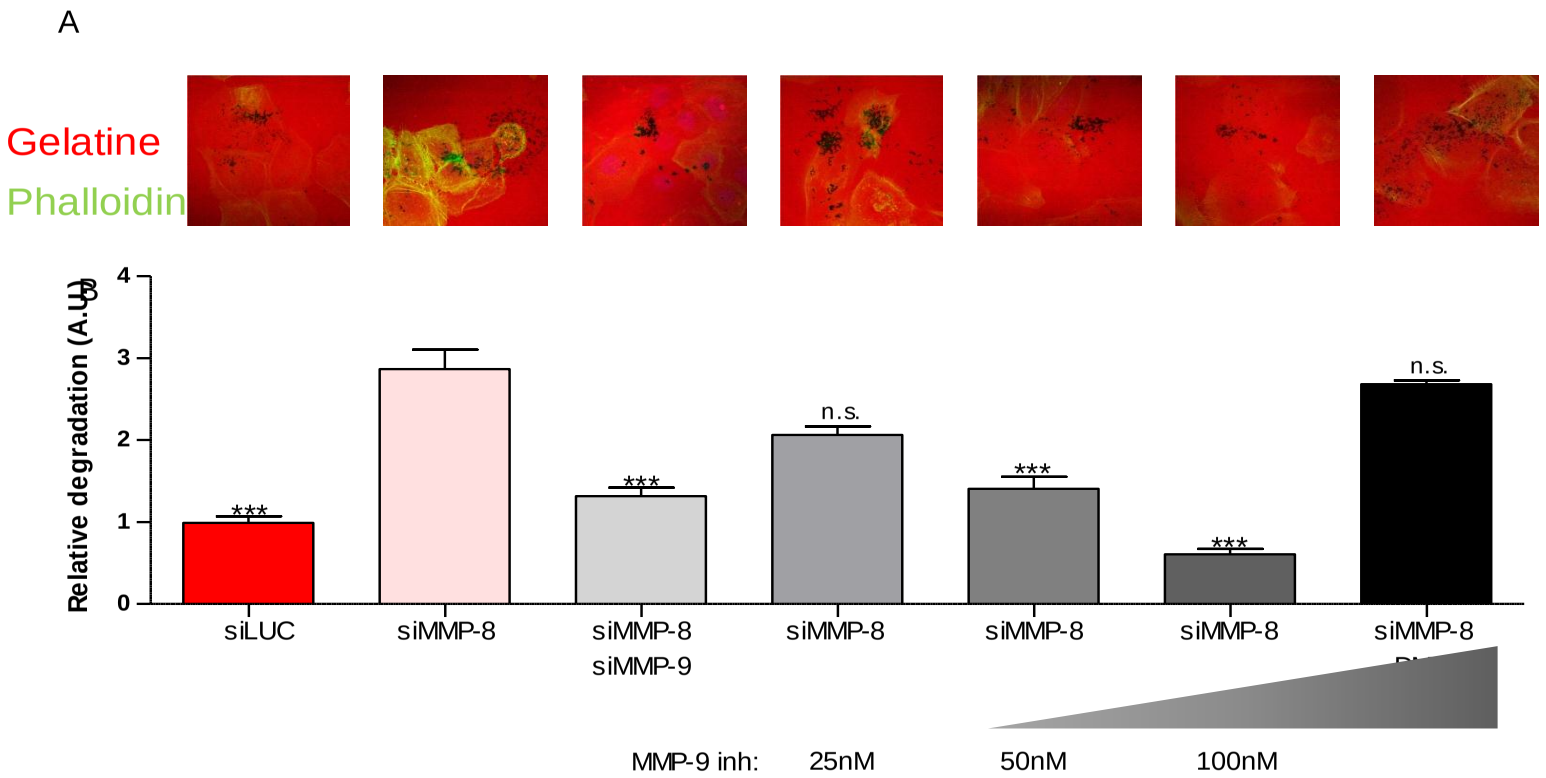

Figure 3-23: Effect of MMP-9 knock-down or inhibition on gelatine degradation in MMP-8 siRNA treated Myo-Puro cells. A; *In vitro* zymography assay was done as described in materials and methods. Images match with the graphic column in Bar 20µm. B; There was a significant decrease in gelatine degradation in MMP-8 and MMP-9 double knock-downs when compared to MMP-8 only knocked down cells. There was also reduced gelatine degradation by MMP-8 knock-down Myo-Puro cells treated with an MMP-9 inhibitor, with a step-wise reduction in degradation evident with increasing inhibition concentration. No significant difference in gelatine degradation was observed when MMP-8 siRNA treated Myo-Puro cells were incubated with DMSO vehicle. A.U., arbitrary unit, n.s., not significant, representative for 1 experiment.

3.3 Discussion

3.3.1 Culturing of Myo-β6 and Myo-Puro Cells

The cell lines used to model normal and DCIS-associated MEC were Myo-Puro and Myo-β6, respectively. The parental cell line from which these were derived was an h-TERT immortalised MEC line (MEC 1089) [294] derived from reduction mammoplasty material. This cell line consists of a mixture of MECs which express high, intermediate or low levels of α6β4 integrin. These cells were subjected to a selection procedure with an α6β4 integrin antibody on magnetic beads to enrich the cells which have high α6β4 integrin expression. It was found that this sub-population exhibited expected characteristics of MECs including expression of P-cadherin, CK17 and Dsg3. Previous work in our lab has shown that DCIS-associated MECs exhibit an altered phenotype with the most consistent change being up-regulation of αvβ6 integrin. Experimental work demonstrated that this is a functionally relevant change, and alters MEC tumour suppressor function. Therefore in order to establish a DCIS model this α6β4 enriched myo-1089 population was transfected with a retroviral vector containing a β6 integrin insert and further sorted using αvβ6 integrin antibody-coated magnetic beads to select αvβ6 integrin over-expressing cells. The cell line generated here was called Myo-β6 cells and represents αvβ6 up-regulated DCIS MECs. A control retroviral system (Empty vector) was also used and these cells were used as a normal breast MEC model and called Myo-Puro.

Myo-β6 and Myo-Puro cells show a drift in their myoepithelial phenotype over time *in vitro*. Most notably, the α6β4 integrin expression is down-regulated. Therefore these cell lines are regularly selected for α6β4 integrin expression. In order to maintain the difference in αvβ6 expression between Myo-β6 and Myo-Puro cells, they are subjected to a routine re-sorting protocol in which Myo-β6 cells were positively selected for αvβ6 whereas Myo-Puro cells were negatively selected. The confluency of the cell lines also increases the αvβ6 integrin expression. The cell lines were grown at no more than 70% confluency. By rigorously controlling culture conditions and regular selection, a consistent phenotype reflecting normal and DCIS-associated MEC was maintained throughout the study.

Initial experiments carried out by a colleague (Dr M. Allen) compared behaviour of these cell lines to primary MEC population and, showed they exhibit similar behaviour *in vitro* (Prof. L. Jones personal communication).

3.3.2 Source of MMP-8 in Normal and DCIS Breast

MECs isolated from normal breast were confirmed to be the source of MMP-8 and the loss of MMP-8 in DCIS associated MECs was demonstrated by QRT-PCR run on mRNA extracted from primary cells.

In an earlier study investigating the expression of MMP-8 in breast tissue, we found on IHC that MMP-8 localised to the MEC-BM interface in normal breast ducts but was not detected in ducts containing DCIS [215].

Unfortunately the antibody used in that study is no longer available. Therefore a series of other antibodies were tested for IHC staining on FFPE or frozen tissues using a number of antigen retrieval techniques; for frozen samples no antigen retrieval was done. For all antibodies used, high level of background staining was observed and no specific staining was present (data not shown), which implies that the MMP-8 antibodies available were not adequate for using in IHC staining. Whilst disappointing, there are limitations to using IHC to detect MMPs: IHC shows the localisation of the protein which may not reflect the cell type making the protein. MMPs are secreted proteins therefore, in order to detect MMP-8 at mRNA level in tissue samples, an *in situ* hybridization (ISH) approach was planned; a specific region in the MMP-8 mRNA sequence that would allow generation of an ISH probe was investigated. The great similarity shared between MMP family members made it difficult to identify an MMP-8-specific region. A region spanning exon 10 was identified as potentially specific for MMP-8; however PCR on normal MECs or Myo-Puro targeting this region did not generate a product (data not shown). This may be a result of alternative splicing, known to affect both exon 8 and exon 10 (Personal communication Prof. Dylan Edwards) and therefore this was not pursued further. Therefore primary normal breast and DCIS associated MECs, LECs and fibroblasts were purified and QRT-PCR was done. This technique is a powerful approach to investigate the source of a secreted protein since it allows discrimination of the cell group expressing the mRNA. The MMP-8 transcript has a low copy number therefore a nested PCR approach was taken. The total mRNA was isolated from freshly purified cells before passaging therefore these cells

provide conditions close to *in vivo*. This analysis confirmed the MEC population to be the source of MMP-8 in normal breast, with lack of expression in MEC isolated from DCIS.

Having shown that normal MEC are the source of MMP-8, the expression levels of MMP-8 in cell line systems was further analysed. Since MMP-8 is a secreted protein CM collected from Myo-β6 or Myo-Puro cells were used. Cell lysate preparations were also used in WB but no specific signal was observed for MMP-8 (data not shown). The amount of protein in the CM is considerably lower than in the cell lysates therefore the CM were concentrated using centrifugal filters. The problems encountered with MMP-8 antibodies in IHC also caused difficulties for WB. Two antibodies were found to give a signal for MMP-8 in WB. This signal was specific for MMP-8 since the band observed with these antibodies was no longer present in samples from siMMP-8 treated MECs. Using these approaches, the mRNA and protein levels of MMP-8 were found to be down-regulated in the DCIS associated system (Myo-β6) when compared to the normal system (Myo-Puro), which recapitulates the alterations identified *in vivo*. Therefore these cell lines were considered to be good models to study the role of MMP-8 in normal breast versus DCIS. WT and a catalytically inactive mutant form of MMP-8 was over-expressed in Myo-β6 cells and MMP-8 activity was evaluated by Collagen-I zymography by adapting the analysis done by Palavalli et al [217], to qualitatively analyse the presence of MMP-8 activity. For specific detection and concentration of MMP-8; prior to Collagen-I zymography CM were immunoprecipitated for MMP-8 by adapting the

method shown by Palavalli et al [217] and these samples were added to gels. Addition of non-reducing loading buffer and incubating samples at RT for 15 minutes was sufficient to release the immunoprecipitates from the protein A beads as shown by the WB.

Zymographic approaches allow monitoring of the enzymatic activity of proteases by exposure to a substrate *in vitro* [304, 305]. During the washing step after electrophoresis, non-ionic detergent Triton 100X substitutes for SDS which partially renaturates the triple helix structure and permits degradation by MMPs [305]. Collagen-I degradation was observed in MMP-8 WT-carrying Myo-β6 cells as anticipated, however, although MMP-8 protein expression was confirmed in MMP-8 EA Myo-β6 cells, as shown by WB, Collagen-I degradation was absent, confirming the inactivity of the mutated EA vector. This approach therefore was appropriate to study the role of MMP-8 enzymatic activity in its biological function, as well as expression; furthermore this system will provide a tool to understand whether the action of MMP-8 is dependent on its proteolytic properties or influencing other proteins to exert its tumour suppressor role. Whilst β6 over-expressing MEC showed loss of MMP-8, αvβ6 levels were not altered on over-expression of MMP-8 WT or MMP-8 EA (data not shown). However in the Myo-β6 cell system, expression of αvβ6 is controlled by a potent retroviral promoter, therefore the over-expression of MMP-8 may not result in significant change. To address whether MMP-8 influences αvβ6 expression primary DCIS associated MECs could be analysed following transfection with MMP-8.

3.3.3 MMP-8 Down-regulates Migration but, Conversely Up-regulates Adhesion and Spread on ECM

Having generated the tools to study the gain-of-function effects of MMP-8; firstly the effect of MMP-8 on MEC adhesion was analysed. The concentrations of ECM proteins used in this assay were determined by seeding Myo-β6 cells in SFM (growth factor deprived media) on serial dilutions of each ECM protein and monitoring cell behaviour after 1 hour. The cells showed rounded morphology in higher dilutions, rounded and spread cells were observed in intermediate dilutions and rounded morphology was detected again in lower dilutions. This response in cell spread has previously been explained by a 'receptor saturation model' by Gaudet and colleagues [306]. At low ligand concentration the integrin receptor ligand engagement (adhesion) is not enough to induce spreading or to create a traction force needed for migration. As the ligand concentration increases more integrins bind the ligand, therefore the cell spreads. At the highest matrix concentrations the receptors become saturated and more clustered therefore cells exhibit a rounded morphology which also blocks migration [306]. Therefore the matrix concentrations were selected from intermediate dilutions which allow optimum adhesion and migration [306-308]. It was found that MMP-8 significantly enhanced MEC adhesion to fibronectin, Collagen-I, laminin-I-I-I and tenascin-C, dependant on its protease activity. Conversely; adhesion to LAP, which is a well-established ligand of αvβ6 during TGF-β activation, was down-regulated. It has previously been shown in our lab that Myo-β6 cells show significantly enhance adhesion to LAP

when compared to Myo-Puro cells [275]. Therefore this result may reflect decreased αvβ6 activity upon MMP-8 WT over-expression in Myo-β6 cells. However this evidence is limited, though the effect of MMP-8 on TGF-β signalling was further dissected, as described in result Section 5.

Secondly, it was found that MEC migration in MMP-8 WT over-expressing but not in MMP-8 EA transfected Myo-β6 cells over fibronectin, Collagen-I, laminin-I-I-I, tenascin-C and LAP was significantly decreased. In the transwell migration assay, in which the underside of the transwell was coated with ECM, the cells were separated from ECM by a porous membrane therefore cells migrate towards a protein gradient. Since the ECM is insoluble and bound to a surface, and cells migrate towards a gradient, this migration is a model for haptotaxis. The cells were seeded in SFM and the outer chamber contained SFM therefore the only gradient established is for ECM [309]. Since the quantification was done on cell number after incubation this assay gives an end-point result. It was previously shown in our lab that Myo-β6 cells show a more migratory phenotype when compared to Myo-Puro cells [275]. It can be hypothesised that the stress from the uncontrolled growth of the tumour cells in the duct generated by physical forces may trigger a wound response in MECs and therefore acquisition of migratory properties may be considered as a DCIS related phenotype (Section 1.5.3).

The down-regulation in migration towards ECM proteins seen in Myo-β6 cells over-expressing MMP-8 WT is in contrast to adhesion data which showed that MMP-8 WT enhances adhesion of Myo-β6 cells to ECM proteins. Thus

MMP-8 appears to mediate anchorage of MECs to their environment in a mechanism dependent upon its enzymatic properties since these changes were not seen in cells over-expressing mutant MMP-8 EA. Considering the central role of MECs in preserving normal tissue architecture, the disruption of which is characteristic of DCIS [59, 310], and the disruption of MEC layer integrity is a determining factor in the progression of pre-invasive to invasive disease, it may be hypothesised that MMP-8 can contribute to MEC tumour suppressor function by promoting maintenance of an intact cell layer through cell-matrix interactions.

Based on these results the next aim was to analyse how MMP-8 may be involved in mediating stationary attachment. MEC share some characteristics with basal keratinocytes, forming an epithelial-BM interface, with generation of unique adhesive HD structures. Dissociation of HD in wound healing and migration is well studied in keratinocytes (Section 1.5.3). Given the effect of MMP-8 on MEC migration we postulated this might be mediated through modulation of HD. Therefore these structures were analysed in modified Myo-β6 cells and showed that HD formation is enhanced in MMP-8 WT when compared to MMP-8 EA or control cells. This was shown by co-localisation analysis of two components of HD; the α6β4 integrin and plectin. This analysis allows investigation of cellular structures while the cells are still under culture conditions. Immunoprecipitation analysis is an alternative approach to analyse physical contact between proteins, however, for this technique the cells need to be detached from the plate or ligand on which they are seeded, and possibly, to analyse a structure involved in cell

attachment, this approach might not be appropriate. The modified Myo-β6 cells were also stained for MMP-8 (using the same antibody list as with the IHC Section 3.2.1), but no specific staining was observed. This is may be due to MMP-8 being secreted or due to failure of the antibodies. Staining for α6β4 revealed spike-like patterns at cell edges as well as the characteristic HD structures. These protrusions were stained with phalloidin. In the absence of dynamic information filopodial protrusions cannot be distinguished from retraction fibres, therefore these structures were referred as 'filopodia/retraction fibres'. Further analysis of these structures showed that MMP-8 WT abrogates filopodia/retraction fibre formation, which is a characteristic of reduced migratory phenotype [311]. This analysis was done on PFA-fixed cells which could affect cell protrusions. In order to investigate the motion of a cell group, time lapse microscopy is a better approach so the actual movement of the cells can be monitored, and the mode of migration (directed or random) as well as the speed of the cells could be quantified. To confirm the effect of secreted MMP-8, parental Myo-β6 cells were incubated with recombinant MMP-8 as described in Section 2.21. Recombinant MMP-8 stimulation significantly down-regulated filopodia/retraction fibre number in Myo-β6 cells (Section 7.1), supporting the over-expression results. In parallel with filopodia/retraction fibre analysis, phalloidin staining also provided data on cell size. MMP-8 WT expressing Myo-β6 cells spread more on fibronectin. This is concomitant with the increased adhesion and decreased migration observed on fibronectin as described earlier. Taking these results together the conclusion can be drawn that MMP-8 promotes a more adhesive

phenotype with enhanced HD formation, and this may be one mechanism by which it contributes to MEC tumour suppressor phenotype.

3.3.4 MMP-8 Reduces Matrix Degradation by MECs

Primary invasion of breast cancer cells is accompanied by BM degradation. One distinct characteristic reported for DCIS-associated MECs by gene expression studies is the enhanced expression of proteases [12]. It has been postulated that this may contribute to the initiation of cancer cell invasion through BM. Concomitantly our lab has shown that Myo-β6 cells up-regulate MMP-9 expression compared to Myo-Puro cells via a TGF-β –dependent mechanism. Here, gelatine degradation analysis was done using an *in vitro* zymography assay which was originally developed for invadopodia analysis and permits visualisation of fluorescent gelatine [312]. The total degraded area per field was quantified, and in parallel the cell number per field was counted. MMP-8 WT but not EA over-expression led to a significant reduction in the gelatinolytic activity of Myo-β6 cells. MECs secrete the gelatinase MMP-2 in addition to MMP-9, therefore the proteolytic activity determined by this assay may not be fully attributed to MMP-9 activity. Therefore to discriminate between MMP-9 and MMP-2 activity, a substrate gel zymography in which gelatine was co-polymerised with acrylamide that allows separation of MMPs according to MW was done [305, 313, 314]. CM derived from MMP-8 WT but not from MMP-8 EA over-expressing Myo-β6 cells showed evidence of reduced MMP-9 activity, however this reduction did not reach significance (MMP-8 WT vs empty p=0.057, MMP-8 WT vs MMP-8

EA p=0.067). Whilst a band for MMP-2 was seen with the positive control (data not shown), no bands were seen for Myo-β6 populations. There are certain limitations to be considered with gelatine zymography [313, 314]. The fact that the refolding of MMPs after electrophoresis is partially recovered might cause problems with insensitivity when a change in levels (reduction or induction) of an MMP is quantified [305]. It is also should be considered that during electrophoresis, SDS disassociates MMP-TIMP complexes which makes the inactive TIMP-bound MMP activity eligible for detection, thus the actual activity level in the CM might not be accurately reflected [305]. The pro-MMP forms can also be detected due to post electrophoresis treatment of Triton 100X and activation buffer, since they are covalenty bound to the pro-domain the pro-forms appear at a higher MW. Moreover, over-staining of gels with Coomassie blue might also introduce sensitivity problems. Therefore, there are several factors that interfere with the quantitative use of zymographic techniques and, limit the information about net proteolytic activity [313, 314]. It can be argued that MMP-8 activity might be detected by gelatine zymography, however this signal should be very weak since gelatine is not the preferential substrate of MMP-8. In this study, no bands corresponding to MMP-8 were observed on gelatine zymography. Also no proteolytic zone corresponding to MMP-9 was observed in Collagen-I zymography. In addition the recombinant MMP-9 and MMP-2 could not be consistently detected. This might be due to the low concentration of recombinant proteins or high concentration of gelatin in the gel, the recombinants might be visible if the gelatin concentration is reduced [313]. Different dilutions of MMP-9 and MMP-2 recombinants were run on gelatine

zymography but a consistent degraded gel area could not be observed. Alternatively, recombinant standards might include reducing agents which destroy the MMP activity [313].

From the *in vitro* zymography and gel zymography there is some evidence, though not conclusive, that MMP-8 might exert an inhibitory role on MMP-9 activity. PCR analysis showed no change in MMP-9 gene expression therefore based on previous reports that MMP-8 and MMP-9 could establish a complex [208], we hypothesised that MMP-8 might bind to MMP-9 and inhibit its action. In addition, MMP-9 is of particular interest since it has been shown that MMP-9 can bind to the extracellular domain of α6β4 and inhibit wound closure [315]. Therefore MMP-9 might interfere with the mechanism of MMP-8.

3.3.5 Loss of MMP-8 Reduces Adhesion and Promotes Migration and BM Degradation by MECs

To confirm the physiological relevance of the over-expression model, in parallel to this DCIS associated model, we generated a normal MEC system and demonstrated endogenous MMP-8 expression, confirming that the system is appropriate to work on MMP-8. Here it was shown that, MMP-8 knock-down in Myo-Puro cells reduced adhesion but increased migration to several ECM components. However migration to fibronectin and Collagen-I did not alter with the loss of MMP-8. Considering the decrease in migration in MMP-8 WT expressing Myo-β6 cells, an increase in migration in Myo-Puro

cells lacking MMP-8 might be expected. Since in normal breast MECs are facing BM which is rich in Collagen-IV but not in fibronectin or Collagen-I it was hypothesised that normal MECs may not be conditioned to respond to these two ECM components. However we could not exclude the possibility that the variation between different experiments in migration towards fibronectin and Collagen-I (errors of mean) could mask the significant difference between siMMP-8 or siLUC transfected Myo-Puros. To evaluate whether the length of incubation could mask the significant effect of MMP-8 loss over Collagen-I, migration assays incubated for 4 hours were conducted. However, no significant difference was observed (Section 7.1.2). Moreover in DCIS, fibronectin is up-regulated spatiotemporally concomitantly with αvβ6 expression probably through a TGF-β dependent mechanism (Personal communication Prof L. Jones). Interestingly there was also no significant change in response to LAP. This may reflect the absence of αvβ6 dependent activity in Myo-Puro cells. Further investigation of the actin cytoskeleton revealed that filopodia/retraction fibre formation is enhanced in the absence of MMP-8. Preliminary data shows that MMP-8 knock-down also increased gelatinase activity, and this increase is MMP-9 dependent since when MMP-9 is inhibited with siRNA or inhibitor the enhanced gelatine degradation of MMP-8 knocked down Myo-Puro cells was abolished. This data requires confirmation but together the results suggest that MMP-8 loss promotes the gain of DCIS-related properties in normal MECs.

Chapter 4: Effect of MMP-8 on Myoepithelial Tumour Suppressor Functions

4 Effect of MMP-8 on Myoepithelial Tumour Suppressor Function

4.1 Introduction and Aims

The role of the microenvironment in promoting tumour cell invasion is now well established [64, 65]. Much of this work focuses on the role of tumour-associated fibroblasts [67], but in the breast the MEC population also influences epithelial cell behaviour [58-60, 117, 275].

Normal MECs have been shown to exhibit tumour suppressor properties [117]. They establish a physical barrier around LECs and produce the BM [79]. MECs also secrete a number of tumour suppressor proteins, proteinase inhibitors and anti-angiogenic factors indicative of the paracrine mechanisms involved in this tumour suppressor function [114, 115]. In fact, normal MECs have been shown to inhibit breast cancer cell invasion in transwell invasion assays, in part, by down-regulating MMP expression and activity in breast cancer cells [117].

In DCIS, MECs become altered and work in our laboratory has shown that certain changes, such as the up-regulation of αvβ6, lead to acquisition of tumour promoter properties [275]. In the current study, it is also evident that DCIS-associated MECs lose MMP-8 expression and this also impacts on MEC function.

Other studies also have demonstrated a tumour suppressor role for MMP-8. It was demonstrated that MMP-8 knockout mice show a higher incidence of skin tumours in a chemically induced carcinogenesis model compared to WT mice [208]. Similarly Gutierrez-Fernandez et al. showed that when B16F10 melanoma cells were inoculated into MMP-8 knock out or WT mice via tail vein injection the number of lung metastasis was up-regulated in MMP-8 knockout mice when compared to WT counterparts [215]. These studies underline the importance of host-derived MMP-8 on the behaviour of cancer cells.

The aims of this chapter are:

- To analyse the effect of MEC derived MMP-8 on breast cancer cell invasion in two dimensional (2D) and three dimensional (3D) systems. Specifically:
    - To co-culture modified Myo-β6 or Myo-Puro cells with breast cancer cells to analyse direct interactions between the two cell groups
    - To build organotypic cultures to analyse the MEC-cancer cell and stromal interactions in breast tissue context

4.2 Results

4.2.1 Effect of MEC Derived MMP-8 on Breast Cancer Cell Invasion in Boyden Chamber Invasion Assays

In order to analyse whether MMP-8 has a role in the paracrine interactions between MECs and breast cancer cells during primary breast cancer cell invasion; modified Myo-β6 cells and the breast cancer cell lines SUM159 or MDA MB 231 were co-cultured in a Boyden chamber invasion assay for 24 hours. In this assay transwells were either coated with Matrigel to represent BM or the MMP-8 substrate Collagen-I, and the number of invaded breast cancer cells were quantified as described in Section 2.8. All experiments were repeated a minimum of 4 times. The number of breast cancer cells invading through Matrigel matrix was significantly reduced when co-cultured with MMP-8 WT (MDA MB 231 $p=0.004$, SUM159 $p=0.04$) but not with MMP-8 EA over-expressing Myo-β6 cells (MDA MB 231 $p=0.61$, SUM159 $p=0.64$), in comparison to Empty vector transfected MEC (Figure 4-1). Addition of recombinant human MMP-8 also resulted in a significant reduction in invading breast cancer cells ($p=0.001$, $n=2$, data not shown).

In order to exclude the possibility that the reduction in invasion identified in the presence of MMP-8 WT was a result of decreased proliferative activity; the proliferation of MDA MB 231 or SUM159 breast cancer cells was evaluated using the MTS assay, after 24 hours treatment with CM collected from MMP-8 WT, MMP-8 EA or Empty vector transfected Myo-β6 cells (as in

the invasion assay) as described in Section 2.9. There was no significant difference in proliferation rate between the different treatment groups for each cell line (Figure 4-2).

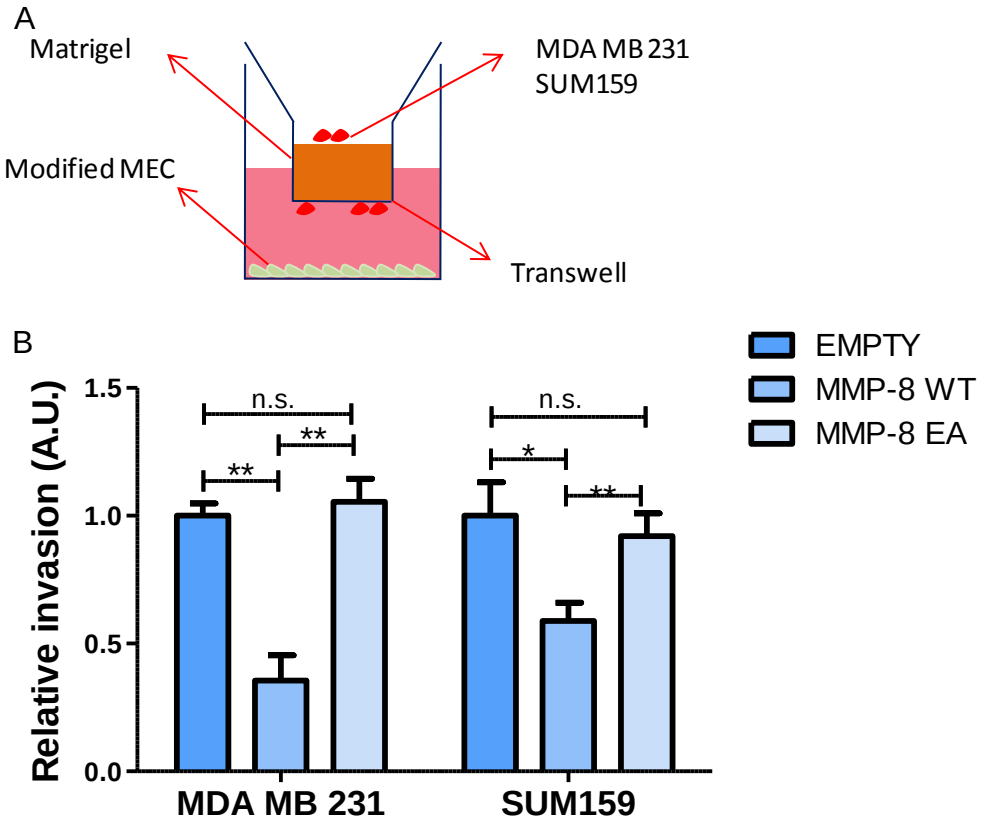

Figure 4-1: Effect of MMP-8 over-expression in Myo-β6 cells on breast cancer cell invasion through Matrigel. A; Schematic representation of Boyden chamber invasion assay using Matrigel as a BM barrier. B; The number of breast cancer cells invading through the membrane was counted as described in Section 2.8, and normalised to the number of invading cells in the assays using Empty vector over-expressing Myo-β6 cells. There was a significant reduction in invasion by SUM159 and MDA MB 231 cells after 24 hours in the presence of MMP-8 WT over-expressing Myo-β6 cells. The SUM159 and MDA MB 231 cell invasion did not change significantly after co-cultured with MMP-8 EA over-expressing Myo-β6 cells for 24 hours. *, $P \leq 0.05$, **, $P \leq 0.01$ (Student's *t* test). Error bars show means +/- SEM. A.U., arbitrary unit, n.s., not significant, representative for 4 independent experiments.

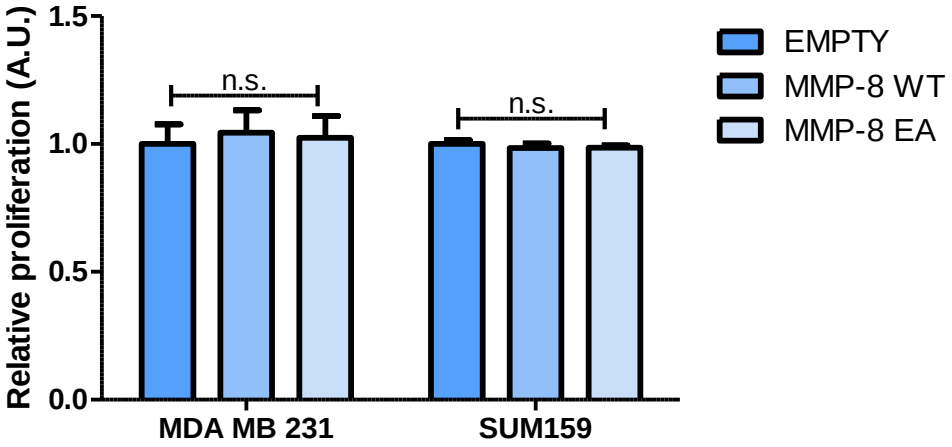

Figure 4-2: Effect of MMP-8 over-expression in Myo-β6 cells on breast cancer cell proliferation. MDA MB 231 or SUM159 breast cancer cells were treated with conditioned media collected from modified Myo-β6 cells as described in Section 2.9. MTS assay was done and the proliferation rate was normalised to the proliferation of breast cancer cells when treated with CM from Myo-β6 cells transfected with Empty vector. There was no significant change in proliferation under different co-culture conditions. Error bars show means +/- SEM. A.U., arbitrary unit, n.s., not significant, representative for 3 independent experiments.

Based on the observation that functioning WT but not the inactive EA form of MMP-8 reduced invasion of breast cancer cells in this 2D system, the effect of MMP-8 on breast cancer cell invasion through its ligand Collagen-I was analysed in a Boyden chamber invasion assay, set up by coating the transwells with Rat tail Collagen-I in place of Matrigel, as described in Section 2.8. There was a significant reduction in the number of SUM159 cells invading through Collagen-I when co-cultured with MMP-8 WT over-expressing Myo-β6 cells compared to control Myo-β6 cells over-expressing Empty vector (p=0.001, n=2) (Figure 4-3). When SUM159 cells were co-

cultured with MMP-8 EA over-expressing Myo-β6 cells, there was no significant difference in invasion (p=0.43, n=2).

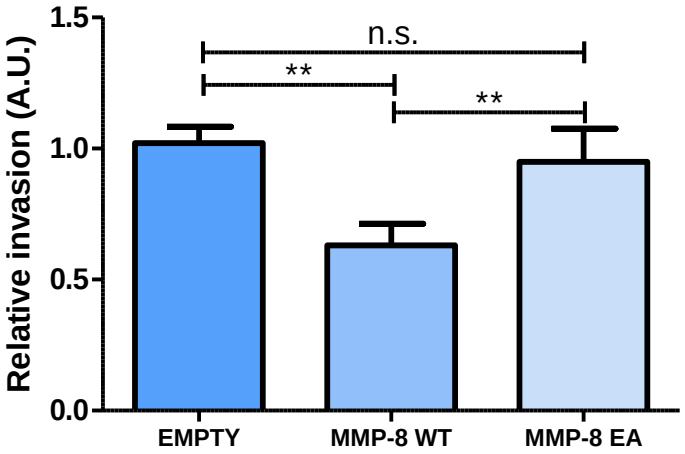

Figure 4-3: Effect of MMP-8 over-expression in Myo-β6 cells on breast cancer cell invasion through Collagen-I. The number of invading breast cancer cells was analysed as described in Section 2.8 and normalised to the invading cell number in the presence of Myo-β6 cells over-expressing Empty vector. Invasion by SUM159 cells was significantly reduced in the presence of MMP-8 WT over-expressing Myo-β6 cells but not in the presence of MMP-8 EA over-expressing Myo-β6 cells. **, P ≤ 0.01 (Student's *t* test). Error bars show means +/- SEM. A.U., arbitrary unit, n.s., not significant, representative for 2 independent experiments.

4.2.2 Effect of MEC Derived MMP-8 on Breast Cancer Cell Invasion in Organotypic Models

To recapitulate the DCIS associated stromal microenvironment an organotypic culture model approach was taken. In this model organotypic gels were constructed from a Matrigel and Collagen-I mixture and embedded with MRC5 fibroblasts. Following 24 hours equilibration, modified Myo-β6 cells and MDA MD 231 or SUM159 breast cancer cells were overlaid on top

of the gel then raised to air-liquid interface as described in Section 2.16 (Figure 4-4 A).

After 11 days incubation; gels were fixed, processed and sectioned then stained with H&E or specific antibodies as described in Section 2.19. Antibodies used were proliferation marker Ki67, MEC marker p63 and invasive breast cancer cell marker Neso which is the Neonatal splice variant of voltage gate channel Nav1.5 [317]. H&E stained sections are shown in the Figure 4-4 B and based on these; invasion was quantified as the combination of the number, depth and the area occupied by the invaded breast cancer cells to give an invasion index. At least 3 organotypic gels were prepared per condition in each experiment and the whole gel section was quantified except the edges. All experiments were done at least 4 times. As shown in the Figure 4-5 the invasion index was significantly reduced when MDA MB 231 or SUM159 breast cancer cells were co-cultured with MMP-8 WT over-expressing Myo-β6 cells (MDA MB 231 p=1.68E-13, SUM159 p=4.04E-04) but not when co-cultured with MMP-8 EA over-expressing Myo-β6 cells (MDA MB 231 p=0.15, SUM159 p=0.54) compared to the invasion in the presence of Empty vector transfected Myo-β6 cells. In order to consider the probability that this decrease in invasion index is because of a reduction in breast cancer cell proliferation in the presence of MMP-8 WT; gels were stained for Ki67 which is a proliferation marker. Proliferation index of cells invaded in the gel was quantified as the number of cells positive for Ki67 divided by the total cell number (determined by the number of nuclei stained by DAPI) and normalised to the proliferation index when breast cancer cells

were co-cultured with Empty vector transfected Myo-β6 cells. There was no significant difference in the proliferation of breast cancer cells co-cultured with Myo-β6 cells transfected with either MMP-8 WT, MMP-8 EA or Empty vector (Figure 4-6) (n=3).

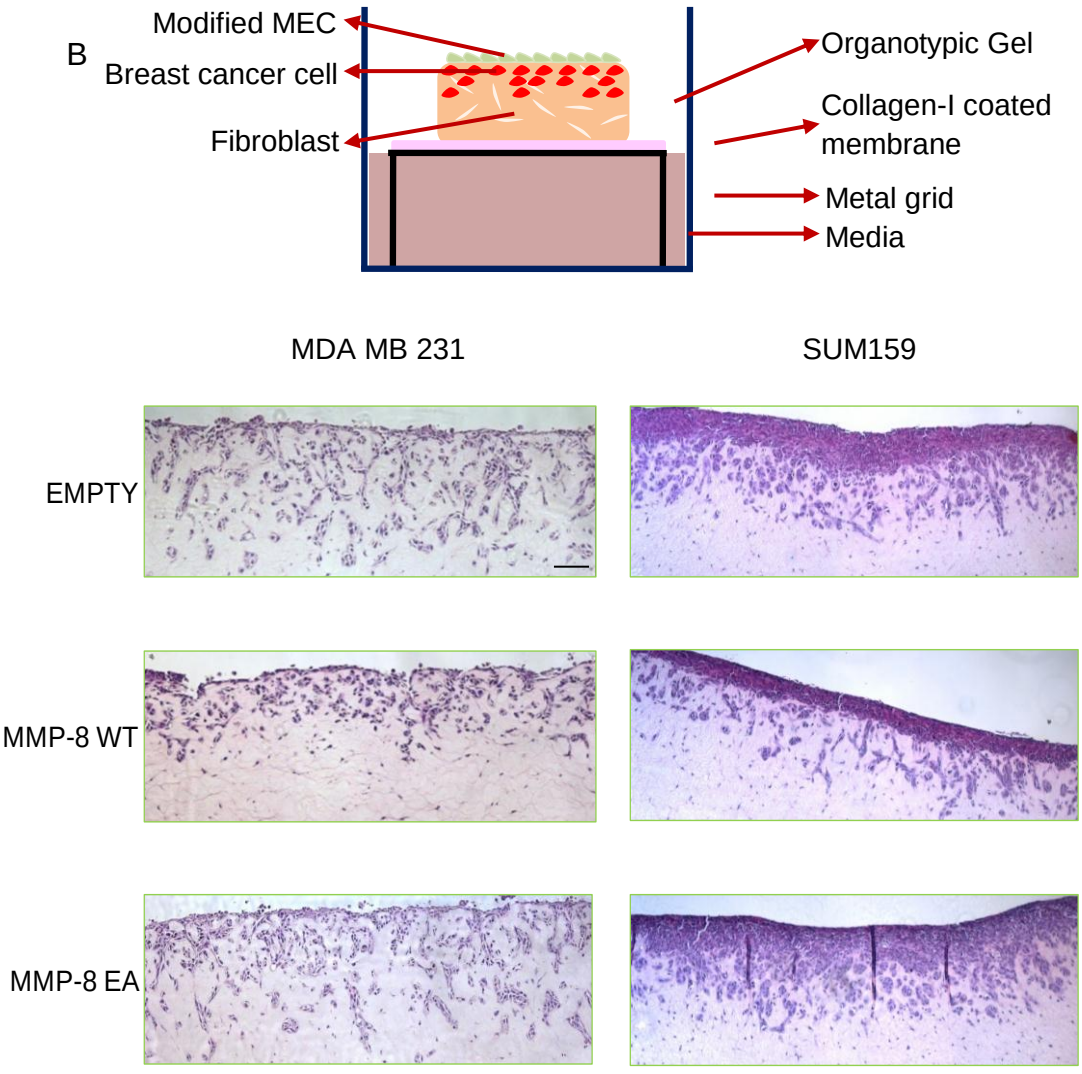

Figure 4-4: Organotypic culture set up A; Schematic representation of organotypic cultures adapted from Froeling et al., 2008, Froeling et al., 2011, and Chioni and Grose, 2012 [297, 300, 316]. Bar 100μm. B; H&E staining of organotypic gels. After the incubation period organotypic gels were processed and sectioned as described in Section 2.16. Images are representative for 4 independent experiments.

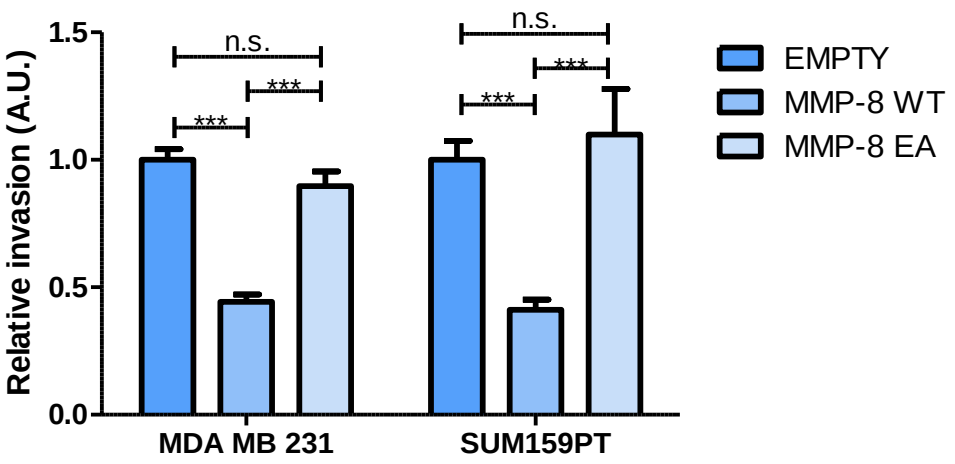

Figure 4-5: Effect of MMP-8 over-expression in Myo-β6 on invasion of MDA MB 231 and SUM159 breast cancer cells in 3D organotypic systems. Based on H&E staining an invasion index was quantified as described in Section 2.16. The invasion index when MDA MB 231 or SUM159 were co-cultured with MMP-8 WT over-expressing Myo-β6 cells was significantly lower than when co-cultured with MMP-8 EA or Empty vector transfected cells. ***, P ≤ 0.001 (Student's *t* test). Error bars show means +/- SEM. A.U., arbitrary unit, representative for 4 independent experiments

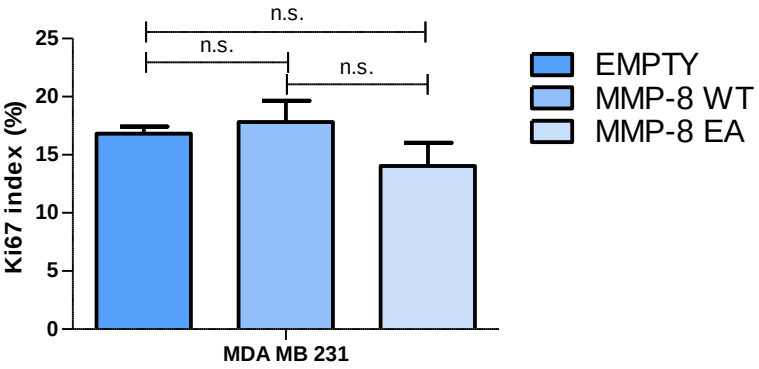

Figure 4-6: Effect of MMP-8 on proliferation of MDA MB 231 breast cancer cells in 3D organotypic systems. Gels were stained for Ki67 proliferation marker as described in Section 2.16 and the proliferation index was quantified as the ratio of Ki67 positive cells to total cell number. There was no significant difference in proliferation index in breast cancer cells co-cultured with MMP-8 WT, MMP-8 EA or Empty vector. Error bars show means +/- SEM., n.s., not significant, representative for 3 independent experiments.

Organotypic cultures were repeated incorporating primary normal breast fibroblasts in place of MRC5 fibroblasts. The fibroblasts were isolated from reduction mammoplasty tissue as described in Section 2.3. The invasion index of MDA MB 231 cells was significantly reduced when co-cultured with MMP-8 WT over-expressing Myo-β6 cells (Figure 4-7) ($p=0.0002$, $n=2$) but not with MMP-8 EA over-expressing group ($p=0.64$, $n=2$) when compared to control Empty vector co-cultures, reflecting the pattern of invasion seen in the presence of MRC5 fibroblasts.

In order to confirm that the invaded cells counted in the organotypic gels are breast cancer cells, and to exclude the possibility that modified Myo-β6 cells are also invading, gels were co-stained for the MEC marker p63 and an invasive breast cancer cell marker Neso [317]. The p63 staining revealed the layer of MEC on top of the gels and Neso staining selectively picked up the invading cells (Figure 4-7 B).

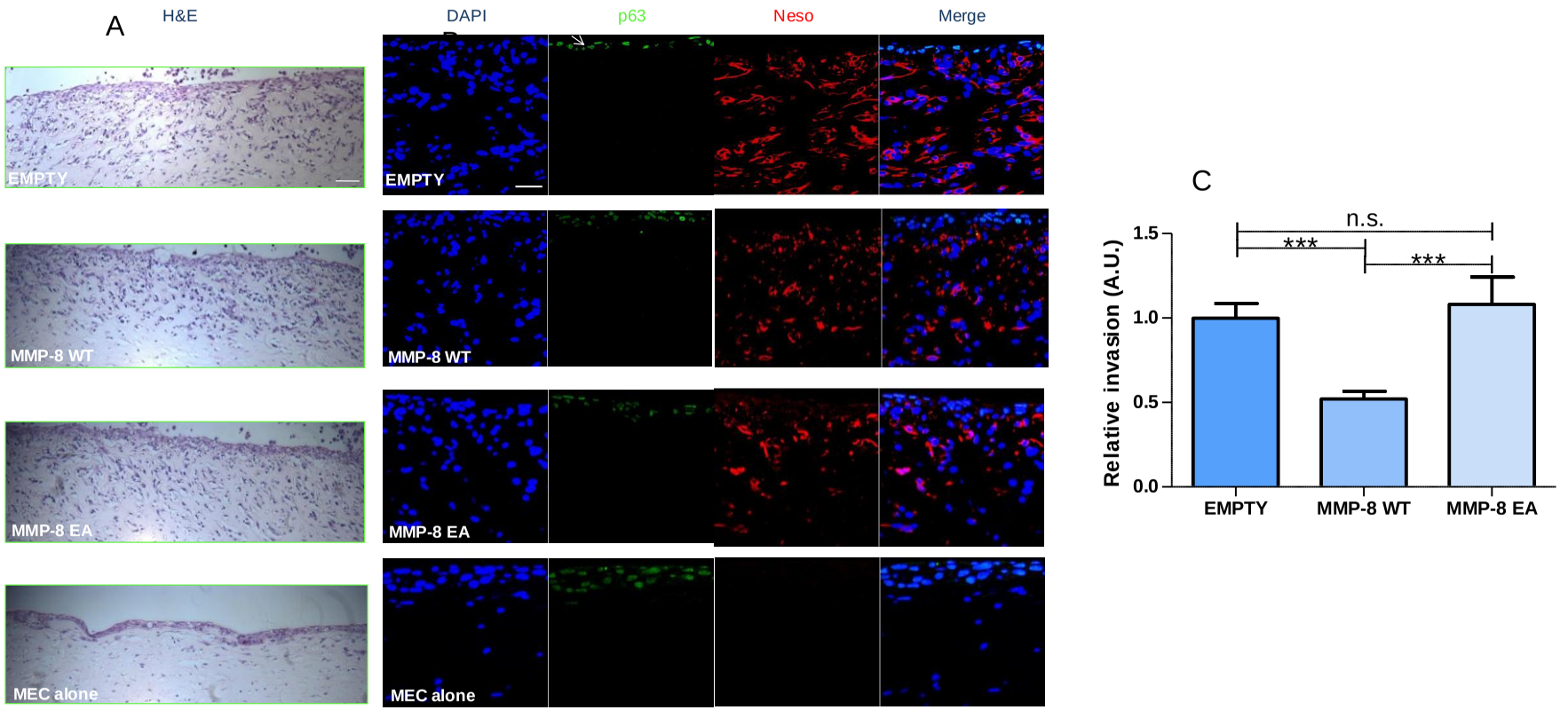

Figure 4-7: Effect of MMP-8 on breast cancer cell invasion in organotypic gels A; H&E staining was done after gels were fixed and sectioned as described in Section 2.16. Bar 100µm B; The organotypic gels were dual-stained for the MEC marker p63 (arrow) and invading breast cancer cell marker Neso as described in Section 2.19. Bar 50µm. C; The invasion index was significantly decreased only when MDA MB 231 cells were co-cultured with MMP-8 over-expressing Myo-β6 cells compared to control or MMP-8 EA co-cultures. ***, P ≤ 0.001 (Student's *t* test). Error bars show means +/- SEM. A.U., arbitrary unit, representative for 2 independent experiments.

4.2.3 Effect of Loss of Myo-Puro Derived MMP-8 on Breast Cancer Cell Invasion in Boyden Chamber Invasion Assays

In order to analyse the loss-of-function effect of endogenous MMP-8 expression in a normal myoepithelial system on breast cancer cell invasion Myo-Puro cells were treated with MMP-8 siRNA or control siRNA. Knock-down was confirmed by RT-PCR and WB (Section 3.3.9). The modified Myo-Puro cells were then co-cultured with MDA MB 231 or SUM159 for 24 hours or with MCF-7 for 48 hours as described in Section 2.8. All experiments were repeated a minimum of 4 times. The number of MCF-7, MDA MB 231 or SUM159 cells invaded through Matrigel was significantly enhanced when co-cultured with MMP-8 knock-down Myo-Puro cells compared to control siRNA treated Myo-Puro co-cultures (MCF-7 $p=0.0003$, MDA MB 231 $p=0.001$, SUM159 $p=0.0003$) (Figure 4-8).

In order to examine the effect of loss of MMP-8 expression in normal MEC on breast cancer cell proliferation; MCF-7, MDA MB 231 and SUM159 cells were treated with CM collected from modified Myo-Puro cells (MDA MB 231 and SUM159 for 24 hours or MCF-7 for 48 hours), followed by an MTS assay as described in Section 2.9. All experiments were repeated 3 times. As shown in Figure 4-9 there was no significant difference in proliferation rate of MCF-7, MDA MB 231 and SUM159PT cells under different CM treatments.

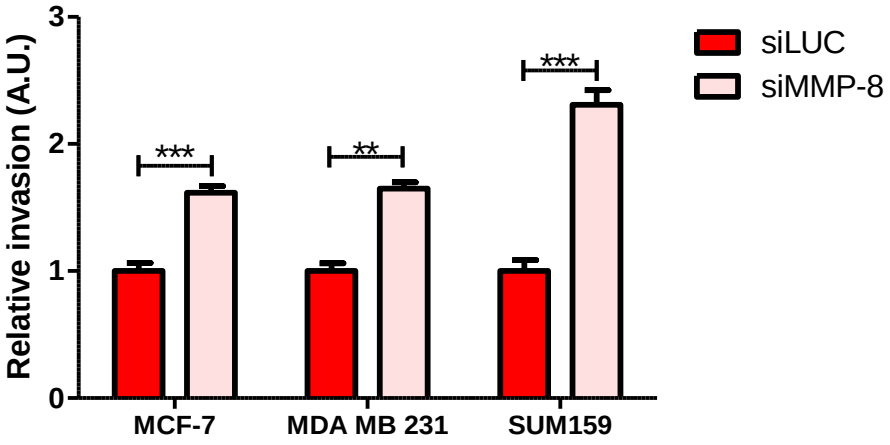

Figure 4-8: Effect of endogenous MMP-8 loss in Myo-Puro on breast cancer cell invasion through Matrigel. Modified Myo-Puro cells were co-cultured with MCF-7, MDA MB 231 or SUM159PT cells as described in 2.8. After incubation the number of invaded breast cancer cells were counted and normalised to cell number in co-cultures with Myo-Puro transfected with control siRNA (siLUC). MCF-7, MDA MB 231 and SUM159 cell invasion through Matrigel was significantly up-regulated when co-cultured with siMMP-8 treated Myo-Puro cells. **, P ≤ 0.01; ***, P ≤ 0.001 (Student's *t* test*)*. Error bars show means +/- SEM. A.U., arbitrary unit, representative for 4 independent experiments.

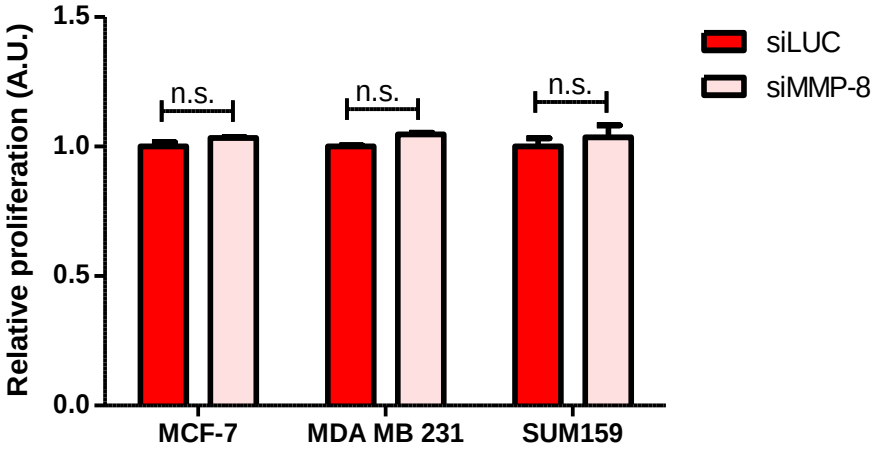

Figure 4-9: Effect of endogenous MMP-8 loss in Myo-Puro cells on breast cancer cell proliferation. MCF-7, MDA MB 231 and SUM159 cells were treated with CM from modified Myo-Puro cells as described in 2.9. MCF-7 cells were treated for 48 hours and MDA MB 231 and SUM159 cells were treated for 24 hours to reflect the invasion assays. An MTS assay was done to assess the proliferation. There was no significant difference in proliferation of the breast cancer cells under any of the assay conditions. Error bars show means +/- SEM. , n.s., not significant, representative for 3 independent experiments.

4.2.4 Investigation of the Effect of MMP-8 Knock-down in Myo-Puro Cells on Breast Cancer Cell Invasion in 3D Culture

In order to analyse whether the loss of Myo-Puro derived MMP-8 has an effect on breast cancer cell invasion in a 3D system, organotypic cultures were set up as described in Section 2.16 by co-culturing the MDA MB 231 cells with modified Myo-Puro cells for 5 days. After that gels were processed and stained for H&E as described and the invasion index was calculated. All experiments were repeated a minimum of 3 times with at least 3 gels per condition (Figure 4-10 A). The invasion index of MDA MB 231 cells was significantly enhanced when co-cultured with siMMP-8 transfected Myo-Puro cells compared to the control system ($p=0.007$) (Figure 4-10 B).

A

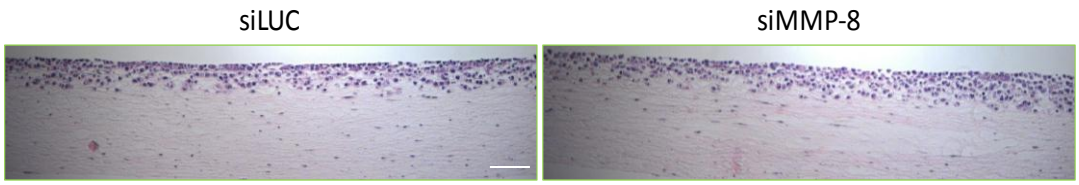

B

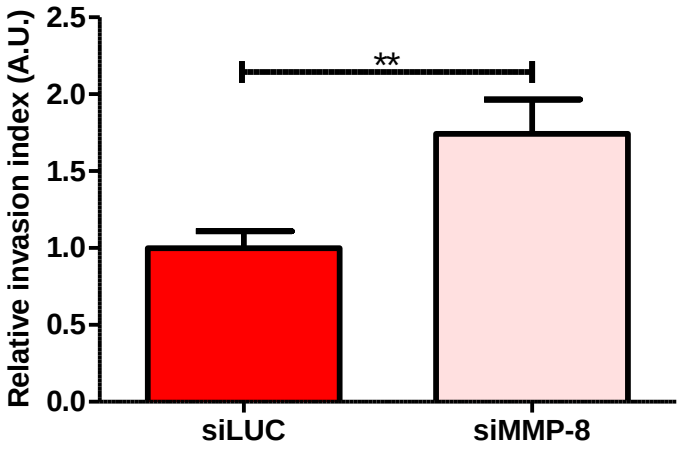

Figure 4-10: Effect of MMP-8 knock-down in Myo-Puro cells on invasion of MDA MB 231 breast cancer cells in 3D organotypic systems. A; 3D organotypic systems were built as described in Section 2.16 in which MDA MB 231 cells were co-cultured with modified Myo-Puro cells and stained for H&E. Bar, 100µm. B; Breast cancer cell invasion was significantly up-regulated when co-cultured with MMP-8 knock-down Myo-Puro compared to the control cell population. **, P ≤ 0.01; (Student's *t* test). Error bars show means +/- SEM. A.U., arbitrary unit, representative for 3 independent experiments.

4.3 Discussion

4.3.1 MEC Derived MMP-8 Can Down-regulate Breast Cancer Cell Invasion in 2D Invasion Assay Models

The data presented here show that MEC derived MMP-8 can reduce breast cancer cell invasion through paracrine interations in 2D Boyden chamber invasion assays. Transwell invasion assays were constructed by coating the transwell (which possess a cell permeable membrane) with Matrigel, to mimic the BM barrier tumour cells encounter *in vivo,* and seeding breast cancer cells onto this matrix and MECs in the outer chamber of the assay. The cancer cells degrade Matrigel, cross the membrane and attach to the underside of the transwell, thus reflecting a process requiring matrix degradation and cell migration. The breast cancer cells selected for these this experiments are the highly invasive, ER^- MDA MB 231 and SUM159 cells because a "suppression effect" on invasion was being investigated. Matrigel is extracted from Englebreth-Holm Swarm (EHS) murine sarcoma and contains Collagen-IV, laminin, perlecan and various growth factors [318, 319] and is considered therefore to resemble BM *in vivo*. As in the transwell assay assembly the different cell groups are not in contact; this system permits investigation of paracrine interactions of the two cell groups via secreted factors. This assay is quick, creates reproducible data, and can be prepared with low number of cells (20,000-30,000 per transwell). Despite the simple set up, Transwell invasion assays allow screening of the effect of an antibody, inhibitor, knock-down or over-expression of a particular protein

[320]. However this approach only produces an end-point result since the readout is the number of invaded cells after a particular incubation period. Moreover this system is certainly oversimplified, since the microenvironment is not represented and the 3D structural architecture of breast tissue is not reflected. Therefore this assay generates limited information about the full process of cancer cell invasion [309, 319, 320].

Here it was shown that MMP-8 can play a role in modulating breast cancer cell invasion through a Matrigel barrier. This invasion suppressor role of MMP-8 was found to be dependent on its enzymatic activity since Myo-β6 cells expressing inactive MMP-8 failed to show an effect when co-cultured with breast cancer cells. Since Matrigel resembles BM this system can be considered representative of primary invasion of breast cancer cells. MEC-derived MMP-8 was shown not to have an effect on breast cancer cell proliferation. This is in agreement with the literature that MMP-8 does not influence primary tumour growth [215]. Thus it can be concluded that the higher cell counts reflect increased invasion rather than an absolute increase in cell number.

Based on the observation that active but not inactive MMP-8 acts as an invasion suppressor, the next aim was to investigate invasion through the preferential MMP-8 ligand Collagen-I. Since Collagen-I is the major component of the interstitial matrix in breast, this approach also provides insights into the invasion into the ECM [107]. The Collagen-I invasion assay was an adaptation of the method used by Sheddin et al [107]. The Collagen-I

used here is acid-extracted from rat tail. At acidic pH Collagen fibril cross-links are reversibly broken and the resultant (aldehyde-bearing) Collagen is soluble in acidic buffer. Collagen-I was reconstituted by adjusting to neutral pH, when cross-links are spontaneously reformed. This reconstituted Collagen-I has been widely used as a model of ECM [107, 309, 319, 320]. A similar pattern to Matrigel invasion was observed, with WT but not catalytically inactive MMP-8 leading to reduced breast cancer cell invasion through Collagen-I.

4.3.2 MEC Derived MMP-8 Loss Promotes Breast Cancer Cell Invasion in 2D model

MMP-8 deficient normal MECs (Myo-Puro) were found to enhance breast cancer cell invasion. This supports results from the over-expression system described above and implies physiological relevance. Having shown an increase in cell invasion in highly invasive breast cancer models, the less invasive ER positive breast cancer cell line MCF-7, was also included in the experiments to broaden the significance of the data. These cells also responded in same way and exhibited enhanced invasion in the presence of MMP-8 knocked down Myo-Puro cells. Similarly to the DCIS MEC model, loss of MMP-8 in Myo-Puro cells did not alter breast cancer cell proliferation; once again showing that MMP-8 is not involved in primary cancer cell growth but suppresses the invasive activity of the breast cancer cells.

4.3.3 MEC Derived MMP-8 Can Reduce Breast Cancer Cell Invasion in 3D Organotypic Models

The effect of MEC derived MMP-8 on breast cancer cell invasion was further analysed using 3D organotypic cell cultures which allow the co-culture of different cell populations; in this study MECs, breast cancer cells and fibroblasts, in juxta-position reflects the architecture of the tissue context thus recapitulating physiological conditions *in vivo* [309, 319, 320]. Here, organotypic gels were prepared with a Matrigel/Collagen-I mixture and fibroblasts embedded in the gel [17, 297-301]. The gels were then overlaid with MECs, then breast cancer cells were seeded on top of the MECs. This set up recapitulates the relationship of tumour cells with a MEC barrier to the stromal microenvironment.

Breast cancer cell invasion was quantified by generating a numerical "invasion index" which combines the depth, number and sum of cell area invaded in the gel, as described by Nystrom et al [301]. This approach provides quantifiable, accurate and reproducible analysis however the pattern of invasion (single cell or collective) is not analysed.

The results found in 3D cultures reflect the same pattern observed in Transwell assays. In the presence of Myo-β6 cells over-expressing MMP-8 WT the invasion of breast cancer cells in 3D cultures was suppressed. This supports a role for MMP-8 in protecting against breast cancer cell invasion through the MEC layer. Considering that the organotypic gels are mainly

constructed from Collagen-I, which is the major target for MMP-8 degradation, these findings raise the possibility of alternative functions for MMP-8, which could down-regulate breast cancer cell invasion.

Conversely, knocking down endogenous MMP-8 in the normal MEC system enhanced cancer cell invasion. The effect observed here is moderate when compared to the over-expression system. This may be a result of the shortened incubation period for the cultures, necessary because of the transient siRNA knock-down system (5 days of incubation in comparison to 11 days in the over-expression system). This incubation time might not be long enough to observe a substantial degree of invasion. In keeping with this, the tumour suppressor nature of MECs could down-regulate the invasion in organotypic gels [275]. In the future for better investigation of the effect of loss of endogenous normal MEC derived MMP-8, Myo-Puro will be treated with shRNA targeting MMP-8 to generate stable knock-downs which will allow extended co-culturing incubation time.

In the data presented, it was shown that MECs do not invade into the gel, but remain on the surface. This shows that the organotypic set up permits discrimination of non-invasive and invasive cell populations. MECs were identified with the established MEC marker p63 and the breast cancer cells were labelled with Neso. The latter antibody, which specifically detects neonatal isoform of $Na_v1.5$ voltage-gated Na^+ channel was generated and used for identification of breast cancer during invasion [321]. The selective detection of invading MDA MB 231 breast cancer cells in organotypic

cultures by Neso staining was previously demonstrated by Chioni and co-workers [322]. The fibroblasts are negative with this marker which makes this antibody a valuable tool to specifically identify invasive breast cancer cells [322].

Here the use of invasive MDA MB 231 cells and normal fibroblasts in a DCIS model system might seem to be conflicting: in particular MDA MB 231 cells are certainly not pre-invasive breast cancer cells but derived from pleural metastasis. However gene expression studies comparing DCIS tumour cells and their invasive tumour cell counterparts repeatedly demonstrate the great similarity between the two cell groups; the DCIS tumour cells already show the spectrum of genetic alterations seen in invasive cells [12, 28, 323]. In regards to the fibroblast population previous studies have shown that when co-cultured with breast cancer cells, the normal fibroblasts are sufficient to promote invasion, tumour cells presumably inducing a myofibroblast phenotype [74, 117, 130]. Also co-injection of mice with normal fibroblasts together with the DCIS model MCF10ADCIS.com cells were sufficient to generate invasive tumours [130]. In keeping with normal fibroblasts being sufficient to enhance cancer cell invasion therefore being appropriate to use in DCIS system; CAFs show significant differences [66, 67]. Therefore in the future fibroblasts isolated from DCIS tissue will be used in organotypic cultures for better investigation of the cancer stroma and cancer cells.

The organotypic cultures are fed from underneath by complete media which mimics the blood vessel. However, *in vivo* blood is continuously circulated

but in the organotypic system the nutrient source is stationary. In order to analyse the effect of blood flow and other features of the microenvironment, in the future, these organotypic gels will be transplanted in mice [297, 301].

In summary, these experiments have shown that MEC derived MMP-8 suppresses breast cancer cell invasion in a proteolytic-dependent mechanism, and loss of MMP-8 leads to enhanced invasion. The mechanism by which MMP-8 influences invasive behaviour is unclear, but will be further investigated in Chapter 5.

Chapter 5: Investigating the Mechanism Involved in MMP-8 Suppressor Function

5 Investigating the Mechanism Involved in MMP-8 Suppressor Function

5.1 Introduction and Aims

The data from this study demonstrate that normal MEC are the major source of MMP-8 in the breast and that this is lost in DCIS. Using over-expression and knock-down systems it is evident that MMP-8 alters the adhesive and migratory capacity of MEC, appears to stabilise HD formation.

Furthermore, co-culture systems demonstrate that MEC-derived MMP-8 exerts an invasion suppressor effect and this is dependent on its proteolytic activity.

Previous work in our lab has shown that the introduction of αvβ6 in MEC in DCIS increased adhesion to LAP, activation of TGF-β and TGF-β dependent up-regulation of MMP-9 leading to invasion promoting action [275]. Moreover it was recently shown that prolonged exposure of epithelial cells to TGF-β could result in a decrease in MMP-8 expression [324].

The aims of this chapter are:

- To start to investigate how MMP-8 contributes to the tumour-suppressor activity of MECs
- Specifically to investigate whether MMP-8 can abrogate TGF-β activation and signalling in MEC since this appears to be an important mechanism leading to promotion of invasion by MEC

5.2 Results

5.2.1 Effect of MMP-8 Over-expression in Myo-β6 Cells on TGF-β Activation

Two approaches were taken to dissect the TGF-β pathway: analysis of the ability of Myo-β6 cells to activate TGF-β, and assessment of the cellular response to exogenous TGF-β stimulation.

Firstly, active TGF-β levels in modified Myo-β6 cells were analysed using a luciferase reporter assay by co-culturing MDA MB 231 cells carrying a TGF-β responsive luminescent vector (MDA MB 231-Luc) with MMP-8 WT, MMP-8 EA or Empty control vector transfected Myo-β6 cells overnight as described in Section 2.22. The experiment was done 3 times using 1000pg/ml human active TGF-βI as a positive control. The luminescence observed from each co-culture system was used as a readout for active TGF-β levels in the system. No significant difference in luminescence levels was detected between different co-cultures (Figure 5-1).

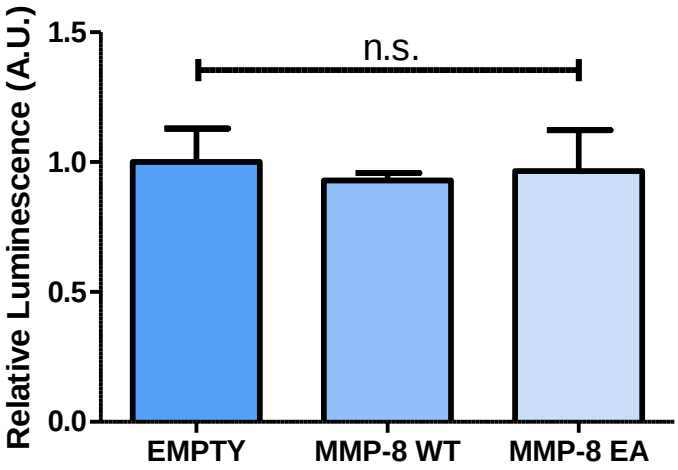

Figure 5-1: Effect of MMP-8 over-expression in Myo-β6 on active TGF-β levels. The levels of active TGF-β was analysed as described in Section 2.22. There was no significant difference in luminescence levels in co-cultures with MMP-8 WT or inactive MMP-8 over-expressing Myo-β6 cells when compared to Empty vector control transfected cells. n.s., not significant; (Student's *t* test). Error bars show means +/- SEM. A.U., arbitrary unit, representative for 3 independent experiments.

Secondly, to analyse the effect of MMP-8 over-expression on response of MEC to active TGF-β, Myo-β6 cells were seeded on a 6 well plate and starved for 24 hours then treated with 5ng/ml active TGF-βI for 5, 10 and 15 minutes as described in Section 2.20. As a readout for TGF-β signalling activity the phosphorylation levels of TGF-β downstream elements SMAD-2 and SMAD-3 was evaluated by WB as described in Section 2.7. This experiment was repeated 3 times and results analysed by densitometry using ImageJ. The expression levels of total and phosphorylated forms of SMAD-2 and SMAD-3 were normalised to that of actin. Then the ratios of phosphorylated form to total protein levels were calculated.

The phosphorylation levels of SMAD-2 and SMAD-3 appeared to be decreased in MMP-8 WT over-expressing Myo-β6 cells when compared to Empty vector over-expressing control cells (Figure 5-2). There also was a reduction in phospho-SMAD-2 and SMAD-3 levels in MMP-8 EA over-expressing Myo-β6 cells when compared to Empty vector transfected cells. These levels were higher than the phospho-SMAD-2 and SMAD-3 levels in MMP-8 WT. In the Myo-β6 cells over-expressing MMP-8 EA the phosphorylated SMAD-2 and SMAD-3 levels and the total SMAD-3 levels appeared to be higher than that of MMP-8 WT or Empty vector transfected Myo-β6 cells without TGF-β stimulation. In addition the total SMAD-3 levels appeared to decrease. The changes in phospho-SMAD-2 and SMAD-3 levels did not reach significance due to the variation observed between experiments.

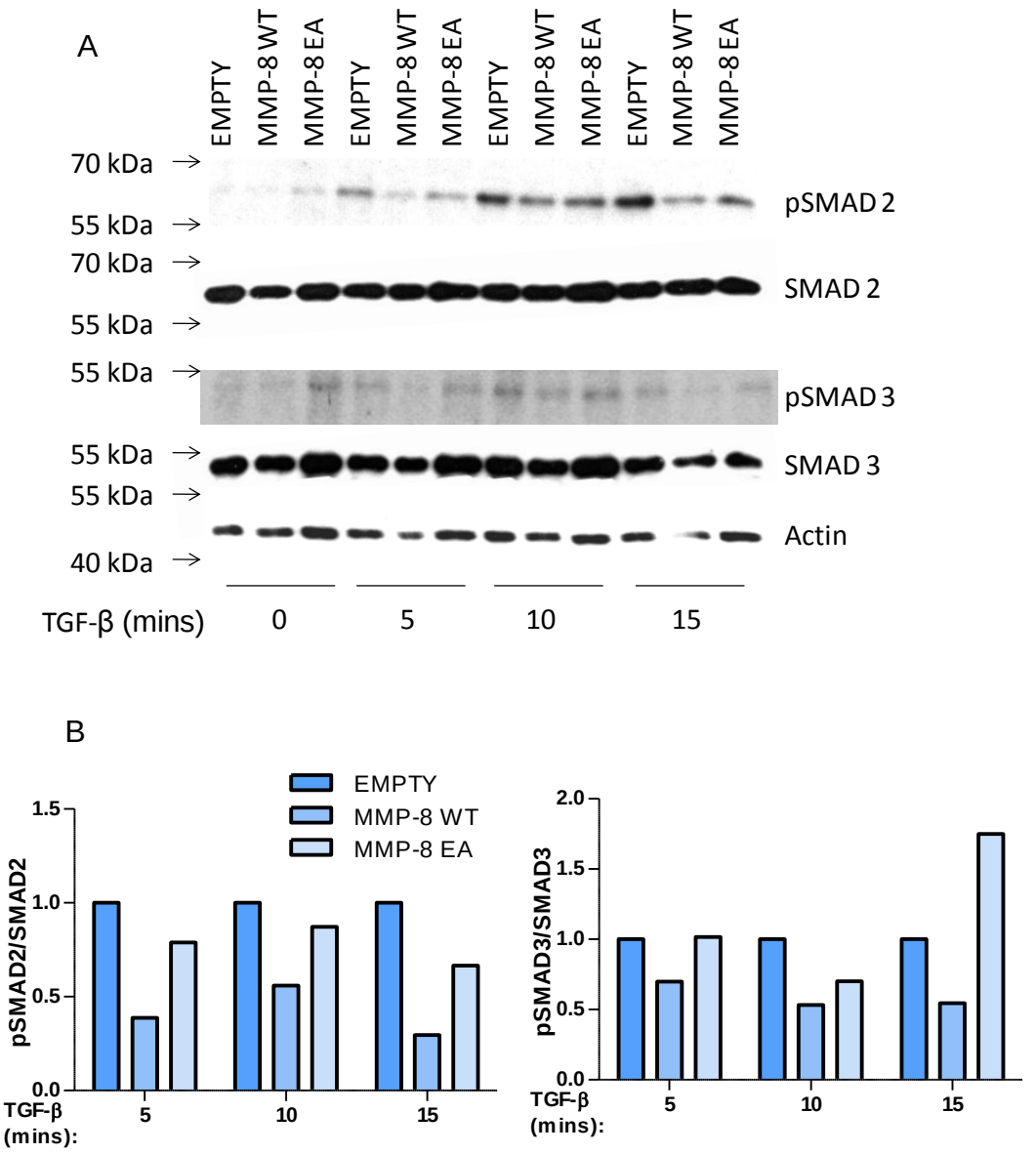

Figure 5-2: The effect of MMP-8 over-expression on response to TGF-β stimulation. MMP-8 WT, MMP-8 EA or Empty vector transfected Myo-β6 cells were stimulated with 5 ng/ml TGF-β for 5,10 and 15 minutes after 24 hours of serum starvation. A; Cell lysates were subjected to WB to check SMAD-2 and SMAD-3 phosphorylation. B; Phosphorylation levels of SMAD-2 and SMAD-3 were examined by ImageJ. The expression level of each protein is normalised to actin loading control. In order to evaluate the changes in phosphorylated froms; the phosphorylated levels were divided by the total levels. These values were normalised to that of Empty vector for each time point. There was a decreased in phosphorylated SMAD-2 and SMAD-3 levels in MMP-8WT over-expressing group compared to inactive MMP-8 or Empty vector over-expressing Myo-β6 cells. pSMAD-2., phosphorylated SMAD-2 , pSMAD-3., phosphorylated SMAD-3, A.U., arbitrary unit, representative for 3 independent experiments (Result shown for 1 experiment).

5.2.2 Effect of Lack of MMP-8 in Myo-Puro Cells on TGF-β Activation

In order to analyse the effect of the loss of endogenous MMP-8 on active TGF-β levels in Myo-Puro cells; cells were treated with MMP-8 siRNA or siLUC control and co-cultured with TGF-β responsive MDA MB 231-Luc cells overnight as described in Section 2.22. This experiment was repeated 3 times. The luminescence obtained when MDA MB 231-Luc cells were co-cultured with siMMP-8 transfected Myo-Puro cells was normalised to the luminescence obtained in siLUC control co-cultures and no difference was observed in MMP-8 knocked down Myo-Puro cells in comparison to control cells (Figure 5-3).

To investigate the effect of the loss of MMP-8 on TGF-β downstream signalling; modified Myo-Puro cells were treated with active TGF-βI as described in Section 2.20. This experiment was performed twice. The WB analysis of phosphorylation of SMAD-2 and SMAD-3 was done by ImageJ as described in Section 5.2.1 and revealed an increase in phosphorylated SMAD-2 and SMAD-3 in MMP-8 knock-down Myo-Puro cells compared to control siRNA transfected cells (Figure 5-4). The highest level of SMAD-2 phosphorylation was observed at 10 minutes time point and the signal appeared to decrease at 15 minutes time point in siMMP-8 transfected Myo-Puro cells. The SMAD-3 phosphorylation was observed only in Myo-Puro cells treated with siMMP-8 at 10 minutes and 15 minutes time point. This signal was also highest at 10 minutes time point.

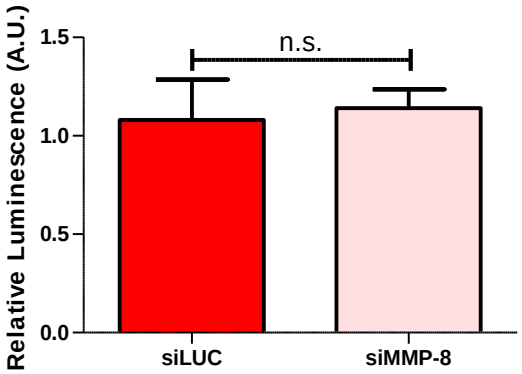

Figure 5-3: Effect of MMP-8 loss in Myo-β6 on active TGF-β levels. The level of TGF-β activity was explored by luciferase reporter assay by co-culturing modified Myo-Puro cells with MDA MB 231 cells carrying a TGF-β responsive vector as described in Section 2.22. There was no difference in luminescence observed levels in MMP-8 knock-down Myo-Puro cells when compared to control siRNA transfected cells. n.s., not significant; (Student's *t* test*)*. Error bars show means +/- SEM. A.U., arbitrary unit, representative for 3 independent experiments (Result shown for 1 experiment).

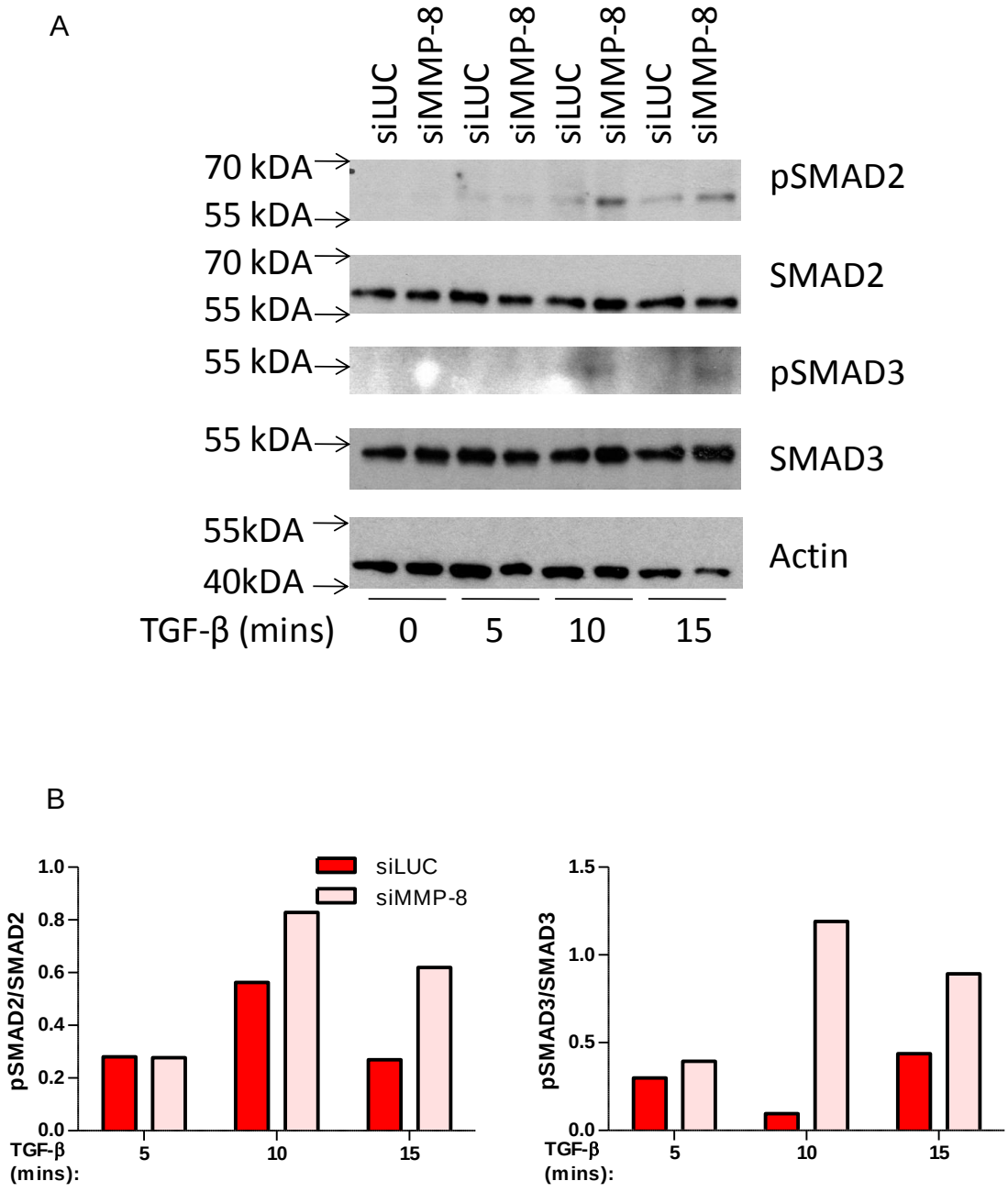

Figure 5-4: The effect of lack of MMP-8 on response to TGF-β stimulation. Modified Myo-Puro cells were activated with 5 ng/ml TGF-β, A; WB analysis and B; Densitometric quantification was done by ImageJ. Levels of phosphorylated forms of SMAD-2 and SMAD-3 were normalised to total SMAD-2 and SMAD-3 respectively for each time point. The phosphorylated SMAD-2 and SMAD-3 forms were up-regulated in MMP-8 knock-down Myo-Puro cells in comparison to control siRNA transfected Myo-Puro cells. pSMAD-2., phosphorylated SMAD-2 , pSMAD-3., phosphorylated SMAD-3, A.U., arbitrary unit, representative for 2 independent experiments.

5.3 Discussion

5.3.1 MMP-8 Expression does not Affect the Level of TGF-β Activity Potentially Down-regulates Downstream Signalling

The preliminary data presented here showed that there was no significant difference in level of TGF-β activation upon MMP-8 WT or MMP-8 EA over-expression in Myo-β6 cells. Similarly knock-down of MMP-8 in Myo-Puro did not result in a significant difference in TGF-β activity. The analysis of level of TGF-β activity was done using a TGF-β luciferase assay [325-327]. In this assay, modified MECs were co-cultured with the TGF-β responsive cell population MDA MB 231-Luc. The latter carries a TGF-β responsive PAI-promoter fused with a renilla and a firefly luciferase gene [328, 329]. Therefore the level of active TGF-β in the test cell is reflected in the amount of luciferase activity of TGF-β responsive cells. In order to test the sensitivity of this assay TGF-β responsive cells were also treated with increased amounts (pg/ml levels) of active TGF-β and this resulted in a stepwise increase in luciferase activity as expected (data not shown). This Dual-Luciferase reporter assay system allows quantification of the background luciferase activity created by background control renilla luciferase gene. Therefore this assay is sensitive and also carries an internal control. Myo-β6 cells are over-expressing αvβ6 which is responsible for the activation of TGF-β by MECs. Therefore MMP-8 over-expression might not result in a significant difference in behaviour since Myo-β6 cells are engineered to express high levels of a TGF-β activator. Conversely in the Myo-Puro system

the levels of active TGF-β may be lower than the sensitivity level of the experiment [325]. In the future this assay will be repeated co-culturing a greater number of modified Myo-Puro cells with the responsive cell line.

Further investigation of TGF-β downstream elements showed that MMP-8 appears to have an inhibitory effect on TGF-β signalling. This analysis was done by checking phosphorylation levels of SMAD-2 and SMAD-3 after stimulating the MECs with active TGF-β. SMAD-2 and SMAD-3 phosphorylation levels appear to decrease in cells following MMP-8 WT over expression. There also was a trend of reduced phospho SMAD-2 and SMAD-3 in MMP-8 EA over-expressing Myo-β6 cells. In addition there appears to be a change in total SMAD-2 or SMAD-3 levels after MMP-8 WT or MMP-8 EA over-expression. The variation in SMAD-2 and SMAD-3 phosphorylation levels meant that a significant difference could not be determined, and these experiments need to be repeated. In MMP-8 knock out Myo-Puro system SMAD-2 and SMAD-3 appeared to increase. This assay was performed twice only due to time constraints therefore statistical analysis could not be run. In the future these experiments need to be repeated to obtain a significant result. This is of particular importance since it would provide insight into the mechanism of MMP-8 action.

Chapter 6: Final Discussion and Future Work

6 Final Discussion and Future Work

6.1 Overview of the Aims

MECs of normal breast are robust tumour suppressor cells surrounding LECs and establishing the interface with BM [79, 117]. During breast cancer progression at the stage of DCIS stage they exhibit phenotypic alterations and eventually disruption of an intact MEC layer leads progression to invasion [58-60, 79]. One of the changes in DCIS MECs shown by our group was the apparent down-regulation of the tumour suppressor protein MMP-8 [215]. In this study we aimed to study the functional significance of this change; whether MMP-8 contributes to the in tumour suppressor function of MECs in normal breast and whether its loss in DCIS is implicated in altered MEC phenotype which ultimately contributes to breast cancer cell invasion.

6.2 MMP-8 Expression Influences Phenotype of DCIS MEC Model

A consistent alteration observed in MECs of DCIS is the up-regulation of αvβ6 integrin, which we have shown to alter MEC suppressor function [275]. In the current study we established cell lines to study the re-introduction of MMP-8 expression in DCIS-associated MECs using a MEC line over-expressing αvβ6, to recapitulate the *in vivo* phenotype. Investigation of MEC-ECM interaction was analysed by means of MEC spread, adhesion and migration on several ECM proteins. This showed that MMP-8 can induce

spread and adhesion and reduces migration towards a number of ECM molecules. These results led to the hypothesis that MMP-8 could be involved in stationary anchorage of MECs to the ECM which implicates a role for MMP-8 in preserving the normal tissue architecture.

It was previously shown by our lab that the DCIS-associated MEC model up-regulates adhesion and migration to the αvβ6 ligand LAP [275] and this could be ablated by an αvβ6 blocking antibody. Adhesion and migration to LAP can be used as readout for αvβ6 activity. In the current study it was shown that MMP-8 over-expression down-regulates adhesion and migration to LAP therefore it can be hypothesised that MMP-8 over-expression might result in a reduction in αvβ6 activity. Since binding of αvβ6 to LAP triggers TGF-β activation; active TGF-β levels and TGF-β down-stream signalling was further studied.

MECs are the basal cells of breast tissue and express the unique basal cell integrin α6β4 [234-237]. The extensive study on the role of this integrin in cell migration, especially in basal skin keratinocytes [244, 245], showed that shuttling of α6β4 from adhesive HDs to filopodial structures dictates whether cells will migrate [248, 253]. Here we showed that in the presence of MMP-8 α6β4 localises more to HDs and filopodia/retraction fibre formation is down-regulated, which corresponds to a reduced migratory phenotype. Together these results suggest a role for MMP-8 in modulating integrin activity.

The effect of MMP-8 appears to be dependent on its proteolytic function since over-expression of a catalytically dead mutant in DCIS associated MEC system did not result in significant effect on MEC phenotype.

One of the striking differences found in DCIS associated MEC is the over-expression of proteases. Considering the MEC layer establishes a barrier between LECs and BM in normal breast tissue it was speculated that enhanced protease expression by MEC could contribute to primary breast cancer cell invasion through BM. In fact it was shown by our lab that DCIS associated MECs up-regulate MMP-9 as a downstream response to TGF-β activity [275]. Intriguingly in the current study the gelatinase activity of DCIS associated MEC is down-regulated by MMP-8 expression.

In our normal MEC model MMP-8 was knocked down and this showed that, conversely to the over-expression system, the loss of MMP-8 reduces adhesion but induces migration to several ECM proteins and enhanced gelatinase activity of Myo-Puro cells. Moreover in the absence of MMP-8 formation of filopodia/retraction fibres were shown to be up-regulated which suggests an increased migratory phenotype in MECs.

In the future, time lapse microscopy will be done to quantify the migratory phenotype of modified MECs. This would allow investigation of cell movement, speed and behaviour on different ECM proteins.

To gain a better understanding of the contribution of MMP-8 in preserving normal tissue architecture modified MECs and breast cancer cells will be embedded in organotypic gels to recapitulate the microenvironmental cues of cell-cell interactions. The generation of dual layered duct like formations in Collagen based gels have previously been developed in our lab [299].

It was previously shown that MMP-8 and MMP-9 could establish a complex [209] but the functional significance of this complex is not known. In this study we showed that MMP-8 might have an inhibitory role on MMP-9 activity without changing MMP-9 expression levels. Therefore it was hypothesised that MMP-8 might bind and therefore inhibit MMP-9 action. For detailed analysis of MMP-8 interactor proteins, MMP-8 will be purified from modified MECs and a mass spectrometry approach will be taken to dissect the MMP-8 complexes. Furthermore a microarray approach will be taken to analyse differentially expressed genes upon MMP-8 over-expression in Myo-β6 cells or MMP-8 knock-down in Myo-Puro cells.

Taken together, these results lead to the hypothesis that MMP-8 contributes to reversion of the DCIS related MEC phenotype into a normal tumour suppressor phenotype, by modulating integrin activity and other members of MMP family (MMP-9).

6.3 MEC Derived MMP-8 Reduces Breast Cancer Cell Invasion

The interaction of cancer cells with cells of the microenvironment is needed to generate an invasive phenotype [64, 65]. It was previously shown by our lab that DCIS associated MECs up-regulate breast cancer cell invasion compared to normal MECs [275]. Interestingly in the current study over-expression of MMP-8 WT down-regulates breast cancer cell invasion in 2D and 3D organotypic systems. In contrast the loss of normal MEC derived MMP-8 resulted in up-regulation of breast cancer cell invasion. This result underlines the importance of microenvironmental control of breast cancer cell invasion and implicates a role for an MMP to suppress invasion. The results also emphasise the unique role of MECs in early stages of breast cancer.

In the future the organotypic cultures will be implanted into the flanks of mice to determine whether any effects on breast cancer cell invasion *in vitro* 3D cultures are replicated *in vivo*. These assays will be repeated with primary MEC and fibroblast populations.

For detailed investigation of how MEC-derived MMP-8 interacts in paracrine way with breast cancer cells, receptors such as chemokine receptors expressed by breast cancer cells will be studied. For example LIX was shown to be processed by MMP-8 [208]. In the future cleavage of this chemokine by MECs will be investigated.

6.4 MMP-8 might Modulate TGF-β Signalling

In this study we present preliminary data to imply that MMP-8 could inhibit TGF-β activity. TGF-β is a protein involved in many stages of breast cancer and exhibit dual function dependent on disease stage (Section 1.6) [284-286]. We are particularly interested in the involvement of TGF-β activity in crosstalk between MECs, breast cancer cells and the fibroblasts during primary breast cancer cell invasion. In the future the detailed analysis of MMP-8 and TGF-β interaction could provide information on mechanism of action of MMP-8.

6.5 MMP-8 as an Anti-target for Cancer Therapy

Here we presented data that microenvironmental derived MMP-8 can act as a tumour suppressor by influencing cell-ECM as well as cell-cell interactions, in part, by modulating integrin, growth factor and other MMP family members function. This further supports the growing evidence that the role of MMPs is much more complex than just ECM degradation.

Based on the data presented in this study we proposed that MMP-8 is an anti-target for breast cancer therapy. It is of crucial importance to identify the anti-target proteins in order to tailor MMPI trials to spare anti-targets over tumour favouring MMPs [147]. Several other MMP family members have been shown to exert tumour suppressor roles, for example MMP-12 [135, 174-176]. Moreover, according to disease stage some members could act as

tumour suppressor or promoter (MMP-9) [135, 165, 174-176]. Therefore spatiotemporal regulation of MMP function needs to be dissected carefully to create a detailed knowledge which is likely to be essential to develop successful inhibitor approaches.

Chapter 7: Appendices

7 Appendices

7.1 Appendix 1

7.1.1 The Effect of Recombinant MMP-8 Stimulation of Myo-β6 Cells on Filopodia/Retraction Fibre Formation

In order to confirm the autocrine effect of MEC derived MMP-8, (parental) Myo-β6 cells were seeded on fibronectin and cultured overnight, then treated with 50ng/ml rhMMP-8 (prepared in SFM) for 24 hours. After that IF staining for α6β4 and phalloidin was done as described in Section 2.18. Control group was generating by treatment with vehicle only.

There was a significant reduction in filopodia/retraction fibre number per cell ($p=0.03$, $n=1$) in recombinant MMP-8 treated group. This result corresponds to the observations in MMP-8 over-expression.

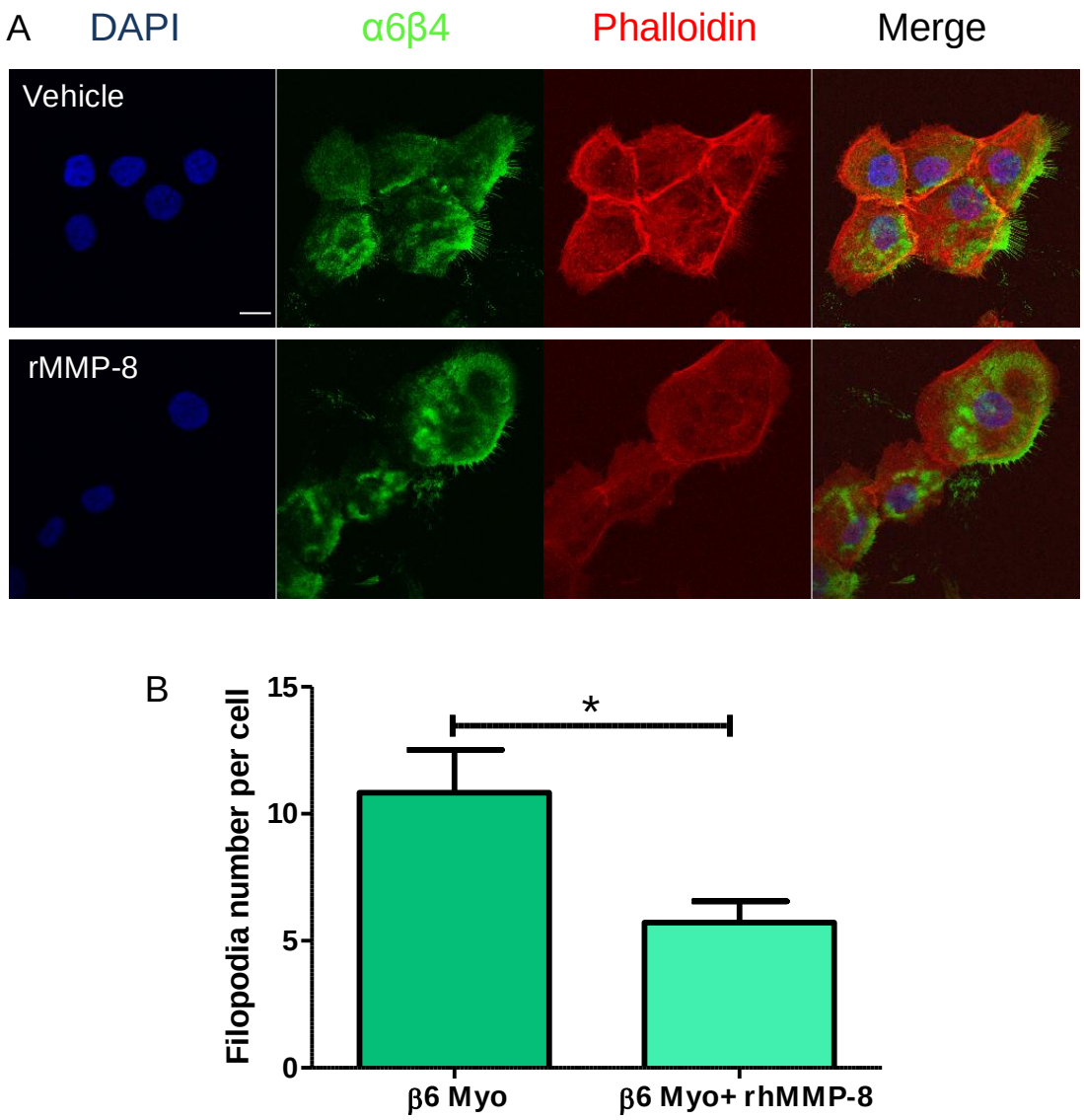

Figure 7-1: Effect of recombinant MMP-8 stimulation on Myo-β6 filopodia/retraction fibre formation. A. Myo-β6 cells were stimulated with rMMP-8 for 24 hours and filopodia/retraction fibre number per cell was counted by using ImageJ. Bar 20 μm. B. A significant reduction in filopodia/retraction fibre number was observed in recombinant MMP-8 treated group when compared to vehicle control. rMMP-8., recombinant MMP-8, representative for 1 experiment.

7.1.2 Effect of MMP-8 Knock-down on Myo-Puro Migration Over Collagen-I in Short Incubation Period

In order to investigate the effect of MMP-8 knock-down on Myo-Puro migration in short incubation to analyse whether the length of incubation time mask the significant effect of MMP-8, the migration assay was set up as described in Section 2.15, but incubated for 4 hours rather than 8 hours. MMP-8 loss showed no significant effect in Myo-Puro migration over Collagen-I after 4 hours incubation (p=0.55, n=1). This result is concomitant to observations after 8 hours incubation (Section 3.3.11).

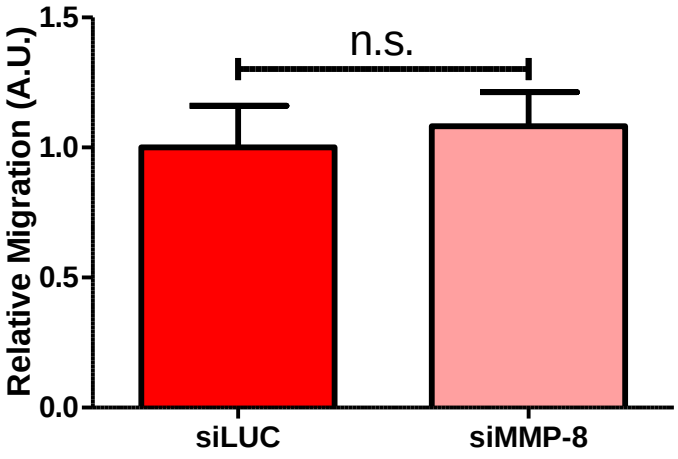

Figure 7-2: Effect of MMP-8 knock-down in Myo-Puro cell migration over Collagen-I in short incubation. Migration assay was done as described in Section 2.18. Incubation was done for 4 hours. There was no significant difference in migration to Collagen-I between siMMP-8 treated Myo-Puro cells or control group. A.U., arbitrary unit, n.s., not significant, representative for 1 experiment.

7.2 Appendix 2

7.2.1 List of MMP-9 Antibodies Used in WB

Two MMP-9 antibodies were used in WB, however failed to reveal a specific band for MMP-9.

Company	Host	Cat no	Outcome
Santa Cruz	Goat	sc-6841	Unspecific bands
Calbiochem	Mouse	IM09L	No band

Table 7-1: List of antibodies MMP-9 antibodies

7.3 Appendix 3

7.3.1 Plasmid Digest

To check the presence of MMP-8 WT insert in pcDNA4 vector, 4 clones of pcDNA4-MMP8 construct were digested as described in Section 2.4. MMP-8 EA containing pcDNA4 vector was also analysed and digest generated 5000 bp and 1400 bp expected bands (data not shown).

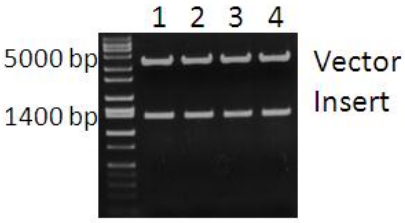

Figure 7-3: MMP-8 insert containing pcDNA4 digest result. Expected 5kb and 1.4kb bands were seen. Bp., base pair.

7.3.2 Plasmid DNA Sequencing

MMP-8 was sequenced using T7 primers and subsequent primers designed for the MMP-8 sequence. The sequencing reaction was carried out by genome centre using Big Dye Terminator v3.1 protocol. Resultant sequences were joined together using CLL sequence viewer (version:6) and the resultant sequence compared with the NCBI sequence for NM 002424.2. This analysis identified mutations in the sequence. This result in a T>I (translation frame position: 34) and K>E (translation frame position: 89) as shown on following pages.

Primer	Sequence 5'-3'
Sequence-1	CACATTTTGATGCCGAAG
Sequence-2	TAATCAACTATGCCTCCAGC

Table 7-2: Primers used to check the presence of full length coding sequence of MMP-8 in pcDNA4 V5 His vector.

References

References

1. Robinson, D., L. Holmberg, and H. Moller, *The occurrence of invasive cancers following a diagnosis of breast carcinoma in situ.* Br J Cancer, 2008. **99**(4): p. 611-5.
2. Beral, V., *Breast cancer and hormone-replacement therapy in the Million Women Study.* Lancet, 2003. **362**(9382): p. 419-27.
3. Hery, C., et al., *Changes in breast cancer incidence and mortality in middle-aged and elderly women in 28 countries with Caucasian majority populations.* Ann Oncol, 2008. **19**(5): p. 1009-18.
4. Kingsmore, D., et al., *Specialisation and breast cancer survival in the screening era.* Br J Cancer, 2003. **88**(11): p. 1708-12.
5. Autier, P., et al., *Disparities in breast cancer mortality trends between 30 European countries: retrospective trend analysis of WHO mortality database.* BMJ. **341**: p. c3620.
6. Ronnov-Jessen, L., O.W. Petersen, and M.J. Bissell, *Cellular changes involved in conversion of normal to malignant breast: importance of the stromal reaction.* Physiol Rev, 1996. **76**(1): p. 69-125.
7. Allred, D.C., *Ductal carcinoma in situ: terminology, classification, and natural history.* J Natl Cancer Inst Monogr, 2010. **2010**(41): p. 134-8.
8. Sopel, M., *The myoepithelial cell: its role in normal mammary glands and breast cancer.* Folia morphologica, 2010. **69**: p. 1-14.
9. Bussolati, G., et al., *Immunolocalization and gene expression of oxytocin receptors in carcinomas and non-neoplastic tissues of the breast.* Am J Pathol, 1996. **148**(6): p. 1895-903.
10. McCready, J., et al., *The contribution of dynamic stromal remodeling during mammary development to breast carcinogenesis.* Breast Cancer Res. **12**(3): p. 205.
11. McCready, J., et al., *The contribution of dynamic stromal remodeling during mammary development to breast carcinogenesis.* Breast Cancer Res, 2010. **12**(3): p. 205.
12. Allinen, M., et al., *Molecular characterization of the tumor microenvironment in breast cancer.* Cancer cell, 2004. **6**: p. 17-32.
13. Gudjonsson, T., et al., *Myoepithelial cells: their origin and function in breast morphogenesis and neoplasia.* Journal of mammary gland biology and neoplasia, 2005. **10**: p. 261-72.
14. Visvader, J.E., *Keeping abreast of the mammary epithelial hierarchy and breast tumorigenesis.* Genes & development, 2009. **23**: p. 2563-77.
15. Deugnier, M.-a., et al., *The importance of being a myoepithelial cell.* Breast cancer research : BCR, 2002. **4**: p. 224-30.
16. Glukhova, M., et al., *Adhesion systems in normal breast and in invasive breast carcinoma.* Am J Pathol, 1995. **146**(3): p. 706-16.
17. Cichon, M.a., et al., *Microenvironmental influences that drive progression from benign breast disease to invasive breast cancer.* Journal of mammary gland biology and neoplasia, 2010. **15**: p. 389-97.
18. Burstein, H.J., et al., *Ductal carcinoma in situ of the breast.* N Engl J Med, 2004. **350**(14): p. 1430-41.
19. Jones, J.L., *Overdiagnosis and overtreatment of breast cancer: progression of ductal carcinoma in situ: the pathological perspective.* Breast cancer research : BCR, 2006. **8**: p. 204.

20. Polyak, K., *Molecular markers for the diagnosis and management of ductal carcinoma in situ.* J Natl Cancer Inst Monogr, 2010. **2010**(41): p. 210-3.
21. Hannemann, J., et al., *Classification of ductal carcinoma in situ by gene expression profiling.* Breast cancer research : BCR, 2006. **8**: p. R61.
22. Deryugina, E.I. and J.P. Quigley, *Matrix metalloproteinases and tumor metastasis.* Cancer metastasis reviews, 2006. **25**: p. 9-34.
23. Jorgensen, K.J. and P.C. Gotzsche, *Breast screening Fundamental errors in estimate of lives saved by screening.* British Medical Journal, 2009. **339**.
24. Payne, S.J.L., et al., *Predictive markers in breast cancer--the present.* Histopathology, 2008. **52**: p. 82-90.
25. Bethwaite, P., et al., *Reproducibility of new classification schemes for the pathology of ductal carcinoma in situ of the breast.* J Clin Pathol, 1998. **51**(6): p. 450-4.
26. Clark, S.E., et al., *Molecular subtyping of DCIS: heterogeneity of breast cancer reflected in pre-invasive disease.* British journal of cancer, 2010. **104**: p. 120-127.
27. Kurose, K., et al., *Frequent somatic mutations in PTEN and TP53 are mutually exclusive in the stroma of breast carcinomas.* Nat Genet, 2002. **32**(3): p. 355-7.
28. Allred, D.C., et al., *Ductal carcinoma in situ and the emergence of diversity during breast cancer evolution.* Clinical cancer research : an official journal of the American Association for Cancer Research, 2008. **14**: p. 370-8.
29. Perou, C.M., et al., *Molecular portraits of human breast tumours.* Nature, 2000. **406**: p. 747-52.
30. Sørlie, T., et al., *Gene expression patterns of breast carcinomas distinguish tumor subclasses with clinical implications.* Proceedings of the National Academy of Sciences of the United States of America, 2001. **98**: p. 10869-74.
31. Sorlie, T., et al., *Repeated observation of breast tumor subtypes in independent gene expression data sets.* Proceedings of the National Academy of Sciences of the United States of America, 2003. **100**: p. 8418-23.
32. Ho-Yen, C., R.L. Bowen, and J.L. Jones, *Characterization of basal-like breast cancer: an update.* Diagnostic Histopathology, 2012. **18**(3).
33. Vincent-Salomon, A., et al., *Integrated genomic and transcriptomic analysis of ductal carcinoma in situ of the breast.* Clinical cancer research : an official journal of the American Association for Cancer Research, 2008. **14**: p. 1956-65.
34. van 't Veer, L.J., et al., *Gene expression profiling predicts clinical outcome of breast cancer.* Nature, 2002. **415**(6871): p. 530-6.
35. Cheang, M.C., et al., *Basal-like breast cancer defined by five biomarkers has superior prognostic value than triple-negative phenotype.* Clin Cancer Res, 2008. **14**(5): p. 1368-76.
36. Dawson, S.J., et al., *BCL2 in breast cancer: a favourable prognostic marker across molecular subtypes and independent of adjuvant therapy received.* Br J Cancer. **103**(5): p. 668-75.
37. Park, K., et al., *HER2 status in pure ductal carcinoma in situ and in the intraductal and invasive components of invasive ductal carcinoma determined by fluorescence in situ hybridization and immunohistochemistry.* Histopathology, 2006. **48**(6): p. 702-7.
38. Hoque, A., et al., *Her-2/neu gene amplification in ductal carcinoma in situ of the breast.* Cancer Epidemiol Biomarkers Prev, 2002. **11**(6): p. 587-90.
39. Houghton, J., et al., *Radiotherapy and tamoxifen in women with completely excised ductal carcinoma in situ of the breast in the UK, Australia, and New Zealand: randomised controlled trial.* Lancet, 2003. **362**(9378): p. 95-102.
40. Muthuswamy, S.K., et al., *ErbB2, but not ErbB1, reinitiates proliferation and induces luminal repopulation in epithelial acini.* Nat Cell Biol, 2001. **3**(9): p. 785-92.

41. Sgroi, D.C., *Preinvasive breast cancer.* Annu Rev Pathol, 2009. **5**: p. 193-221.
42. Wulfkuhle, J.D., et al., *Proteomics of human breast ductal carcinoma in situ.* Cancer research, 2002. **62**: p. 6740-9.
43. Simpson, P.T., et al., *Molecular evolution of breast cancer.* J Pathol, 2005. **205**(2): p. 248-54.
44. Balleine, R.L., et al., *Molecular grading of ductal carcinoma in situ of the breast.* Clin Cancer Res, 2008. **14**(24): p. 8244-52.
45. Lopez-Garcia, M.A., et al., *Breast cancer precursors revisited: molecular features and progression pathways.* Histopathology. **57**(2): p. 171-92.
46. Buerger, H., et al., *Comparative genomic hybridization of ductal carcinoma in situ of the breast-evidence of multiple genetic pathways.* J Pathol, 1999. **187**(4): p. 396-402.
47. Abdel-Fatah, T.M., et al., *High frequency of coexistence of columnar cell lesions, lobular neoplasia, and low grade ductal carcinoma in situ with invasive tubular carcinoma and invasive lobular carcinoma.* Am J Surg Pathol, 2007. **31**(3): p. 417-26.
48. Abdel-Fatah, T.M., et al., *Morphologic and molecular evolutionary pathways of low nuclear grade invasive breast cancers and their putative precursor lesions: further evidence to support the concept of low nuclear grade breast neoplasia family.* Am J Surg Pathol, 2008. **32**(4): p. 513-23.
49. Ma, X.J., et al., *Gene expression profiles of human breast cancer progression.* Proc Natl Acad Sci U S A, 2003. **100**(10): p. 5974-9.
50. Roylance, R., et al., *A comprehensive study of chromosome 16q in invasive ductal and lobular breast carcinoma using array CGH.* Oncogene, 2006. **25**(49): p. 6544-53.
51. Ma, X.-J., et al., *Gene expression profiling of the tumor microenvironment during breast cancer progression.* Breast cancer research : BCR, 2009. **11**: p. R7.
52. Lacroix, M., R.A. Toillon, and G. Leclercq, *Stable 'portrait' of breast tumors during progression: data from biology, pathology and genetics.* Endocr Relat Cancer, 2004. **11**(3): p. 497-522.
53. Natrajan, R., et al., *Loss of 16q in high grade breast cancer is associated with estrogen receptor status: Evidence for progression in tumors with a luminal phenotype?* Genes Chromosomes Cancer, 2009. **48**(4): p. 351-65.
54. Porter, D., et al., *Molecular markers in ductal carcinoma in situ of the breast.* Mol Cancer Res, 2003. **1**(5): p. 362-75.
55. Chin, K., et al., *In situ analyses of genome instability in breast cancer.* Nat Genet, 2004. **36**(9): p. 984-8.
56. Schuetz, C.S., et al., *Progression-specific genes identified by expression profiling of matched ductal carcinomas in situ and invasive breast tumors, combining laser capture microdissection and oligonucleotide microarray analysis.* Cancer Res, 2006. **66**(10): p. 5278-86.
57. Kerlikowske, K., et al., *Biomarker expression and risk of subsequent tumors after initial ductal carcinoma in situ diagnosis.* J Natl Cancer Inst. **102**(9): p. 627-37.
58. Man, Y.-g., *Focal degeneration of aged or injured myoepithelial cells and the resultant auto-immunoreactions are trigger factors for breast tumor invasion.* Medical hypotheses, 2007. **69**: p. 1340-57.
59. Man, Y.-G. and Q.-X.A. Sang, *The significance of focal myoepithelial cell layer disruptions in human breast tumor invasion: a paradigm shift from the "protease-centered" hypothesis.* Experimental cell research, 2004. **301**: p. 103-18.
60. Man, Y.-g., et al., *Cell clusters overlying focally disrupted mammary myoepithelial cell layers and adjacent cells within the same duct display different*

immunohistochemical and genetic features: implications for tumor progression and invasion. Breast cancer research : BCR, 2003. **5**: p. R231-41.
61. Hu, M. and K. Polyak, *Microenvironmental regulation of cancer development.* Curr Opin Genet Dev, 2008. **18**(1): p. 27-34.
62. Kim, J.B., R. Stein, and M.J. O'Hare, *Tumour-stromal interactions in breast cancer: the role of stroma in tumourigenesis.* Tumour Biol, 2005. **26**(4): p. 173-85.
63. Bissell, M.J. and D. Radisky, *Putting tumours in context.* Nat Rev Cancer, 2001. **1**(1): p. 46-54.
64. Allen, M. and J. Louise Jones, *Jekyll and Hyde: the role of the microenvironment on the progression of cancer.* J Pathol. **223**(2): p. 162-76.
65. Polyak, K. and R. Kalluri, *The role of the microenvironment in mammary gland development and cancer.* Cold Spring Harb Perspect Biol, 2010. **2**(11): p. a003244.
66. Olumi, A.F., et al., *Carcinoma-associated fibroblasts direct tumor progression of initiated human prostatic epithelium.* Cancer Res, 1999. **59**(19): p. 5002-11.
67. Maffini, M.V., et al., *Stroma as a crucial target for mammary gland carcinogenesis.* J Cell Science, 2004. **117**(8): p. 1495-1502.
68. Orimo, A., et al., *Stromal fibroblasts present in invasive human breast carcinomas promote tumor growth and angiogenesis through elevated SDF-1/CXCL12 secretion.* Cell, 2005. **121**(3): p. 335-48.
69. Ramos, E.A., et al., *Epigenetic changes of CXCR4 and its ligand CXCL12 as prognostic factors for sporadic breast cancer.* PloS one. **6**(12): p. e29461.
70. Hu, M., et al., *Role of COX-2 in epithelial-stromal cell interactions and progression of ductal carcinoma in situ of the breast.* Proc Natl Acad Sci U S A, 2009. **106**(9): p. 3372-7.
71. Miller, F.R., et al., *MCF10DCIS.com xenograft model of human comedo ductal carcinoma in situ.* J Natl Cancer Inst, 2000. **92**(14): p. 1185-6.
72. Oyama, F., et al., *Coordinate oncodevelopmental modulation of alternative splicing of fibronectin pre-messenger RNA at ED-A, ED-B, and CS1 regions in human liver tumors.* Cancer Res, 1993. **53**(9): p. 2005-11.
73. Hancox, R.A., et al., *Tumour-associated tenascin-C isoforms promote breast cancer cell invasion and growth by matrix metalloproteinase-dependent and independent mechanisms.* Breast Cancer Res, 2009. **11**(2): p. R24.
74. Serini, G., et al., *The fibronectin domain ED-A is crucial for myofibroblastic phenotype induction by transforming growth factor-beta1.* J Cell Biol, 1998. **142**(3): p. 873-81.
75. Campbell, I., W. Qiu, and I. Haviv, *Genetic changes in tumour microenvironments.* J Pathol. **223**(4): p. 450-8.
76. Radisky, D.C., et al., *Rac1b and reactive oxygen species mediate MMP-3-induced EMT and genomic instability.* Nature, 2005. **436**(7047): p. 123-7.
77. Direkze, N.C. and M.R. Alison, *Bone marrow and tumour stroma: an intimate relationship.* Hematol Oncol, 2006. **24**(4): p. 189-95.
78. Dudley, A.C., et al., *Calcification of multipotent prostate tumor endothelium.* Cancer cell, 2008. **14**(3): p. 201-11.
79. Hu, M., et al., *Regulation of in situ to invasive breast carcinoma transition.* Cancer cell, 2008. **13**: p. 394-406.
80. Sharma, M., et al., *Analysis of stromal signatures in the tumor microenvironment of ductal carcinoma in situ.* Breast Cancer Res Treat. **123**(2): p. 397-404.
81. Eng, C., et al., *Genomic alterations in tumor stroma.* Cancer Res, 2009. **69**(17): p. 6759-64.
82. Jessani, N., et al., *Carcinoma and stromal enzyme activity profiles associated with breast tumor growth in vivo.* Proc Natl Acad Sci U S A, 2004. **101**(38): p. 13756-61.

83. Fukino, K., et al., *Combined total genome loss of heterozygosity scan of breast cancer stroma and epithelium reveals multiplicity of stromal targets.* Cancer Res, 2004. **64**(20): p. 7231-6.
84. Fukino, K., et al., *Genomic instability within tumor stroma and clinicopathological characteristics of sporadic primary invasive breast carcinoma.* Jama-Journal of the American Medical Association, 2007. **297**(19): p. 2103-2111.
85. Patocs, A., et al., *Breast-cancer stromal cells with TP53 mutations and nodal metastases.* N Engl J Med, 2007. **357**(25): p. 2543-51.
86. Wernert, N., et al., *Presence of genetic alterations in microdissected stroma of human colon and breast cancers.* J Mol Med (Berl), 2000. **78**(7): p. B30.
87. Wernert, N., et al., *Presence of genetic alterations in microdissected stroma of human colon and breast cancers.* Anticancer Res, 2001. **21**(4A): p. 2259-64.
88. Fukino, K., et al., *Genomic instability within tumor stroma and clinicopathological characteristics of sporadic primary invasive breast carcinoma.* JAMA, 2007. **297**(19): p. 2103-11.
89. Campbell, I.G., et al., *Breast-cancer stromal cells with TP53 mutations.* N Engl J Med, 2008. **358**(15): p. 1634-5; author reply 1636.
90. Hosein, A.N., et al., *Breast carcinoma-associated fibroblasts rarely contain p53 mutations or chromosomal aberrations.* Cancer Res. **70**(14): p. 5770-7.
91. Orimo, A. and R.A. Weinberg, *Stromal fibroblasts in cancer: a novel tumor-promoting cell type.* Cell Cycle, 2006. **5**(15): p. 1597-601.
92. Lawrenson, K., et al., *Senescent fibroblasts promote neoplastic transformation of partially transformed ovarian epithelial cells in a three-dimensional model of early stage ovarian cancer.* Neoplasia. **12**(4): p. 317-25.
93. Hu, M., et al., *Distinct epigenetic changes in the stromal cells of breast cancers.* Nature genetics, 2005. **37**: p. 899-905.
94. Fiegl, H., et al., *Breast cancer DNA methylation profiles in cancer cells and tumor stroma: association with HER-2/neu status in primary breast cancer.* Cancer Res, 2006. **66**(1): p. 29-33.
95. Yu, H.M., J.K. Mouw, and V.M. Weaver, *Forcing form and function: biomechanical regulation of tumor evolution.* Trends in Cell Biology, 2011. **21**(1): p. 47-56.
96. Tanner, K., *Regulation of the basement membrane by epithelia generated forces.* Physical Biology, 2012. **9**(6).
97. Paszek, M.J., et al., *Tensional homeostasis and the malignant phenotype.* Cancer cell, 2005. **8**(3): p. 241-54.
98. Engler, A.J., et al., *Matrix elasticity directs stem cell lineage specification.* Cell, 2006. **126**(4): p. 677-89.
99. Volokh, K.Y., *Stresses in growing soft tissues.* Acta Biomaterialia, 2006. **2**(5): p. 493-504.
100. Padera, T.P., et al., *Cancer cells compress intratumour vessels.* Nature, 2004. **427**(6976): p. 695-695.
101. Tlsty, T.D. and L.M. Coussens, *Tumor stroma and regulation of cancer development.* Annual Review of Pathology-Mechanisms of Disease, 2006. **1**(1): p. 119-150.
102. Butcher, D.T., T. Alliston, and V.M. Weaver, *A tense situation: forcing tumour progression.* Nature Reviews Cancer, 2009. **9**(2): p. 108-122.
103. Ng, C.P., B. Hinz, and M.A. Swartz, *Interstitial fluid flow induces myofibroblast differentiation and collagen alignment in vitro.* J Cell Sci, 2005. **118**(Pt 20): p. 4731-9.
104. Erler, J.T., et al., *Lysyl oxidase is essential for hypoxia-induced metastasis.* Nature, 2006. **440**(7088): p. 1222-1226.

105. Levental, K.R., et al., *Matrix Crosslinking Forces Tumor Progression by Enhancing Integrin Signaling.* Cell, 2009. **139**(5): p. 891-906.
106. Kass, L., et al., *Mammary epithelial cell: Influence of extracellular matrix composition and organization during development and tumorigenesis.* International Journal of Biochemistry & Cell Biology, 2007. **39**(11): p. 1987-1994.
107. Lyons, T.R., et al., *Postpartum mammary gland involution drives progression of ductal carcinoma in situ through collagen and COX-2.* Nature medicine, 2011. **17**(9): p. 1109-U116.
108. Adriance, M.C., et al., *Myoepithelial cells: good fences make good neighbors.* Breast Cancer Res, 2005. **7**(5): p. 190-7.
109. Runswick, S.K., et al., *Desmosomal adhesion regulates epithelial morphogenesis and cell positioning.* Nat Cell Biol, 2001. **3**(9): p. 823-30.
110. Barcellos-Hoff, M.H., et al., *Functional differentiation and alveolar morphogenesis of primary mammary cultures on reconstituted basement membrane.* Development, 1989. **105**(2): p. 223-35.
111. Bissell, M.J. and D. Bilder, *Polarity determination in breast tissue: desmosomal adhesion, myoepithelial cells, and laminin 1.* Breast cancer research : BCR, 2003. **5**: p. 117-9.
112. Gudjonsson, T., et al., *Normal and tumor-derived myoepithelial cells differ in their ability to interact with luminal breast epithelial cells for polarity and basement membrane deposition.* Journal of cell science, 2002. **115**: p. 39-50.
113. Yeh, I.-T. and C. Mies, *Application of immunohistochemistry to breast lesions.* Archives of pathology & laboratory medicine, 2008. **132**: p. 349-58.
114. Barsky, S., *Myoepithelial mRNA expression profiling reveals a common tumor-suppressor phenotype.* Experimental and Molecular Pathology, 2003. **74**: p. 113-122.
115. Barsky, S.H. and N.J. Karlin, *Myoepithelial cells: autocrine and paracrine suppressors of breast cancer progression.* Journal of mammary gland biology and neoplasia, 2005. **10**: p. 249-60.
116. Watabe, K., P.R. Pandey, and J. Saidou, *Role of myoepithelial cells in breast tumor progression.* Frontiers in Bioscience-Landmark, 2010. **15**: p. 226-236.
117. Jones, J.L., et al., *Primary breast myoepithelial cells exert an invasion-suppressor effect on breast cancer cells via paracrine down-regulation of MMP expression in fibroblasts and tumour cells.* The Journal of pathology, 2003. **201**: p. 562-72.
118. Stingl, J. and C. Caldas, *Molecular heterogeneity of breast carcinomas and the cancer stem cell hypothesis.* Nature reviews. Cancer, 2007. **7**: p. 791-9.
119. Bissell, M.J., P.A. Kenny, and D.C. Radisky, *Microenvironmental regulators of tissue structure and function also regulate tumor induction and progression: the role of extracellular matrix and its degrading enzymes.* Cold Spring Harb Symp Quant Biol, 2005. **70**: p. 343-56.
120. Wysolmerski, J.J., et al., *Overexpression of parathyroid hormone-related protein or parathyroid hormone in transgenic mice impairs branching morphogenesis during mammary gland development.* Development, 1995. **121**(11): p. 3539-47.
121. Witty, J.P., J.H. Wright, and L.M. Matrisian, *Matrix metalloproteinases are expressed during ductal and alveolar mammary morphogenesis, and misregulation of stromelysin-1 in transgenic mice induces unscheduled alveolar development.* Mol Biol Cell, 1995. **6**(10): p. 1287-303.
122. Srinivasan, K., et al., *Netrin-1/neogenin interaction stabilizes multipotent progenitor cap cells during mammary gland morphogenesis.* Dev Cell, 2003. **4**(3): p. 371-82.

123. Ke, Y., et al., *The expression of basic fibroblast growth factor and its receptor in cell lines derived from normal human mammary gland and a benign mammary lesion.* J Cell Sci, 1993. **106 (Pt 1)**: p. 135-43.
124. Simian, M., et al., *The interplay of matrix metalloproteinases, morphogens and growth factors is necessary for branching of mammary epithelial cells.* Development, 2001. **128**(16): p. 3117-31.
125. Sternlicht, M.D., et al., *The human myoepithelial cell is a natural tumor suppressor.* Clin Cancer Res, 1997. **3**(11): p. 1949-58.
126. Guelstein, V.I., et al., *Myoepithelial and basement membrane antigens in benign and malignant human breast tumors.* Int J Cancer, 1993. **53**(2): p. 269-77.
127. Reis-Filho, J.S., et al., *Maspin expression in myoepithelial tumors of the breast.* Pathol Res Pract, 2001. **197**(12): p. 817-21.
128. Shao, Z.M., et al., *The human myoepithelial cell exerts antiproliferative effects on breast carcinoma cells characterized by p21WAF1/CIP1 induction, G2/M arrest, and apoptosis.* Experimental cell research, 1998. **241**: p. 394-403.
129. Tobacman, J.K., M. Hinkhouse, and Z. Khalkhali-Ellis, *Steroid sulfatase activity and expression in mammary myoepithelial cells.* The Journal of steroid biochemistry and molecular biology, 2002. **81**: p. 65-8.
130. Hu, M., et al., *Regulation of in situ to invasive breast carcinoma transition.* Cancer cell, 2008. **13**(5): p. 394-406.
131. Hilson, J.B., S.J. Schnitt, and L.C. Collins, *Phenotypic alterations in ductal carcinoma in situ-associated myoepithelial cells: biologic and diagnostic implications.* The American journal of surgical pathology, 2009. **33**: p. 227-32.
132. Jones, J.L., et al., *DCIS-Associated Myoepithelial Cells Expressing the alpha v beta 6 Integrin Modify Tumour Cell Behaviour: A Predictor of Invasive Progression?* Cancer research, 2009. **69**(24): p. 759s-759s.
133. Thomas, G.J., et al., *alpha v beta 6 Integrin upregulates matrix metalloproteinase 9 and promotes migration of normal oral keratinocytes.* The Journal of investigative dermatology, 2001. **116**: p. 898-904.
134. Yousefi, M., et al., *Mammary ducts with and without focal myoepithelial cell layer disruptions show a different frequency of white blood cell infiltration and growth pattern: implications for tumor progression and invasion.* Applied immunohistochemistry & molecular morphology : AIMM / official publication of the Society for Applied Immunohistochemistry, 2005. **13**: p. 30-7.
135. López-Otín, C. and L.M. Matrisian, *Emerging roles of proteases in tumour suppression.* Nature reviews. Cancer, 2007. **7**: p. 800-8.
136. Lopez-Otin, C. and C.M. Overall, *Protease degradomics: a new challenge for proteomics.* Nat Rev Mol Cell Biol, 2002. **3**(7): p. 509-19.
137. Overall, C.M., et al., *Protease degradomics: mass spectrometry discovery of protease substrates and the CLIP-CHIP, a dedicated DNA microarray of all human proteases and inhibitors.* Biol Chem, 2004. **385**(6): p. 493-504.
138. Bachmeier, B.E., et al., *Matrix metalloproteinases in cancer: comparison of known and novel aspects of their inhibition as a therapeutic approach.* Expert Rev Anticancer Ther, 2005. **5**(1): p. 149-63.
139. Kessenbrock, K., V. Plaks, and Z. Werb, *Matrix metalloproteinases: regulators of the tumor microenvironment.* Cell, 2010. **141**: p. 52-67.
140. Lafleur, M.a., M.M. Handsley, and D.R. Edwards, *Metalloproteinases and their inhibitors in angiogenesis.* Expert Reviews in Molecular Medicine, 2004. **5**: p. 1-39.
141. Liotta, L.A., et al., *Metastatic Potential Correlates with Enzymatic Degradation of Basement-Membrane Collagen.* Nature, 1980. **284**(5751): p. 67-68.

142. Cauwe, B., P.E. Van den Steen, and G. Opdenakker, *The biochemical, biological, and pathological kaleidoscope of cell surface substrates processed by matrix metalloproteinases.* Crit Rev Biochem Mol Biol, 2007. **42**(3): p. 113-85.
143. Overall, C.M. and R.A. Dean, *Degradomics: systems biology of the protease web. Pleiotropic roles of MMPs in cancer.* Cancer Metastasis Rev, 2006. **25**(1): p. 69-75.
144. McCawley, L.J. and L.M. Matrisian, *Matrix metalloproteinases: they're not just for matrix anymore!* Curr Opin Cell Biol, 2001. **13**(5): p. 534-40.
145. Nagase, H., R. Visse, and G. Murphy, *Structure and function of matrix metalloproteinases and TIMPs.* Cardiovascular research, 2006. **69**: p. 562-73.
146. Kruger, A., R.E. Kates, and D.R. Edwards, *Avoiding spam in the proteolytic internet: future strategies for anti-metastatic MMP inhibition.* Biochim Biophys Acta, 2009. **1803**(1): p. 95-102.
147. Overall, C.M. and O. Kleifeld, *Tumour microenvironment - opinion: validating matrix metalloproteinases as drug targets and anti-targets for cancer therapy.* Nature reviews. Cancer, 2006. **6**: p. 227-39.
148. Farr, M., et al., *The N-terminus of collagenase MMP-8 determines superactivity and inhibition: a relation of structure and function analyzed by biomolecular interaction analysis.* Biochemistry, 1999. **38**: p. 7332-8.
149. Vincenti, M.P. and C.E. Brinckerhoff, *Signal transduction and cell-type specific regulation of matrix metalloproteinase gene expression: can MMPs be good for you?* Journal of cellular physiology, 2007. **213**: p. 355-64.
150. Tallant, C., A. Marrero, and F.X. Gomis-Ruth, *Matrix metalloproteinases: fold and function of their catalytic domains.* Biochim Biophys Acta. **1803**(1): p. 20-8.
151. Rosenblum, G., et al., *Molecular structures and dynamics of the stepwise activation mechanism of a matrix metalloproteinase zymogen: challenging the cysteine switch dogma.* J Am Chem Soc, 2007. **129**(44): p. 13566-74.
152. Ala-aho, R. and V.-M. Kähäri, *Collagenases in cancer.* Biochimie, 2005. **87**: p. 273-86.
153. García-Prieto, E., et al., *Resistance to bleomycin-induced lung fibrosis in MMP-8 deficient mice is mediated by interleukin-10.* PloS one, 2010. **5**: p. e13242.
154. Chung, L., et al., *Collagenase unwinds triple-helical collagen prior to peptide bond hydrolysis.* EMBO J, 2004. **23**(15): p. 3020-30.
155. Lauer-Fields, J.L., et al., *Identification of specific hemopexin-like domain residues that facilitate matrix metalloproteinase collagenolytic activity.* J Biol Chem, 2009. **284**(36): p. 24017-24.
156. Brinckerhoff, C.E. and L.M. Matrisian, *Matrix metalloproteinases: a tail of a frog that became a prince.* Nature reviews. Molecular cell biology, 2002. **3**: p. 207-14.
157. Murray, G.I., et al., *Matrix metalloproteinase-1 is associated with poor prognosis in colorectal cancer.* Nature medicine, 1996. **2**(4): p. 461-462.
158. Airola, K., et al., *Expression of collagenases-1 and -3 and their inhibitors TIMP-1 and -3 correlates with the level of invasion in malignant melanomas.* British journal of cancer, 1999. **80**(5-6): p. 733-743.
159. Johansson, N., et al., *Collagenase-3 (MMP-13) is expressed by hypertrophic chondrocytes, periosteal cells, and osteoblasts during human fetal bone development.* Developmental Dynamics, 1997. **208**(3): p. 387-397.
160. Allan, J.A., et al., *Binding of gelatinases A and B to type-I collagen and other matrix components.* Biochem J, 1995. **309 (Pt 1)**: p. 299-306.
161. Tester, A.M., et al., *Pro-matrix metalloproteinase-2 transfection increases orthotopic primary growth and experimental metastasis of MDA-MB-231 human breast cancer cells in nude mice.* Cancer research, 2004. **64**(2): p. 652-658.

162. van de Vijver, M.J., et al., *A gene-expression signature as a predictor of survival in breast cancer.* The New England journal of medicine, 2002. **347**: p. 1999-2009.
163. Li, H.C., et al., *Prognostic value of matrix metalloproteinases (MMP-2 and MMP-9) in patients with lymph node-negative breast carcinoma.* Breast Cancer Research and Treatment, 2004. **88**(1): p. 75-85.
164. Jinga, D.C., et al., *MMP-9 and MMP-2 gelatinases and TIMP-1 and TIMP-2 inhibitors in breast cancer: correlations with prognostic factors.* Journal of Cellular and Molecular Medicine, 2006. **10**(2): p. 499-510.
165. Egeblad, M. and Z. Werb, *New functions for the matrix metalloproteinases in cancer progression.* Nat Rev Cancer, 2002. **2**(3): p. 161-74.
166. Coussens, L.M., et al., *MMP-9 supplied by bone marrow-derived cells contributes to skin carcinogenesis.* Cell, 2000. **103**(3): p. 481-90.
167. Bergers, G., et al., *Matrix metalloproteinase-9 triggers the angiogenic switch during carcinogenesis.* Nat Cell Biol, 2000. **2**(10): p. 737-44.
168. Cornelius, L.A., et al., *Matrix metalloproteinases generate angiostatin: effects on neovascularization.* J Immunol, 1998. **161**(12): p. 6845-52.
169. Pozzi, A., et al., *Elevated matrix metalloprotease and angiostatin levels in integrin alpha 1 knockout mice cause reduced tumor vascularization.* Proc Natl Acad Sci U S A, 2000. **97**(5): p. 2202-7.
170. Chabottaux, V. and A. Noel, *Breast cancer progression: insights into multifaceted matrix metalloproteinases.* Clin Exp Metastasis, 2007. **24**(8): p. 647-56.
171. Folgueras, A.R., et al., *Matrix metalloproteinases in cancer: from new functions to improved inhibition strategies.* The International journal of developmental biology, 2004. **48**: p. 411-24.
172. Murphy, G., *Tissue inhibitors of metalloproteinases.* Genome Biol. **12**(11): p. 233.
173. Minn, A.J., et al., *Genes that mediate breast cancer metastasis to lung.* Nature, 2005. **436**(7050): p. 518-524.
174. López-Otín, C., L.H. Palavalli, and Y. Samuels, *Protective roles of matrix metalloproteinases: from mouse models to human cancer.* Cell cycle (Georgetown, Tex.), 2009. **8**: p. 3657-62.
175. Decock, J., et al., *Matrix metalloproteinases: protective roles in cancer.* Journal of Cellular and Molecular Medicine, 2011. **15**(6): p. 1254-1265.
176. Noel, A., et al., *New and paradoxical roles of matrix metalloproteinases in the tumor microenvironment.* Front Pharmacol, 2012. **3**: p. 140.
177. Radisky, E.S. and D.C. Radisky, *Matrix metalloproteinase-induced epithelial-mesenchymal transition in breast cancer.* J Mammary Gland Biol Neoplasia. **15**(2): p. 201-12.
178. Andarawewa, K.L., et al., *Dual stromelysin-3 function during natural mouse mammary tumor virus-ras tumor progression.* Cancer Res, 2003. **63**(18): p. 5844-9.
179. Rudolph-Owen, L.A., et al., *The matrix metalloproteinase matrilysin influences early-stage mammary tumorigenesis.* Cancer Res, 1998. **58**(23): p. 5500-6.
180. Del Casar, J.M., et al., *Comparative analysis and clinical value of the expression of metalloproteases and their inhibitors by intratumor stromal fibroblasts and those at the invasive front of breast carcinomas.* Breast Cancer Res Treat, 2009. **116**(1): p. 39-52.
181. Poola, I., et al., *Identification of MMP-1 as a putative breast cancer predictive marker by global gene expression analysis.* Nature medicine, 2005. **11**(5): p. 481-483.
182. Gorrin Rivas, M.J., et al., *Expression of human macrophage metalloelastase gene in hepatocellular carcinoma: correlation with angiostatin generation and its clinical significance.* Hepatology, 1998. **28**(4): p. 986-93.

183. Yang, W., et al., *Human macrophage metalloelastase gene expression in colorectal carcinoma and its clinicopathologic significance.* Cancer, 2001. **91**(7): p. 1277-83.
184. Hofmann, H.S., et al., *Matrix metalloproteinase-12 expression correlates with local recurrence and metastatic disease in non-small cell lung cancer patients.* Clin Cancer Res, 2005. **11**(3): p. 1086-92.
185. Acuff, H.B., et al., *Analysis of host- and tumor-derived proteinases using a custom dual species microarray reveals a protective role for stromal matrix metal loproteinase-12 in non-small cell lung cancer.* Cancer research, 2006. **66**(16): p. 7968-7975.
186. Kerkela, E., et al., *Metalloelastase (MMP-12) expression by tumour cells in squamous cell carcinoma of the vulva correlates with invasiveness, while that by macrophages predicts better outcome.* Journal of Pathology, 2002. **198**(2): p. 258-269.
187. Margheri, F., et al., *Systemic Sclerosis-Endothelial Cell Antiangiogenic Pentraxin 3 and Matrix Metalloprotease 12 Control Human Breast Cancer Tumor Vascularization and Development in Mice.* Neoplasia, 2009. **11**(10): p. 1106-1115.
188. Kotzsch, M., et al., *Prognostic relevance of uPAR-del4/5 and TIMP-3 mRNA expression levels in breast cancer.* European Journal of Cancer, 2005. **41**(17): p. 2760-2768.
189. Lipton, A., et al., *Elevated plasma tissue inhibitor of metalloproteinase-1 level predicts decreased response and survival in metastatic breast cancer.* Cancer, 2007. **109**(10): p. 1933-1939.
190. Guo, Y.P., et al., *Growth factors and stromal matrix proteins associated with mammographic densities.* Cancer Epidemiology Biomarkers & Prevention, 2001. **10**(3): p. 243-248.
191. Sjoblom, T., et al., *The consensus coding sequences of human breast and colorectal cancers.* Science, 2006. **314**(5797): p. 268-274.
192. Viloria, C.G., et al., *Genetic Inactivation of ADAMTS15 Metalloprotease in Human Colorectal Cancer.* Cancer research, 2009. **69**(11): p. 4926-4934.
193. Wei, X.M., et al., *Mutational and Functional Analysis Reveals ADAMTS18 Metalloproteinase as a Novel Driver in Melanoma.* Molecular Cancer Research, 2010. **8**(11): p. 1513-1525.
194. Lind, G.E., et al., *ADAMTS1, CRABP1, and NR3C1 identified as epigenetically deregulated genes in colorectal tumorigenesis.* Cellular Oncology, 2006. **28**(5-6): p. 259-272.
195. Lo, P.H.Y., et al., *Identification of a tumor suppressive critical region mapping to 3p14.2 in esophageal squamous cell carcinoma and studies of a candidate tumor suppressor gene, ADAMTS9.* Oncogene, 2007. **26**(1): p. 148-157.
196. Moncada-Pazos, A., et al., *The ADAMTS12 metalloprotease gene is epigenetically silenced in tumor cells and transcriptionally activated in the stroma during progression of colon cancer.* Journal of cell science, 2009. **122**(16): p. 2906-2913.
197. Jin, H., et al., *Epigenetic identification of ADAMTS18 as a novel 16q23.1 tumor suppressor frequently silenced in esophageal, nasopharyngeal and multiple other carcinomas.* Oncogene, 2007. **26**(53): p. 7490-7498.
198. Dejonckheere, E., R.E. Vandenbroucke, and C. Libert, *Matrix metalloproteinase8 has a central role in inflammatory disorders and cancer progression.* Cytokine & growth factor reviews, 2011. **22**: p. 73-81.
199. Owen, C.A., et al., *Membrane-bound matrix metalloproteinase-8 on activated polymorphonuclear cells is a potent, tissue inhibitor of metalloproteinase-resistant collagenase and serpinase.* Journal of immunology (Baltimore, Md. : 1950), 2004. **172**: p. 7791-803.

200. Moilanen, M., et al., *Expression and regulation of collagenase-2 (MMP-8) in head and neck squamous cell carcinomas.* The Journal of pathology, 2002. **197**: p. 72-81.
201. Van Lint, P. and C. Libert, *Matrix metalloproteinase-8: cleavage can be decisive.* Cytokine & growth factor reviews, 2006. **17**: p. 217-23.
202. Hasty, K.A., et al., *The Collagen Substrate-Specificity of Human Neutrophil Collagenase.* Journal of Biological Chemistry, 1987. **262**(21): p. 10048-10052.
203. DeNardo, D.G. and L.M. Coussens, *Inflammation and breast cancer. Balancing immune response: crosstalk between adaptive and innate immune cells during breast cancer progression.* Breast cancer research : BCR, 2007. **9**: p. 212.
204. Liotta, L.a. and E.C. Kohn, *The microenvironment of the tumour-host interface.* Nature, 2001. **411**: p. 375-9.
205. Kiili, M., et al., *Collagenase-2 (MMP-8) and collagenase-3 (MMP-13) in adult periodontitis: molecular forms and levels in gingival crevicular fluid and immunolocalisation in gingival tissue.* Journal of clinical periodontology, 2002. **29**: p. 224-32.
206. Kostamo, K., et al., *In vivo relationship between collagenase-2 and interleukin-8 but not tumour necrosis factor-alpha in chronic rhinosinusitis with nasal polyposis.* Allergy, 2005. **60**(10): p. 1275-1279.
207. Hu, S., *Identification of a splice variant of neutrophil collagenase (MMP-8).* FEBS Letters, 1999. **443**: p. 8-10.
208. Balbín, M., et al., *Loss of collagenase-2 confers increased skin tumor susceptibility to male mice.* Nature genetics, 2003. **35**: p. 252-7.
209. Gutiérrez-Fernández, A., et al., *Increased inflammation delays wound healing in mice deficient in collagenase-2 (MMP-8).* The FASEB journal : official publication of the Federation of American Societies for Experimental Biology, 2007. **21**: p. 2580-91.
210. Khatwa, U.a., et al., *MMP-8 promotes polymorphonuclear cell migration through collagen barriers in obliterative bronchiolitis.* Journal of leukocyte biology, 2010. **87**: p. 69-77.
211. Tester, A.M., et al., *LPS responsiveness and neutrophil chemotaxis in vivo require PMN MMP-8 activity.* PloS one, 2007. **2**(3): p. e312.
212. Thirkettle, S., et al., *Matrix metalloproteinase 8 (collagenase 2) induces the expression of interleukins 6 and 8 in breast cancer cells.* J Biol Chem, 2013. **288**(23): p. 16282-94.
213. Cox, J.H., et al., *Matrix metalloproteinase 8 deficiency in mice exacerbates inflammatory arthritis through delayed neutrophil apoptosis and reduced caspase 11 expression.* Arthritis and rheumatism, 2010. **62**: p. 3645-55.
214. Coussens, L.M. and Z. Werb, *Inflammation and cancer.* Nature, 2002. **420**: p. 860-7.
215. Gutiérrez-Fernández, A., et al., *Matrix metalloproteinase-8 functions as a metastasis suppressor through modulation of tumor cell adhesion and invasion.* Cancer research, 2008. **68**: p. 2755-63.
216. Korpi, J.T., et al., *Collagenase-2 (matrix metalloproteinase-8) plays a protective role in tongue cancer.* British journal of cancer, 2008. **98**: p. 766-75.
217. Palavalli, L.H., et al., *Analysis of the matrix metalloproteinase family reveals that MMP8 is often mutated in melanoma.* Nature genetics, 2009. **41**: p. 518-20.
218. Khanna-Gupta, A., et al., *Human neutrophil collagenase expression is C/EBP-dependent during myeloid development.* Experimental hematology, 2005. **33**: p. 42-52.
219. Stadlmann, S., et al., *Cytokine-regulated expression of collagenase-2 (MMP-8) is involved in the progression of ovarian cancer.* European Journal of Cancer, 2003. **39**: p. 2499-2505.

220. Kader, A.K., et al., *Matrix metalloproteinase polymorphisms and bladder cancer risk.* Cancer Res, 2006. **66**(24): p. 11644-8.
221. Jones, L.E., et al., *Comprehensive analysis of matrix metalloproteinase and tissue inhibitor expression in pancreatic cancer: increased expression of matrix metalloproteinase-7 predicts poor survival.* Clinical cancer research : an official journal of the American Association for Cancer Research, 2004. **10**: p. 2832-45.
222. Tanaka, M., et al., *Suppression of gastric cancer dissemination by ephrin-B1-derived peptide.* Cancer science, 2010. **101**: p. 87-93.
223. Tanaka, M., et al., *The C-terminus of ephrin-B1 regulates metalloproteinase secretion and invasion of cancer cells.* Journal of cell science, 2007. **120**: p. 2179-89.
224. Quintero, P.A., et al., *Matrix metalloproteinase-8 inactivates macrophage inflammatory protein-1 alpha to reduce acute lung inflammation and injury in mice.* J Immunol, 2010. **184**(3): p. 1575-88.
225. Blackburn, J.S. and C.E. Brinckerhoff, *Wild-type versus mutant MMP-8 in melanoma: 'when you come to a fork in the road, take it'.* Pigment Cell Melanoma Res, 2009. **22**(3): p. 248-50.
226. Decock, J., et al., *Association of matrix metalloproteinase-8 gene variation with breast cancer prognosis.* Cancer research, 2007. **67**: p. 10214-21.
227. Takada, Y., X.J. Ye, and S. Simon, *The integrins.* Genome Biology, 2007. **8**(5).
228. Desgrosellier, J.S. and D.A. Cheresh, *Integrins in cancer: biological implications and therapeutic opportunities.* Nature Reviews Cancer, 2010. **10**(1): p. 9-22.
229. Guo, W.J. and F.G. Giancotti, *Integrin signalling during tumour progression.* Nature Reviews Molecular Cell Biology, 2004. **5**(10): p. 816-826.
230. Hynes, R.O., *Integrins: Bidirectional, allosteric signaling machines.* Cell, 2002. **110**(6): p. 673-687.
231. Thomas, G.J., M.L. Nyström, and J.F. Marshall, *Alphavbeta6 integrin in wound healing and cancer of the oral cavity.* Journal of oral pathology & medicine : official publication of the International Association of Oral Pathologists and the American Academy of Oral Pathology, 2006. **35**: p. 1-10.
232. Hynes, R.O., *Integrins: bidirectional, allosteric signaling machines.* Cell, 2002. **110**(6): p. 673-87.
233. Gilcrease, M.Z., *Integrin signaling in epithelial cells.* Cancer Letters, 2007. **247**(1): p. 1-25.
234. Allen, M.D., et al., *Clinical and functional significance of alpha9beta1 integrin expression in breast cancer: a novel cell-surface marker of the basal phenotype that promotes tumour cell invasion.* J Pathol, 2011. **223**(5): p. 646-58.
235. Koukoulis, G.K., et al., *Immunohistochemical localization of integrins in the normal, hyperplastic, and neoplastic breast. Correlations with their functions as receptors and cell adhesion molecules.* Am J Pathol, 1991. **139**(4): p. 787-99.
236. Shaw, L.M., *Integrin function in breast carcinoma progression.* J Mammary Gland Biol Neoplasia, 1999. **4**(4): p. 367-76.
237. Lambert, A.W., S. Ozturk, and S. Thiagalingam, *Integrin signaling in mammary epithelial cells and breast cancer.* ISRN Oncol, 2012. **2012**: p. 493283.
238. Diaz, L.K., et al., *Beta4 integrin subunit gene expression correlates with tumor size and nuclear grade in early breast cancer.* Mod Pathol, 2005. **18**(9): p. 1165-75.
239. Friedrichs, K., et al., *High Expression Level of Alpha-6 Integrin in Human Breast-Carcinoma Is Correlated with Reduced Survival.* Cancer research, 1995. **55**(4): p. 901-906.
240. Diaz, L.K., et al., *Chromogenic in situ hybridization for alpha6beta4 integrin in breast cancer: correlation with protein expression.* J Mol Diagn, 2004. **6**(1): p. 10-5.

241. Bergstraesser, L.M., et al., *Expression of hemidesmosomes and component proteins is lost by invasive breast cancer cells.* Am J Pathol, 1995. **147**(6): p. 1823-39.
242. Geuijen, C.A. and A. Sonnenberg, *Dynamics of the alpha6beta4 integrin in keratinocytes.* Mol Biol Cell, 2002. **13**(11): p. 3845-58.
243. Koster, J., et al., *Analysis of the interactions between BP180, BP230, plectin and the integrin alpha 6 beta 4 important for hemidesmosome assembly.* Journal of cell science, 2003. **116**(2): p. 387-399.
244. Tsuruta, D., et al., *Hemidesmosomes and focal contact proteins: Functions and cross-talk in keratinocytes, bullous diseases and wound healing.* Journal of Dermatological Science, 2011. **62**(1): p. 1-7.
245. Santoro, M.M. and G. Gaudino, *Cellular and molecular facets of keratinocyte reepithelization during wound healing.* Exp Cell Res, 2005. **304**(1): p. 274-86.
246. Rezniczek, G.A., et al., *Linking integrin alpha(6)beta(4)-based cell adhesion to the intermediate filament cytoskeleton: Direct interaction between the beta(4) subunit and plectin at multiple molecular sites.* Journal of Cell Biology, 1998. **141**(1): p. 209-225.
247. Rabinovitz, I., L. Tsomo, and A.M. Mercurio, *Protein kinase gat phosphorylation of specific serines in the connecting segment of the beta 4 integrin regulates the dynamics of type II hemidesmosomes.* Molecular and Cellular Biology, 2004. **24**(10): p. 4351-4360.
248. Rabinovitz, I., A. Toker, and A.M. Mercurio, *Protein kinase C-dependent mobilization of the alpha 6 beta 4 integrin from hemidesmosomes and its association with actin-rich cell protrusions drive the chemotactic migration of carcinoma cells.* Journal of Cell Biology, 1999. **146**(5): p. 1147-1159.
249. Sterk, L.M., et al., *The tetraspan molecule CD151, a novel constituent of hemidesmosomes, associates with the integrin alpha6beta4 and may regulate the spatial organization of hemidesmosomes.* J Cell Biol, 2000. **149**(4): p. 969-82.
250. Litjens, S.H.M., J.M. de Pereda, and A. Sonnenberg, *Current insights into the formation and breakdown of hemidesmosomes.* Trends in Cell Biology, 2006. **16**(7): p. 376-383.
251. Steffensen, B., L. Hakkinen, and H. Larjava, *Proteolytic events of wound-healing-coordinated interactions among matrix metalloproteinases (MMPs), integrins, and extracellular matrix molecules.* Critical Reviews in Oral Biology & Medicine, 2001. **12**(5): p. 373-398.
252. vanderNeut, R., et al., *Epithelial detachment due to absence of hemidesmosomes in integrin beta 4 null mice.* Nature genetics, 1996. **13**(3): p. 366-369.
253. Mariotti, A., et al., *EGF-R signaling through Fyn kinase disrupts the function of integrin alpha 6 beta 4 at hemidesmosomes: role in epithelial cell migration and carcinoma invasion.* Journal of Cell Biology, 2001. **155**(3): p. 447-457.
254. Rabinovitz, I., I.K. Gipson, and A.M. Mercurio, *Traction forces mediated by alpha 6 beta 4 integrin: Implications for basement membrane organization and tumor invasion.* Molecular Biology of the Cell, 2001. **12**(12): p. 4030-4043.
255. Dans, M., et al., *Tyrosine phosphorylation of the beta(4) integrin cytoplasmic domain mediates Shc signaling to extracellular signal-regulated kinase and antagonizes formation of hemidesmosomes.* Journal of Biological Chemistry, 2001. **276**(2): p. 1494-1502.
256. Mainiero, F., et al., *The intracellular functions of alpha(6)beta(4) integrin are regulated by EGF.* Journal of Cell Biology, 1996. **134**(1): p. 241-253.
257. Santoro, M.M., G. Gaudino, and P.C. Marchisio, *The MSP receptor regulates alpha 6 beta 4 and alpha 3 beta 1 integrins via 14-3-3 proteins in keratinocyte migration.* Developmental Cell, 2003. **5**(2): p. 257-271.

258. Borradori, L. and A. Sonnenberg, *Structure sand function of hemidesmosomes: More than simple adhesion complexes.* Journal of Investigative Dermatology, 1999. **112**(4): p. 411-418.
259. Cantley, L.C. and Z. Songyang, *Specificity in recognition of phosphopeptides by src-homology 2 domains.* J Cell Sci Suppl, 1994. **18**: p. 121-6.
260. Sudhakaran, P.R., et al., *Endothelial cell-laminin interaction: modulation of LDH expression involves alpha6beta4 integrin-FAK-p38MAPK pathway.* Glycoconj J, 2009. **26**(6): p. 697-704.
261. Hintermann, E., et al., *Inhibitory role of alpha 6 beta 4-associated erbB-2 and phosphoinositide 3-kinase in keratinocyte haptotactic migration dependent on alpha 3 beta 1 integrin.* J Cell Biol, 2001. **153**(3): p. 465-78.
262. Shaw, L.M., et al., *Activation of phosphoinositide 3-OH kinase by the alpha 6 beta 4 integrin promotes carcinoma invasion.* Cell, 1997. **91**(7): p. 949-960.
263. Chung, J., et al., *Integrin (alpha 6 beta 4) regulation of eIF-4E activity and VEGF translation: a survival mechanism for carcinoma cells.* J Cell Biol, 2002. **158**(1): p. 165-74.
264. Zahir, N., et al., *Autocrine laminin-5 ligates alpha6beta4 integrin and activates RAC and NFkappaB to mediate anchorage-independent survival of mammary tumors.* J Cell Biol, 2003. **163**(6): p. 1397-407.
265. Weaver, V.M., et al., *beta4 integrin-dependent formation of polarized three-dimensional architecture confers resistance to apoptosis in normal and malignant mammary epithelium.* Cancer cell, 2002. **2**(3): p. 205-16.
266. Tsuruta, D., et al., *Hemidesmosomes and focal contact proteins: functions and cross-talk in keratinocytes, bullous diseases and wound healing.* J Dermatol Sci, 2011. **62**(1): p. 1-7.
267. Ozawa, T., et al., *Dynamic relationship of focal contacts and hemidesmosome protein complexes in live cells.* J Invest Dermatol. **130**(6): p. 1624-35.
268. Kitajima, Y., et al., *Control of the distribution of hemidesmosome components in cultured keratinocytes: Ca2+ and phorbol esters.* J Dermatol, 1992. **19**(11): p. 770-3.
269. Giannelli, G., et al., *Induction of cell migration by matrix metalloprotease-2 cleavage of laminin-5.* Science, 1997. **277**(5323): p. 225-8.
270. Pirila, E., et al., *Matrix metalloproteinases process the laminin-5 gamma 2-chain and regulate epithelial cell migration.* Biochem Biophys Res Commun, 2003. **303**(4): p. 1012-7.
271. Koshikawa, N., et al., *Role of cell surface metalloprotease MT1-MMP in epithelial cell migration over laminin-5.* J Cell Biol, 2000. **148**(3): p. 615-24.
272. Goldfinger, L.E., M.S. Stack, and J.C. Jones, *Processing of laminin-5 and its functional consequences: role of plasmin and tissue-type plasminogen activator.* J Cell Biol, 1998. **141**(1): p. 255-65.
273. Stanton, H., et al., *The activation of ProMMP-2 (gelatinase A) by HT1080 fibrosarcoma cells is promoted by culture on a fibronectin substrate and is concomitant with an increase in processing of MT1-MMP (MMP-14) to a 45 kDa form.* Journal of cell science, 1998. **111**: p. 2789-2798.
274. Thomas, G.J., et al., *alpha v beta 6 Integrin upregulates matrix metalloproteinase 9 and promotes migration of normal oral keratinocytes.* J Invest Dermatol, 2001. **116**(6): p. 898-904.
275. Allen, M., et al., *Altered Microenvironment Promotes Progression of Preinvasive Breast Cancer: Myoepithelial Expression of αvβ6 Integrin in DCIS Identifies High-risk Patients and Predicts Recurrence.* Clin Cancer Research, 2014. **20**: p. 344-357.
276. Li, X., et al., *Alphavbeta6-Fyn signaling promotes oral cancer progression.* J Biol Chem, 2003. **278**(43): p. 41646-53.

277. Agrez, M., et al., *The Alpha-V-Beta-6 Integrin Promotes Proliferation of Colon-Carcinoma Cells through a Unique Region of the Beta-6 Cytoplasmic Domain.* Journal of Cell Biology, 1994. **127**(2): p. 547-556.
278. Gu, X., et al., *Integrin alpha(v)beta6-associated ERK2 mediates MMP-9 secretion in colon cancer cells.* Br J Cancer, 2002. **87**(3): p. 348-51.
279. Yang, G.Y., et al., *Integrin alpha v beta 6 mediates the potential for colon cancer cells to colonize in and metastasize to the liver.* Cancer Sci, 2008. **99**(5): p. 879-87.
280. Bates, R.C., *Colorectal cancer progression: integrin alphavbeta6 and the epithelial-mesenchymal transition (EMT).* Cell Cycle, 2005. **4**(10): p. 1350-2.
281. Marsh, D., et al., *alpha vbeta 6 Integrin promotes the invasion of morphoeic basal cell carcinoma through stromal modulation.* Cancer Res, 2008. **68**(9): p. 3295-303.
282. Janes, S.M. and F.M. Watt, *Switch from alphavbeta5 to alphavbeta6 integrin expression protects squamous cell carcinomas from anoikis.* J Cell Biol, 2004. **166**(3): p. 419-31.
283. Munger, J.S., et al., *The integrin alpha v beta 6 binds and activates latent TGF beta 1: a mechanism for regulating pulmonary inflammation and fibrosis.* Cell, 1999. **96**: p. 319-28.
284. Akhurst, R.J. and R. Derynck, *TGF-beta signaling in cancer--a double-edged sword.* Trends Cell Biol, 2001. **11**(11): p. S44-51.
285. Bierie, B. and H.L. Moses, *Tumour microenvironment: TGFbeta: the molecular Jekyll and Hyde of cancer.* Nat Rev Cancer, 2006. **6**(7): p. 506-20.
286. Margadant, C. and A. Sonnenberg, *Integrin-TGF-beta crosstalk in fibrosis, cancer and wound healing.* EMBO Rep, 2010. **11**(2): p. 97-105.
287. Aluwihare, P., et al., *Mice that lack activity of alpha v beta 6-and alpha v beta 8-integrins reproduce the abnormalities of Tgfb1- and Tgfb3-null mice.* Journal of cell science, 2009. **122**(2): p. 227-232.
288. Barcellos-Hoff, M.H. and K.B. Ewan, *Transforming growth factor-beta and breast cancer: Mammary gland development.* Breast Cancer Res, 2000. **2**(2): p. 92-9.
289. Dalal, B.I., P.A. Keown, and A.H. Greenberg, *Immunocytochemical localization of secreted transforming growth factor-beta 1 to the advancing edges of primary tumors and to lymph node metastases of human mammary carcinoma.* Am J Pathol, 1993. **143**(2): p. 381-9.
290. Kong, F.M., et al., *Elevated plasma transforming growth factor-beta 1 levels in breast cancer patients decrease after surgical removal of the tumor.* Ann Surg, 1995. **222**(2): p. 155-62.
291. Yang, Y.A., et al., *Lifetime exposure to a soluble TGF-beta antagonist protects mice against metastasis without adverse side effects.* J Clin Invest, 2002. **109**(12): p. 1607-15.
292. Yin, J.J., et al., *TGF-beta signaling blockade inhibits PTHrP secretion by breast cancer cells and bone metastases development.* J Clin Invest, 1999. **103**(2): p. 197-206.
293. Gomm, J.J., et al., *Isolation of Pure Populations of Epithelial and Myoepithelial Cells from the Normal Human Mammary-Gland Using Immunomagnetic Separation with Dynabeads.* Analytical Biochemistry, 1995. **226**(1): p. 91-99.
294. O'Hare, M.J., et al., *Conditional immortalization of freshly isolated human mammary fibroblasts and endothelial cells.* Proceedings of the National Academy of Sciences of the United States of America, 2001. **98**: p. 646-51.
295. Elbashir, S.M., et al., *Duplexes of 21-nucleotide RNAs mediate RNA interference in cultured mammalian cells.* Nature, 2001. **411**(6836): p. 494-498.
296. Lyons, T.R., et al., *Postpartum mammary gland involution drives progression of ductal carcinoma in situ through collagen and COX-2.* Nat Med. **17**(9): p. 1109-15.

297. Froeling, F.E., et al., *Organotypic culture modelling of pancreatic cancer.* Gastroenterology, 2008. **134**(4): p. A586-A586.
298. Froeling, F., et al., *Retinoic Acid-Induced Stellate Cell Quiescence Results in Sfrp4 Secretion Which Abrogates Wnt-beta-Catenin Signalling Pathway Modulating Human Pancreatic Tumour Cell Behaviour.* Gastroenterology, 2011. **140**(5): p. S156-S157.
299. Holliday, D.L., et al., *Novel multicellular organotypic models of normal and malignant breast: tools for dissecting the role of the microenvironment in breast cancer progression.* Breast cancer research : BCR, 2009. **11**: p. R3.
300. Chioni, A.M. and R. Grose, *FGFR1 cleavage and nuclear translocation regulates breast cancer cell behavior.* Journal of Cell Biology, 2012. **197**(6): p. 801-817.
301. Nyström, M.L., et al., *Development of a quantitative method to analyse tumour cell invasion in organotypic culture.* The Journal of pathology, 2005. **205**: p. 468-75.
302. Thies, a., et al., *Clinically proven markers of metastasis predict metastatic spread of human melanoma cells engrafted in scid mice.* British journal of cancer, 2007. **96**: p. 609-16.
303. Nuttall, R.K., et al., *Elevated membrane-type matrix metalloproteinases in gliomas revealed by profiling proteases and inhibitors in human cancer cells.* Molecular cancer research : MCR, 2003. **1**: p. 333-45.
304. Gogly, B., et al., *Collagen zymography as a sensitive and specific technique for the determination of subpicogram levels of interstitial collagenase.* Analytical Biochemistry, 1998. **255**(2): p. 211-216.
305. Snoek-van Beurden, P.A.M. and J.W. Von den Hoff, *Zymographic techniques for the analysis of matrix metalloproteinases and their inhibitors.* Biotechniques, 2005. **38**(1): p. 73-83.
306. Gaudet, C., et al., *Influence of type I collagen surface density on fibroblast spreading, motility, and contractility.* Biophysical Journal, 2003. **85**(5): p. 3329-3335.
307. Cox, E.A., S.K. Sastry, and A. Huttenlocher, *Integrin-mediated adhesion regulates cell polarity and membrane protrusion through the Rho family of GTPases.* Mol Biol Cell, 2001. **12**(2): p. 265-77.
308. Palecek, S.P., et al., *Integrin-ligand binding properties govern cell migration speed through cell-substratum adhesiveness.* Nature, 1997. **385**(6616): p. 537-40.
309. Chen, H.C., *Boyden chamber assay.* Methods Mol Biol, 2005. **294**: p. 15-22.
310. Bissell, M.J., A. Rizki, and I.S. Mian, *Tissue architecture: the ultimate regulator of breast epithelial function - Commentary.* Current Opinion in Cell Biology, 2003. **15**(6): p. 753-762.
311. Mattila, P.K. and P. Lappalainen, *Filopodia: molecular architecture and cellular functions.* Nature Reviews Molecular Cell Biology, 2008. **9**(6): p. 446-454.
312. Artym, V.V., K.M. Yamada, and S.C. Mueller, *ECM degradation assays for analyzing local cell invasion.* Methods Mol Biol, 2009. **522**: p. 211-9.
313. Hawkes, S.P., H.X. Li, and G.T. Taniguchi, *Zymography and Reverse Zymography for Detecting MMPs and TIMPs.* Matrix Metalloproteinase Protocols, Second Edition, 2010. **622**: p. 257-269.
314. Vandooren, J., et al., *Zymography methods for visualizing hydrolytic enzymes.* Nature Methods, 2013. **10**(3): p. 211-220.
315. Pal-Ghosh, S., et al., *MMP9 cleavage of the beta 4 integrin ectodomain leads to recurrent epithelial erosions in mice.* Journal of cell science, 2011. **124**(15): p. 2666-2675.

316. Froeling, F.E.M., et al., *Retinoic Acid-Induced Pancreatic Stellate Cell Quiescence Reduces Paracrine Wnt-beta-Catenin Signaling to Slow Tumor Progression.* Gastroenterology, 2011. **141**(4): p. 1486-U503.
317. Chioni, A.M., et al., *A novel polyclonal antibody specific for the Na(v)1.5 voltage-gated Na(+) channel 'neonatal' splice form.* J Neurosci Methods, 2005. **147**(2): p. 88-98.
318. Kleinman, H.K. and G.R. Martin, *Matrigel: basement membrane matrix with biological activity.* Semin Cancer Biol, 2005. **15**(5): p. 378-86.
319. Marshall, J., *Transwell((R)) invasion assays.* Methods Mol Biol, 2011. **769**: p. 97-110.
320. Moutasim, K.A., M.L. Nystrom, and G.J. Thomas, *Cell migration and invasion assays.* Methods Mol Biol, 2011. **731**: p. 333-43.
321. Chioni, A.M., et al., *A novel polyclonal antibody specific for the Na-v 1.5 voltage-gated Na+ channel 'neonatal' splice form.* Journal of Neuroscience Methods, 2005. **147**(2): p. 88-98.
322. Chioni, A.M., et al., *Protein kinase A and regulation of neonatal Nav1.5 expression in human breast cancer cells: Activity-dependent positive feedback and cellular migration.* International Journal of Biochemistry & Cell Biology, 2010. **42**(2): p. 346-358.
323. Ma, X.J., et al., *Gene expression profiles of human breast cancer progression.* Proceedings of the National Academy of Sciences of the United States of America, 2003. **100**(10): p. 5974-5979.
324. Briones-Orta, M.A., et al., *Arkadia Regulates Tumor Metastasis by Modulation of the TGF-beta Pathway.* Cancer research, 2013. **73**(6): p. 1800-1810.
325. Mazzieri, R., J.S. Munger, and D.B. Rifkin, *Measurement of active TGF-beta generated by cultured cells.* Methods Mol Biol, 2000. **142**: p. 13-27.
326. Abe, M., et al., *An Assay for Transforming Growth-Factor-Beta Using Cells Transfected with a Plasminogen-Activator Inhibitor-1 Promoter Luciferase Construct.* Analytical Biochemistry, 1994. **216**(2): p. 276-284.
327. Dennler, S., et al., *Direct binding of Smad3 and Smad4 to critical TGF beta-inducible elements in the promoter of human plasminogen activator inhibitor-type 1 gene.* EMBO J, 1998. **17**(11): p. 3091-100.
328. Daly, A.C., R.A. Randall, and C.S. Hill, *Transforming Growth Factor beta-Induced Smad1/5 Phosphorylation in Epithelial Cells Is Mediated by Novel Receptor Complexes and Is Essential for Anchorage-Independent Growth.* Molecular and Cellular Biology, 2008. **28**(22): p. 6889-6902.
329. Dennler, S., et al., *Direct binding of Smad3 and Smad4 to critical TGF beta-inducible elements in the promoter of human plasminogen activator inhibitor-type 1 gene.* Embo Journal, 1998. **17**(11): p. 3091-3100.
330. Calvo, F., et al., *Mechanotransduction and YAP-dependent matrix remodelling is required for the generation and maintenance of cancer-associated fibroblasts.* Nat Cell Biology, 2013. **15** (6): p.637-646.